Spectrophotometric Determination of Beryllium with Eriochrome Cyanine R

By Shunji UMEMOTO

(Received June 11, 1956)

For the colorimetric determination of beryllium with organic reagents, various reagents have been used. The following reagents are known; *p*-nitrobenzeneazoorcinol[1,2,3,4,5], quinalizarin[6,7,8,9] curcumin[2,10], alkanin[11,12], naphthazarin[11,12], naphthacrome green G[13] aluminon[14,15,16], quinizarine-2-sulfonic acid[17,18,19], acetylacetone[20], sulfo-salicylic acid[21], sodium salt of chlorophenol-azo-dioxynaphthalene disulfonic acid[22], 8-hydroxyquinaldine[23] solochrome cyanine[24], benzene-2-arsonic acid-(1-azo-2)-1,8-dioxynaphthalene-3,6-disulfonic acid[25], solochrome brilliant blue B (sodium salt of sulfo-dichloro-hydroxy-dimethyl fuchson dicarboxylic acid[25] etc.. Beryllium fails to give a specific color change on a reaction with these reagents; but in general some other ions including iron, aluminum, alkali earth metals and rare earth metals give color change. Therefore, on their application, any of the above mentioned reagents is to be chosen according to the purpose. The method here proposed also seems possible of utilization for some purpose.

Introduction

The color reaction of the following three organic reagents of a similar structure with beryllium was examined at pH 1.42–11.0.

To 2 ml. of the buffer solution, 2 drops of metal solutions containing 50 p. p. m. metals

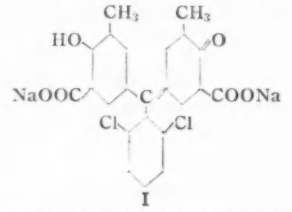

I

Sodium salt of dichloro-hydroxy-dimethyl fuchson dicarboxylic acid

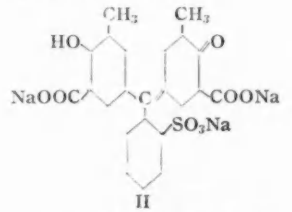

II

Sodium salt of sulfo-hydroxy-dimethyl fuchson dicarboxylic acid (Eriochrome cyanine R)

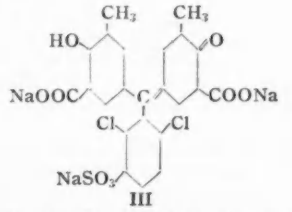

III

Sodium salt of sulfo-dichloro-hydroxy-dimethyl fuchson dicarboxylic acid (Solochrome brilliant blue B)

CHEMISTRY HALL LIBRARY

1) F.A. Vinci, *Anal. Chem.*, 25, 1580 (1953).
2) T. Furuhata, *Repts. Sci. Research Inst.* (Tokyo), 26, 15 (1950).
3) A. S. Komarovskii and N. S. Poluektov, *Mikrochemie*, 14, 315 (1934).
4) L.W. Neidrach, A.M. Mitchell and C. J. Rodden, Natl. Nuclear Energy Ser., Div. VIII, 1, Anal. Chem. Manhattan Project, 350 (1950).
5) W. Stross and G.H. Osborn, *J. Soc. Chem. Ind.*, 63, 249 (1644).
6) M. Bose, *J. Indian Chem. Soc., Ind. & News Ed.*, 14, 61 (1951).
7) G. Charlot, *Anal. Chim. Acta*, 1, 218 (1947).
8) H.Z. Fischer, *Z. anal. Chem.*, 73, 54 (1928).
9) T. Furuhata, *Repts. Sci. Research Inst.* (Tokyo), 26, 9 (1950).
10) I.M. Kolthoff, *J. Am. Chem. Soc.*, 50, 393 (1928).
11) T.Y. Toribara and A.L. Underwood, *Anal. Chem.*, 21, 1352 (1949).
12) A.L. Underwood and W.F. Neuman, ibid, 1348 (1949).
13) W.N. Aldridge and H.G. Liddell, *Analyst*, 73, 607 (1948).
14) H. Goto and Y. Kakita, *Sci. Repts, Research Insts. Tôhoku Univ.*, 5, 163 (1953).
15) G.E. Kosel and W.F. Neuman, *Anal. Chem.*, 22, 936 (1950).
16) C.L. Luke and M. E. Campbell, ibib, 24, 1056 (1952).
17) M.W. Cucci, W.F. Neuman and B.J. Mulryan, *U.S. Atomic Energy Commission*, AECD-1990 (1948).
18) M.W. Cucci, W. F. Neuman and B. J. Mulryan, *Anal. Chem.*, 21, 1358 (1949).
19) F. Hyslop, E. D. Palmes, Wm. C. Alford, A.R. Monaco and L.T. Fairhall, *Natl. Inst. Health Bull.*, 181, 49 (1943).
20) J.A. Adam, E. Booth and J.D.H. Strickland, *Anal. Chim. Acta*, 6, 462 (1952).
21) H.V. Meek and C. V. Banks, *Anal. Chem.*, 22, 1512 (1950).
22) T. Furuhata, *Repts. Sci. Research Inst.* (Tokyo), 26, 139 (1950).
23) K. Motojima, This Bulletin, 29, 71 (1956).
24) C.H. Wood and H. Isherwood, *Metallurgia*, 39, 321 (1949).
25) V.I. Kuznetsov, *J. Anal. Chem. U.S.S.R.*, 10, 276 (1955).
26) J.H. Wood, *Mikrochim. Acta*, 1955, 11.

and 2 drops of 0.1% reagent solution were added. After three hours the color change was observed. For the pH ranges of 1.42–5.2, 7.0–9.2 and 9.2–11.0, the following buffer solutions were used respectively; hydrochloric acid–sodium acetate, hydrochloric acid-barbital and borax–sodium carbonate. In a buffered solution, pH 9.2, the color is yellow for all three blanks (water), and in the presence of beryllium, the color changes to brownish red (I), pinkish red (II) and dark reddish brown (III) respectively. Titanium changes the color of I to brownish yellow. But the same amounts of alminum, iron (ferric and ferrous), titanium (with II and III), copper, thorium and zirconium do not give any color change. The same amounts of calcium, magnesium, manganese and uranium ($(UO_2)^{2+}$) also fail to give any color change to II. In the other buffered solution, beryllium gives a color change, but fails to give a specific color change on reaction with these reagents as in pH 9.2.

Concerning eriochrome cyanine R[27] and solochrome brilliant blue B[28], their application to spectrophotometric determination has been already suggested.

Apparatus

Light absorption was measured against water by means of Shimadzu photoelectric spectrophotometer with 10 mm. absorption cells.

Reagents

Distilled Water.—Redistilled water is obtained by using a water distilling apparatus made of quartz.

Standard Beryllium Solution.—In 5 ml. of concentrated sulfuric acid, 0.1417 g. of beryllium oxide is dissolved. The resulting solution is transferred to a 500 ml. measuring flask containing about 100 ml. of water and is diluted to volume. This solution contains 0.1022 mg. of beryllium per ml.

0.05M Borax Buffer Solution.—In 1000 ml. of distilled water, 19.10 g. of borax are dissolved.

5% Potassium Sodium Tartrate Solution.—In 1000 ml. of distilled water, 50 g. of potassium sodium tartrate are dissolved.

Dye Solutions.—In 1000 ml of distilled water, 1, 3 or 5 g. of dyes are dissolved. The solutions thus obtained contain 0.1, 0.3 or 0.5% of dyes. Dye solutions should not be stored for more than one week.

Absorption Spectra

Absorption spectra of the reagents I, II and III, and of the complexes formed with beryllium are respectively presented in Figs. 1, 2 and 3. These curves were measured in buffered solutions of pH 9.2. The blank solution was prepared by mixing 20 ml. of 0.05 M borax solution with 1 ml. of water and 1 (I) or 2 ml. (II, III) of 0.1% reagent solution, whilst for the preparation of the complex solution 1 ml. of beryllium solution (50 micrograms of beryllium) was used in place of water. The solutions were made to stand for three hours at room temperature before the light absorption was measured.

Inspection of the curves shows that the reagent II is the most desirable for the spectrophotometric determination and that a wave length of 527 mμ gives the greatest difference in light absorption between the blank and the complex of reagent II, eriochrome cyanine R.

Therefore, the following experiments were carried out only with eriochrome cyanine R.

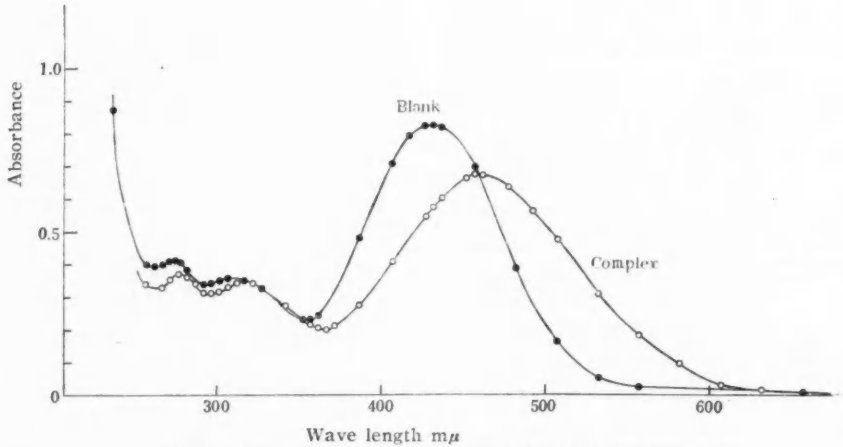

Fig. 1. Absorption spectra of reagent I and its complex.

27) T.Y. Toribara and R.E. Sherman, *Anal. Chem.*, **25**, 1594 (1953).

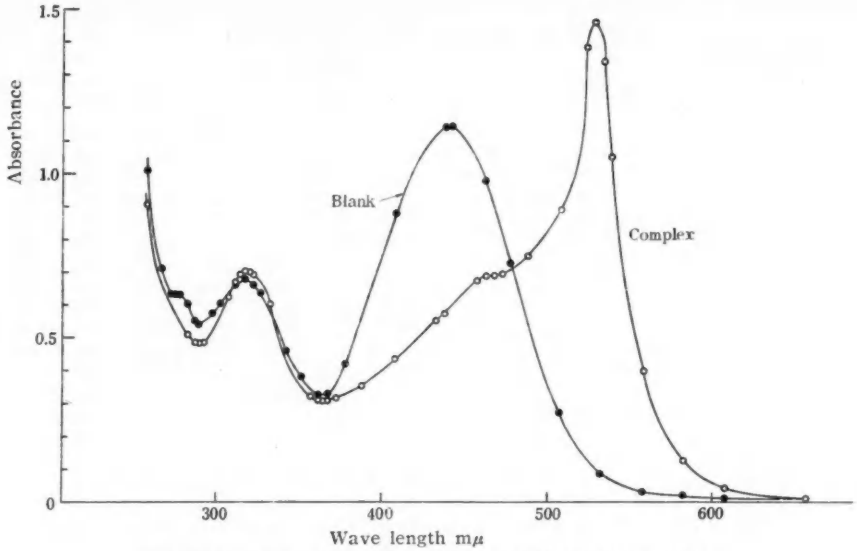

Fig. 2. Absorption spectra of reagent II and its complex.

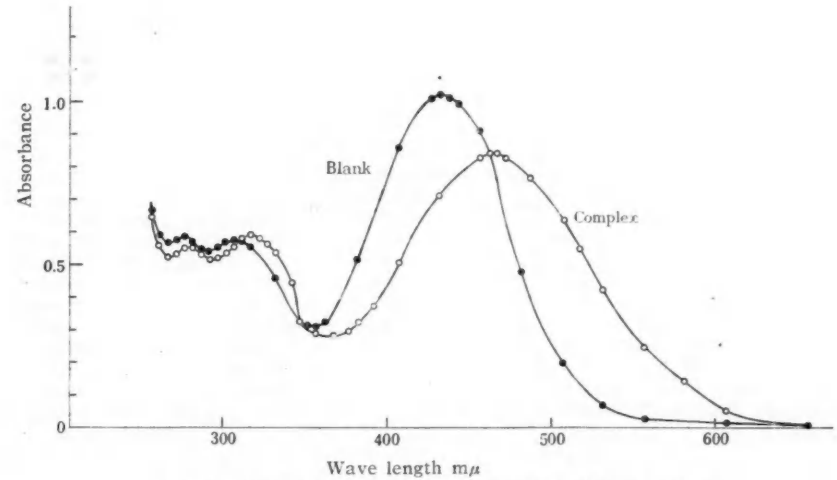

Fig. 3. Absorption spectra of reagent III and its complex.

Effect of Temperature and Time

In general, the organic reagents and beryllium may react slowly in an alkaline medium and at a low temperature. Consequently the effect of temperature and time of standing on the color change was studied.

Five ml. of beryllium solution and 100 ml. of 0.05 M borax solution were mixed, and made to stand for one hour in an ice box or in an air bath, its temperature being controlled. Five ml. of 0.1% eriochrome cyanine R solution were added. Light absorption at 527 mμ was measured ten, twenty and thirty minutes, one, two, three, five, eight, twenty-four and forty-eight hours after the development of the color for aliquots of the beryllium solutions of various concentrations. The results are presented in Table I and II and also in Fig. 4.

From these results, the color intensity was found to be dependent on the temperature and on the time after color development. At a lower temperature, color intensity is high but develops slow, but at a higher temperature, color intensity is low but develops fast. Therefore, the temperature has to be strictly controlled and the mesure-

TABLE I

EFFECT OF TEMPERATURE AND STANDING TIME

Temperature °C	Concentration of Beryllium Solution Mixed with Borax Solution p. p. m.	Standing Time									
		10min.	20min.	30min.	1 hr.	2 hr.	3 hr.	5 hr.	8 hr.	24 hr.	48 hr.
0	25	34.2	39.9	43.4	51.0	65.1	75.1	88.3	97.9	100	98.6
	20	37.8	41.3	44.6	52.9	66.2	74.5	89.1	100	100	100
	15	47.0	50.1	53.1	60.5	69.6	78.7	90.6	99.7	99.5	100
	10	58.9	63.1	63.7	70.3	76.7	83.3	92.5	99.6	98.9	100
	5	79.9	80.8	83.0	87.9	89.7	92.4	96.0	98.2	97.3	100
	0	90.9	96.1	92.2	94.8	98.7	100	96.1	97.4	97.4	97.4
15	25	39.7	66.8	73.4	89.0	94.3	100	100	100	87.7	82.7
	20	61.8	71.2	76.9	87.1	93.3	99.9	100	99.9	88.5	84.1
	15	72.7	80.2	83.5	92.7	97.3	100	100	100	94.0	89.3
	10	86.6	88.3	90.4	96.8	99.1	100	99.4	100	97.1	94.8
	5	90.9	93.9	94.4	97.0	98.5	100	98.0	99.0	94.4	92.9
	0	97.1	92.9	94.3	100	100	100	100	100	95.7	100
25	25	92.2	99.4	99.9	99.7	98.7	99.3	100	99.0	91.3	77.3
	20	89.6	100	98.0	98.7	98.2	97.7	97.3	97.5	91.0	89.6
	15	93.5	99.3	100	98.6	98.6	98.8	99.3	98.8	93.3	92.3
	10	97.7	100	100	100	98.0	99.3	99.7	99.7	96.7	93.0
	5	91.9	99.5	100	98.4	98.9	100	99.5	99.5	94.1	91.4
	0	87.2	87.2	93.6	97.4	94.9	93.6	94.9	92.3	100	97.4
50	25	99.3	98.5	97.6	98.2	97.5	98.4	100	98.5	71.8	65.4
	20	98.9	98.7	99.3	99.6	99.8	100	100	99.1	77.3	72.6
	15	99.2	100	97.2	98.1	97.8	96.7	95.0	96.7	87.3	82.3
	10	96.3	98.1	98.9	100	98.1	98.9	100	100	93.7	92.6
	5	94.1	97.1	96.5	95.9	100	97.1	98.8	100	94.1	89.4
	0	89.5	89.5	96.1	100	97.4	96.1	97.4	94.7	98.7	98.7

Figures shown are the percentages of light absorptions for the maximum light absorption of the solutions which contained same amount of beryllium and were kept at the same temperatures.

TABLE II

ANALYSIS OF VARIANCE

Source of Variation		Degrees of Freedom	Sum of Squares	Mean Square
Main Effects	Temperature (T)	3	9,681.15	3,227.05**
	Time (H)	9	7,217.42	801.94**
	Concentration (C)	5	3,930.46	786.09**
2-Factor Interactions	T×H	27	16,846.31	623.94**
	C×H	45	2,052.73	45.62**
	T×C	15	4,018.36	267.89**
3-Factor Interaction	T×H×C	135	3,097.32	22.94
Total		239	46,843.45	

** Highly significant * Significant

TABLE III

EFFECT OF DYE CONCENTRATION AND TARTRATE

Figures are the readings of the photometer

	20 ml. 0.05M Borax				10 ml. 0.05M Borax +10 ml. 5% Tartrate			
	Concentration of Beryllium Solutions Added p. p. m.*							
	0	3	7	10	0	3	7	10
0.1% Eriochrome Cyanine R	0.090	0.152	0.234	0.314	0.092	0.152	0.223	0.273
0.3% Eriochrome Cyanine R	0.267	0.393	0.593	0.769	0.273	0.423	0.609	0.755
0.5% Eriochrome Cyanine R	0.442	0.616	0.880	1.10_0	0.452	0.663	0.947	1.15_3

* Beryllium content of the solutions, the light absorptions of which were measured is 1/22 of these figures.

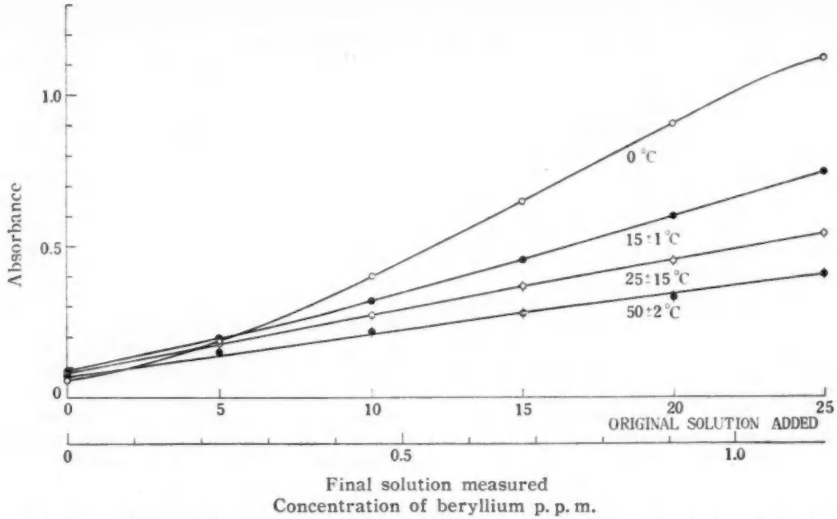

Fig. 4. Effect of temperature and relations between beryllium content and maximum light absorption.

ment of the maximum absorption has to be made at an adequate time after color development.

For an easier control, it seems convenient to select the temperature at 15–30°C and the measuring time in accordance with the temperature.

Effect of Dye Concentration and Tartrate

At pH 9.2, various metals are precipitated; when these elements are present in a large amount, beryllium is coprecipitated and the color change of eriochrome cyanine R by beryllium is inhibited. To avoid this, the presence of potassium sodium tartrate is desirable.

To determine the effect of potassium sodium tartrate and of the concentration of eriochrome cyanine R solution, 0.1, 0.3 and 0.5% eriochrome cyanine R solutions, 3 p. p. m., 7 p. p. m. and 10 p. p. m. of beryllium solutions and 5% potassium sodium tartrate in 0.05 M borax solution were used respectively. One ml. of beryllium solution and 10 ml. of tartrate solution were mixed and 10 ml. of 0.05 M borax solution were added. After standing for one hour in an air bath of 15°C (±1°C), 1 ml. of eriochrome cyanine R solution was added. After four hours, light absorptions were measured at 527 mμ. The results are shown in Table III and IV and in Fig. 5.

The larger the quantity of eriochrome cyanine R, the more intensive is the color (see the inclination of the curve in Fig. 5). Since, however, the light absorption of the blank should not be too high for an accurate determination, the concentration of eriochrome cyanine R cannot be higher than 0.5%.

As the results of presence of tartrate, the relations between the beryllium concentration and the light absorption of the complex holds linear. Moreover, the rate of increase in light absorption with increase in the concentration of eriochrome cyanine R is greater in the presence of tartrate than in its absence.

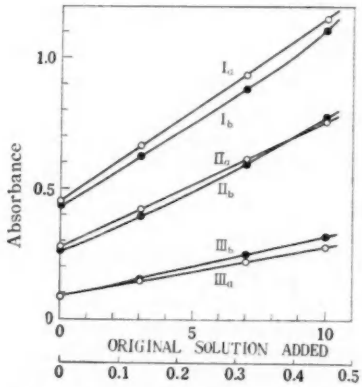

Fig. 5. Effect of dye concentration and tartrate.
Ia: 0.5% dye solution, presence of tartrate
Ib: 0.5% dye solution, absence of tartrate
IIa: 0.3% dye solution, presence of tartrate
IIb: 0.3% dye solution, absence of tartrate
IIIa: 0.1% dye solution, presence of tartrate
IIIb: 0.1% dye solution, absence of tartrate

TABLE IV
ANALYSIS OF VARIANCE

Source of Variation		Degrees of Freedom	Sum of Squares	Mean Square
Main Effects	Concentration of Dye (D)	2	1,397,195	698,597.5**
	Concentration of Beryllium (B)	3	728,133	242,711.0**
	Tartrate (T)	1	1,135	1,135.0**
2-Factor Interactions	D×B	6	135,318	22,553.0**
	T×D	2	3,274	1,637.0
	B×T	3	771	257.0
3-Factor Interaction	D×B×T	6	1,220	203.3
Total		23	2,267,046	

** Highly significant * Significant

Thus, the addition of tartrate gives many benefits for an accurate determination.

For the most sensitive condition at 15°C, i.e. for the application of 0.5% eriochrome cyanine R and the presence of tartrate, the calibration curve for beryllium is shown in Fig. 6.

ing 3 p.p.m. of beryllium and various amounts of a metal or of an anion were prepared. One ml. of a metal or anion solution and 10 ml. of 5% potassium sodium tartrate solution were mixed with 10 ml. of 0.05M borax solution, and set aside for one hour at 15°C. One ml. of 0.5% eriochrome

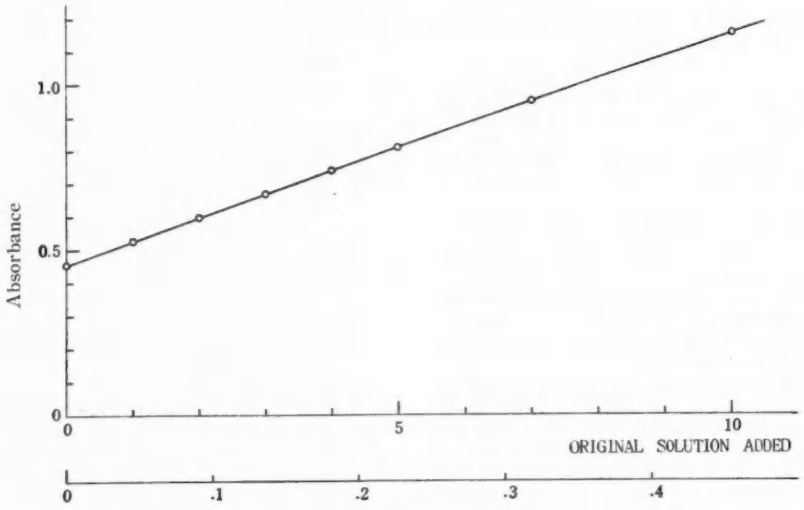

Final solution measured
Concentration of beryllium p.p.m

Fig. 6. Calibration curve of beryllium.
(15°C, presence of tartrate, 0.5% eriochrome cyanine *R* solution)

Effect of Metals and Anions

It has already been mentioned that small amounts of various metals fail to give any color change to eriochrome cynine R in a medium of 0.05 M borax solution, pH 9.2. In the presence of tartrate, however, many metal ions can be held in solution and are expected to give color change of the dye.

In order to disclose the limit of interference of various metals and anions with the color development of beryllium, one series of solutions containcyanine R solution was added, and the light absorption at 527 mμ was measured after four hours. The limit and mode of interference of various metals and anions were shown in Table V.

When a dilute solution of eriochrome cynine R was used, the limit of interference of each metal or anion became greater and the color change caused by beryllium smaller. An example is shown in Table VI and VII (c.f. Table V). Experimental conditions were the same as in the case of the above experiment except for the use of 0.1% dye solution instead of 0.5%.

TABLE V

INTERFERENCE LIMIT OF METALS AND ANIONS

Metal or Anion	Compound	Interference Limit: For the Metal or Anion Solutions Mixed with Tartrate Solution	Interference Limit: For the Final Solutions, Light Absorption of which were measured p. p. m.†	Mode of Interference
Fe^{3+}	Ferric chloride	250	12	Color enhancement
Al^{3+}	Alum	250	12	ditto
Ti^{4+}	Titanium sulfate	>300	>14	—
Mg^{2+}	Magnesium sulfate	250	12	Color inhibition
Ca^{2+}	Calcium chloride	700	32	ditto
Th^{4+}	Thorium nitrate	2000	91	ditto
Fe^{2+}	Ferrous ammonium sulfate	—*	—*	—
$(ZrO)^{2+}$	Zirconium oxychloride	100	4.5	Color inhibition
$(UO_2)^{2+}$	Uranyl acetate	>1000	>45	—
SiO_3^{2-}	Sodium silicate	300	14	Color inhibition
F^-	Sodium fluoride	1000	45	ditto
PO_4^{3-}	Potassium phosphate, monobasic	3000	136	ditto

* For standing, Fe^{2+} is oxidized to Fe^{3+}, and same figure was obtained as Fe^{3+}.

† The concentration of beryllium was 0.17 p. p. m. in this experiment.

TABLE VI

EFFECT OF METAL IONS

One milliliter of 20 p. p. m. beryllium solution containing various amounts of metals and 10 ml. of tartrate solution were mixed and added 10 ml. of 0.05M borax solution. After standing for one hour at 15°C, 1 ml. of 0.1% eriochrome cyanine R solution is added and after four hours light absorption of the solution was measured. Figures of light absorptions are as follows.

Concentration of Iron p. p. m.*	Concentration of Titanium p. p. m.* 0			50		
	Concentration of Aluminum p. p. m. 0	200	1000	0	200	1000
0	0.441	0.453	0.446	0.452	0.452	0.451
200	0.446	0.447	0.448	0.449	0.453	0.445
1000	0.456	0.459	0.451	0.452	0.442	0.447

* These concentrations are the concentration of the metal solutions mixed with tartrate. For the final solutions, these concentrations must be devided by 22.

Discussion

In the case of the determination of beryllium using eriochrome cyanine R, temperature, standing time, concentration of the dye solution, the presence of tartrate, and the concentration of various other ions are the factors which regulate the accuracy, precision and reproducibility.

Above all, the concentration of dye solution should be as high as possible. When it is high, one of the beneficial effects of tartrate, increase in color intensity, is promoted.

Concerning further advantages brought about by tartrate, it makes the working curve linear and prevents the coprecipitation of beryllium with metal ions such as iron, aluminum, calcium and magnesium. Thus, the addition of tartrate is essential.

Temperature is also an important factor; at a lower temperature the color intensity is

TABLE VII

ANALYSIS OF VARIANCE

Source of Variation		Degrees of Freedom	Sum of Squares	Mean Square
Main Effects	(Ti)	1	1.39	1.39
	(Fe)	2	31.45	15.73
	(Al)	2	24.11	12.06
2-Factor Interactions	(Ti)×(Fe)	2	141.44	70.72
	(Fe)×(Al)	4	46.22	11.56
	(Al)×(Ti)	2	44.11	22.06
3-Factor Interaction	(Ti)×(Fe)×(Al)	4	75.56	18.89
Total		17	364.28	

** Highly significant * Significant

higher, but to get maximum light absorption it requires a long time to obtain it and the temperature control is difficult; at a higher temperature standing time for obtaining the maximum light absorption is shorter but the resulting color intensity is lower, the temperature control being also difficult.

Consequently, temperature of 15–30°C will also be recommended from these respects. The interfering cations and anions should not be present with beryllium over the interference limit. The latter is a function of the concentration of the dye solution as mentioned above.

The following procedure is recommended.

One ml. of the sample solution containing from 1 to 10 micrograms of beryllium and 10 ml. of 5% potassium sodium tartrate solution are mixed with 10 ml. of 0.05M borax solution. After standing for one hour at 15°C, 1 ml. of 0.5% eriochrome cyanine R solution is added. After three hours the light absorption of the colored solution is measured at 527 mμ. With the aid of the calibration curve, the amounts of beryllium can be determined (see Table V and Fig. 6).

To a dilute solution of beryllium containing from 0.05 to 0.5 milligram Be per liter, the following procedure is applied. Into a 25 ml. measuring flask, 0.5 g. of potassium sodium tartrate is taken and 20 ml. of the sample solution are poured. After dissolution of tartrate, 0.191 g. of borax is added, dissolved and the whole diluted to 25 ml. After being kept for one hour at 15°C, 1 ml. of 0.5% eriochrome cyanine R solution is added and the light absorption is measured at 527 mμ after four hours. In this case, the calibration curve must be used, which is prepared by the same procedure for a standard beryllium solution.

In any case, when an interfering substance is present in greater quantity than the interfering limit, its amount has to be diminished below the interfering limit.

The author wishes to thank Professor Kenjiro Kimura and Nobufusa Saito of the University of Tokyo for their kind guidance and encouragement, Mr. Shunichi Soma for his kind supply of information, and Mr. Kenji Umemoto for his assistance with a part of the experiment.

Balneological Laboratory, Okayama University, Misasa Hot Springs Tottori Prefecture

Study on the Molecular Structure of Bisacetylacetone-Copper(II) by Electron Diffraction[1]

By Shuzo SHIBATA and Kôzô SONE*

(Received June 27, 1956)

Although the structures and properties of metallic chelate compounds have attracted considerable attention of many recent investigators, the number of compounds whose molecular structures have been accurately determined by X-rays seems to be rather limited on account of their highly complicated crystal structures. However, it is well known that some of these compounds can readily be vaporized. Therefore, it is possible to apply the gas electron diffraction method to the determination of their molecular structures. The present paper deals with the study on the molecular structure of copper chelate of acetylacetone by this method.

The structure of copper acetylacetonate is of interest, particularly, in respect to the question whether the configuration of four oxygen atoms relative to the divalent copper atom is square or tetrahedral, from the point of view of the metallic chelate chemistry. Such a problem has not yet been completely clarified in spite of many earlier investigations, e.g. X-ray analysis[2], dipole moment[3] and infra-red absorption[4] measurements. Our present electron diffraction study was intended to obtain such information, and directly clarified the fact that the chelate possesses a square planar configuration with

1) Presented at Symposium on the metallic complex compounds held on November 13, 1951.

* Present address: Aichi College of Liberal Arts, Higashiku, Nagoya.

2) E. G. Cox and K. C. Webster, *J. Chem. Soc.*, 1935, 731.

3) A. E. Finn, G. C. Hampson, and L. E. Sutton, *J. Chem. Soc.*, 1938, 1254.

4) e.g. J. Lecomte, *Discussions Faraday Soc.*, 1950, 125.

Cu-O distance equal to 1.95 Å. Our results were in good agreement with the recent X-ray investigations[5,6].

Experimental

The sample was prepared by the reaction of aqueous cupric acetate solution with acetylacetone. It was recrystallized from alcohol. The sample was evaporated at about 170°C in a high temperature nozzle and was led into a vacuum chamber to interfere with an electron beam of about 0.06 Å in wave length. The diffraction photographs were taken in the usual way[7]. The camera length was about 11 cm.

Analysis

Measurements were made visually of the q values and the intensities of maxima and minima below $q=70$ in the photographs. Only the intensity of the 14th maximum could be measured. The measured q values are listed in Table I.

TABLE I
OBSERVED AND CALCULATED q VALUES OF THE MAXIMA AND MINIMA

Max.	Min.	$q_{obs.}$	q_c(Model C)	$q_c/q_{obs.}$[a]
	2	7.56	7.6	(1.005)
2		10.05	10.2	1.015
3		14.61	14.7	1.006
4		17.82	17.4	(0.976)
5		21.05	21.0	0.998
6		24.83	23.6	(0.950)
7		29.18	29.6	1.014
8		33.71	33.5	0.994*
9		37.85	36.9	(0.975)
10		43.32	43.3	1.000*
11		52.06	52.2	1.003*
12		57.29	56.4	0.984
13		62.77	62.0	0.988
Average of $q_c/q_{obs.}$				1.000
Average Deviation				0.007

a) The values in parentheses were omitted in calculating the average and values marked with asterisk were given double weight.

The positions of the minima except the 2nd were not measured because of the highly short period of the halos. Curve V_1 in Fig. 3 shows the visual curve which was drawn so as to reproduce the feature of halos and to have the intensities corresponding to the following formula.

$$I(q)=\sum_{i\neq j}(Z_iZ_j/r_{ij})\sin(\pi qr_{ij}/10)$$

Here notations have their usual significances. However, the accurate measurement of intensity in the region of small q values is considerably difficult on account of the intense background of photographs; hence it is probable that the inaccuracy of intensity measurement introduces errors into the radial distribution curve. Therefore the intensity of the first visual curve in this region was corrected by the preliminary theoretical intensity curves in a way described below. The R.D. curve was calculated from the visual curve by use of the formula

$$rD(r)=\sum_i I(q_i)\exp(-aq_i^2)\sin(\pi q_i r/10),$$

where the constant a was chosen so that $\exp(-aq_t^2)=0.1$ for the last term ($q_t=65$). In this case, the unobservable part of q below 7 which is shown by a dotted curve in V_1 in Fig. 3 was appropriately estimated from the feature of the theoretical intensity curve. The R.D. curve thus obtained is shown by R.D. 1 in Fig. 1. The interatomic distances obtained from this

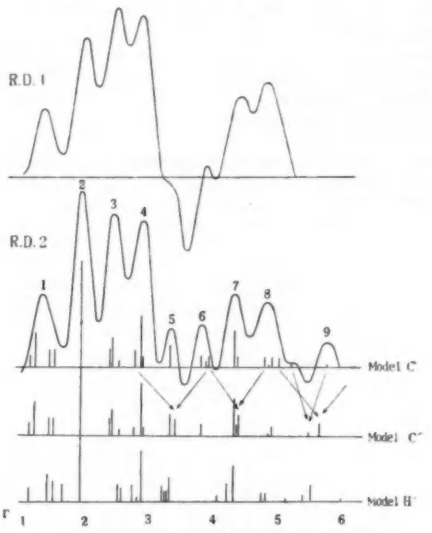

Fig. 1. The radial distribution curves of copper acetylacetonate.
The vertical bars in R.D. 2 indicate all atomic distances (below 6 Å) calculated for model C (square planar), model C′ (rectangular twisted) and model H′ (tetrahedral).

curve are given in Table 2 with assignments to these distances. It must be mentioned here that the following assumption was made throughout the present analysis; the ligand is planar and possesses D_{2h} symmetry. Using the values obtained for the interatomic distances, especially, Cu-O_1**, Cu-C_1, Cu-C_2, and Cu-C_4, preliminary theoretical intensity curves were calculated for various reasonable models. Then, it can be seen that these models*** did not seriously change the

5) E. A. Shugam, *Doklady Akad. Nauk S.S.S.R.* **81**, 853 (1951); *Chem. Abst.*, **46**, 3894 (1952).
6) H. Koyama, Y. Saito and H. Kuroya, *Journal of the Institute of Polytechnics, Osaka City University*, **4**, No. 1, Series C., 43 (1953).
7) e.g. L. O. Brockway, *Rev. Mod. Phys.*, **8**, 231 (1936).

** The notation "Cu-O_1" also means Cu-O_1', Cu-O_2 and Cu-O_2'. In the case of other atomic pairs the situation is the same as in the Cu-O_1 by the above assumption.
*** A twisted model is also taken into consideration together with a planar model.

TABLE II
THE POSITIONS AND THE ASSIGNMENTS OF THE PEAKS IN THE R.D. CURVES

Peak	Distance Å R.D. 1	R.D. 2	Assignment[a]
1	1.34	1.34	$C_1O_1(3)$ $C_1C_2(2)$ $C_1C_4(2)$ CH(1)
2	1.97	1.95	*Cu*$O_1(10)$
3	2.44	2.41	$C_2O_1(2)$ $C_4O_1(2)$ $C_2C_4(1)$
4	2.84	2.87	*Cu*$C_1(5)$ O_1O_2, O_1O_2'*(2) $O_1C_3(1)$
5	3.25	3.32	*Cu*$C_2(2)$
6	3.82	3.80	C_1C_3*(1) $O_1C_3'(1)$
7	4.32	4.30	*Cu*$C_4(3)$ $O_1C_5(1)$
8	4.80	4.81	O_1C_1'*(1) $O_1C_2'(1)$ $O_1C_5'(1)$
9		5.72	C_1C_1'

a) These assignments correspond to the most probable model C. Numbers in parentheses show approximately the relative magnitudes of the ratio Z_iZ_j/r_{ij}. Here the atomic pairs contributing predominantly to each peak are listed. Also the italicized atomic distances are assumed in the calculation of the intensity curves. The bond distances marked with asterisks vary depending on the configuration of the molecule.

intensities for small q values, and therefore the features of these curves can be used to modify the intensity of the first visual curve for small q values (below about 15). The visual curve thus corrected is shown by V_2 in Fig. 3. For example, it was found that the height of the 2nd maximum and the depths of the 2nd and 3rd minima were overestimated in the first visual curve.

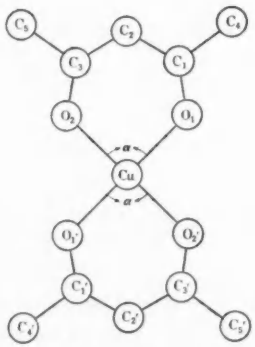

Fig. 2. The shape of the best model and the numbering of atoms.

The corrected R.D. curve was further calculated from the second visual curve in the same way as before, and is shown by R.D. 2 in Fig. 1. This curve is almost non-negative, and this fact is a desirable feature in general. Table II lists the positions and assignments of peaks in its curve. The 2nd, 4th, 5th and 7th peaks are definitely assigned to the Cu-O_1, Cu-C_1, Cu-C_2 and Cu-C_4 atomic pairs, respectively, since these peaks are taken as single or nearly single peaks because of their great scattering powers, so these distances seem to be probably correct. If the structures of the ligands are assumed as mentioned above, the geometrical consideration of the 3rd peak (assigned to C_2-O_1, C_4-O_1 and C_2-C_4) with the above four distances leads to the value of $\angle O_1CuO_2(\angle\alpha)$ nearly equal to 90°. Furthermore, the complete structure of the ligand is probably estimated with use of the 6th peak (C_1-C_5); thus the structure of ligand of the square model C is selected as the most probable model. Thus the structure of the molecule is determined by the configuration dependent on the angle between two ligand planes. Therefore, to determine particularly whether the configuration of molecule is coplanar (model C) or rectangular (model C'), computed radial distributions for each model were compared with the observed one. The vertical bars under the R.D. 2 in Fig. 1 show the interatomic distances for each model and the heights of the bars are drawn proportional to Z_iZ_j/r_{ij} of the respective atomic pairs. Oblique arrows in this figure show the corresponding atomic pairs by the change of the molecular configuration. The comparison of the two computed radial distributions with the observed one leads to the fact that the planar model is superior to the rectangular twisted model, because in the latter the areas of the 5th, 6th, 7th and 8th peaks are not in quantitative accordance with the sum of the heights of the bars. This fact will be made clear by the comparison of both theoretical intensity curves with the observed curve as described later.

Furthermore, a large number of theoretical intensity curves were calculated for various molecular models in order to check the acceptability of the most probable model C mentioned above and to determine the molecular structure in more detail. However, on account of the many parameters involved a complete analysis on the molecular structure of copper acetylacetonate would be a very laborious task. Therefore this analysis was carried out by means of the following assumptions: Cu-O_1, Cu-C_1, Cu-C_2, and Cu-C_4 distances are 1.95 Å, 2.87 Å, 3.32 Å and 4.30 Å, respectively, which are the most probable values obtained from R.D. method. Then other parameters determining the structure are $\angle\alpha$, C_1-C_2, and C_1-C_4 for the ligands, and the configuration of the molecule dependent on the angle between the two ligand planes. The values of the parameters $\angle\alpha$ and C_1-C_2 were taken over the range from 80° to 110° and from 1.33 Å to 1.62 Å respectively, and the position of the C_4 atom was taken in such a way that the C_1-C_4 bond nearly bisects $\angle O_1C_1C_2$. In regard to the configuration of molecule, a coplanar and a rectangular form (including a tetrahedral form) are taken into account. A number of intensity curves were calculated for these carefully selected models with various values for the above parameters and were compared with the observed one. These intensity curves contain the contributions from all the atomic pairs, the pairs pertaining to hydrogen being ignored except H-C bondings.

Some of the calculated intensity curves are

depicted in Fig. 3. The corresponding models are listed in Table III. The relative positions

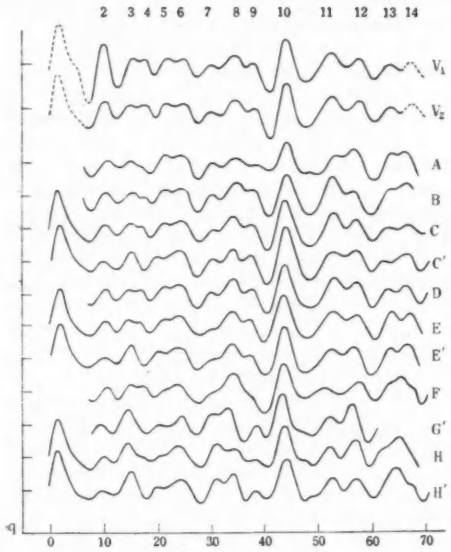

Fig. 3. Visual and theoretical intensity curves.

of maxima and minima of these curves will be compared with those of the visual curve as follows. Curve A is unsatisfactory since the 8th maximum is low and since the 10th minimum is shallow, and since the 11th maximum is lower than the 12th maximum. If the value of $\angle\alpha$ is smaller than 80°, the intensity curves cannot be obtained in agreement with the observed one in regard to the points mentioned above, even though various values of other parameters**** were used. Therefore model A provides the lower limit of $\angle\alpha$. Curves B and E are satisfactory. Curves C and D are more satisfactory. Curve F is unsatisfactory because of the feature of the 9th maximum (depressed to an unacceptable extent) and the relative heights and the positions of the 11th and 12th maxima, and this model provides the upper limit of $\angle\alpha$. Model H*****, a planar model with $\angle\alpha$ equal to a tetrahedral angle, is very unsatisfactory because it requires that the heights of the 3rd and 6th maxima and especially the features of the 7th, 8th and 9th maxima disagree with observations. If the molecule takes a configuration with one ligand plane at a right angle to the plane of the other ligand, such as in models C', E', G' and H' (the latter two are tetrahadral), the features of the 3rd and 4th (disappearing) maxima and position of 5th maximum disagree remarkably with those of the visual curve as seen in Fig. 3, so that these twisted models (including the tetrahedral) are rejected. This conclusion was also confirmed by the computed R.D. as shown by C' and H' (tetrahedral) in Fig. 1. If the molecule would take the twisted form, the 5th and 7th peaks in the observed R.D. should be larger and the 6th and 8th peaks should be smaller. After all, the general qualitative appearance of the photographs is well reproduced by the square planar model. A quantitative comparison of the q values of maxima calculated for the best model C with the observed one is shown in Table I. The discrepancies in the positions

TABLE III

THE MODELS OF THE THEORETICAL INTENSITY CURVES SHOWN IN FIG. 3

Model	$\angle$OCuO	C_1-C_2, Å	C_1-O_1, Å	C_1-C_4, Å	Configuration*
A	80°	1.33	1.15	1.55	Coplanar
B	90°	1.33	1.28	1.55	,, (Square form)
C	90°	1.46	1.21	1.51	,, (,,)
C'	,,	,,	,,	,,	Rectangular
D	90°	1.46	1.21	1.56	Coplanar (Square form)
E	93°	1.46	1.25	1.56	,,
E'	,,	,,	,,	,,	Rectangular
F	98°	1.45	1.32	1 51	Coplanar
G'	110°	1.46	1.50	1.51	Rectangular (Nearly tetrahedral form)
H	110°	1.62	1.40	1.50	Coplanar
H'	,,	,,	,,	,,	Rectangular (Nearly tetrahedral form)

* The configuration is determined by the twisted angle between two ligand planes.

From the analysis described above, the molecular structure of copper acetylacetonate was

**** In general the feature of intensity curves are not seriously sensitive to the parameters C_1-C_2 and C_1-C_4.

***** The models with $\angle\alpha$ equal to a tetrahedral angle seems to be unresonable since the ligand require unreasonably long C_1-C_2 or C_1-O_1 distances from the previous assumption.

determined as follows: Cu–O_1=1.95 Å, Cu–C_1=2.87 Å, Cu–C_2=3.32 Å and Cu–C_4=4.30 Å. (These values were obtained from the R.D. method and the correctness of these values were checked by the calculations of the theoretical intensity curves.), $\angle O_1CuO_2=90\pm10°$, and planar configuration. The latter two are more important conclusions. On the basis of the present photographs it is not possible to make any definite statements as to the distances of C_1–C_2, C_1–O_1 and C_1–C_4 on account of the complexity of the chelate, but for these distances the following average values are obtained from the acceptable models: 1.42 Å, 1.25 Å and 1.55 Å, respectively.

Discussion

Our gas electron diffraction study lead to the conclusion that copper acetylacetonate has a square coplanar configuration with Cu–O distance equal to 1.95 Å.

The result that this chelate takes a square coplanar configuration agrees with the earlier indication of Cox and Webster[2] and also with the recent data of Shugam[5] and Koyama et al.[7] (The $\angle O_1CuO_2$ was determined to be 93° by Shugam and 87.5° by Koyama et al., respectively.) The fact that the chelate forms the square coplanar (not tetrahedral) configuration seems to be due to the fact that an unpaired electron in the 3d orbital of Cu (II) is promoted to the 4p orbital so that Cu (II) constructs dsp^2 hybrid orbitals which have higher bond strengths than sp^3 hybrid orbitals, as suggested by Pauling[8]. Also in this case the conjugation between $d\pi$ orbital of Cu atom and $p\pi$ orbitals of the ligand atoms may highly strengthen the Cu–O bonds, so that this configuration will become more stable.

The observed value of the Cu–O distance was 1.95 Å. It is in good agreement with the sum of the covalent radius of oxygen (0.66 Å) and the metallic radius[8] of copper with a coordination number of 12 (1.28 Å), but is much smaller than the sum (2.4 Å) of ionic radii****** of the two atoms. This supports the evidence of covalent bond character of Cu–O bond. The Cu–O distances in various molecules hitherto reported are: 1.95 Å for cupric oxide[9], 2.01 Å for $CuCl_2\cdot 2H_2O$[9], 1.97 Å for $K_2CuCl_4\cdot 2H_2O$ and $(NH_4)_2CuCl_4\cdot 2H_2O$[9], 1.98 Å and 2.01 Å (mean values) for two types of Cu atoms of malachite[10], 1.98 Å for bandylite[11], 2.03 Å for copper proline dihydrate[12], and 1.91 Å and 1.96 Å (mean values) for copper acetylacetonate (by Shugam and Koyama et al., respectively). The observed Cu–O distance agrees fairly well with these values, but better with that of cupric oxide than with others. This seems to be due probably to the fact that in cupric oxide Cu (II) takes a square coplanar configuration with four covalent Cu–O bonds as in a free molecule of copper acetylacetonate, rather than a distorted octahedral configuration as found in other examples mentioned above. Consequently the observed Cu–O distance of 1.95 Å corresponds to the covalent radius 1.29 Å for Cu (II) in square configuration with coordination number of 4, in contrast with the known radius[8], 1.35 Å in tetrahedral configuration.

The authors express their deep appreciation to Prof. M. Kubo and Dr. M. Kimura for their valuable advice and also to the Ministry of Education for supporting this research.

Department of Chemistry
Faculty of Science
Nagoya University
Chikusa, Nagoya

8) L. Pauling, "Nature of the Chemical Bond", Cornell University Press, New York (1939).

****** Pauling's univalent ionic radii were used after the correction for the ionic valence and coordination number.

9) Ref. 8). R. W. G. Wyckoff, "Crystal Structures", Vol. I, Interscience Publishers, Inc., New York (1948). ibid., (Vol. II) (1951).

10) A. F. Wells, *Acta Cryst.*, **4**, 200 (1951).

11) R. L. Collin, *Acta Cryst.*, **4**, 204 (1951).

12) A. McL. Mathieson and H.K. Walsh, *Acta Cryst.*, **5**, 599 (1952).

*Measurement of Solubilities of Sparingly Soluble Liquids in Water and Aqueous Detergent Solution Using Non-ionic Surfactant**

By Makoto HAYASHI** and Tsunetaka SASAKI

(Received June 26, 1956)

Introduction

During the past few years, numerous studies were reported with regard to the solubilization of various substances into the aqueous solutions of surface active agents. But in the region of concentration below cmc., little is known as to the behavior of solutes in solution. To know such characteristics of the surface active agents in aqueous solution, particularly their interactions with the solutes, it is necessary to begin with the determination of the solubility of solutes in water as well as in aqueous solutions of detergents, since we have unfortunately no reliable data available up to the present. This lack of correct data may come partly from the roughness of the method itself, and partly from the fact that the sparingly soluble substances usually show a tendency to be dispersed as colloidal particles, which make obscure the true solubility determination. Formerly, one of the present authors also determined the solubility of iso-amyl alcohol in water taking account of this fact[1]. In the present paper we determined the solubility of iso-amyl alcohol, *n*-butyl alcohol and benzene in water, making use of the influence on solubility of these substances produced by the addition of non-ionic surfactant, Tween 80.

Experiment

(a) Materials.—The surfactant used in this experiment was a kind of non-ionic surfactant, Tween 80, of Atlas Powder Co., which was kept in vacuum until a constant weight was attained.

For the purification of iso-amyl alcohol and *n*-butyl alcohol, they were boiled with a concentrated sodium hydroxide solution, washed with water, dried with anhydrous potassium carbonate and distilled over calcium oxide. Distillation was repeated over calcium metal, and the fractions distilled at 131°C for the former and 118°C for the latter were collected. Benzene was purified by the ordinary method, that is, it was shaken repeatedly with concentrated sulfuric acid, boiled with mercuric oxide, recrystallized several times and distilled over sodium metal.

(b) Principle and Apparatus.—A definite amount of iso-amyl alcohol is added to a varying amount of Tween 80 solution of known concentration in the cylindrical tube with a well-ground stopper. The mixture is then shaken vigorously, and is stood in the thermostat for about fifteen minutes. If the alcohol concentration is higher than its solubilization limit, the system becomes turbid due to emulsification. The turbidity decreases and finally disappears with an increasing amount of Tween 80 solution added. The diagram is drawn between the turbidity and the concentration (wt. %) of iso-amyl alcohol in the mixture taking the concentration of Tween 80 constant as shown in Fig. 1. From these curves

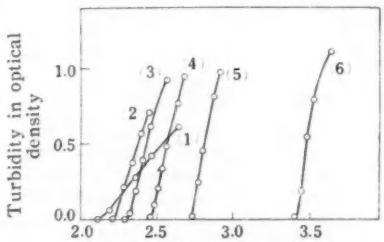

Fig. 1. Relation between turbidity and iso-amyl alcohol concentration in Tween 80 solution of concentration: (1) 0.0998%, (2) 0.228%, (3) 0.52%, (4) 1.046%, (5) 2.00%, (6) 3.86%.

we can estimate the limit of solubilization by extrapolating the linear parts of these curves to zero turbidity. The values of solubilization thus obtained are plotted against the concentration of Tween 80, which is shown as f(c) in Fig. 2. In this figure the point A represents the solubility of iso-amyl alcohol in pure water which is determined as follows. The saturate solution of iso-amyl alcohol in water is prepared and is titrated using Tween 80 solution of the concentration corresponding to the point C in Fig. 2. Hereby, turbidity increases, passes through a maximum, and then decreases gradually, when plotted against the concentration of Tween 80 added, as in Fig. 3. The decreasing portion of the curve is linear. From the extrapolation of this portion to zero turbidity, we can obtain the concentration of Tween 80 (D) required just to dissolve alcohol, which in turn corresponds to the ordinate of the

* This work was presented at the Symposium of Colloid Chemistry, held at Osaka, in November 13, 1954.

** Present address, Kassui Women's Junior College, Higashi Yamate-machi, Nagasaki.

1) S. Mitsui and T. Sasaki, *J. Chem. Soc. Japan*, **63**, 1766 (1942).

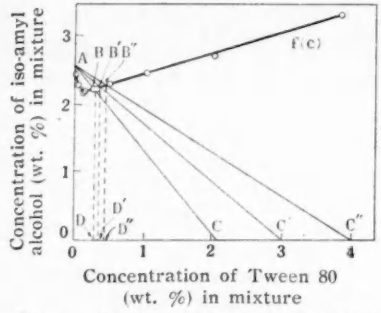

Fig. 2. Solubility of iso-amyl alcohol in aqueous Tween 80 solution. Concentration of Tween 80 in aqueous solution: C=2.061%, C'=2.988%, C''=3.99%; D=0.272%, D'=0.346%, D''=0.436%; A, Saturate solution of iso-amyl alcohol in water; B, B', B'', End point of titration of saturate solution A.

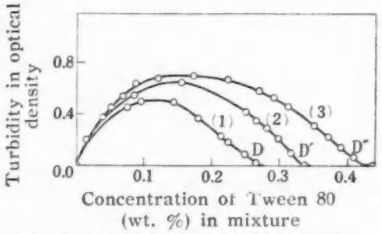

Fig. 3. Turbidities of saturate iso-amyl alcohol solution when titrated with aqueous Tween 80 solution. Concentration of Tween 80 solution used: (1) 2.061%, (2) 2.988%, (3) 3.99%.

point of intersection (B) made by the curve f(c) and the straight line AC in Fig. 2. Inversely, the point B can be determined from D and f(c); thus we can determine the point A, namely the solubility of iso-amyl alcohol, by extrapolating the straight line BC. The turbidity was measured by the photocell type photometer, and expressed in terms of the optical density of transmitted light. The monochromatic light (550 mμ) from a 50 watt lamp with an interference filter was used as a light source.

The temperature of the cell containing solution was regulated within 30.1±0.1°C by the thermostatted water circulating through a water mantle surrounding it.

(c) Experimental Procedure and Results.— For the determination of f(c) of iso-amyl alcohol, about 0.7 g. of it was accurately weighed and mixed with known weight (about 20 g.) of Tween 80 solution of the concentration from 0.0998 to 3.86%. For the determination of the steeply inclined portion of f(c) near the point A, aqueous iso-amyl alcohol was usen instead of pure alcohol. For the preparation of saturate solution, about 7 g. of iso-amyl alcohol and about 200 cc. of water were well shaken together at a temperature lower than that of the measurement (30.1°C), and then stood in the thermostat for about twenty-four hours. After the excess solute particles cleared up, a transparent saturate solution was obtained which was taken out from the bottom of the vessel by a siphon. A known amount of this solution (about 20 g.) was titrated with Tween 80 solution corresponding to C(2.061%), C'(2.988%) and C''(3.99%) as indicated in Fig. 2, under the constant temperature (30.1°C). The points D, D' and D'' were thus obtained and the corresponding points B, B' and B'' were found on f(c) of Fig. 2. The extrapolation of the straight lines BC, B'C' and B''C'' gave nearly the same values of solubility corresponding to the point A in Fig. 2, which were also listed in Table I.

The solubility of *n*-butyl alcohol could be obtained similarly.

In the case of benzene, however, the above method could not be applied directly as the turbidity plotted aginst the concentration of benzene was not linear as shown in Fig. 4. This fact

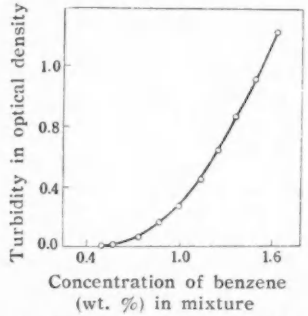

Fig. 4. Relation between turbidity and benzene concentration in 1.07% Tween 80 aqueous solution.

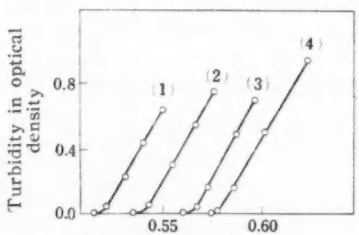

Fig. 5. Relation between turbidity and benzene concentration in aqueous solution of Tween 80-ethyl alcohol mixture. Concentration of 1.67% Tween 80-ethyl alcohol mixture in total mixture: (1) 25.8%, (2) 26.8%, (3) 28.0%, (4) 28.6%.

made the extrapolation inaccurate. In this case, however, the addition of ethyl alcohol enabled us to overcome this difficulty. Fig. 5 shows the opacity curve of benzene emulsion using the ethyl alcohol solution of Tween 80 (1.67%) instead of Tween 80 alone as the solubilizer. Further procedures were the same as in the case of iso-amyl

alcohol. The curve g(c) was thus obtained and shown in Fig. 6.

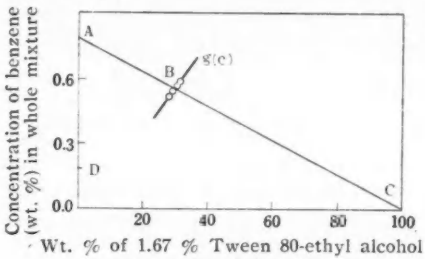

Fig. 6. Solubility of benzene in aqueous solution of Tween 80-ethyl alcohol mixture.
A, Heterogeneous benzene-water mixture obtained by the addition of benzene to the saturate solution
B, End point of titration of heterogeneous system A
C, 1.67% alcohol solution of Tween 80
D, Saturate solution of benzene in water

The saturate solution of benzene expressed as D in Fig. 6 was prepared by the same method as iso-amyl alcohol except for the temperature of shaking being higher than that of the measurement. Actually 0.5244 g. of benzene was added to 92.9926 g. of the saturate solution thus obtained, so as to bring the system in favorable conditions for titration. The point A in Fig. 6 represents the composition of the heterogeneous system thus obtained which was titrated with the solution C, namely 1.67% alcohol solution of Tween 80 containing no water. Now, the titration easily went on just as in the case of iso-amyl alcohol and the point A was obtained similarly. From the composition of A, the solubility of benzene in water could be obtained by subtracting the excess concentration of benzene added to the saturate solution. Solubility data for *n*-butyl alcohol and benzene were also listed in Table I.

TABLE I

Substance	Temperature	Solubility in Water (wt. %)		Reference	
Iso-amyl alcohol	30.1°C	2.587 2.565 2.577	2.57±0.01	2.56	(30°C)[5]
				2.31	(29°C)[7]
Benzene	20.0°C	0.137		0.179	(25°C)[2]
	25.0°C	0.180		0.174	(25°C)[3]
				0.1865	(25°C)[4]
n-Butyl alcohol	30.0°C	7.01		7.08	(30°C)[7]

2) R. L. Bohn and W. F. Claussen, *J. Am. Chem. Soc.*, **73**, 1571 (1951).
3) L. J. Andrews and R. M. Keefer, *J. Am. Chem. Soc.*, **71**, 3645 (1949).
4) Landolt-Börnstein, "Physikalische-Chemisch Tabellen", IIIA, 667 (1935).
5) I. A. Kablukov and V. T. Malischeva, *J. Am. Chem. Soc.*, **47**, 1553 (1925).
6) F. Fontein, *Z. physik. Chem.*, **73**, 212 (1910).
7) Int. Crit. Table, III, p. 388 (1928).

Discussion

As shown in the earlier part of this paper, we proposed a new method of determining a sparlingly soluble solute in water. This method offers advantages in that the process of preparing a saturate solution and that of the determination of a saturate concentration were separated, whereas in other methods such as the determination of the amount of a solute added to a solvent before the turbidity appears, the above two processes are not separated from each other, so the errors are inevitably introduced due to the inaccuracy of the judgement of saturation, especially in the case where the solute shows a tendency to be dispersed colloidally. The accuracy of our method is satisfactory compared with that of the other method as shown in Table I. We should like further to draw attention to the curve f(c) in Fig. 2 which shows a distinct minimum in solubility of iso-amyl alcohol in Tween 80 solution. Such a behavior is interesting in relation to the mechanism of surfactant in solution from the standpoint of solubilizate versus surfactant interaction. But we need further study for a more precise discussion.

Summary

1. The solubility of iso-amyl alcohol, *n*-butyl alcohol and benzene were determined by the titration using the surfactant, Tween 80.

2. In the case of iso-amyl alcohol and *n*-butyl alcohol, the relation between the turbidity and the quantity of solute in surfactant solution is linear, and the solubility limits are both lower than the solubilities in pure water in the dilute region of the surfactant. This makes the determination of their solubility easy and accurate both in pure water and aqueous solution of the detergent.

3. The above method cannot be applied directly for the determination of the solubility of benzene. Ethyl alcohol–Tween 80 mixture is used instead of Tween 80 to overcome this difficulty.

4. The solubilities obtained by this method are accurate enough compared with other methods, in the case of iso-amyl alcohol and *n*-butyl alcohol, possible error being estimated to be 0.4%. In benzene, the error is somewhat larger, but is in good agreement with the values of the literature.

Chemical Institute, College of Arts and Sciences, Chiba University, Chiba and Department of Chemistry, Faculty of Science, Tokyo Metropolitan University, Tokyo

A New Spectrophotometric Method for the Determination of Small Amounts of Chloride Using the Mercuric Thiocyanate Method

By Iwaji IWASAKI, Satori UTSUMI, Ken HAGINO and Takejiro OZAWA

(Received February 28, 1956)

Introduction

A more rapid and accurate method for the determination of a very small amount of chloride ion in natural waters such as rain water, river waters, etc., has been desired.

An indirect colorimetric determination of chloride using solid silver chromate and diphenylcarbazide has been reported[1]. A small amount of chloride can also be estimated by the effect on suppression of reaction of mercuric ion with diphenylcarbazide or diphenylcarbazone[2]. K. Kuroda and E. B. Sandell[3] have studied a photometric method for the determination of chloride which is based on the formation of a colloidal suspension of silver sulfide by treatment of the ammoniacal solution of silver chloride with sulfide. Recently, chloride ion has been determined colorimetrically after exchanging for iodate ion with granular silver iodate in a column[4].

In the previous paper[5], the authors presented a new rapid colorimetric method for the determination of low concentrations of chloride using a very slightly ionizing mercuric thiocyanate solution and an iron alum solution. Chloride ion reacts with $Hg(SCN)_2$ to form $HgCl_2$, $HgCl_4^{2-}$, and SCN^-, which gives a reddish-orange color with ferric ion in nitric acid solution. The orange color of ferric thiocyanate ($FeSCN^{2+}$) formed in the solution is determined colorimetrically. The colored solution obtained has an absorption maximum at 460 mμ, and this colored substance is not extracted with ethyl ether[6]. The calibration curves (absorbance-concentration curves) do not show a linear relationship with the concentrations of chloride.

Lately we have found that the calibration curves of chloride conform to Beer's law at concentrations up to 50 p. p. m. when dioxane is used in the determination of chloride by the mercuric thiocyanate method. This improved spectrophotometric method for the determination of chloride, which is satisfactory for the range of 0.05–80 p. p. m. of chloride, is described in this report.

Experiments and Discussion

Reagents.—*Standard chloride solution* (1,000 p. p. m. Cl^-): 2.103 g. of potassium chloride (guaranteed reagent) was dissolved in 1 l. of distilled water. Solutions of suitable concentrations were prepared by diluting this stock solution.

Potassium Thiocyanate Solution.—About 10 g. of potassium thiocyanate (guaranteed reagent) was dissolved in 1 l. of water. This solution (about 0.1 M) was then standardized by the Volhard's method. Solutions of suitable concentrations were prepared by diluting this standard solution.

Solid Mercuric Thiocyanate.—When a potassium thiocyanate solution is added, drop by drop, to a mercuric nitrate solution containing nitric acid, using iron alum as an indicator, white crystalline $Hg(SCN)_2$ is precipitated. This precipitate is filtered off through a glass filter, and washed with cold water, and then dried in the air. Utilizing this procedure, solid mercuric thiocyanate was prepared. (This compound is stable for a long time.)

1,4-Dioxane (b.p. 102°C, m. p. 11.3°C, Dielectric const. 2.1).—Dioxane (guaranteed reagent) was used after being purified. Purification was accomplished by distilling with an adequate amount of metallic sodium, and collecting at 102°C.

*Mercuric thiocyanate solution (A)** was prepared by dissolving 100 mg. of mercuric thiocyanate in 100 cc. of a mixed solvent consisting of 9 volumes of dioxane and 1 volume of absolute ethyl alcohol. The freezing point of this mixed solvent was about 4°C. Mercuric thiocyanate solution (B) was prepared by dissolving 100 mg. of mercuric thiocyanate in 100 cc. of a mixed solvent consisting of 2 volumes of dioxane and 1 volume of alcohol. Mercuric thiocyanate solution (C)[5] was prepared by dissolving 300 mg. of mercuric thiocyanate in 100 cc. of alcohol. All these mercuric thiocyanate solutions mentioned above were stable.

* Mercuric thiocyanate is difficultly soluble in cold water and dioxane, but more soluble in ethyl alcohol.

1) F.D. and C.T. Snell, "Colorimetric Methods of Analysis", (1949) Vol. II, p. 715; K. Imai, *J. Japan Biochem. Soc.*, 20, 147 (1948).

2) Yu. Yu. Luré and Z. V. Nikoraeva, *Zavodskaya Lab.*, 12, 161 (1946); *C. A.*, 40, 7070 (1946); S.M. Drachev and F.I. Ginzburg, *J. Applied Chem. (U.S.S.R.)*, 11, 879 (1938); F. E. Clark, *Anal. Chem.*, 22, 553 (1950).

3) K. Kuroda and F.B. Sandell, *Anal. Chem.*, 22, 1144 (1950).

4) J.L. Lambert, S.K. Yasuda, *Anal. Chem.*, 27, 444 (1955).

5) I. Iwasaki, S. Utsumi and T. Ozawa, This Bulletin, 25, 226 (1952). S. Utsumi, *J. Chem. Soc. Japan (Pure Chem. Sect.)*, 73, 835, 838 (1952).

6) I. Iwasaki and H. Shimojima, ibid., 76, 749 (1955). H.S. Frank and R.L. Oswalt, *J. Am. Chem. Soc.*, 69, 1321 (1947).

Iron alum solution (A) was prepared by dissolving 8 g. of ferric ammonium sulfate (guaranteed reagent) in 100 cc. of 6 N nitric acid, free from chloride. Iron alum solution (B) was prepared by dissolving 6 g. of ferric ammonium sulfate in 100 cc. of 6 N nitric acid. Iron alum was used as a reagent of ferric ion, because it is easily obtained in the purely crystallized state, free from chloride, whereas ferric nitrate is hygroscopic and often contains chloride.

Apparatus.—Absorption measurements were carried out with a Beckman Model DU spectrophotometer using 10 mm. cells at 460 mμ.

Effect of Dioxane.—The influence of the addition of dioxane upon the colorimetric determination of chloride by the mercuric thiocyanate method was studied. Results obtained are shown in Fig. 1, in which line (I) corresponds to the calibration curve of chloride obtained by the former method[5] reported previously. The experiments were carried out under the following conditions: 10 cc. of the sample solution were pipetted into a test tube equipped with a glass stopper. Then 2 cc. of iron alum solution (B) and 1 cc. of mercuric thiocyanate solution (C) were added. The absorbances were plotted against the concentrations of chloride at 20°C, ten minutes after mixing.

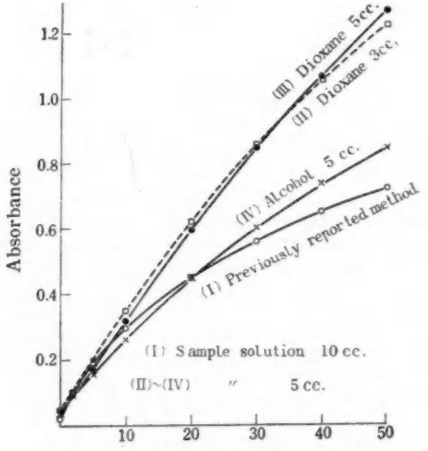

Fig. 1. Absorbance-concentration curves and effect of dioxane and alcohol at 460 mμ, 20°C.

As will be seen in Fig. 1, the calibration curve (I) was not linear with respect to the concentrations of chloride. When 2 cc. of iron alum solution (B), 1 cc. of mercuric thiocyanate solution (C) and then 3 cc. of dioxane were added to 5 cc. of the sample solution, the absorbance-concentration curve shown in the broken line (II) was obtained. When 5 cc. of dioxane, and ethyl alcohol were added respectively instead of 3 cc. of dioxane, the calibration curves corresponding to line (III) and (IV) respectively were obtained.

In this mercuric thiocyanate method, it is clear that the intensity of the color obtained is markedly affected by the addition of dioxane, but not of alcohol. The calibration curve of line (III) can be seen to conform nearly to Beer's law. After preliminary experiments the authors established a new spectrophotometric method available for the determination of chloride over the range of 0.05 to 80 p. p. m. of chloride.

Determination for a Range of 3 to 80 p.p.m. of Chloride.—Procedure (A).—To 2.5 cc. of the sample solution, 1 cc. of iron alum solution (A) and 3 cc. of mercuric thiocyanate solution (A) were added. The absorption measurements were carried out with a Beckman Model DU spectrophotometer using 10 mm. cells ten minutes after mixing.

Absorption Spectral Curves.—The absorption of the colored solutions (blank test, 10 and 30 p. p. m. Cl^-) was measured over the range of 390–600 mμ; absorbance was plotted against wave length in Fig. 2, in which there is one absorption maximum at 460 mμ. In addition, the solution has an absorption below 430 mμ, owing to the formation of a yellow ferric sulfate complex ion.

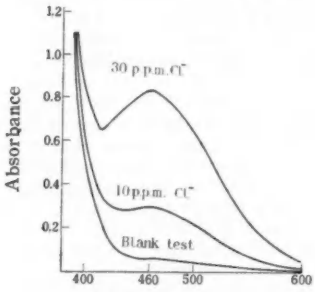

Fig. 2. Absorption Curves.

Time of Standing and Stability of Color.—Constant absorbance values of colored solutions (blank test, 10 and 30 p. p. m. Cl^-) were obtained after then minutes at room temperature (about 10°C). The color of the solution was stable. The results obtained are shown in Table I.

TABLE I

TIME OF STANDING AND STABILITY OF COLOR AT ABOUT 10°C

Time	Absorbance		
	Blank test	10 p. p. m. Cl^-	30 p. p. m. Cl^-
2 min.	0.065	0.285	0.824
3 "	0.055	0.280	0.810
4 "	0.051	0.275	0.801
5 "	0.050	0.272	0.799
10 "	0.050	0.272	0.791
15 "	0.050	0.272	0.791
1 hr.	0.050	0.273	0.793
3 "	0.050	0.272	0.793

Calibration Curves and Effect of Temperature.—The calibration curves shown in Fig. 3 were prepared by the Procedure (A) mentioned

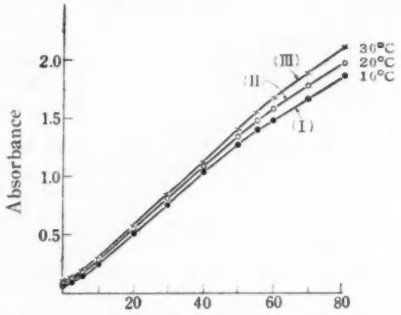

Concentration of chloride P. P. M.

Fig. 3. Calibration curves and effect of temperature, at 460 mμ.

above using standard chloride solutions of known concentrations at 10°, 20° and 30°C. As will be seen in Fig. 3, the calibration curves show good agreement with Beer's law over the concentration range of 2–50 p. p. m. of chloride. But, for the concentrations higher than 50 p. p. m. of chloride, and lower than 2 p. p. m., the calibration curves do not show linear relation-ships, curving very slightly as shown in Fig. 3.

Since absorbance is considerably affected by temperature, as shown in Fig. 3, it is necessary to measure the absorbance under the same conditions of temperature in order to determine the concentration of chloride with good accuracy by this method. For the determination of concentrations lower than 3 p. p. m. Cl^-, the Procedure (B) described later in this report should be used.

A faintly colored blank solution was obtained when redistilled water was treated. The absorbance of the blank test was small, but constant, and was probably due to the dissociation of mercuric thiocyanate. The calibration curves shown in Fig. 3 were reproducible within ±1% for the range of 5–80 p. p. m. Cl^-.

Effect of the Reagent Concentrations.—The absorbance was affected by the amounts of mercuric thiocyanate solution and the concentrations of iron alum reagents. The experimental results obtained are shown in Fig. 4, in which line (I) corresponds to the calibration curve for line (II) in Fig. 3, and lines (II) and (III) show the experimental results obtained under the following conditions: for line (II), to 2.5 cc. of sample solution, 1 cc. of iron alum solution (B) and 3 cc. of mercuric thiocyanate solution (A) were added; for line (III), to 2.5 cc. of sample solution, 1 cc. of iron alum solution (A) and 2.5 cc. of mercuric thiocyanate solution (A) were added.

As will be seen in Fig. 4, it is necessary to use 3 cc. of mercuric thiocyanate solution (A) for 2.5 cc. of the sample solutions. On the other hand, when the amount of iron alum is increased, the color obtained is deeper, as in the case reported previously[5].

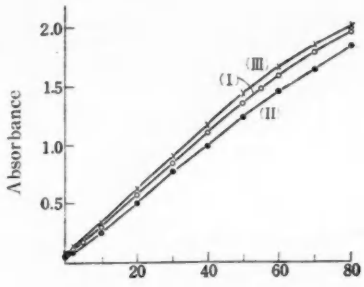

Concentration of chloride P. P. M.

Fig. 4. Absorbance-concentration curves. Effect of the reagent concentration at 460 mμ. 20°C.

(I) $Hg(SCN)_2$ Soln. (A) 3 cc.
Fe-Alum Soln. (A) 1 cc.
(II) $Hg(SCN)_2$ Soln. (A) 3 cc.
Fe-Alum Soln. (B) 1 cc.
(III) $Hg(SCN)_2$ Soln. (A) 2.5 cc
Fe-Alum Soln. (A) 1 cc.

In this method the color intensity was slightly affected by the concentration of nitric acid. The effect of the concentration of nitric acid in iron alum reagent on this colorimetric method was observed in the presence of 30 p. p. m. of chloride at 15°C. The results obtained are shown in Table II.

TABLE II

EFFECT OF THE CONCENTRATION OF NITRIC ACID

Concns. of HNO_3 (N)	5	5.5	6	6.5	7
Absorbance	0.760	0.788	0.815	0.836	0.860

When the concentration of nitric acid was increased, the reddish-orange color became deeper.

Color Reaction.—In order to explain this color reaction some experiments were carried out. The results obtained are shown in Fig. 5, in which the line (I) corresponds to the calibration curve (II) in Fig. 3, and the other lines are obtained under the following conditions: for broken line (II), to 2.5 cc. of standard thiocyanate solutions of known concentrations, 1 cc. of iron alum solu-

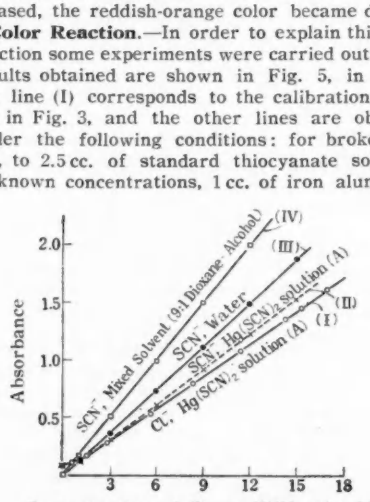

Concentration of Cl^- or SCN^- 10^{-4} M

Fig. 5. Absorbance-concentration curves. Equilibrium of the color reaction.

tion (A) and 3 cc. of mercuric thiocyanate solution (A) were added; for line (III), to 2.5 cc. of the thiocyanate solution 3 cc. of distilled water and 1 cc. of iron alum solution (A) were added; and for line (IV), to 2.5 cc. of the thiocyanate solution, 1 cc. of iron alum solution (A) and 3 cc. of mixed solvents consisting of 9 volumes of dioxane and 1 volume of alcohol were added. The absorbances were plotted against the concentrations in 10^{-4} moles per liter at 20°C.

The calibration curve for chloride (line (I)) falls approximately along the calibration curve for thiocyanate (line (II)) containing the same amounts of mercuric thiocyanate solution. This fact indicates that the following reaction takes place from left to right almost completely.

$$2Cl^- + Hg(SCN)_2 \rightleftarrows HgCl_2 + 2SCN^-$$

The liberated SCN^- reacts with Fe^{3+} to give a reddish-orange color, as follows:

$$SCN^- + Fe^{3+} \rightleftarrows FeSCN^{2+}$$

The fact that the orange color of ferric thiocyanate formed in the solution becomes stronger in the presence of dioxane seems to indicate that the equilibrium of the above equation is largely shifted from left to right (lines (III) and (IV)). On the other hand, the difference between line (II) and (IV) seems to be due to the formation of mercuric thiocyanate complex ion[7] as follows:

$$n\,SCN^- + Hg(SCN)_2 \rightleftarrows [Hg(SCN)_{2+n}]^{n-}$$

Determination for a Range of 0.05 to 5 p.p.m. of Chloride.—The determination of lower concentrations of chloride was carried out by the following Procedure (B).

Procedure (B). Five cubic centimetres of the sample solution were pipetted into a test tube equipped with a glass stopper. Then 1 cc. of iron alum solution (A) and 1.5 cc. of mercuric thiocyanate solution (B) were added.

Calibration Curves and Effect of Temperature.—The calibration curves, (I) and (II) in Fig. 6, were prepared by Procedure (B) described above using standard chloride solutions of known concentrations at 15°C and 25°C respectively. Line (III) corresponds to the calibration curve obtained by the previously reported method[5] at 15°C (i.e., to 10 cc. of the sample solution, 2 cc. of iron alum solution (B) and 1 cc. of mercuric thiocyanate solution (C) were added). These calibration curves in Fig. 6 show good agreement with Beer's law over the range 0.05–3 p.p.m. of chloride.

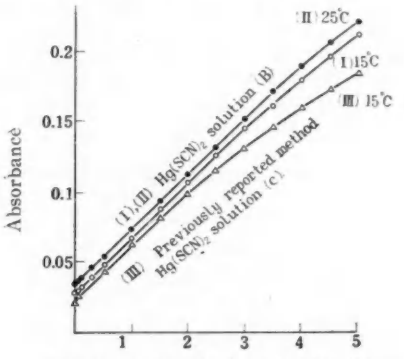

Fig. 6. Calibration curves for the lower range of chloride (I—II).

These curves were affected slightly by temperature as will be seen in Fig. 6. The absorbance of the blank test was very small, but constant. The lowest concentration of the standard solution whose color could be distinguished from that of the blank test was 0.05 p.p.m. Cl^- (1.4×10^{-5} M). The calibration curves shown in Fig. 6 were reproducible within ±0.05 p.p.m. Cl^-. In this method a better result will be obtained by the use of 100 mm. cells instead of 10 mm. cells. Especially in the determination of lower concentrations of chloride, the operator must be properly careful of contamination from outside.

Effect of Various Ions.—Bromide, iodide, cyanide, sulfide and thiosulfate react with $Hg(SCN)_2$ solution to liberate SCN^- ion, which gives a reddish-orange color with ferric ion in the same way as chloride[8], even in this improved method. Among the substances which interfere intrinsically with this method, sulfide, thiosulfate, cyanide, and thiocyanate are destroyed by heating with hydrogen peroxide in alkaline solution[9].

The effect of various ions except the interfering ions described above on this method (Procedure A) was examined in the presence of 30 p.p.m. Cl^- and blank test. Some of the results obtained are given in Table III.

TABLE III

EFFECT OF IONS ON PROCEDURE (A) AT 15°C

Substance	Concentration	Absorbance	
None	p.p.m. 0	Blank test 0.053, 0.053	30 p.p.m. Cl^- 0.815, 0.813
$NaNO_3$	85,000 (1 M)	0.070	0.907
〃	8,500 (0.1 M)	0.053	0.818
SO_4^{2-}	5,000	0.052	0.738
〃	500	0.053	0.813
H_2O_2	1,000 (0.1%)	0.053	0.813
PO_4^{3-}	100	0.048	0.772
〃	10	0.053	0.815
F^-	100	0.052	0.793
〃	10	0.053	0.807
Ca^{2+}	1,000	0.053	0.818
Al^{3+}	1,000	0.053	0.815
Cu^{2+}	100	0.053	0.813
Ba^{2+}	100	0.053	0.818
Cr^{3+}	100	0.053	0.815
Fe^{3+}	100	0.054	0.821

7) F. Gallais and J. Mounier, *Compt. rend.*, **223**, 722, 790 (1946).

8) S. Utsumi, *J. Chem. Soc. Japan (Pure Chem. Sect.)*, **73**, 889 (1952); ibid., **74**, 32, 301 (1953).

9) S. Utsumi, ibid., **74**, 608 (1953); I. Iwasaki, S. Utsumi and T. Ozawa, This report was presented at a symposium of the Japan Soc. for Anal. Chem. May, 1953.

Substance	Concentration	Absorbance	
None	p. p. m. 0	Blank test 0.053, 0.053	30 p. p. m. Cl^- 0.815, 0.813
Fe^{2+}	100	0.053	0.818
Ni^{2+}	100	0.052	0.813
Co^{2+}	100	0.053	0.815
SO_3^{2-}	100	0.053	0.813
NO_2^-	100	0.053	0.815
ClO_4^-	100	0.053	0.815
ClO_3^-	100	0.052	0.813
BrO_3^-	100	0.777	1.523
〃	10	0.103	0.903
IO_3^-	100	0.053	0.886
〃	10	0.053	0.815
$[Fe(CN)_5]^{4-}$	10	0.255	0.824
〃	1	0.063	0.815
$[Fe(CN)_5]^{3-}$	10	0.130	0.830
〃	1	0.060	0.815

The experimental results are summarized as follows:

(1) Na^+, K^+, Mg^{2+}, Ca^{2+}, Al^{3+}, acetate and silicate (calculated as SiO_2) ions have no effect even when found to be of the magnitude of 1,000 p. p. m.

(2) Cu^{2+}, Sr^{2+}, Ba^{2+}, Zn^{2+}, Cd^{2+}, Pb^{2+}, Ti^{4+}, Ce^{3+}, Th^{4+}, Bi^{3+}, Cr^{3+}, Mn^{2+}, Fe^{3+}, Fe^{2+}, Ni^{2+}, Co^{2+}, SO_3^{2-}, AsO_4^{3-}, BO_2^- and $C_2O_4^{2-}$ ions do not interfere when the concentration is as high as 100 p. p. m. Since a precipitate is formed in the case of barium, it should be centrifuged off in order to remove it. The color of Cu^{2+}, Cr^{3+}, Ni^{2+} and Co^{2+} ions is negligible up to 100 p. p. m. in this method.

(3) Sodium nitrate** does not interfere when present even in the amount of 0.1 M (8,500 p. p. m.); but at a very large concentration higher results are obtained.

(4) 500 p. p. m. of sulfate do not interfere; but 5,000 p. p. m. give lower results probably due to the reaction with ferric ion.

(5) 10 p. p. m. of fluoride and phosphate do not interfere; but 100 p. p. m. give lower results probably owing to the formation of complex ion with ferric ion.

(6) The presence of nitrite at the concentration of 100 p. p. m. does not interfere at 15°C, but at 30°C a slight interference is observed.

(7) Hydrogen peroxide does not interfere at 0.1% (1,000 p. p. m.).

(8) 100 p. p. m. of chlorate and perchlorate, and 10 p. p. m. of iodate do not interfere; but 10 p. p. m. of bromate and 100 p. p. m. of iodate give higher results.

(9) Ferrocyanide and ferricyanide interfere when present in small amounts.

** For the determination of chloride in silicate rocks, large amounts of sodium nitrate are formed[10].

As mentioned above, interfering substances are few. Bromide, iodide, cyanide, thiocyanate, sulfide, thiosulfate, bromate, ferrocyanide and ferricyanide interfere; but they are not usually present in natural waters in such concentrations as would give a serious error. This rapid and accurate spectrophotometric method for the determination of a small amount of chloride can possibly be applied widely to the determination of chloride in rocks[10], natural waters[11] and metals[12].

Summary

A new spectrophotometric method suitable for the determination of a small amount of chloride using iron alum solution in nitric acid solution, and mercuric thiocyanate solution in a mixture of dioxane and alcohol solution has been established.

The calibration curves conform to Beer's law at concentrations up to 50 p. p. m. of chloride. The calibration curves are reproducible within ±1% for the range of 5–80 p. p. m. Cl^- (Procedure A), and within ±0.05 p. p. m. for the range of 0.05–5 p. p. m. Cl^- (Procedure B). As the calibration curves are affected by temperature, it is necessary to measure the absorbance always under the same conditions of temperature in order to achieve good accuracy.

The colored solution is stable. A very small volume of the sample solution such as 5 cc. or 2.5 cc. is good enough for the determination. Interfering substances are few, because this method is carried out in acid medium. Br^-, I^-, CN^-, SCN^-, S^{2-}, $S_2O_3^{2-}$, BrO_3^-, $[Fe(CN)_5]^{4-}$ and $[Fe(CN)_6]^{3-}$ interfere, but usually they are not present in natural waters in concentrations that would give a serious error.

This simple method is suitable for rapid determinations, because it is unnecessary to control pH or filter the precipitate. It is suggested that this method can be widely applied to the determination of chloride in waters, rocks, etc.

Laboratory of Analytical Chemistry and Geochemistry, Tokyo Institute of Technology, Tokyo

10) I. Iwasaki, T. Katsura and N. Sakato, *J. Chem. Soc. Japan (Pure Chem. Sect.)*, **76**, 1116 (1955).
11) I. Iwasaki, T. Nitta and T. Tarutani, ibid., **74**, 1003 (1953).
12) I. Iwasaki, T. Tashiro and T. Ozawa, *Japan Analyst*, 5, 275 (1956).

Molecular Structure Investigations by Electron Diffraction Method. II. The Molecular Structure of Ethylene Chlorohydrin

By Mashio YAMAHA

(Received December 7, 1955)

Introduction

Many physico-chemical investigations such as the dipole moment measurements by C. T. Zahn[1], I. Watanabe[2], the spectroscopic studies by Kohlrauch and Ypsilanti[3], R. M. Badger[4,5], S. Mizushima et al[5,7] have shown that the ethylene chlorohydrin molecule in the gaseous state consists of two rotational isomers. Badger[5] investigated the temperature variation of the infrared and Raman spectra in relation to the intramolecular hydrogen, bonding and established the fact that, in the gaseous state, at room temperature, the molecule consists of a *trans* form and another stable one. Watanabe concluded that the latter stable form of this molecule is one for which the rotational angle φ (see Fig. 1) is $0\sim60°$.

However, the interatomic distances, C–C, C–O, C–Cl, Cl″···O etc., cannot be determined directly by measurement of dipole moments or other spectroscopic methods. Recently, O. Bastiansen[8] determined them directly by means of an electron diffraction method using a rotating sector, as follows: C–C=1.54; C–Cl=1.76; C–O=1.43; and O″···Cl=3.17 Å. Consequently, the *gauche* form of this molecule is characterized by $\varphi=74°$.

In the discussion of the molecular structure of ethyl alcohol by M. Kimura[9], the interatomic distance C–O in this molecule was considered greater than in the case of the normal covalent bond, namely, 1.42 Å. In this report, the author has investigated the molecular parameters of ethylene chlorohydrin, and has also tried to investigate, if possible, the height of the potential barrier of internal rotation, including hydrogen bonding, in this molecule.

Experimental Procedure

(1) *Sample.* — The commercial reagent of ethylene chlorohydrin, colored slightly yellowish, after dehydrated sodium sulphate had been immersed in it for many days, was distilled several times with a flask having a 5–10 cm. long rectifying column. The colorless viscous distillate (b. p. 128°–128.5°C) was obtained for the experiment.

(2) Details of the apparatus and methods of measurement are omitted, because they are the same as in our previous report[10].

Apparatus: Hot cathode, vertical type.
Camera length: 91 to 110 mm.
Wave length: 0.053–0.056 Å

The sample was spurted from the nozzle at room temperature, 25°–35°C.

The diffraction pattern thus obtained is comparatively indistinct and yet eleven diffracted

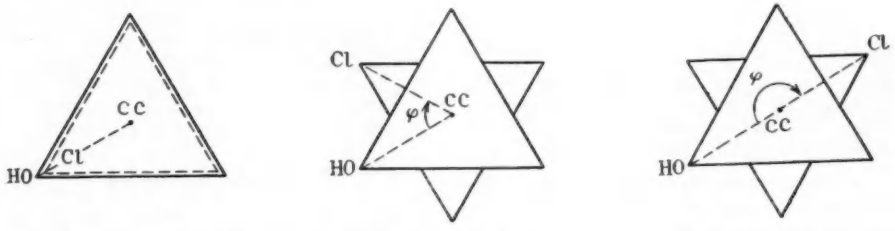

Cis form $\varphi=0°$ *Gauche* form $\varphi=60°$ *Trans* form $\varphi=180°$

Fig. 1. Schematic models showing the rotational angle φ about the C–C bond for ethylene chlorohydrin molecule.

1) C.T. Zahn, *Trans. Acad. Soc.*, **30**, 804 (1934).
2) I. Watanabe, *Riken Iho* (in Japanese), **20**, 838 (1941).
3) K.W. Kohlrauch and G.P. Ypsilanti, *Z. Physik. Chem.*, **B 29**, 274 (1935).
4) R.M. Badger and S.H. Baner, *J. Chem. Phys.*, **4**, 711 (1936).
5) L.R. Zumwalt and R.M. Badger, *J. Chem. Phys.*, **7**, 87 (1939); *J. Am. Chem. Soc.*, **62**, 305 (1940).
6) S. Mizushima, Y. Morino and T. Kubota, This Bulletin, **14**, 15 (1939).
7) S. Mizushima, Y. Morino and S. Nakamura, *Sci. Papers I.P.C.R.*, **37**, 205 (1940).
8) O. Bastiansen, *Acta Chem. Scand.*, **3**, 415 (1949).
9) M. Kimura, *J. Chem. Soc. Japan* (in Japanese), **71**, 18 (1950).
10) T. Yuzawa and M. Yamaha, This Bulletin, **26** (No. 8), 414 (1953).

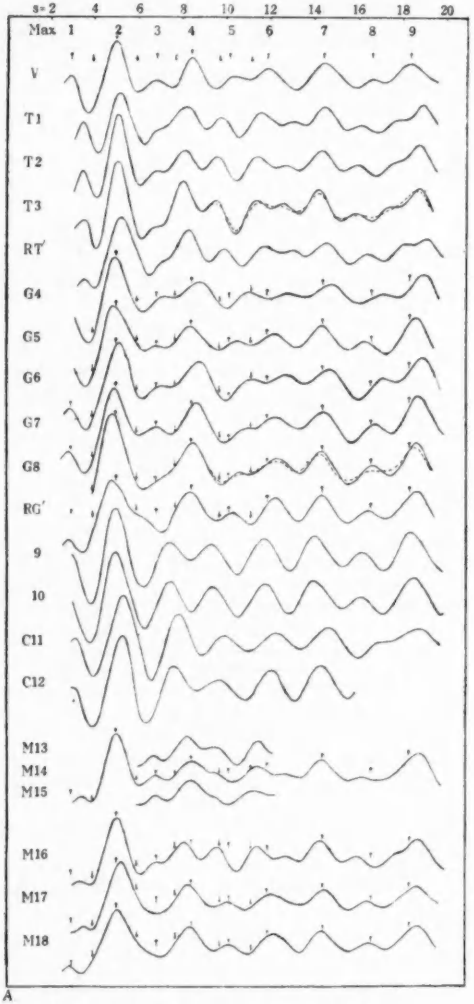

Fig. 2. Visual (V) and theoretical intensity curves for ethylene chlorohydrin molecule. (cf. Table I and II). (The curves are shown in the *s*-scale).

halos have been measured by means of a visual method up to the limit of $q<80$. The measured *s-values* (or *q-values*) of the maxima and minima are shown in Table I, and the visual intensity curves shown at the top of Figs. 2 and 3.

Molecular Models

In constructing the assumed molecular models, the combinations of various molecular parameters have been considered and are given in Table II. First, the models were divided into several groups according to the rotational equilibrium positions about the

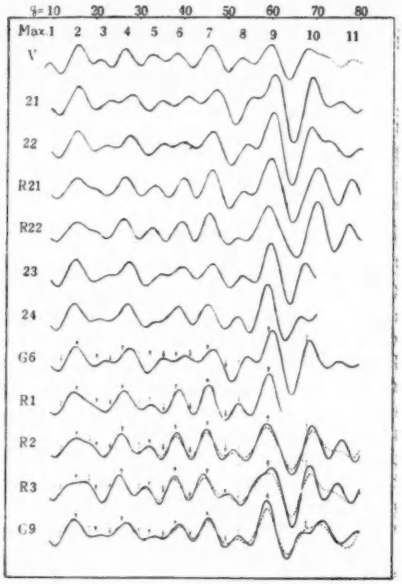

Fig. 3. Visual (V) and theoretical intensity curves for ethylene chlorohydrin molecule. (cf. Table II). (The curves are shown in the *q*-scale).

C-C bond: that is, the groups of *trans, gauche* and *cis* forms including the slight variations of φ close to each form (see Fig. 1). In each groups, the interatomic distance C-O was varied from 1.43 to 1.49 Å, and the valence angles ∠CCCl and ∠CCO were varied within the range 109.5° to 112°, assuming C-H=1.09 and C-C=1.54 Å. Then assuming the other parameters inclusive of the several combinations of bond lengths, bond angles and rotational angle φ to be constant, the mixtures of *trans* and *gauche* forms were considered (see Fig. 2). Subsequently, the bond length C-C was varied from 1.50 to 1.58 Å. Finally, in better models,the rotational angle φ was varied from 60° to 80° (see Fig. 3).

Intensity Curves

The theoretical intensity curves corresponding to the models mentioned above as calculated by the use of the well-known Pauling formula are given in Fig. 2:

$$I(s)=k\sum_i\sum_j Z_iZ_j\cdot\sin(sr_{ij})/sr_{ij},$$

where $s=(4\pi\sin\theta/2)/\lambda$; θ, the scattering angle: λ, the wave length; and r_{ij}, the interatomic distance between atoms i and j, and those as calculated by the use of Pauling-Schomaker formula in Fig. 3:

TABLE I

LIST OF MOLECULAR MODELS AND ASSUMED CORRESPONDING MOLECULAR CONSTANTS (cf. Fig. 2) Other assumed constants: C-C=1.54 Å, C-H=1.10 Å, ∠CCH=109.5°

Groups	Models	(φ°)	∠CCO°	∠CCCl°	C-O (Å)	O''···Cl (Å)
Trans	T1	180	109.5	109.5	1.43	
	T2	〃	112	112	1.43	
	T3	〃	109.5	112	1.49	
	RT′	150	109.5	112	1.46	3.93
Gauche	G4	60	109.5	109.5	1.43	
	G5	〃	112	112	1.43	
	G6	〃	109.5	109.5	1.46	3.03
	G7	〃	109.5	112	1.46	3.09
	G8	〃	109.5	112	1.49	
	RG′	70	109.5	112	1.46	3.15
Forms of $0<\varphi<60°$	9	30	109.5	112	1.43	
	10	15	112	112	1.43	
Cis	C11	0	109.5	109.5	1.43	
	C12	0	112	112	1.43	

TABLE II

LIST OF MOLECULAR MODELS AND ASSUMED CORRESPONDING MOLECULAR CONSTANTS, SHOWING THE PROPORTION OF COEXISTENCE OF TWO DIFFERENT ISOMERS (cf. Fig. 2)

Models	Components of Two Isomer Types		Proportion %	C-O (Å)	∠CCO°	∠CCCl°
M13	*Trans*	and *Gauche*	75:25	1.43	109.5	112
M14	〃	〃	50:50	〃	〃	〃
M15	〃	〃	25:75	〃	〃	〃
M16	〃	〃	50:50	1.43	112	112
M17	*Trans* (RT′)	and *Gauche* (RG′)	20:80	1.46	109.5	112
M18	〃	〃	50:50	〃	〃	〃

TABLE III

LIST OF MOLECULAR MODELS AND ASSUMED CORRESPONDING MOLECULAR CONSTANTS, SHOWING THE VARIATIONS OF OTHER CONSTANTS φ AND C-C AS COMPARED WITH TABLES I AND II

Other assumed constants: C-O=1.46 Å, C-H=1.10 Å, ∠CCH=109.5°

Models	(φ°)	∠CCO°	∠CCCl°	C-C (Å)	O''...Cl (Å)	q/q_{obs}	Mean dev.
21	60	109.5	109.5	1.50	3.01		
22	60	〃	112	〃	3.05		
R21	70	〃	109.5	〃	3.12		
R22	70	〃	112	〃	3.17		
23	60	〃	109.5	1.58	3.07		
24	60	〃	112	〃	3.14		
G6	60	109.5	109.5	1.54	3.03	1.015	0.020
R1	70	〃	112	〃	3.15	1.001	0.023
R2	75	〃	〃	〃	3.22	0.995	0.009
R3	80	〃	〃	〃	3.28	0.988	0.013
G9	60	112	〃	〃	3.13	1.005	0.023

$$I(q)=k\sum_{i}\sum_{j}(Z_iZ_j/r_{ij})\sin(\pi qr_{ij}/10)\cdot\exp(-b_{ij}q^2),$$

where $q=10s/\pi$; and b_{ij}, the temperature factor.

The values of b_{ij}'s are shown in Table V. As regards the factor relating to the interatomic distance O''···Cl_{gauche}, whose contribution to

TABLE IV
OBSERVED s AND q-*values* AND CALCULATED q/q_{obs} VALUES FOR BEST MOLECULAR MODELS

Max.	Min.	s_{obs}	q_{obs}	q/q_{obs} R1	q/q_{obs} R2
1		(2.93)	(9.23)		
	2′	(3.91)	(12.33)		
2		5.00	15.84	0.953	1.007
	3′	(5.92)	(18.84)	—	—
3		6.83	20.44	0.952	—
	4′	7.70	23.63		
4		(8.42)	(26.22)	1.022	0.995
	5′	9.72	30.06	1.021	0.988
5		10.15	32.31	1.018	0.994
	6′	11.17	35.56	1.004	0.984
6		11.90	38.32	1.019	1.007
	7′		41.66	1.020	1.005
7		(14.42)	45.59	1.005	0.995
	8′		49.67	1.001	0.995
8		(16.67)	52.73	0.998	0.979
9		18.39	59.28	1.004	0.995
		Mean average:		1.001_4	0.995_0
		Mean deviation:		0.023	0.009

the intensity relations is large, the calculation was made according to the method of J. Karle[11] in consideration of the effect of the hindered rotation about the C C bond. The details are dealt with in a later section.

To the curves T3, G8, R2, R3 and G9, the dotted curves, in which temperature factors were taken into account, are added in Figs. 2 and 3 (see later).

Selection of the Best Model

The theoretical intensity curves of different groups which correspond to the structure of *trans*, *gauche* and *cis* forms are compared with the visual intensity curve V.

(1) In the case of *cis* form, the maximum which corresponds to the minor max. 3 of curve V does not appear and the intensity curve becomes almost sinusoidal up to $s \approx 14$.

In successive variations of the rotational angle φ up to $\varphi = 30°$ from this *cis* position, the *s-value* of each maximum or minimum varies slightly, and the intensity curves still show simple sinusoidal features. This intensity relation is different from the actual measurement (curve V), so that the *cis* group, including the model with $\varphi = 0°$–$30°$, must be rejected.

(2) In comparing cases of the *trans* and *gauche* forms, three maxima appear between max. 4 and max. 7 in the case of the *trans* form, but two maxima appear in the case of the *gauche* form. In the casc of the *trans* form, max. 3 accompanies max. 4, but in the visual curve, max. 3 seems to accompany max. 2. In this respect, the intensity relations of the visual curve are similar to those of the *gauche* form.

(3) Special attention was paid to the curves in the *gauche* group, which seem preferable for the present. The *s-values* vary slightly when the valence angle ∠CCCl is changed from tetrahedral to 112°. The *s-values* of max. 4 and max. 7 agree most closely with those of the visual curve when this angle is taken to be 112°.

Further, even when the valence angle ∠CCO is varied from tetrahedral to 112°, the variation of *s-values* is not distinct, because it seems to be obscured by the resultant intensity relation due to the variation of the O″···Cl distance and other distances.

(4) As the C–O distance is extended from 1.43 to 1.49 Å, max. 3 acquires a shelf-like feature, approaches max. 4, and almost disappears as shown in curve G8. Furthermore, the *s-value* for each maximum does not coincide with the actual measurement.

The above-mentioned discussion cannot be made independently in regard to the variations of each parameter. Since no satisfactory result has been obtained thus far as shown in Fig. 2, cases wherein the *trans* and *gauche* forms coexist and cases wherein C–C=1.50 and C−C=1.58 Å have been examined (see Figs. 2 and 3).

(5) The curves in which the *trans* and *gauche* forms are mixed are M13∼M18 of Fig. 2 (see Table II).

The result does not necessarily coincide with the actual measurement, but it shows better agreement. Recently S. Mizushima and collaborators confirmed the co-existence of rotational isomers through the analyses of Raman- and infrared spectra, and our result coincides with theirs in general. The visual intensity curve is close to that of the *gauche* form; so that, in view of the ratio of mixing at room temperature, the *gauche* form may be considered predominant.

(6) Good results have been obtained by taking the co-existence of the *trans* and *gauche* forms into consideration, but, on account of the intensity relation of max. 5 and max. 6 in the actual measurement, the models were not sufficient. Therefore, assuming tentatively that the *trans* and *gauche* forms do not co-exist, that is, that the molecule exists in only one form, further investigations have been made in cases of $\varphi = 70°$, 75°, 80°, and 150° (Fig. 3—the curves G6, R1, R2, R3, G9).

11) J. Karle, *J. Chem. Phys.* **15**, 202 (1947).

Upon varying φ from 70° to 80°, the shelf-like feature appears in max. 2 and 3, but this intensity relation is not apparent in the actual measurement. Max. 5 shifts towards a smaller *s-value* than in the case of the *gauche* form, so as to coincide with the visual curve. This tendency is similar to cases of C–C=1.50 Å, φ=70° (see curves R21 and R22).

O. Bastiansen reported that the rotational angle φ of the *gauche* form has been determined to be 74°. In our investigation, the curve φ=75° seems to show very excellent agreement with the actual measurement (see curve R2 in Fig. 3).

(7) In the cases of C–C=1.50 and 1.58 Å, the curves 21 to 24 of the *gauche* form are shown in Fig. 3. Their intensity relations are mostly not different from those of the *gauche* form in Fig. 2, but the *q-value* of each maximum or minimum changes appreciably. By assuming φ=70°, the *s-values* (*q-values*) of max. 3 and max. 5 and their intensity relations are in better agreement than by assuming the *gauche* form (φ=60°).

Radial Distribution Curve

The radial distribution curve has been calculated by using the following formula:

$$rD(r)=\sum_{q=1}^{q=\max} I(q)\cdot\sin(\pi qr/10)\cdot\exp(-aq^2),$$

where the a is determined to be $\exp(-aq_{\max}^2)=0.1$, $q_{\max}$ being the largest *q-value* observed (about $q_{\max}=80$) in the actual measurement. For the numerical function $I(q)$, the visual intensity curve has been used.

Each maximum (peak) of radial distribution curve (Fig. 4) is interpreted as follows:

1.46 Å=C–O, 1.76 Å=C–Cl,
2.75 Å=C′···Cl, 3.10 Å=O″···Cl_{gauche}.

Maxima other than the above-mentioned are considered to be the superpositions of maxima of corresponding interatomic distances, and they are difficult to separate individually. Further, a maximum, though not sufficiently distinct, appears close to r=3.90 Å, which is supposed to be due to the co-existence of a *trans* form.

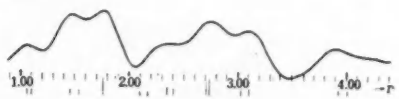

Fig. 4. Radial distribution curve for ethylene chlorohydrin molecule.
The interatomic distance corresponding to each peak is shown under the curve.

The distance which corresponds to the O″···Cl in this *trans*-form seems slightly shorter than the calculated O″···Cl_{trans} (about 4.13 Å). If this distance is considered for the moment to be correct, the following three conditions can be given;

(1) Angle $\varphi<180°$,
(2) Valence angles ∠CCO, and ∠CCCl may be smaller than 112°,
(3) Bond length C–C<1.54 Å.

Calculation of Temperature Dependence Affecting the Intensity Curves

According to the report by J. Karle, in the case of the XY_2C–CY_2X type molecule, the contribution of each atom pair X″···X to the intensity curve is represented by the following formula, in which the variation of the following intensity relation caused by the restricted rotation about the C–C single bond in the vicinity of the "*gauche*" form is taken into consideration:

$$(\cos\Theta)^{1/2}\sin[\tau_1-(\gamma^2\tau_1\cdot\sin^2\Theta/4\beta)+\Theta/2]\times\exp[-\gamma^2\tau_1\cos^2\Theta/4b^2]/\tau_1, \quad (1)$$

where: than $\Theta=\beta\tau_1/b^2$,

$\beta=C_2/[8(C_1-C_2/2)]-3[C_2/(C_1-C_2/2)]^2/32$,
$b^2=\alpha\tanh(h\nu/2kT)$, $\nu=\sigma(V_0/2I)^{1/2}/2\pi$,
$\tau_1=s(C_1-C_2/2)^{1/2}$, $\alpha^2=2\sigma^2\pi^2IV_0/h^2$,
$\sigma=3$,
$I=\sum' mr^2=I_1I_2/(I_1+I_2)$,
$\gamma=\sqrt{3}C_2/[4(C_1-C_2/2)]$,
$C_1=(l_1^2+l_2^2)/2$,
$C_2=(l_1^2-l_2^2)/2$, $s=(4\pi\sin\theta/2)/\lambda^*$,

and where V_0 is the assumed potential barrier of the hindered rotation about C–C bond. In the case of the ethylene chlorohydrin molecule, V_0 includes the potential

TABLE V
APPROXIMATE TEMPERATURE FACTORS USED FOR EACH ATOM PAIR EXCEPT THAT OF O′···Cl (For the factor $\exp(-b_{ij}q^2)$ in pauling-schomaker formula

Atom Pairs	r_{ij}(Å)	$(\pi^2/200)<l_{ij}^2>_{av.}$	b_{ij} (used)
C–H	1.10	0.00030	0.00015
C–O	1.43–1.49	0.000145	0
C–C	1.50–1.58	0.000148	0
C–Cl	1.74–1.80	0.000139	0
O′···H	(2.10)	0.00041	0.00026
C′···H	(2.17)	0.00037	0.00022
Cl′···H	(2.35)	0.00053	0.00037
C′···O	(2.44)	0.00022	0.00007
C′···Cl	2.67–2.78	0.00022	0.00007
O″···Hg			0.0008**
O″···Ht			0.0006**
Cl″···Hg			0.0006**
Cl″···Ht			0.0004**

** Roughly assumed values.

TABLE VI

NUMERCIAL VALUES IN FORMULA (1) RELATING TO THE ESTIMATED HINDERED-ROTATIONAL POTENTIAL BARRIER V_0 CORRESPONDING TO THE ATOM PAIR O''···Cl_{gauche} FOR ETHYLENE CHLOROHYDRIN (C–Cl=1.77 Å assumed)

V_0 kcal./mol.	τ_1	γ^2	$\gamma^2/4b^2$	C–O (Å)	∠CCO°	∠CCCl°
3	3.0943 s	0.0439$_7$	0.00098$_7$	1.48	109.5	112
5	〃	〃	0.00059$_4$	〃	〃	〃
10	〃	〃	0.00030$_3$	〃	〃	〃
20	〃	〃	0.00014$_3$	〃	〃	〃
3	3.0789 s	0.0408$_4$	0.00091$_8$	1.43	〃	〃
10	〃	〃	0.00028$_2$	〃	〃	〃

energy of hydrogen bonding. (In other words, it includes, in the *gauche* form, the portion of the potential energy caused by the hydrogen bond O–H···Cl.) l_1 is the largest interatomic distance of X''···X (i.e. at the *trans* position) and l_2 the smallest (i.e. at the *cis* position). I_1 and I_2 are the moments of inertia of the atoms X's (that is, atoms O and Cl in our case respectively) around the axis C–C, h is Planck's constant and k is Boltzmann's constant. The computed values τ_1, γ^2 and $\gamma^2/4b^2$ in the case of the ethylene chlorohydrin molecule are shown in Table VI with the assumed values V_0, C–O (Å), ∠CCO° and ∠CCCl°.

Strictly speaking, however, this formula is originally to be applied to the case in which two X-atoms are the same, for instance, the case of 1,2-dichloroethane molecule, which has a threefold symmetry axis, namely $\sigma=3$. When the restricted rotation of this molecular type becomes infinitesimal, that is, the molecule is assumed to be rigid, the formula (1) approaches the form:

$$(\sin sl_{ij})/sl_{ij}. \qquad (2)^*$$

In the strict calculation of the contribution of intensity variations made by the restricted rotation, all atomic distances whose variations contribute to the intensity variations should be taken into account (that is, the distances assigned to the form Y''···Y, Y''···X). Because the two X atoms are O and Cl in our case, that is, not identical, and also because similar calculation regarding the other interatomic distances Cl''···H, O''···H, and H''···H etc., whose contributions may be appreciable but have actually been neglected, the approximation resulting from the application of this principle proposed by J. Karle may be considered comparatively rough for our case of the ethylene chlorohydrin molecule.

* Since the τ_1 in the formula (1) corresponds to sl_{ij} of the formula (2), the part of $(\cos\theta^{l/2}\cdot\sin(\cdots\cdots)$ in the former approaches $(\sin sl_{ij})/sl_{ij}$ and the part of the exponential approaches 1 in the latter.

Assuming the approximations in our case to be admissible, the contributions have been calculated for the cases in which V_0 is chosen as 3, 5, 10 and 20 kcal./mol. It has been found that V_0 is about 10 kcal./mol. or more as a result of the comparisons of the observed intensity relations. The dotted lines on the curves T3, G8, G9, R2 have been calculated for the presumed V_0 value. If the value V_0 is assumed to be $V_0<10$ kcal./mol., the curves become of a very much more damped form in the range $q>50$, and it would become impossible to observe clearly the maxima which can actually be detected in this range of our experiment.

Discussion and Summary of Results

From the above considerations, the intensity curves RG', R1, R2, R21, R22, M17 and M18 seem to be nearly satisfactory, and thus the final results of the molecular structure of ethylene chlorohydrin have been obtained as follows:

C–O=1.46 Å±0.02 Å, O''···Cl=3.20 Å±0.06 Å,
∠CCCl=111°±2°, ∠CCO=110°±2°.

The stable form of the internal rotation about the C–C bond seems to be nearly a *gauche* form, that is, the exact position $\varphi=75°$ is regarded as the most reasonable one from the overall intensity relation of diffracted pattern.

These results are considered to agree with those from the electron diffraction method using a rotating sector by O. Bastiansen[8] and also with those from the dipole moment measurement[2].

From the analysis of the radial distribution curve and of the intensity curves, the *gauche* ($\varphi=75°$) and *trans* forms might be supposed to co-exist, and this has been confirmed from the spectroscopic results, but the proportion of these co-existing forms has not been determined from our study.

The fact that the *gauche* form is predominant at room temperature is thought to be caused by the formation of the intramolecular

hydrogen bond[12]. The potential V_0 of the internal hindered rotation including the contribution of the hydrogen bond is presumed to be approximately from 7 to 10 kcal./mol. or more, as judged from the examination of the approximate calculation and of the degree of damping of the experimental intensity curve.

It would be very interesting, but hardly possible, to determine V_0 precisely by an experimental method other than the electron diffraction. Even by the electron diffraction method (using the visual method), it is very difficult to confirm precisely the height of the potential barrier of internal hindered rotation to which the intramolecular hydrogen bond contributes, because the variation of the intensity relation is not so obvious as to allow conclusions in the order of several kcal. per mol.

The author would like to express his gratitude to Professor Y. Morino of the Faculty of Science, Tokyo University, Professor A. Kotera of this University and Assistant Professor M. Kimura of Nagoya University for their very kind guidance, advice and discussions throughout this work.

12) S. Mizushima, T. Shimanouchi, T. Miyazawa, K. Abe and M. Yasumi, *J. Chem. Phys.*, **19**, 1477 (1951), *J. Am. Chem. Soc.* **74**, 1378 (1952). L.P. Kuhn, "The Hydrogen Bond. I. Intra- and Intermolecular Hydrogen Bonds in Alcohols", *J. Am. Chem. Soc.*, **74**, 2492 (1952).

Chemical Institute, Faculty of Science
Tokyo University of Education
Ootsuka, Tokyo

Molecular Structure Investigations by Electron Diffraction Method. III. The Molecular Structure of Ethylene Fluorohydrin

By Masato IGARASHI and Mashio YAMAHA

(Received December 7, 1955)

Introduction

In regard to the molecular structure of ethylene chlorohydrin, many investigations were made as mentioned in the previous report[1]. From electron diffraction studies of this molecule, it was concluded that the structure having the rotational angle $\varphi=75°$ about the C–C bond is predominant at room temperature.

A few structural investigations of ethylene fluorohydrin molecule have been made[2]. In this report the structure has been investigated in relation to the rotationally stable form of this molecule including the problem of intramolecular hydrogen bonding. Moreover, the problem of the bond length C–F of fluorine-substituted compounds is very interesting, and this problem has also been taken into consideration.

Experimental Procedures

(1) Sample.—The ethylene fluorohydrin has been synthesized according to F. W. Hoffmann's method[3].

122.5 g. potassium fluoride (previously dried by heating and powdered) is mixed with 112 g. dried ethylene glycol and 45.5 g. diethylene glycol in a flask, and then heated with continuous stirring at a temperature about 175°–185°C, while 114.5 g. ethylene chlorohydrin is being gradually dropped into the flask. The addition of the chlorohydrin takes about 2.5 hours. Gaseous evaporate is distilled out through a rectifying column filled with small glass balls, the temperature at the top of the column being held constant at 100°C.

Finally, air is blown into the reaction product in the flask, and the distillate is completely distilled. Sodium fluoride is added to the distillate, and the ethylene fluorohydrin thus produced is collected by distillation at a temperature between 95°–105°C (boiling point). As traces of water mixed in the fluorohydrin cannot be removed by distillation, the product is left with dehydrated Glauber's salt (sodium sulfate anhydride) for many days for dehydration before final distillation.

(2) Photograph of Diffracted Pattern.—The apparatus of electron diffraction is the same as that described in the previous report[5], and a horizontal type camera having a camera length of 130 mm. was also used.

Generally the halos of this pattern are lacking in sharpness and are comparatively diffused. Eight diffracted halos have been measured

1) M. Yamaha, This Bulletin publised **29**, 865 (1956).
2) For Example, H.D. Cowan, M. Herman, et al., "Raman spectra of single fluorine compounds", *Ind. chim. belge.*, **16**, 86 (1951).
3) F. W. Hoffmann, *J. Am. Chem. Soc.*, **70**, 2596 (1948).
4) M. Kimura, *J. Chem. Soc. Japan* (in Japanese), **71**, 18 (1950).
5) T. Yuzawa and M. Yamaha, This Bulletin, **26**, 414 (1953).

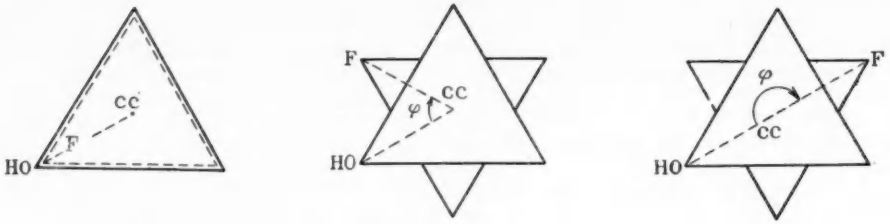

Cis Form $\varphi=0°$ | *Gauche* Form $\varphi=60°$ | *Trans* Form $\varphi=180°$

Fig. 1. Schematic models showing the rotational angle φ about the C-C bond for ethylene fluorohydrin molecule.

TABLE I

THE MOLECULAR MODELS AND CORRESPONDING ASSUMED MOLECULAR CONSTANTS

(cf. Fig. 2)

Groups	Models	C-O (Å)	C-F (Å)	∠CCO°	∠CCF°	O$^{\gamma}$···F (Å)
Trans	T1	1.43	1.36	109.5	107	3.58
	T2	1.48	1.40	109.5	112	3.71
Gauche	G3	1.43	1.36	109.5	107	2.75
	G4	1.45	1.36	108	109.5	2.75 (C-C=1.50
	G5	1.45	1.36	109.5	109.5	2.77 (C-C=1.50
	G6	1.45	1.33	109.5	109.5	2.80
	G7	1.48	1.40	109.5	107	2.80
Form of $\varphi=30°$	8	1.43	1.36	109.5	107	
Cis	C9	1.43	1.36	109.5	107	2.42
	C10	1.48	1.40	109.5	112	2.56

visually, up to the limit of the range $q<75$ from about 20 photographed plates.

The measured *q-values* of the maxima and minima are shown in Table III, and the visual intensity curve is shown at the top of Fig. 2.

Molecular Models and Theoretical Curves

(1) The theoretical intensity curves for the assumed molecular models have been calculated by the use of the well-known Pauling-Schomaker formula:

$$I(q)=k\sum_i\sum_j(Z_iZ_j/r_{ij})\cdot\sin(\pi qr_{ij}/10)\cdot\exp(-b'_{ij}q^2),$$

where Z_i is the atomic number of the atom i. Z_H is assumed to 1.25.

$q=10s/\pi$, $s=(4\pi\sin\theta/2)/\lambda$, θ: the scattering angle,

r_{ij}: the distance between the ith and jth atoms,

λ: the wave length of the electron beam used,

b'_{ij}: the temperature factor for the atom pair i-j.

(2) The assumed molecular models corresponding to the theoretical intensity curves in Figs. 2 and 3 are tabulated in Tables I and II. In constructing the models, the bond distance C-H=1.09 Å and the angle ∠CCH=109.5° are assumed.

The models are divided into several groups according to the rotational equilibrium positions about the C-C bond, that is, the *trans*, *gauche*, the form of $\varphi=30°$ and *cis* groups (see Fig. 1). Secondly, in each group, the bond length C-O varies from 1.43 to 1.48 Å, C-F from 1.33 to 1.40 Å, and ∠CCF from 107° to 112°. Thirdly, in the case of the *gauche* group, the angle φ varies from 30° to 75°. In this case, the other parameters are assumed to be C-C=1.54, C-O=1.43, C-F=1.36 Å and ∠CCF=∠CCO=109.5°.

The value b_{ij}'s used for each atom-pair are shown in Table VI.

TABLE II

THE MOLECULAR MODELS AND CORRESPONDING ASSUMED MOLECULAR CONSTANTS IN REGARD TO THE VARIATION OF ANGLE φ

C-C=1.54 Å, C-O=1.43 Å, C-F=1.36 Å and ∠CCF=∠CCO=109.5 are assumed constantly

Models	φ°	O$^{\gamma}$...F(Å)
A	75	2.94
B	68	2.88
C	60	2.80
D	45	2.67
E	38	2.62
F	30	2.56

TABLE III

OBSERVED q-VALUES AND CALCULATED q/q_{obs}. VALUES FOR THE BETTER MOLECULAR MODELS

Max.	Min.	q_{obs}	q/q_{obs} G4	G5	B	C
1		(10.87)	(0.892)	—	—	—
	2′	(14.37)	(0.905)	—	(0.891)	(0.898)
2		18.99	0.995	1.006	0.995	0.979
	3′	24.80	1.008	0.980	0.996	1.008
3		29.39	1.034	1.028	1.014	1.044
	4′	33.39	(1.045)	—	0.994	—
4		36.09	1.006	—	0.975	—
	5′	39.56	1.001	0.996	0.998	1.001
5		44.17	0.998	0.994	0.988	1.003
	6′	49.82	0.974	0.965	0.959	0.976
6		52.88	0.970	0.953	0.957	0.978
	7′	56.18	0.970	0.961	0.968	0.981
7		60.19	0.990	0.985	0.995	0.995
	8′	65.58	1.016	1.016	1.019	0.988
8		70.20	1.019	1.010	1.004	0.957
Mean Average:			0.998_4	0.990_4	0.989_4	0.991_8
Mean sq. deviation:			0.019	0.023	0.019	0.022

(3) The radial distribution curve

$$rD(r)=\sum_{q=1}^{q=\max} I(q)\cdot\sin(\pi qr/10)\cdot\exp(-aq^2)$$

is calculated by using the best visual intensity curve V for the function $I(q)$, where the value a is determined to be $\exp(-aq^2_{max})=0.1$, q_{max} being about 75.

Comparisons of the Intensity Curves and the Selection of the Best Model

From the comparison of the visual and theoretical intensity curves as shown in Fig. 2 and from the analysis of the radical distribution curve as shown in Fig. 4, the characteristic features for the selection of the best model are specified as follows:

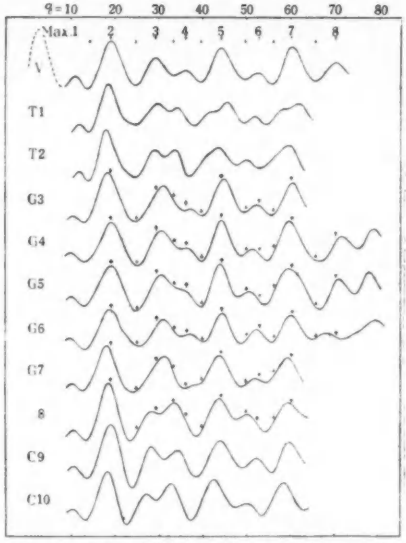

Fig. 2. Visual (V) and theoretical intensity curves for ethylene fluorohydrin molecule. (cf. Table I).

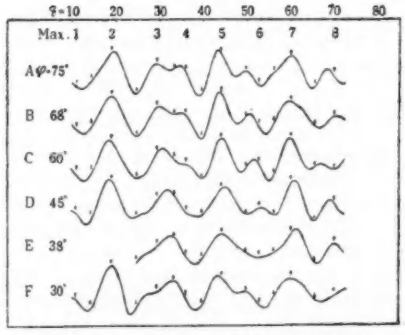

Fig. 3. Theoretical intensity curves showing the variations of models according to the changes of angle φ. (cf. Table II).

TABLE IV

THE DISTANCE O$^{\gamma}$···F *gauche* IN RELATION TO OTHER MOLECULAR CONSTANTS

C-C (Å)	C-O (Å)	C-F (Å)	∠CCO°	∠CCF°	O$^{\gamma}$···F (Å)	Models
1.54	1.43	1.36	109.5	109.5	2.75	G3
1.50	1.45	1.36	108	109.5	2.75	G4
1.54	1.43	1.40	109.5	107	2.77	
1.50	1.45	1.36	109.5	109.5	2.77	G5
1.54	1.48	1.36	109.5	107	2.78	
1.54	1.43	1.36	109.5	109.5	2.80	C
1.54	1.45	1.33	109.5	109.5	2.80	G6
1.54	1.48	1.40	109.5	107	2.80	G7
1.54	1.43	1.36	109.5	112	2.84	
1.54	1.43	1.40	109.5	112	2.87	
1.54	1.48	1.36	109.5	112	2.87	
1.54	1.48	1.40	109.5	112	2.89	

TABLE V

THE LIST OF MOLECULAR CONSTANTS OF FLUORINE-SUBSTITUTED COMPOUNDS

Molecules	C-C (Å)	C-F (Å)	C-Cl (Å)	Other Parameters	References
CCl_3F		1.40			6), 7)
$CHCl_2F$		1.40	1.76		6)
CCl_2F_2		1.35	1.74	$\angle FCF = 108°48'$	6), 7)
CH_3F		1.332			8)
CHF_2		1.39 (1.384)			9)
$CClF_3$		1.328	1.740	$\angle FCF = 108°$, $\angle FCF = 110°$	10)
CF_3-COOH		1.36			11)
CH_3-CCl_2F		1.40	1.78	$\angle CCF = 109.5°$, $\angle CCCl = 111°$	12)
CH_3-$CClF_2$		1.37	1.77	$\angle CCF = \angle CCCl = 111°$, $\angle FCF = \angle FCCl = 108°$	12)
CH_3-COF		1.41			13)
CH_3-CF_3	1.45	1.33		$\angle FCF = 108.5°$	14)
	1.53	1.36		$\angle CCF = 112°$, $\angle FCF = 107°$	12)
	1.54	1.33			15)
CF_3-CF_3	1.45 (±0.06)				16)
($CClF_2$-$CClF_2$)	1.45 (ass.)	1.33	1.74		17)

(1) Comparison of each group corresponding to the *trans*, *gauche* and *cis* forms of molecular models.

a) The curves corresponding to the *trans* and *cis* groups are comparatively similar in shape, but the *q-values* of each maximum or minimum are different from one another. Further, the intensity relations of max. 3 and max. 4 differ slightly from one another, and also the shapes of max. 5 and max. 7 are broad with the shelf-like feature in the *trans* form.

b) Max. 3 and the accompanying shelf-like max. 4 are characteristic of the *gauche* group. These features are slightly different from those of the other groups.

So far as the considerations of these features, as compared with those of the visual curve, are concerned, the curves of the *gauche* group appear to be in best agreement (see Fig. 2, curves G4 and G5, and section (4)).

(2) In the *gauche* form, the variation of the O″···F distance, depending upon the variations of the parameters C-O, C-F and ∠CCF, is listed in Table IV, (not all of the corresponding curves are shown in Figs. 2 and 3).

The variation of the intensity relation of each curve is not so clear as to determine each allowable range of the respective parameters C-O, C-F and ∠CCF independently. However, from the analysis of the radial distribution curve, the distance O″···F seems to be in the vicinity of the value $r = 2.81$ Å (see (4)). The intensity curves for which O″···F is about 2.81 Å are generally satisfactory.

The curve G6, having a smaller distance C-F = 1.33 Å, is hardly satisfactory, because the *q-values* of max. 3, max. 4 and max. 8 clearly show disagreement with those of the visual curve.

(3) When the rotational angle φ is varied from 30° to 75°, the smaller the angle φ becomes, the more max. 3 shifts toward larger *q-values*, accompanied by the disappearance of the shelf-like max. 4 and the later appearance of a small shelf-like maximum at about the position of max. 3 in the visual curve.

Up to a point, the larger the angle φ becomes, the more the intensity relations of all the maxima and minima agree with that of the measured visual curve; but when $\varphi = 75°$, the features of max. 3, max. 4 and max. 7 become similar to those of the *trans* form, that is, max. 4 approaches max. 3, max. 7 becomes broader with a small shelf, and the *q-values* of each maximum shift slightly from those of the visual curve.

6) L. O. Brockway, *J. Phys. Chem.*, **41**, 185, 747 (1937).
7) J. Wouters and M. de Hemptinne, *Nature* (London), **141**, 412 (1938).
8) V. Schomaker and D.P. Stevenson, *J. Am. Chem. Soc.*, **63**, 37 (1941), W. Gordy, J.W. Simmons and A.G. Smith, *Phys. Rev.*, **74**, 243 (1948) (Microwave Spectra).
9) S.N. Chosh, R. Trambarulo and W. Gordy, *J. Chem. Phys.*, **20**, 605 (1952) (Microwave Spectra).
10) D.K. Coles and R.H. Hughes, *Phys. Rev.*, **76**, 858 (1949). (Microwave Spectra).
11) J. Karle and L.O. Brockway, *J. Am. Chem. Soc.*, **66**, 574 (1944).
12) R.A. Spurr and W. Shand (private communication to L. Pauling and V. Schomaker).
13) H.A. Skinner, Thesis (Oxford).
14) L.O. Brockway, J.H. Secrist and F. Lucht, Am. Chem. Soc. Meeting, Buffalo, N. Y.
15) W.F. Edgell, *J. Chem. Phys.*, **16**, 1002 (1948) (Microwave Spectra).
16) See, J.R. Nielsen and C.M. Richards, *J. Chem. Phys.*, **16**, 67 (1948).
17) M. Iwasaki, S. Nagase and R. Kojima, *J. Chem. Phys.*, **22**, 959 (1954) (Letter).

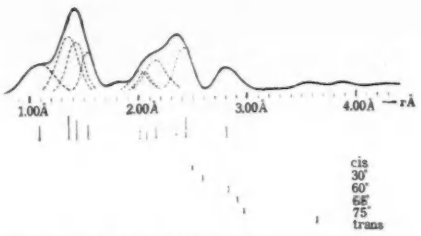

Fig. 4. Radial distribution curve for ethylene fluorohydrin molecule.
Under the curve, the interatomic distance corresponding to each peak is shown by the short line.
O″···F distance which corresponds to the variation of rotational angle φ from 0° (*cis*) to 180° (*trans*) is also shown in due order under the corresponding position of the curve. (cf. Tables I and II).

The model which has the rotational angle about $\varphi=60°$–$70°$ (see Fig. 3, B and C) seems to be the best.

(4) When attention is paid to the radial distribution curve (Fig. 4), two broad peaks appear in the range of $r<2.6$ Å, each of the peaks being the superposition of several interatomic distances: that is, one corresponds to the peaks of the distances C–F, C–O and C–C, and the other to those of F′···H, O′···H and C′...O, etc. However, all the broad peaks cannot be analyzed accurately as peaks of respective component distances.

For the present purpose, particular peaks corresponding to the assumed interatomic distances (for example, C–H, C–F, C–O, C–C, F′···H, O′···H, C′···O, etc.) are indicated by dotted lines on the distribution curve (Fig. 4).

It is expected that the comparatively large peak corresponding to the distance C′···O which is related to the angle ∠CCO and the length C–C appears at the point about $r=$ 2.4 Å. On the distribution curve, there seems to be a corresponding peak at the point $r=$ 2.38 Å. The distance 2.38 Å seems to be slightly smaller than 2.44 Å, the normal distance of C′···O.

The shortening of this distance can be interpreted in two ways: the angle ∠CCO may be slightly smaller than 109.5° (nearly 108°), or the distance C–C may be about 1.50 Å*, in both cases the distance C–O being assumed to be 1.45 Å.

The intensity curves G4 and G5 correspond to the models which have the distance C–C= 1.50 Å. G4, having ∠CCO=108°, and G5, having ∠CCO=109.5°, coincide better with the visual curve than the others in the *gauche* group.

(5) On the radial distribution curve, the peak corresponding to the distance O″···F appears distinctly at about $r=2.81$ Å, and this distance agrees rather well with the O″···F distance of the *gauche* form.

In the cases of C–C=1.50 Å mentioned above (G4, G5), the O″···F distance seems to be slightly smaller than the value 2.81 Å. As a result, the cases of $\varphi>60°$, that is, those which allow slightly longer O″···F, are considered. Upon comparing the curves of the group of the *gauche* form with B and C, the curves B and C are seen to coincide fairly well with the visual one with respect to the intensity relations and *q-values*.

(6) No peak corresponding to the *trans* distance of O″···F appears in the presumable r range in the radial distribution curve, and therefore the *trans* and *gauche* isomers of this molecule hardly seem to co-exist.

(7) In the curves A to F in Fig. 3, the effects of temperature factors are taken into account (as tabulated in Table VI). However, since the characteristic features of these curves appear to change very little, these factors are not considered in further details.

Discussion and Summary of Results

From the preceding considerations, the intensity curves G4, G5, B and C seem to be regarded as satisfactory, and the final results of the molecular structure of ethylene fluorohydrin have been obtained as follows:

C–O=1.45 Å±0.02 Å O″···F=2.82 Å±0.03 Å,
C–C=1.50 Å~1.55 Å ∠CCF=109°±2°,
C–F=1.35 Å~1.40 Å ∠CCO=109.5°±2°.

Through many other investigations, that is, the results of ethylene chlorohydrin[1], ethyl alcohol[4], and isopropyl alcohol[5], the same conclusion has been reached as regards the bond distance C–O=1.45 Å.

According to many structural investigations of fluorine-substituted compounds, the slightly shorter distances C–C<1.54 Å and C–F= 1.36 Å~1.40 Å seem to be satisfactory (see Table V).

TABLE VI
APPROXIMATE TEMPERATURE FACTORS b'_{ij} USED IN CALCULATIONS

$b'_{ij}=0$	for C–C,
$b'_{ij}=-0.00016$	for C–O, C–F, C′···O, C′···F and C″···F,
$b'_{ij}=-0.00030$	for C′···H, O′···H, F′···H, O″···H and F″···H.

* In the investigations flourine-substituted compounds, it has often been observed tha. the distance c-c is slightly smaller than the normal covalent distance 1.54Å (see Table V).

In regard to paraffines in which two or more hydrogen atoms have been substituted by fluorine atoms, a smaller value of distance C–F>1.35 Å has often been found, but the distance C–F<1.35 Å seems adequate in the case of this molecule.

In the case of ethylene chlorohydrin, it was concluded that the *gauche* and the *trans* forms co-exist, but a similar conclusion can not be reached in the present compound. From the analysis of the radial distribution curve, it is concluded that there is almost certainly one form of this molecule at room temperature. That is, the ethylene fluorohydrin molecule is of the *gauche* form (φ= 60°–70°), and is considered to form the intramolecular hydrogen bond. This is a reasonable interpretation by virtue of the fact that hydrogen bonding of the type O–H···F seems to be stronger than that of the type O–H···Cl[18]: even in the case of ethylene chlorohydrin, the *gauche* from seems to be predominant at room temperature.

The author wishes to express his deep gratitude to the late Professor H. Oosaka of this University and to Professor Y. Morino of Tokyo University, for their kind advice throughout this work.

Chemical Institute, Faculty of Science
Tokyo University of Education
Otsuka, Tokyo

18) L. Pauling, "The Nature of the Chemical Bond", p. 284; "Hydrogen Bond", Cornell Univ. Press (1940).

Molecular Structure Investigations by Electron Diffraction Method. IV. The Molecular Structures of α, γ-Dichlorohydrin and Ethylene Cyanohydrin

By Mashio YAMAHA

(Received December 7, 1955)

Introduction

The molecular structure of ethylene chlorohydrin has been surveyed by S. Mizushima[1–4] by means of infra-red and Raman spectra studies in regard to the problems of energy and entropy differences between the two intramolecular rotational isomers, i.e., the *trans* and the *gauche* forms of this molecule.

According to the surveys by O. Bastiansen[5] and by the author[6] using an electron diffraction method, a considerable fraction of the molecules in the gaseous state exist in the *gauche* form, in which the intramolecular hydrogen bond is formed between the O and Cl atoms. Previously, Zumwalt and Badger[7], by using infra-red spectroscopic data, established the fact that each of the ethylene chloro-, bromo- and iodo-hydrin, and α,γ-dichlorohydrin molecules, all of which have –O–H radicals, forms an intramolecular hydrogen bond between the oxygen and halogen atoms. Since the publication of the previous report[8], surveys have been continued on the molecular structures of α,γ-dichlorohydrin (1, 3-dichloropropanol (2)) and ethylene cyanohydrin (Hydracrylonitrile) by using the visual electron diffraction method. As to the structure of ethylene cyanohydrin, the molecule does not seem to form the intramolecular hydrogen bond, and the question, in what stable position the molecule exists in a gaseous state, has been examined.

Experimental Procedure

1) Apparatus. — The electron diffraction apparatus of the vertical, hot cathode type was described in the previous publication[8] (camera length: 91 mm. and 101 mm.).

The samples are viscous liquids and they show high boiling points. They were spurted from the high temperature nozzle having a nichrome-wire heating device.

2) Samples.—*α, γ-Dichlorohydrin.*—A commercial sample was purified by distillation under reduced pressure (boiling point: 87°C/35 mmHg).

1) S. Mizushima, Y. Morino and T. Kubota, *Bull. Chem. Soc. Japan*, **14**, 15 (1939).
2) S. Mizushima, Y. Morino and S. Nakamura, *Sci. Paper I.P.C.R.*, **37**, 205 (1940).
3) S. Mizushima et al., *J. Chem. Phys.*, **19**, 1477 (1951).
4) S. Mizushima et al., *J. Am. Chem. Soc.*, **74**, 1378 (1952).
5) O. Bastiansen, *Acta Chim. Scand.*, **3**, 415 (1949).
6) M. Yamaha, This Bulletin, **29**, 865 (1956).
7) L.R. Zumwalt and R.M. Badger, *J. Am. Chem. Soc.*, **62**, 305 (1940); *J. Chem. Phys.*, **7**, 87 (1939).
8) T. Yuzawa and M. Yamaha, This Bulletin, **28**, 414 (1953).

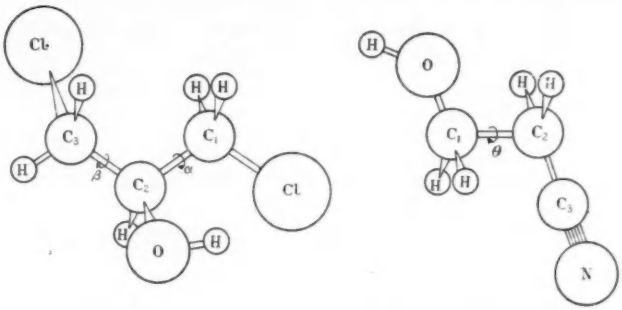

α, γ-Dichlorohydrin Ethylene Cyanohydrin

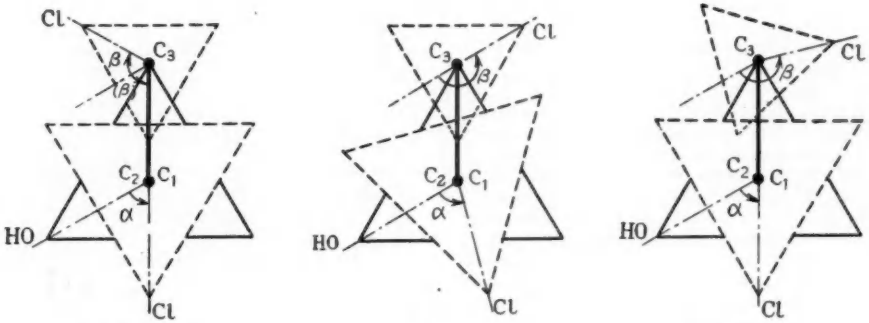

α=60°
β=−60° (or β′=+60°)
(cf. curve G or H)

α=75°
β=180°
(cf. curve N)

α=60°
β=165°
(cf. curve K)

α, γ-Dichlorohydrin

Fig. 1. Schematic models which show the relative atomic configulations for α, γ-dichlorohydrin and ethylene cyanohydrin molecules.
The relative position between O and two Cl atoms of each form varying according to the internal rotation about C-C bonds, is also shown at the lower position for the dichlorohydrin molecule.

TABLE I
THE LIST OF MOLECULAR MODELS AND CORRESPONDING MOLECULAR PARAMETERS OF α, γ-DICHLOROHYDRIN

Models	∠CCC°	∠CCCl°	α°	β°	C-Cl	C″···Cl$_g$	C″···Cl$_t$	O″···Cl$_g$	O″···Cl$_t$	Cl‴···Cl
A	109.5	109.5	60	180	1.77	3.08	4.09	3.03	4.01	4.52
B	〃	112	〃	〃	〃	3.13	4.12	3.09	4.03	4.76
C	112	〃	〃	〃	〃	3.17	4.14	〃	〃	4.73
D	109.5	109.5	〃	150	〃	2.77	4.09	3.03	3.93	4.49
E	〃	112	〃	〃	〃	2.84	4.12	3.09	3.96	4.56
F	〃	109.5	〃	120	〃	3.78	4.09	3.03	3.71	4.93
G	〃	〃	〃	+60	〃		〃	〃		5.40
H	112	112	〃	−60	〃	3.17	4.14	3.09		4.81
I	〃	〃	45	180	〃	3.13	4.13	2.93	4.03	4.80
J	〃	〃	60	〃	1.75	3.17	4.12	3.08	4.01	4.70
K	109.5	〃	〃	165	1.77	2.97	〃	3.09	4.03	4.66
L(=B)	〃	〃	〃	180	〃	3.13	〃	〃	〃	4.76
M	〃	〃	〃	195	〃	3.31	〃	〃	〃	4.90
N	〃	〃	75	180	〃	3.13	4.10	3.22	〃	4.60
O	〃	109.5	60	〃	1.80	3.09	4.12	3.05	〃	〃

TABLE II

THE LIST OF MOLECULAR MODELS AND CORRESPONDING MOLECULAR PARAMETERS OF ETHYLENE CYANOHYDRIN

Models	∠CCC°	θ°	C_1–C_2	C_2–C_3	C≡N (Å)	O″···C (Å)	O‴···N (Å)
A	109.5	180	1.54	1.54	1.16	3.79	4.88
B	〃	〃	〃	1.50	〃	3.76	4.85
C	112	〃	〃	〃	〃	3.78	4.86
D	109.5	〃	1.52	1.46	1.20	3.70	4.83
E	〃	〃	〃	1.42	1.16	3.67	4.76
F	〃	60	1.54	1.50	〃	2.88	3.63
G	112	〃	〃	〃	〃	2.93	3.70
H	109.5	〃	1.52	1.46	1.20	2.84	3.62
I	〃	0	1.54	1.50	1.16	2.52	3.13
J	112	〃	〃	〃	〃	2.59	3.21

Ethylene Cyanohydrin.—A sample synthesized from ethylene bromohydrin by Mr. Kubouchi of the Electrical Communication Laboratory has been used (boiling point: 108°/12 mmHg).

3) Electron Diffraction Patterns. — The maxima and minima of diffracted halos appearing on photographic plates have been measured visually. For dichlorohydrin, nine distinct halos have been observed in the range of $q<80$ in addition to several faint or indistinct halos. For ethylene cyanohydrin, eight halos including weak and indistinct ones have been observed in the range of $q<60$. Measured *q-values* of maxima and minima are shown in Tables IV and V, and visual intensity curves are shown at the top of Figs. 2 and 4, followed by the theoretical intensity curves.

4) Theoretical Intensity Curves and Radial Distribution Curves.—The theoretical intensity curves have been calculated by using the following well-known Pauling-Schomaker formula;

$$I(q)=k\sum_i\sum_j (nZ_iZ_j/r_{ij})\cdot\sin(\pi q r_{ij}/10)\cdot\exp(-b'_{ij}q^2),$$

where, $q=10\,s/\pi$; $s=(4\pi\sin\theta/2)/\lambda$; θ, the scattering angle and λ, the wave length of the beam.

The molecular parameters which are used in the construction of models are listed in Table I for dichlorohydrin and in Table II for cyanohydrin (cf. Fig. 1).

For dichlorohydrin, the temperature factors b'_{ij}, whose values are suggested from the case of

TABLE III

TEMPERATURE FACTORS b'_{ij} FOR THE CALCULATION OF INTENSITY CURVES OF α, γ-DICHLOROHYDRIN MOLECULE

Atompairs	b'_{ij}
C–H	0.00015
C–O	0
C–C	0
C–Cl	0
C′···H	0.00022
C′···O	0.00008
C′···C	0.00017
C′···Cl	0.00008
Cl′···H	0.00040
C″···Cl_g	0.00050
Cl″···O_g	0.00040
C″···Cl_t	0.00040
Cl″···O_t	0.00033
Cl‴···Cl	0.00070

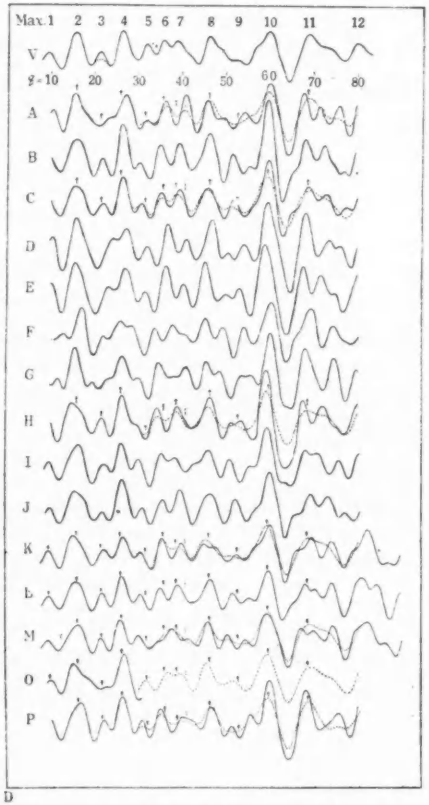

Fig. 2. Visual (V) and theoretical intensity curves for dichlorohydrin molecule.
Dotted curves correspond to the curves in which the temperature factors for each atomic distance as shown in Table III are taken into consideration.

ethylene chlorohydrin[9] and are listed in Table III, are taken into consideration, the corresponding curves being shown by dotted curves in Fig. 2.

For ethylene cyanohydrin, the temperature factors are ignored in the approximate calculation, since the observed intensity curve extends to $q<60$.

Also the radial distribution curves using the visual intensity curves have been calculated by means of the following formula;

$$rD(r)=\sum_{q=1}^{q=\max} I(q)\cdot\sin(\pi qr/10)\cdot\exp(-aq^2).$$

and are shown in Figs. 3 and 5.

5) Analyses of Intensity Curves and Radial Distribution Curves.—a) α,γ-Dichlorohydrin.— In constructing the molecular models, the following parameters are assumed (i), and varied in the ranges (ii):

(i) C-C=1.54 Å, C-O=1.45 Å, C-H=1.10 Å ($Z_H=1.2$),

(ii) C-Cl=1.75 Å~1.80 Å, ∠CCC=109.5°~112°, ∠CCCl=109.5°~112°.

TABLE IV

OBSERVED *q-values* AND CALCULATED q/q_{obs} VALUES FOR BETTER MOLECULAR MODELS OF α,γ-DICHLOROHYDRIN

Max.	Min.	q_{obs}	q/q_{obs}		
			N	C	O
2		16.07	0.996	0.989	0.989
	3′	(19.70)	—	0.990	0.990
3		21.54	(1.040)	1.003	1.010
	4′	23.47	0.997	1.010	0.999
4		26.12	1.015	0.999	0.995
5		31.70	0.987	0.962	0.962
6		35.90	1.008	0.987	0.972
7		(38.72–40.93)			
		(39.82)	1.008	(0.989)	0.997
8		46.41	0.978	0.989	0.991
9		(52.85)	(0.967)	0.973	—
10		59.68	0.995	0.999	0.994
11		68.53	1.008	1.007	0.998
Mean deviation:			0.999_1	0.991_4	0.990_5
Mean sq. average deviation:			0.011_2	0.012_5	0.012_3

9) For molecules having C≡N triple bond, the distance C≡N seems reasonably to be 1.16Å; that is, for example, for methyl cyanide, $CH_3-C\equiv N$,
C≡N=1.16Å by L.O. Brockway, *J. Am. Chem. Soc.*, **58**, 2516 (1936).
C≡N=1.16Å and C−C=1.49Å by L. Pauling et al., *J. Am. Chem. Soc.*, **61**, 927 (1939).
$r_{C\equiv N}$=1.157Å (HCN),
1.163Å (Cl−CN),
1.160Å (Br−CN),
1.159Å (I−CN), by means of microwave spectra by W.J.O. Thomas, *J. Chem. Phys.*, **19**, 1162 (1951),
for Acrylonitrile $CH_2=CH^a-C\equiv N$
$C^a-C=1.44$Å and C≡N=1.16Å.
by T. Saito, reported in the Ann. Meeting of the Chem. Soc. Japan, (1954), April.

TABLE V

OBSERVED *q-values* AND CALCULATED q/q_{obs} VALUES FOR THE BEST MODEL OF ETHYLENE CYANOHYDRIN

Max.	q_{obs}	q/q_{obs} E
(shelf)	13.14	0.989
2	18.00	1.014
(shelf)	21.78	1.010
3	25.86	1.025
4	30.68	0.999
5	34.13	1.002
6	40.40~	0.990
	43.78	0.984
7	49.22	(1.034)
8	55.73~	1.005
	59.00	1.012
Mean deviation:		1.003
Mean sq. average deviation:		0.012_2

In this case, since the molecule has a complicated structure, the values of parameters are confined to the narrower range of variation referring to the values of ethylene chlorohydrin previously determined. It was established that considerable fraction of the ethylene chlorohydrin molecules have the structure of *gauche* form, that is, the structure in which the intramolecular hydrogen bond is formed between Cl and O atoms even at room temperature, the rotational angle α of *gauche* form being about 75°.

The dichlorohydrin molecule has two O···Cl atom pairs, the combinations of two rotational equilibrium angles α and β (see Fig. 1) around the two C-C bonds being taken up as shown in the fourth and fifth columns of Table I, in which atomic distances and valence angles corresponding to each model are listed.

The ranges of variations of angles α and β are as follows*:

α=45°, 60° (*gauche*), 75°.

$\beta=\pm60°$ (*gauche*), 120°, 150°, 165°, 180° (*trans*) and 195°.

(1) As the angles ∠CCC and ∠CCCl are varied from 109.5° to 112°, the *q-values* of maxima 5, 6 and 7 decrease slightly. The intensity relations of maxima 2, 3 and 4, and those in the range $45<q<60$ differ from one another in the curves A, B and C. Also, in the curves D and E, the *q-values* of maxima 4, 5, 6, 7, 8 and 9 decrease according to the similar variation of parameters. The intensity relations and *q-valus* of the models having both 112° of angles ∠CCC and ∠CCCl are clearly different from those of the visual curve.

(2) As the C-Cl distances are changed from 1.75 Å to 1.80 Å, the *q-values* of the maxima and minima change slightly, and the height of maximum 7 becomes lower. However, the intensity relations and *q-values* of maxima 5, 6 and 7 for

* In the combinations of angles α and β, obviously, a model having $\alpha=60°$, $\beta=180°$ and one having $\alpha=180°$, $\beta=60°$, are equivalent.

both models J and P are unsatisfactory, although model O seems better.

(3) If one of the two O···Cl pairs forms the intramolecular hydrogen bond, i.e. with the angle $\alpha \approx 60°$, the other O···Cl pair seems unable to form another hydrogen bond, and consequently the rotational angle $\beta = \pm 60°$ seems inadequate. This fact is made clear from the comparisons of the curves G ($\alpha = 60°$, $\beta = 60°$) and H ($\alpha = 60°$, $\beta = -60°$) with the curves A, B and C, each of which has the combination of $\alpha = 60°$, and $\beta = 180°$.

In the curves G and H, maximum 5 accompanies maximum 4 and shows shelf-like feature, especially in the curve G, the intensity relation seems clearly different from that of the visual one, and also the maxima 6 and 7 shift inward for curve H.

(4) Assuming one O···Cl pair is in a position of $\alpha = 60°$, the relative position of the other O···Cl pair is examined by varying the angle $\beta = 120°$, 150°, 165°, 180° and 195°. In the curves D and E ($\beta = 150°$), maximum 3 accompanies maximum 4 with a shelf-like feature. The curve F ($\beta = 120°$) illustrates the extreme feature in which both maxima 3 and 5 come together with maximum 4 and show deterioration. In the curve M ($\beta = 195°$), the maxima 3, 4, 5 and 8 shift inward, and maxima 6 and 7 seem to become one maximum. In the curves K and L, the intensity relations and the positions of maxima of over-all q-range become better and nearly adequate, but maximum 5 is situated at a smaller *q-value* than the visual curve, in which minimum 5′ seems to be deeper than minimum 6′ and maximum 5 comes comparatively near maximum 6.

(5) In the case of ethylene chlorohydrin, the rotational angle α relating to one O′′···Cl atom pair in the vicinity of *gauche* position was shown to be 75°. Consequently, in the case of this molecule, the combination of $\alpha = 75°$ and $\beta = 180°$ is considered as shown in the curve N. The intensity relations for the entire q-range, except maximum 3, and the *q-values* of the maxima and minima of this curve coincide with those of the visual curve.

(6) The radial distribution curve (Fig. 3) computed by using the experimental intensity curve has been analyzed into various corresponding peaks, and several peaks corresponding to the distances of atom pairs are as follows:

Peak A: 1.15 Å = C–H (a little longer)
B: = C–O and C–C
C: 1.77 Å = C–Cl
D: = O′···H and C′···H
E: = Cl′···H, C′···O, C′···C
F: 2.71 Å = C′···Cl
G: = C′′···Cl, O′′···Cl (in the vicinity of the *gauche* position)
H: = C′′···Cl, O′···Cl (in the vicinity of the *trans* position)
I: 4.45 Å ~ 4.70 Å = Cl′′′···Cl.

The superposed peaks E, G and H can not be clearly separated into the component peaks (corresponding distances), but the corresponding distances of the better models resulting from the

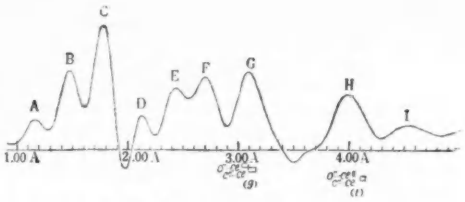

Fig. 3. Radial distribution curve for dichlorohydrin molecule.

Under the curves, the O′′...Cl and C′′... Cl interatomic distances corresponding to the relative positions in the *gauche* (g) and the *trans* (t) forms respectively are shown with small squares.

$O''\cdots Cl_g$ 3.04~3.09 (Å)
$C''\cdots Cl_g$ 3.09~3.16 (Å)
$O''\cdots Cl_t$ 4.03~4.05 (Å)
$C'\cdots Cl_t$ 4.10~4.15 (Å)

selection of intensity curves are fairly consistent with those in the radial distribution curve. That is, two rotationally stable positions of O′′···Cl atom pairs are probable $\alpha = 60°$–75° and $\beta = 165°$–180°. The corresponding O′′···Cl, and C′′···Cl distances in these cases are shown under the corresponding peaks G and H by small rectangles whose respective widths show the allowances according to the slight variations of bond distances and angles (see Table I). The existence of a peak of 4.45 Å–4.70 Å corresponding to the Cl′′′···Cl distance also seems to show adequately the relative position of the two Cl atoms (see column 11 in Table I).

In considering the conclusions in the previous report on ethylene chlorohydrin, that is, the values C–Cl = 1.77 Å, C–O = 1.45 Å, ∠CCC = 109.5° and ∠CCCl = 112° with the assumed C–C = 1.54 Å, the model of dichlorohydrin molecule having the rotational angles $\alpha = 75°$ and $\beta = 180°$ is reasonable (cf. curve N).

b) Ethylene Cyanohydrin.—In constructing molecular models, the following parameters are assumed (i), and varied in the ranges (ii):

(i) C–O = 1.45 Å, C–H = 1.10 Å ($Z_H = 1.2$), C≡N = 1.16 Å[9] and ∠CCO = 109.5°,
(ii) C_1–C_2 = 1.52 Å–1.54 Å, C_2–C_3 = 1.42 Å–1.54 Å and $\angle C_1C_2C_3 = 109.5°$–112°.

The list of models with molecular parameters is shown in Table II, and corresponding theoretical intensity curves in Fig. 4.

Regarding the relative position of –C≡N and –OH radicals, representated by the rotational angle θ, the models are classified into three groups, the *trans* group ($\theta = 180°$, curves from A to E), the *gauche* group ($\theta = 60°$, curves from F to H) and the *cis* group ($\theta = 0°$, curves I and J).

In comparing the intensity relations and *q-values* of maxima and minima of the visual and theoretical intensity curves, the better models are selected by means of the following view-points of analysis;

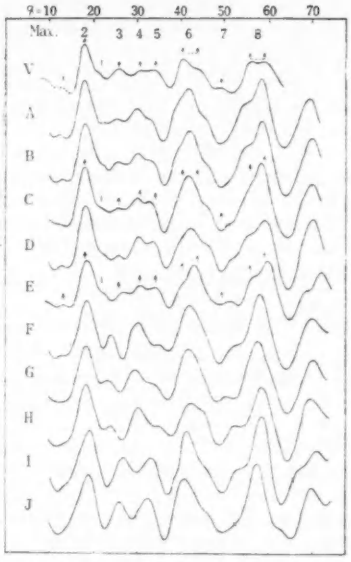

Fig. 4. Visual (V) and theoretical intensity curve for ethylene cyanohydrin molecule.

(1) The *trans*-, *gauche*- and *cis*-forms change clearly in the features of intensity relations as shown in Fig. 4. That is, the maxima 2 and 6 remain almost unchanged throughout the curves; the variation of intensity between maxima 3 and 5 is relatively small in the curves of the *trans*-group (A to E). For the *gauche* group (F to H), both maximum 3 and minimum 4′ shift inward and maximum 4 becomes higher; however, these features do not coincide with those of the visual curve. In the range of $20<q<40$ in the curves I and J (the *cis* group), the simply sinusoidal features differ distinctly from the visual one. The characteristic features of the visual curve are a very low shelf ($q\approx21.8$) accompanying maximum 2 and a slowly-varying intensity between maxima 3, 4 and 5 (i.e. (a) slightly separated low maximum 3 and (b) adjacent maxima 4 and 5 near each other having almost equal heights). These features seem to coincide fairly well with those of the curves in the *trans* group, especially with those of curves E (see later).

(2) From the analysis of the radial distribution curve as shown later, the molecule could be regarded as belonging to the *trans* group, and the C_1–C_2 and C_2–C_3 distances and $\angle C_1C_2C_3$ angles are examined on this assumption.

The C_2–C_3 distance nearest to the triple bond of C≡N can be considered to be short, and the variations of C_2–C_3 distance are compared with one another as: C_2–C_3=1.50 Å (curve B and C), 1.46 Å (curve D) and 1.42 Å (curve E). The case of the angle $\angle C_1C_2C_3=112°$ as shown in the curve C (cf. curve G in the *gauche* form and curve J in the *cis* form having $\angle C_1C_2C_3=112°$) is also compared. In each case, the intensity relation of maxima from 3 to 5 slightly changes, and the heights of maxima 4 and 5 are nearly equal in the visual curve. The curves B, C and D seem comparatively good. The intensity relation of curve E seems the best, although the maxima of curve E shift slightly outward from those of the visual curve in the entire q-range. In spite of the intensity relation of maxima from 3 to 5 being comparatively diffused, it can be safely said, though not conclusively, that the C_2–C_3 distance is slightly shorter than 1.54 Å.

(3) A somewhat obscure and diffuse experimental intensity curve of ethylene cyanohydrin has been obtained up to $q\approx60$, because the sample is a viscous and less volatile liquid having high boiling temperature. Despite this, a radial distribution curve, curve RD1 has been computed with some uncertainty as shown in Fig. 5. From the curve, the corresponding atom pairs and distances between each peak are analyzed as follows:

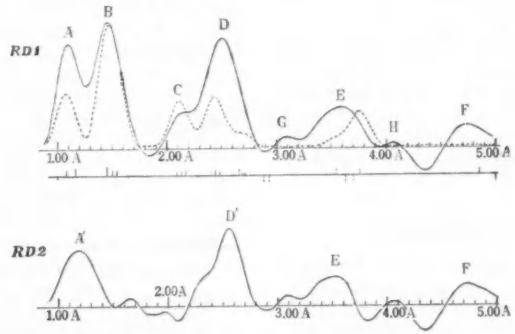

Fig. 5. Radial Distribution curves for ethylene cyanohydrin molecule.
*RD*1, total radial distribution curve. *RD*2, the curve which shows the residual curve produced by the subtraction of the area under the hypothetical partial *RD* curve (as shown by the dotted curve) from the area under the *RD*1 curve.

A: C-H, C≡N,
B: C_1-C_2, C_2-C_3 C-O,
C: C'···H, O'···H,
D: C'···O (≈2.40 Å), C'···C (2.43 Å∼2.55 Å),
O''···H (≈2.70 Å), C'···N (2.66 Å∼2.70 Å),
E: C''···N (3.48 Å∼3.55 Å),
C''...O_{trans} (3.30 Å∼3.79 Å),
F: O'''...N_{trans} (4.83 Å∼4.88 Å).

Each of these analyzed values seems to agree fairly well with each corresponding parameter of the better models. In particular, the *trans*-form seems acceptable as regards the rotational equilibrium position around the C_1-C_2 bond. That is, the peak F (4.70 Å-4.80 Å) does not appear in the cases other than the *trans* form: for example, if the *gauche* formexists, the peak corresponding to O''···O_{gauche}≈2.85 Å∼2.95 Å will appear, but not in RD1. It is not clear, however, whether or not the two rotational isomers may coexist. The distances other than O'''···N_{trans} (peak F) cannot be determined separately from the curve RD1, since the other peaks appear to be the combinations of two or more peaks. From consideration of the intensity curves, the dotted curve which is the hypothetical radial distribution curve of the following eight distances on RD1, is computed;

C-H=1.08 Å, C-O=1.45 Å, C_1-C_2=1.54 Å*,
C'···H=2.17 Å**, C'···O=2.44 Å**,
C''···O_{trans}=3.76 Å**, O''···H_{gauche}=2.69 Å**,
N'···H=3.55 Å**.

In consequence of the subtraction of the area under the dotted curve from that of RD1, the peaks other than those corresponding to eight distances mentioned above appear in the curve RD2.

The new distribution curve RD2 is analyzed with some uncertainty as follows:

A': The peaks corresponding to the distances C≡N and C_2-C_3 should appear, but could hardly be separated.
D': 2.56 Å=C_2'···N,
E': 3.45 Å∼3.60 Å=C''···N,
from this value the angle $\angle C_1C_2C_3$ could not be decided conclusively.

The intensity curve E, which is computed in consideration of the results of radial distribution curve, seems to be the most acceptable one, except the shape of maximum 6 and the slight disagreements of all *q-values*. The structure of ethylene cyanohydrin could not be determined more fully, because only insufficient diffracted patterns were obtained.

Results and Discussions

1) α,γ-Dichlorohydrin.—From the intensity and radial distribution curves, the following results are obtained:

C-Cl=1.76 Å-1.80 Å, $\angle$CCC=109.5°±1.5°,
$\angle$CCCl=111°±1.5°,
α=70°±10°, β=180°±10°.

The results of α, γ-dichlorohydrin seem sufficiently acceptable in comparison with those of ethylene chlorohydrin.

One of the two O''···Cl atom pairs is in the *gauche* position and the other *trans* at room temperature, because probably intramolecular hydrogen bond can only be formed in one or the other set of O''···Cl atom pairs.

2) Ethylene Cyanohydrin.—
C_2-C_3=(1.48 Å±0.04 Å)<C_1-C_2
θ=180° (The stable form of rotation about C_1-C_2 bond is of *trans*.)

Upon consideration of the present results, the C_2-C_3 bond neighboring the triple bond C≡N seems to be comparatively short. In the series of bonds -C_2-C_3≡N, the N atom is capable of becoming a weak "proton-acceptor", while the C_3 atom does not have this capacity. However, it is probably difficult to form the intramolecular hydrogen bond O-H···N in this molecule because of the longer distance of the O···N atom pair and of the repulsive force between the O···C_3 atom pair in the *cis* form (i.e. O···N_{cis}=3.20Å and O···C_{3cis}=2.60Å). Consequently, the molecule exists almost in the *trans* form in the gaseous state, and the coexistence of another isomer forming the intramolecular hydrogen bond can not be confirmed.

Summary of Results

The molecular structures of α, γ-dichlorohydrin and ethylene cyanohydrin in the gaseous state were investigated by a visual electron diffraction method. The results obtained from the analyses of intensity curves and radial distribution curves are as follows:

α, γ-Dichlorohydrin (1, 3-dichloropropanol (2))

Assumption: C-C=1.54 Å, C-O=1.45 Å, and C-H=1.10 Å and $\angle$CCH=$\angle$CCO=109.5°.
Results: C-Cl=1.78 Å±0.02 Å, $\angle$CCC=109.5°±1.5° and $\angle$CCCl=111°±1.5°.
Stable rotational position: α=70°±10°, β=180°±10°.

Ethylene Cyanohydrin

Assumption: C-H=1.10 Å, C_1-C_2=1.52 Å-1.54 Å, C≡N=1.16 Å, $\angle$CCH=10.95°, $\angle C_1C_2C_3$=109.5°-112°
Results: C_2-C_3=(1.48 Å±0.04 Å)<C_1-C_2
Stable rotational position: θ=180° (*trans* form).

* In order to obtain the peak corresponding to C_2-C_3, the value of C_1-C_2 is assumed.
** These values should be varied functionally with the angle $\angle C_1C_2C_3$, but the values are assumed in the first approximation.

The author wishes to express his deep gratitude to Mr. Y. Kubouchi of the Electrical Communication Laboratory for having kindly offered the useful sample of ethylene cyanohydrin, and to Professor A. Kotera of this University, and Dr. S. Nagakura of the Scientific and Technical Laboratory, Tokyo University, for their valuable discussions throughout this work.

Chemical Institute, Faculty of Science
Tokyo University of Education
Ootsuka Tokyo

Studies on the Synthesis of Metal Complexes. I. Synthesis of an Ammine-carbonato Series of Cobalt (III) Complexes*

By Motoshichi MORI, Muraji SHIBATA, Eishin KYUNO and Tomohiko ADACHI

(Received April 30, 1956)

It has been well known that in the presence of alkali bicarbonates cobaltous salts such as chloride and sulfate give green coloration by the action of hydrogen peroxide on the aquous solution, and this reaction has been used for the iodometric or colorimetric determination of cobalt by several workers[1,2].

On the other hand, this reaction product has been regarded as tricarbonatocobalt (III) anion, $[Co(CO_3)_3]^{3-}$, from measurement of the absorption spectrum[2] or chemical analysis of a derivative with hexamminecobalt (III) cation, $[Co(NH_3)_3][Co(CO_3)_3]$[3].

The present study was first directed to the isolation of the complex salt and the determination of its chemical formula and then turned to the synthesis of cobalt (III) complexes belonging to an ammine-carbonato series. All the objects were attained with success.

Experimental

Synthesis—1) Potassium Tricarbonatocobaltate (III), $K_3[Co(CO_3)_3]\cdot 3H_2O$.—Twenty grams of $KHCO_3$ was mixed with 20 cc. of water and the mixture was cooled in an ice-bath. In a separate beaker 10 g. of $CoCl_2\cdot 6H_2O$ was dissolved in 10 cc. of water and 5 cc. of 30% H_2O_2 was added to this solution. This was added to the $KHCO_3$ solution drop by drop with stirring, allowing about an hour for the operation. The green solution obtained was quickly filtered by suction, and the clear filtrate was again cooled and kept in a dark place. When about 15 cc. of alcohol was added to the filtrate, crystals began to appear, but they were contaminated with bicarbonate. The precipitates, therefore, were filtered off and the filtrate was again kept in a dark place at nearly 0°C. Then a little more alcohol was added to the filtrate, and the solution was allowed to stand until the deposition of crystals ceased, which took more than half an hour. The crystals were collected on a glass filter, washed with alcohol and then by ether, and stored in a brown bottle. The yield was 13.5 g. The solid was soluble in water containing potassium bicarbonate, but suffered decomposition by pure water, yielding the hydrous oxide.

Some care had to be exercised in isolating this complex. If the addition of the $CoCl_2$-H_2O_2 mixture was too rapid it brought about precipitation of cobaltic hydroxide, while if too much alcohol was added, it caused co-precipitation of other salts such as potassium chloride.

2) Blue Variety of Potassium Dicarbonatodiamminecobaltate (III), Blue-$K[Co(NH_3)_2(CO_3)_2]$ H_2O.—To the clear green solution, prepared from $KHCO_3$ and $CoCl$-H_2O_2 mixture as described in 1), was added 5 g. of ammonium carbonate and the mixture was warmed on a water-bath until the green color of the solution changed into blue, which took about ten minutes. At the end of this period the vessel containing the warm solution was immediately dipped in the ice-bath in order to stop further progress of the reaction and to effect crystallization of the product. After the removal by filtration of the first crop of crystals another crop could be obtained from the residual solution by gradual addition of alcohol. These crops were collected together, recrystallized from water and washed with pure alcohol. Total yield, about 7 g.

3) Violet Variety of Potassium Dicarbonatodiamminecobaltate (III), Violet-$K[Co(NH_3)_2(CO_3)_2]\cdot H_2O$.—The green solution containing 5 g. of ammonium carbonate was heated on the water-bath until the color of the solution turned into blue and finally violet. Then the solution was

* Presented at the 9th Annual Meeting of the Chemical Society of Japan, Kyoto, April 2, 1956.

1) H.A. Laitinen and L.W. Burdett, *Anal. Chem.*, 23, 1268 (1951).

2) M. Mori and M. Shibata, *J. Chem. Soc. Japan*, 75, 1046 (1954).

3) T.P. McCutcheon and W.J. Schuele, *J. Am. Chem. Soc.*, 75, 1845 (1953).

cooled rapidly and a large amount of alcohol was added to it, and the whole was allowed to stand for some time. The violet precipitate was collected and dissolved in a little cold water to remove impurities as residues, and then the complex sought for was reprecipitated from the solution by the addition of alcohol. After repeating this procedure, the product was washed with alcohol and ether in turn and finally dried in a vacuum desiccator over sulfuric acid. Thus about one gram of violet powder was obtained. The complex was hygroscopic and very readily soluble in water.

4) Carbonatotetramminecobalt (III) Chloride, $[Co(NH_3)_4CO_3]Cl$.—To the green solution were added 15 g. of ammonium carbonate and 30 cc. of conc. ammonia and the mixture was boiled on the water-bath until the color of the solution became blood-red. At the end of this heating the liquid was poured into an evaporating dish and concentrated to a small volume with the addition of a small amount of ammonium carbonate. On adding alcohol, the complex was precipitated, the yield being about 9 g.

5) Hexamminecobalt (III) Chloride and Chloropentammine Cobalt (III) Chloride, $[Co(NH_3)_6]Cl_3$ and $[Co(NH_3)_5Cl]Cl_2$.—Thirty grams of ammonium chloride, 40 cc. of conc. ammonia and 2 g. of active charcoal were introduced into the green solution and the mixture was boiled until its color became reddish-brown (about thirty minutes). In this case, a reflux condenser was used to avoid the escape of ammonia from the solution. After filtering and cooling, conc. hydrochloric acid was gradually added to the filtrate, until a yellow precipitate separated out. The purification of the product was effected by the usual method for this complex. Yield, about 4 g.

On evaporating the mother liquor, chloropentamminecobalt (III) chloride was obtained as a by-product.

6) Hexamminecbalt (III) Tricarbonatocobaltate (III), $[Co(NH_3)_6][Co(CO_3)_3]$.—This compound was quantitatively precipitated from the green solution by the addition of solid hexamminecobalt (III) chloride. The compound appeared as light-green powder. It was extremely insoluble in water, alcohol and acetone and was very stable against day-light.

All the complexes described above are shown in the accompanying flow sheet (Table I).

TABLE I

A FLOW SHEET OF SYNTHESIS OF AMMINE-CARBONATO Co(III) COMPLEXES

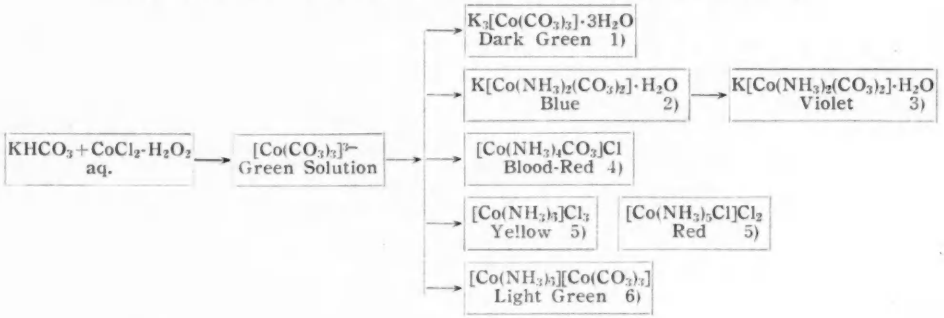

Analysis.—Determination of chemical formulas was carried out for the complexes obtained in 1), 2), 3) and 6). The other complexes were identified by their characteristic properties such as precipitation reaction and absorption spectrum.

Water of crystallization was determined from the loss of weight of the product at 100–130°C by means of a Shimazu Thermano Balance and the fact nothing but water of crystallization has been removed was confirmed by re-dissolving the dehydrated sample in water.

When the dehydrated sample was heated with gradual elevation of temperature up to 300°C, all of the ammonia molecules and part of the carbonate ions attached to the central cobalt atom were expelled from the sample, and the remainder consisted of potassium carbonate and an oxide of cobalt (perhaps, Co_2O_3). The reaction may be represented as follows:

$$2K_3[Co(CO_3)_3] \longrightarrow 3K_2CO_3 + Co_2O_3 + 3CO_2\uparrow$$

$$2K[Co(NH_3)_2(CO_3)_2] \longrightarrow K_2CO_3 + Co_2O_3 + 4NH_3\uparrow + 3CO_2\uparrow$$

$$[Co(NH_3)_6][Co(CO_3)_3] \longrightarrow Co_2O_3 + 6NH_3\uparrow + 3CO_2\uparrow$$

The quantity of ammonia and carbondioxide expelled was estimated from the observed loss of weight. The potassium carbonate was alkalimetrically estimated after the residue was extracted with hot water and the cobalt content was iodometrically determined after the oxide in the residue was dissolved with hot sulfuric acid.

To confirm the validity of the above methods, direct analysis of ammonia and carbondioxide was also carried out.

Absorption Spectra.—The absorption spectra of the above complexes in aqueous solution were measured with a Beckman Model DU Spectrophotometer using a cell 1.0 cm. in thickness.

Results and Discussion

The results of thermal decomposition are shown in Fig. 1 and all the numerical values

TABLE II
ANALYTICAL RESULTS

(amounts in %)

Complexes	H_2O		$CO_2+(NH_3)$		K_2CO_3		Co		CO_2*		NH_3*	
	calcd.	obs.	calcd.	obs.	calcd.	obs.	calcd.	obs.	calcd.	obs.	calcd.	obs.
$K_3[Co(CO_3)_3]\cdot 3H_2O$	13.5	13.2	16.1	15.5	50.4	45.0	14.4	14.9	44.6	46.9	—	—
Blue-$K[Co(NH_3)_2(CO_3)_2]\cdot H_2O$	6.7	6.6	36.7	35.9	25.6	23.5	21.6	22.1	—	—	12.6	12.5
Violet-$K[Co(NH_3)_2(CO_3)_2]\cdot H_2O$	6.7	6.5	36.7	36.0	25.6	23.5	21.6	20.6	—	—	12.6	13.8
$[Co(NH_3)_6][Co(CO_3)_3]$	—	—	58.5	58.0	—	—	29.5	28.0	—	—	—	—

* direct determination

TABLE III
ABSORPTION MAXIMA AND log ε

($10^{13}\cdot sec^{-1}$)

Complexes	ν_1	log ε_1	ν_2	log ε_2	ν_3	log ε_3
$K_3[Co(CO_3)_3]$	46.5	2.19	68.1	2.22	117.6	3.97
$K_3[Co(C_2O_4)_3]$	49.5	2.09	70.8	2.19	122.4	4.42
Blue-$K[Co(NH_3)_2(CO_3)_2]$	52.2	2.14	76.8	2.40	126.6	4.14
Violet-$K[Co(NH_3)_2(CO_3)_2]$	55.5	1.80	80.2	2.04	128.1	4.30
$NH_4[Co(NH_3)_2(C_2O_4)_2]$	54.0	1.95	82.4	2.10	129.3	3.24
Na[Coedta]	55.6	2.48	78.9	2.33	133.3	4.34

are given in Table II. These data seem to justify the assignment of such chemical formulae as $K_3[Co(CO_3)_3]\cdot 3H_2O$, blue- and violet-$K[Co(NH_3)_2(CO_3)_2]\cdot H_2O$ and $[Co(NH_3)_6][CoCO_3)_3]$ to our compounds. Additional evidence of the validity of these formulae exists in the absorptiometric data (Fig. 2 and Table III). Thus, the absorption curve of $K_3[Co(CO_3)_3]$ is similar to that of $K_3[Co(C_2O_4)_3]$, and that of violet-$K[Co[NH_3)_2(CO_3)_2]$ to those of $NH_4[Co(NH_3)_2(C_2O_4)_2]$ and K[Coedta].

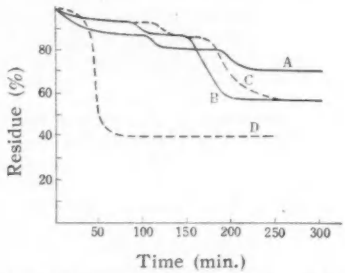

Fig. 1. Thermal decomposition of complexes at 100-300°C.
A. $K_3[Co(CO_3)_3]\cdot 3H_2O$
B. Blue-$K[Co(NH_3)_2(CO_3)_2]\cdot H_2O$
C. Violet-$K[Co(NH_3)_2(CO_3)_2]\cdot H_2O$
D. $[Co(NH_3)_6][Co(CO_3)_3]$

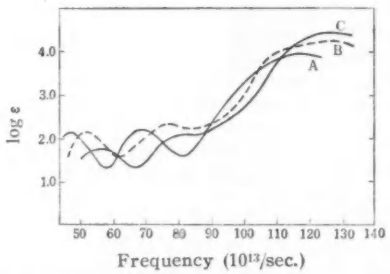

Fig. 2. Absorption spectra of:
A. $K_3[Co(CO_3)_3]$
B. Blue-$K[Co(NH_3)_2(CO_3)_2]$
C. Violet-$K[Co(NH_3)_2(CO_3)_2]$.

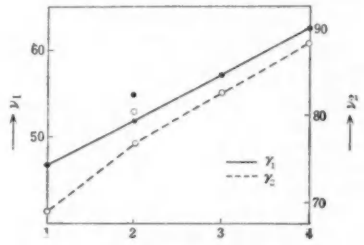

Fig. 3. Frequency positions of the ammine-carbonato Co(III) complexes.
1. $[Co(CO_3)_3]^{3-}$ 2. $[Co(NH_3)_2(CO_3)_2]^-$
3. $[Co(NH_3)_4CO_3]^+$ 4. $[Co(NH_3)_6]^{3+}$

$K_3[Co(CO_3)_3]\cdot 3H_2O$.—The exact formula for this complex had not been determined before. According to reference[1], Job assigned to it the formula K_3CoO_3, Durrant considered it to be $(KCO_2\text{-}O)_2\text{-}Co\text{-}O\text{-}Co\text{-}(O\text{-}O_2CK)_2$ and Duval called it cobalt (III) tricarbonatocobaltiate, $Co[Co(CO_3)_2]$. None of these formulas, however, correctly represents the constitution of the pure substances obtained by the present workers.

From the results of analysis and because of the absorption spectrum of this complex, it is reasonable to give it *tris*-structure. The difficulty of isolating this complex in the pure state will be appreciated by considering the fact that trioxalatocobaltate (III) easily decomposes in day-light. In order to draw a final conclusion, however, it is necessary to resolve the complex into the antipodes. In fact, attempts were carried out by using *l*-strychnine and *d-tris*-(ethylenediamine)-cobalt (III) ion. In both cases, green precipitates were fractionally obtained from the original solution of the complex. But, since decomposition of the complex took place during the process of removing the precipitants, the optical rotation of the fractionated complex was not measured. Further studies will be carried out.

Blue- and Violet-K[Co(NH_3)$_2$(CO_3)$_2$]·H_2O.—Now, it is important to determine the configuration of these stereoisomers. Provided that a bifunctional group such as carbonate ion can span only *cis*-positions and that no intramolecular change of configuration occurs during the reaction of ammonium salt on tricarbonatocobaltate, the blue compound formed at an earlier stage of the reaction must be *cis*-form, while violet one formed through blue complex is regarded as *trans*-form. Studies of the resolution of both complexes may shed light on this problem.

Absorption Spectra.—The frequency values for the first and second bands of a series of ammine-carbonato complexes are plotted in Fig. 3. From the diagram, it is seen that the values of the first band lie on a single line except for one of violet complex. On the other hand, such a linearity can not exist among the frequencies of the second band. It should be added that the violet complex has the absorption maximum at the same frequency as EDTA-Co (III) complex as indicated in Table III.

Synthesis.—Our methods in which green tris-cobaltate is used as starting material, have the advantage of simplicity. For example, carbonatotetramminecobalt (III) salt, which is useful for the synthesis of various complexes, is prepared by the successive substitution of carbonate ions with ammonia groups without atmospheric oxidation, and hexamminecobalt (III) salt is also prepared by further substitution in the presence of active charcoal. It has also been observed that the cobalt (III) complexes belonging to an ethylenediamine-carbonato series is synthesized in the same way, and this will be reported later.

Summary

A green compound is isolated from the concentrated solution obtained by the action of hydrogen peroxide on cobalt (II) ions in the presence of potassium bicarbonate, and the formula $K_3[Co(CO_3)_3]\cdot 3H_2O$ is assigned to it on the basis of the analysis of the solid and of the absorption spectrum of the solution.

A series of ammine-carbonatocobalt (III) complexes, $K_3[Co(CO_3)_3]\cdot 3H_2O$, blue (perhaps, *cis*)- and violet(perhaps, *trans*)-$K[Co(NH_3)_2(CO_3)_2]\cdot H_2O$, $[Co(NH_3)_4CO_3]Cl$ and $[Co(NH_3)_3]Cl_3$, are synthesized from the abovementioned green solution by means of successive substitution of carbonate ions by ammonia groups. Hexamminecobalt (III) tricarbonatocobaltate, $[Co(NH_3)_6]$ $[Co(CO_3)_3]$, is also obtained by adding a hexamminecobalt (III) salt to the green solution of tricarbonato-complex. Three complexes, $K_3[Co(CO_3)_3]\cdot 3H_2O$ and blue- and violet-$K[Co(NH_3)_2(CO_3)_2]\cdot H_2O$, are probably to be regarded as new complexes and may be identified by their absorption spectra.

Department of Chemistry, Faculty of Science, Kanazawa University
Kanazawa

Studies on the Synthesis of Metal Complexes. II. Synthesis and Absorption Spectra of Hydrogen Ethylenediaminetetraacetato-cobaltate (III) and Sodium-hydrogen Chloro-ethylenediaminetetraacetato-cobaltate (III)*

By Motoshichi MORI, Muraji SHIBATA, Eishin KYUNO and Hiroshi NAKAJIMA

(Received April 30, 1956)

The common cobalt (III) complex in which ethylenediaminetetraacetic acid is hexadentate was first prepared by Brintzinger, Thiele and Mueller[1], and nitro-(ethylenediaminetetraacetato)-cobaltate (III) and bromo-(ethylenediaminetetraacetato-cobaltate (III) were later synthesized by Schwarzenbach[2]. Hereafter, ethylenediaminetetraacetic acid, quadrivalent ethylenediaminetetraacetate anion and tervalent anion will be denoted by EDTA, edta and edtaH respectively.

In the present study, free acid of the common complex, H[Coedta]·$4H_2O$ and sodium salt of the chloro-complex, Na[Co(Cl) (edtaH)]·$2H_2O$ were newly synthesized, and absorption spectra of all Co(III)-EDTA complexes including older ones were also measured. The geometrical configuration of the complexes is also discussed in this paper.

Experimental

Synthesis of H[Coedta]·$4H_2O$.—Ten grams of EDTA(edtaH$_4$) and about the same amount of freshly prepared cobaltic hydroxide were introduced into 200 cc. of water, and the mixture was heated on a water-bath for about one hour until the completion of the reaction. After cooling, the solution was filtered and then the filtrate was poured into a column of cation exchanger Amberlite IR-120 which had been converted into H-form. By this operation the alkali ions contained in the cobaltic hydroxide were completely removed. The solution passing through the exchanger was collected and then concentrated by means of vacuum distillation. On cooling the residual solution in an ice-bath, crystals were deposited, which were filtered by suction and recrystallized from the aqueous solution by adding dil. hydrochloric acid in the cold. Yield, about 65%

Anal. Found: H_2O, 17.1; Co, 14.30. Calcd.: H_2O, 17.0; Co, 14.15%.

The crystals obtained were deep lavender in color like the common complex, Na[Coedta]·$4H_2O$, but less soluble than the latter. The pH of a 10^{-3} M aqueous solution was found to be 2.80.

Synthesis of Na[Co(Cl) (edtaH)]·$2H_2O$.—This compound was prepared as blue crystals by the following method. To a conc. solution prepared by dissolving 10 g. of Na[Co(edta)]·$4H_2O$ in water was added 40 cc. of conc. hydrochloric acid, and the solution was evaporated nearly to dryness on a water-bath. After cooling, the blue residue was washed several times with a little water until the washings did not show any reddish-violet color. By this treatment the unchanged salt, Na[Co(edta)], was removed from the complex aimed at. The remainder was dissolved in water containing a small amount of sodium acetate, and then pure alcohol was added to this solution until blue crystals separated out. They were dissolved again in water containing sodium acetate and then recrystallized by adding dil. hydrochloric acid to the cooled solution. Yield, about 45%.

Anal. Found: H_2O, 8.0; Co, 13.08; Cl, 10.0%. Calcd: H_2O, 7.95; Co, 13.02; Cl, 7.84%.

The complex was readily soluble in water containing an acetate and was converted to the common complex when the aqueous solution was heated for a long time or some silver nitrate or an acid was added to it. The pH of a 10^{-3} M aqueous solution was found to be 2.91.

The same complex was synthesized alternatively by using Na[Co(Br) (edtaH)]·$2H_2O$ or Na[Co(NO_2) (edtaH)]·H_2O in place of Na[Coedta]·$4H_2O$. Free acid of the chloro-complex, H[Co(Cl) (edtaH]·$2H_2O$ was prepared by using H[Coedta]·$4H_2O$ in place of Na[Coedta]·$4H_2O$. It came in blue crystals like the sodium salt and the yield was about 50%.

Formation of Blue Co-EDTA Complex.—To an alkaline solution of EDTA prepared by dissolving the disodium salt (Na_2H_2edta·$2H_2O$) in dil. aqueous solution of sodium hydroxide, an aqueous solution of cobalt sulfate was added and the mixture was inserted in an ice-bath. On adding 10% solution of hydrogene peroxide, the reaction mixture changed from pink to blue in color. Attempts to isolate crystals from this solution ended in failure. This blue solution was very unstable and was converted to the violet solution of common complex with elevation of temperature or by acidification of the solution.

Other Complexes.—Na[Coedta]·$4H_2O$, Na[Co(NO_2) (edtaH)]·H_2O and Na[Co(Br) (edtaH)]·$2H_2O$ were synthesized by the methods reported by Schwarzenbach[2].

* Presented at the 9th Annual Meeting of the Chemical Society of Japan, Kyoto, April 2, 1956.

1) H. Brintzinger, H. Thiele and U. Mueller, *Z. anorg. Chem.*, **251**, 285 (1943).

2) G. Schwarzenbach, *Helv. Chim. Acta*, **32**, 839 (1949).

Analysis.—The water of crystallization was determined from the loss of weight of samples at 130°C by means of a Shimazu Thermano Balance, and it was also found that the samples could be dehydrated by the drying with no change in their chemical properties. The cobalt contents were iodometrically determined for samples treated by bisulfate fusion. The chlorine content was determined by Volhard's method.

Measurement.—The visible and ultraviolet absorption spectra were measured by using a Beckman Model DU Spectrophotometer, and the infrared absorption spectrum, by a Hilger Model 800 Recording Spectrophotometer. Potentiometric titration was carried out by a Shimazu Model MT-3 Electronic Titrimeter.

Results and Discussion

The titration curves of the complexes and the infrared spectrum of chloro-complex are shown in Fig. 1 and Fig. 2 respectively. All the absorption curves of the aqueous solution of the complexes are shown in Figs. 3 and 4, and their absorption maxima are given in Table I.

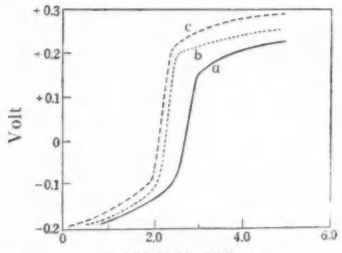

Fig. 1. Titration curves of 10^{-3} M complexes (20 cc) with 10^{-2} N sodium hydroxide.
a. $H[Coedta]\cdot 4H_2O$
b. $Na[Co(Cl)(edtaH)]\cdot 2H_2O$
c. $Na[Co(NO_2)(edtaH)]\cdot H_2O$

TABLE I

ABSORPTION MAXIMA OF Co(III)-EDTA COMPLEXES

Complexes	First Band ν_1	First Band log ε_1	Second Band ν_2	Second Band log ε_2	Third Band ν_3	Third Band log ε_3	Specific Band ν_s	Specific Band log ε_s
Common complex $Na[Coedta]\cdot 4H_2O$	55.9	2.51	78.5	2.34	132.16	4.34	—	—
Blue Complex $[Coedta]^-$?..	51.7	2.47	77.9	2.37	135.14	4.25	—	—
Free Acid of Common Complex $H[Coedta]\cdot 4H_2O$	55.9	2.55	78.5	2.38	133.33	4.45	—	—
Nitro-Complex $Na[Co(NO_2)(edtaH)]\cdot H_2O$.....	53.0 60.6	2.03 2.33	—	—	120.00 133.33	4.26 4.26	88.24	3.52
Bromo-complex $Na[Co(Br)(edtaH)]\cdot 2H_2O$.....	50.9	2.37	75.0 ?	2.39	111.11 130.43	4.18 4.22	—	—
Chloro-complex $Na[Co(Cl)(edtaH)]\cdot 2H_2O$.....	51.3	2.38	74.6	2.31	111.52 132.74	4.18 4.43	—	—

Chemical Formulae of the Synthesized Compounds.—As will be seen in Fig. 1, the titration curve of our chloro-complex is very similar to that of the nitro-complex, and both complexes act as monobasic acids. A like behavior is observed in the free acid of common complex. Further, the two carbonyl bands shown by the infrared spectrum of the chloro-complex are strong evidence for the existence of a free carboxyl group in the coordination sphere of the complex (Fig. 2). The stronger band, which appears at 1610 cm^{-1}, is attributed to the presence of coordinated carboxyl groups. The weaker band, at 1724 cm^{-1}, is associated with the free carboxyl group. Incidentally, the bands for corresponding bromo-complex appear at 1628 cm^{-1} and 1723 cm^{-1} [3]. Thus, in view of the information obtained from the chemical analysis, titration and infrared spectrum measurement, it is reasonable to give our compounds such formulae as given in the experimental section.

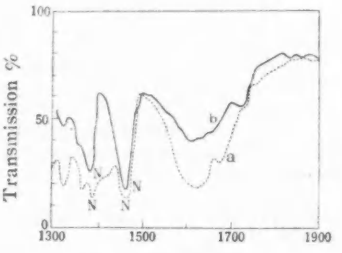

Fig. 2. Infrared absorption spectra of:
a. $Na_2H_2edta\cdot 2H_2O$
b. $Na[Co(Cl)(edtaH)]\cdot 2H_2O$
N. Nujol.

3) D.H. Bush and J.C. Bailar, *J. Am. Chem. Soc.*, **75**, 4574 (1953).

Absorption Spectra of [Coedta] and Blue Co-EDTA Species.—Although the absorption spectrum of the common violet complex had already been measured by Y. Shimura and R. Tsuchida[4], the present workers made new measurements to investigate the pH effect on the absorption spectrum. As is seen in Fig. 3, the absorption curves of buffer solutions prepared in the pH range 2 to 4 are exactly identical with that of an aqueous solution, while those of alkaline solution prepared in the pH range 8 to 10 are different, and further the variation of the optical density shows appreciable deviation from that predicted by Beer's law.

The blue-Co-EDTA complex species described in the experimental section may be identical with the blue complex species regarded as hydroxo-complex, $[Co(OH)(edtaH)]^-$, by Schwarzenbach[2]. The absorption curve of this complex is given in the same figure (Fig. 3d). Discussion of the configuration of species will be given later.

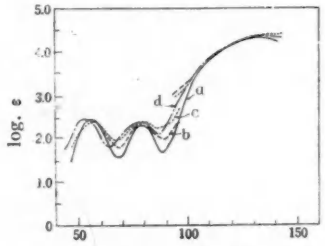

Fig. 3. Absorption spectra of $[Coedta]^-$:
a. in aqueous sol. (pH 6.9), acid sols. (pH>2).
b. in pH 9.5.
c. in pH 10.3.
d. blue Co-EDTA complex species.

Absorption Spectra of [Co(X)(edtaH)].—Although the absorption spectra of nitro-and bromo-complex had already been measured by Y. Shimura and R. Tsuchida*, the same thing was attempted by the present workers in relation to the chloro-complex. As is seen in Fig. 4, the absorption curves of bromo- and chloro-complex are similar to each other in appearance, and the maxima of the first and second bands both show a bathochromical shift from the corresponding maxima of the common complex. A little difference between the two, however, is clearly to be seen from Table I, that is, the maximum of the first band for the bromo-complex is shifted to a slightly longer wave-length than that for chloro-complex. The reason for these bathochromic effects of the ligands may be explained by the familiar empirical rule that the bromide and chloride ions are more bathochromic ligands than the oxalate ion, and the bromide ion is slightly more bathochromic than the chloride ion as ligand. The same relation probably holds for the second set of bands, but it is still uncertain since the absorption curve of bromo-complex does not show a well-defined maximum in the second band.

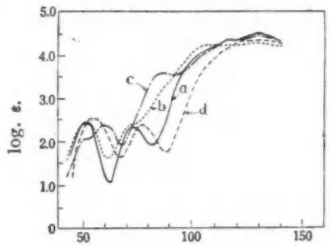

Fig. 4. Absorption spectra of:
a. $Na[Co(Cl)(edtaH)]\cdot 2H_2O$
b. $Na[Co(Br)(edtaH)]\cdot 2H_2O$
c. $Na[Co(NO_2)(edtaH)]\cdot H_2O$
d. $Na[Coedta]\cdot 4H_2O$.

As is seen in the same figure, the first band of nitro-complex clearly splits into two components, and this interesting fact will be reported shortly by other workers*. Inspection of the absorption spectra in the ultraviolet region reveals the interesting fact that there are two absorption maxima in the region. For nitro-complex they appear at 120.00 ($\times 10^{13}$/sec.) and 133.33, for bromo-complex, at 111.11 and 130.43, and for chloro-complex, at 111.52 and 132.74 (Table I). In contrast, the common complex shows a single maximum at 132.16. Accordingly, the appearance of two maxima in the longer wave-lengths may be attributed to the entrance of ligand X into the coordination sphere.

Configuration of the Complexes.—Now, we are in a position to discuss the configuration of the complexes. So far as the absorption spectrum of the blue Co-EDTA complex is concerned, the maximum of the first band is shifted bathochromically to a considerable degree as is seen in Fig. 3d. If the complex in question is hydroxo- or aquo-complex including ethylenediaminetetraacetate anion as a pentadentate ligand, the absorption maximum will be shifted hypsochromically from the maximum of common complex according to the empirical rule of "spectrochemical series". Therefore we regard this blue

4) Y. Shimura and R. Tsuchida, This Bulletin, 28, 572 (1955).

* Private information from Dr. Y. Shimura.

complex as a modification of Co(III)-EDTA complexes in which ethylenediaminetetraacetate anion acts as a hexadentate ligand.

In a previous paper[5], the authors reported the synthesis of a blue and a violet variety of $K[Co(NH_3)_2(CO_3)_2]\cdot H_2O$ and assumed *cis*-form for the former and *trans*-form for the latter. Comparison of the absorption spectra of these complexes with those of the complexes obtained in the present work showed that the maxima of the first and second bands of the two blue complexes occupied similar positions and that the same thing was true about the two violet complexes (for blue Co (III)-EDTA; 51.7 ($\times 10^{12}$/sec.), 77.9; for blue-$[Co(NH_3)_2(CO_3)_2]$, 52.2, 76.8; for violet-[Coedta], 55.9, 78.5; for violet-$[Co(NH_3)_2(CO_3)_2]$, 55.5, 80.2).

By this analogy of the absorption maxima, therefore, it may be assumed that the blue complex has one configuration in which the two nitrogen atoms span in *cis*-positions of octahedron and the violet common complex has another configuration in which the two nitrogen atoms span in *trans*-positions. Of course, the regular octahedron will suffer considerable distortion in the latter configuration. Such hypothesis about the configuration of the common complex, however, gives us a convenient explanation for the origin of the absorption band in the ultraviolet region. Provided that the absorption band in the ultraviolet region—"the third band"—is due to negative ions coordinated in trans-positions, the appearance of two maxima in the absorption spectra of [Co(X) (edtaH)] can be understood by taking into consideration such configuration as is indicated in Fig. 5.

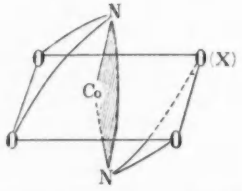

Fig. 5. Assumed configuration.

The present discussion of the configuration of "hexadentate" and "pentadentate" complexes is based on the assumption that the blue Co(III)-EDTA complex is a modification of "hexadentate" complex in spite of our failure to isolate this complex. Furthermore the dimentional restriction of the EDTA molecule makes it appear unnatural that the nitrogen atoms should span in trans-positions. Consequently, further studies must be carried out.

5) M. Mori, M. Shibata, E. Kyuno and T. Adachi, This Bulletin, 29, 883 (1956).

Summary

Two new compounds, $H[Coedta]\cdot 4H_2O$ and $Na[Co(Cl)(edtaH)]\cdot 2H_2O$ were synthesized, and their chemical formulae were confirmed by means of potentiometric titration and by examination of the infrared spectrum.

The absorption spectrum of $Na[Coedta]\cdot 4H_2O$ in solution was measured to investigate the pH effect. The absorption curves in acid solutions ($pH>2$) were wholly identical with that in aqueous solution of the salt, but those of alkaline solutions ($pH<10$) were not identical and further showed deviation from Beer's law.

The absorption curves of $Na[Co(NO_2)(edtaH)]\cdot H_2O$, $Na[Co(Br)(edtaH)]\cdot 2H_2O$ and $Na[Co(Cl)(edtaH)]\cdot 2H_2O$ were also measured. The first band for the chloro-complex and that for the bromo-complex occupied the similar position and shifted bathochromically as compared with the corresponding maximum for the common complex [Coedta]. These results may be explained on the basis of the so-called "spectrochemical series". The absorption spectra of the complexes [Co(X) (edtaH)] were found to have two absorption maxima in the ultraviolet region. This phenomenon may be attributed to the "trans effect" of negative ions.

By oxidation of an alkaline solution containing cobaltous and edta ions with hydrogen peroxide, a blue complex was produced. Although an attempt to isolate it ended in failure, existence of cobalt (III) complex containing hexadentate EDTA was assumed on the basis of the absorption spectrum.

The authors wish to express their sincere thanks to professor K. Yamazaki of Nagoya University for the measurement of the infrared spectra, and to Dr. Y. Shimura of Osaka University for his helpful advice.

Department of Chemistry, Faculty of Science, Kanazawa University
Kanazawa

By-products of Acrylonitrile Synthesis from Acetylene and Hydrocyanic Acid. II. Amines Obtained by Hydrogenation of Nitriles

By Shiro MORIMOTO

(Received April 21, 1956)

Introduction

In the previous paper[1], the presence of propionitrile, benzonitrile and naphthalene was confirmed and that of five olefinic nitriles, i. e., 1-cyanobutadiene, 2-cyanobutadiene, 1-cyanohexatriene, 2-cyanohexatriene, 3-cyanohexatriene, was suggested in the neutral by-products of acrylonitrile synthesis from acetylene and hydrocyanic acid.

The present paper deals with the comfirmation of these suggestions by means of the identification of the amines which were produced by the hydrogenation of the above mentioned by-products.

Results and Discussion

The neutral by-products of acrylonitrile synthesis were hydrogenated with Raney nickel. The hydrogenation products were divided into two parts, neutral and basic. The basic part was fractionated by distillation through a Stedman-type column. The results obtained are shown in Figs. 1 and 2. Thus the two constant boiling fractions were obtained, i. e., A–2 (b. p. 77–78.5°C) and A–7 (b. p. 103–106°C).

A–2 was treated with phenylisothiocyanate, resulting in the formation of crystals which melted at 61–61.5°C and were identified to be N, N′-*n*-butylphenylthiourea after a mixed melting point test. Treatment of A–7 with

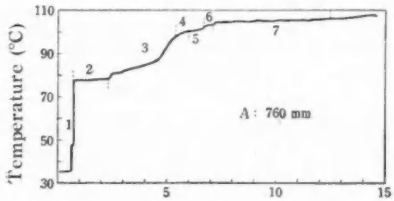

Fig. 1. Distillation curve of A-fractions.

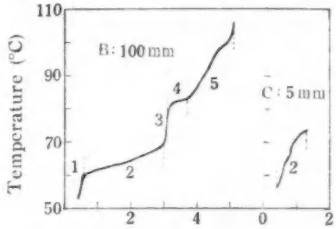

Fig. 2. Distillation curves of B- and C-fractions.

phenylisothiocyanate also gave crystals which melted at 62–63°C. The crystals were identified to be N, N′-*n*-amylphenylthiourea because the mixed melting point showed no depression. So it was confirmed that A–2 and A–7 contained *n*-butylamine and *n*-amylamine, respectively.

The paperchromatograms of hydrochlorides of A–3, A–4, B–2, B–4, B–5 and C–2 showed the presence of butylamines, amylamines, di-propylamine, heptylamines and benzylamine. But this method was not able to separate isomers mutually, i. e., 2-methylbutyl- from *n*-amyl-amine; 2-methylhexyl- and 2-ethylamyl- from *n*-heptyl-amine.

By the chromatography of N-2, 4-dinitrophenylamines (DNP-amines) on the column of cation exchanger the author[2] had already succeeded in separating isomers, i. e., DNP-isopropyl- from DNP-*n*-propyl-amine; DNP-isobutyl- from DNP-*n*-butyl-amine.

By the column-chromatography of DNP-derivatives of A–4, B–4, B–5 and C–2, the presence of *n*-butyl-, 2-methylbutyl-, *n*-amyl-, di-*n*-propyl-, benzyl- and *n*-heptyl-amines and two other primary heptylamines than *n*-heptylamine could be confirmed.

The amines which may be obtained by the hydrogenation of the above mentioned nitriles are as follows:

1) S. Morimoto, This Bulletin, 29, 450 (1956).

2) T. Seki and S. Morimoto, *J. Chm. Soc. Japan* (*Pure Chem. Sect.*), 77, 1124 (1956).

$CH_2=CH-CN$, CH_3-CH_2-CN $\longrightarrow$ $CH_3\cdot CH_2\cdot CH_2-NH_2$, $CH_3\cdot CH_2\cdot CH_2-NH-CH_2\cdot CH_2\cdot CH_3$

$CH_2=CH-CH=CH-CN$ $\longrightarrow$ $CH_3\cdot CH_2\cdot CH_2\cdot CH_2\cdot CH_2-NH_2$

$CH_2=CH-C(CN)=CH_2$ $\longrightarrow$ $CH_3\cdot CH_2\cdot CH(CH_3)\cdot CH_2-NH_2$

$CH_2=CH-CH=CH-CH=CH-CN$ $\longrightarrow$ $CH_3\cdot CH_2\cdot CH_2\cdot CH_2\cdot CH_2\cdot CH_2\cdot CH_2-NH_2$

$CH_2=CH-CH=CH-C(CN)=CH_2$ $\longrightarrow$ $CH_3\cdot CH_2\cdot CH_2\cdot CH_2\cdot CH(CH_3)\cdot CH_2-NH_2$

$CH_2=CH-CH=C(CN)-CH=CH_2$ $\longrightarrow$ $CH_3\cdot CH_2\cdot CH_2\cdot CH(C_2H_5)\cdot CH_2-NH_2$

$\longrightarrow$

The two primary heptylamines other than *n*-heptylamine are possibly 2-methylhexyl- and 2-ethylamyl-amines which may be obtained from 2-cyanohexatriene and 3-cyanohexatriene, respectively.

These facts confirmed the suggestions described in the previous paper. The presence of *n*-butylamine may be explained by the formation of allylcyanide, since the formation of acetonitrile from acetylene and hydrocyanic acid was confirmed in the author's other experiment[3].

Experimental

1. Catalytic Hydrogenation of the Neutral By-products.—The neutral part[1] (109 g.) of by-products which were obtained as the intermediate distillation fraction between acrylonitrile and succinodinitrile was hydrogenated with Raney nickel under the condition shown in Table I.

TABLE I

HYDROGENATION OF THE NEUTRAL BY-PRODUCTS OF ACRYLONITRILE SYNTHESIS

Inhalt of stainless steel autoclave, 330 cc.

Expt. No.	Starting material g.	Catalyst (Alloy) g.	Press. atm.	Temp. °C	Time min.	Hydrogen absorbed mol.	Prod. g.
1	29	5	80–20	130	220	0.90	27
2	80	5	86–18	120	326	1.95	79

TABLE II

FRACTIONAL DISTILLATION OF BASIC HYDROGENATION PRODUCTS

No.	Temp. °C	Distillate cc.	No.	Temp. °C	Distillate cc.
A-Fractions (760 mmHg)			B-Fractions (100 mmHg)		
1	35–47.5	0.7	1	45–59.8	0.6
2	77–78.5	1.6	2	59.9–69.0	2.4
3	79–97.2	3.1	3	69–69.5	0.1
4	97.2–100	0.6	4	77–82.8	0.6
5	100–102	0.7	5	83.4–104.7	1.4
6	102–103	0.4			
7	103–106	5.4	C-Fractions (5 mmHg)		
8	106–107	2.2	1	–56.7	0.4
			2	58–73.5	0.9
			3	74	

The hydrogenation products (106 g.) were dissolved in the same amount of ether and treated with aq. hydrochloric acid solution, resulting in the separation of 11.2 cc. (containing ether and water) of the neutral part and 51 cc. (containing ether and water) of the basic part.

This basic part (51 cc.) was fractionated by distillation through a Stedman-type column (with stainless steel net; plate number 14–18) under different pressures successively: A, 760 mmHg; B, 100 mmHg; C, 5 mmHg; and the results are shown in Table II.

2. N,N'-Alkylphenylthiourea.—To 0.5 cc. of the constant boiling fraction A-2 (b. p. 77–78.5°C), 1 cc. of phenylisothiocyanate was added (exothermic) to form a very viscous liquid. After an addition of petroleum ether, the mixture was allowed to stand for several days to form crystals. These crystals were filtered and melted at 61–61.5°C, after recrystallization from benzene and petroleum ether. Yield 0.1 g. These crystals mixed with N,N'-*n*-butylphenylthiourea (m. p. 65°C[4]) melted at 62.5–63°C, showing no melting point depression.

Anal. Found: C, 63.71; H, 7.46; N, 13.21. Calcd. for $C_{11}H_{16}N_2S$: C, 63.42; H, 7.74; N, 13.44%.

From the mixture of 0.5 cc. of the constant boiling fraction A-7 (b. p. 103–106°C) and 1 cc. of phenylisothiocyanate, 0.1 g. of crystals were obtained, and melted at 62–63°C. These crystals mixed with N,N'-*n*-amylphenylthiourea (m. p. 68–69°C[4]) melted at 65–68°C, showing no melting point depression.

Anal. Found: C, 65.04; H, 8.13; N, 12.53. Calcd. for $C_{12}H_{18}N_2S$: C, 64.81; H, 8.16; N, 12.60%.

3. Paperchromatography of Amine Hydrochlorides.—The paperchromatograms of hydrochlorides of A-3, A-4, B-2, B-4, B-5 and C-2 are shown in Fig. 3.

4. Chromatographic Separation of DNP-Amines on the Column of Cation Exchange Resin.—The aqueous solution of hydrochloride of A-4, B-4, B-5 or C-2 (5–10 cc., containing 0.3–4.0 mg.), the same amount of acetone, 1 cc. of acetone solution of 1-fluoro-2,4-dinitrobenzene

3) S. Morimoto, To be published.

4) Otterbacher and Whitmore, *J. Am. Chem. Soc.*, **51**, 1909 (1929).

TABLE III

MELTING POINTS AND ANALYTICAL RESULTS OF DNP-AMINES

DNP-Amine	Melting point Found °C	Melting point Literat. °C	Analytical results (%) Found C	Found H	Found N	Calcd. C	Calcd. H	Calcd. N
-benzyl-	115–6	115–6[5] 126[5']	57.30	4.78	15.75	57.14	4.06	15.38
-*n*-heptyl-	22–3	20[5]	55.64	6.61	15.33	55.50	6.81	14.94

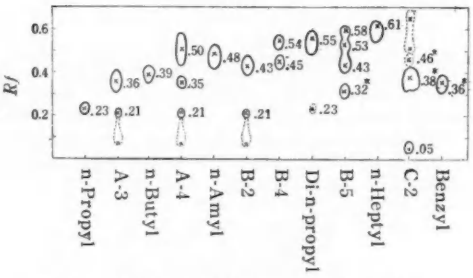

Fig. 3. Paperchromatograms of hydrochlorides of amines.
Developer, Butanol satuarated with water.
*yellow→purple

(FDNB) containing 0.02 g./cc.) and 1 cc. of 2% aqueous sodium bicarbonate solution were mixed and shaken for four hours. Then 1 cc. of aqueous solution of glycine and sodium carbonate (containing 0.008 g. glycine and 0.02 g. sodium carbonate per cc.) was added to the mixture and the resulting mixture was shaken for two more hours. After acetone was evaporated off under reduced pressure, the reaction mixture was extracted with ether three times. From the ether solution, ether was evaporated off under reduced pressure. The residue was dissolved in ten cc. of the mixed solvent (tetrahydrofuran, methylethylketone and water, 4:3:13). Two cc. of the solution was charged on the column (9×400 mm.) of cation exchanger, Amberlite IRC 50 (H-type), and developed with the same solvent.

An ultraviolet spectrophotometer was used to detect and estimate DNP-amines in effluents, taking advantage of the characteristic ultraviolet absorption at 360 mμ. The elution curves are shown in Figs. 4-7. The peaks a, b, c, d, g and h in these figures were identified to be those of DNP-*n*-butyl-, DNP-2-methylbutyl-, DNP-*n*-amyl-, DNP-di-*n*-propyl, DNP-*n*-heptyl- and DNP-benzylamines, by compareing with those of the standard samples, respectively. The peaks e and f are considered to be those of DNP-derivatives of two other primary heptylamines than *n*-heptylamine on the basis of their retention volumes.

5. Preparations of the Standard Samples of DNP-Amines.—N-2, 4-Dinitrophenyl-2-methylbutylamine.—To 30 cc. of aqueous solution containing 0.3 g. of 2-methylbutylamine hydrochloride and 0.6 g. of sodium bicarbonate, 35 cc. of alcoholic (or acetone) solution containing 0.5 g. of FDNB was added and allowed to stand over night in a refrigerator. The oil separated by decantation from the supernatant was dissolved in 30 cc. of alcohol (or acetone). To the solution, 16 cc. of water was added and allowed to stand over night to form 0.35 g. of crystals. The crystals were recrystallized from 25 cc. of alcohol (or acetone) and 11 cc. of water to form 0.3 g. of crystals which melted at 47.3–48°C.

Anal. Found: C, 52.10; H, 5.87; N, 16.87. Calcd. for $C_{11}H_{15}N_3O_4$: C, 52.17; H, 5.97; N, 16.59%. This substance has not been reported in literature up to this time.

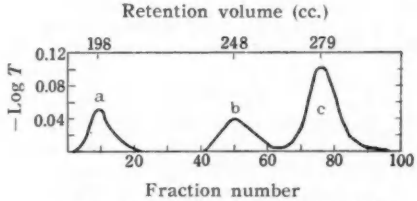

Fig. 4. Elution curve of DNP-A-4
one fraction=1.2 cc.

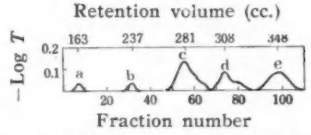

Fig. 5. Elution curve of DNP-B-4
one fraction=1.7 cc.

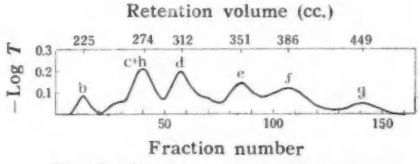

Fig. 6. Elution curve of DNP-B-5
one fraction=1.75 cc.

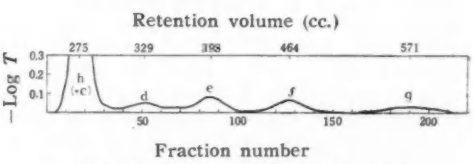

Fig. 7. Elution curve of DNP-C-2
one fraction=1.7 cc.

5) A. Mulder, *Rec. trav. chim. Pay-Bas*, **25**, 111 (1906); H. J. Backer, ibid., **70**, 92 (1951).
5') G. T. Morgan, *J. Chem. Soc.*, **1915**, **107**, 1307.
6) E. J. Van der Kam, *Rec. trav. chim. Pay-Bas*, **45**, 722 (1926).

By the same way, DNP-benzylamine and DNP-*n*-heptylamine were prepared. Their melting points and analytical results are shown in Table III.

The reaction products of di-*n*-propylamine with FDNB did not solidify by the same way. But the sample showed an unique chromatographic band on the column except for DNP-*n*-propylamine. Thus the sample was employed as a qualitative standard.

The preparations of DNP-derivatives of *n*-propyl-, *n*-butyl- and *n*-amyl-amine were reported in the author's other paper[2].

Summary

The basic substances were obtained from the hydrogenation products of the neutral by-products of acrylonitrile synthesis from acetylene and hydrocyanic acid. They were fractionated by distillation through a Stedman-type column. *n*-Butylamine and *n*-amylamine were isolated and identified as derivatives of phenylthiourea. On the basis of chromatograms, i.e., the paperchromatograms of hydrochlorides of amines and chromatograms of N-2,4-dinitrophenyl-derivatives on the column of cation exchanger, the presence of seven amines, i.e., *n*-propyl-, *n*-butyl-, 2-methylbutyl-, *n*-amyl-, di-*n*-propyl-, *n*-heptyl- and benzyl-amines was confirmed and that of two primary heptylamines other than *n*-heptylamine, i.e., 2-methylhexyl- and 2-ethylamyl-amines, was suggested.

Heartfelt thanks are to be returned to Professors Shiro Akabori and Shunsuke Murahashi of Osake University for their kind instruction and suggestions; and to Kazuo Adachi and Masamichi Miura for their helpful technical assistance.

Department of Chemistry, Faculty of Science, Osaka University, Osaka

---

Spectrochemical Study of Microscopic Crystals. XIII[1]. *The Structure of Wolffram's Red Salt,* $Pt(NH_2 \cdot C_2H_5)_4Cl_2 \cdot 2H_2O$ *and a Related Compound*[2]

By Shoichiro YAMADA and Ryutaro TSUCHIDA

(Received July 11, 1956)

Formerly the present authors studied the polarized absorption spectra of those compounds involving apparently tervalent platinum or palladium which display extraordinarily deep colours[1,3]. It was found in the earlier studies[3] that some of the above compounds have chains consisting of platium or palladium atoms in different oxidation states connected through halide ions and that the formation of the chains gives rise to a characteristic charge transfer absorption polarized along the chains. Wolffram's red salt, $Pt(EA)_4Cl_3 \cdot 2H_2O$[4], which contains a platinum atom in an apparently tervalent state, may be supposed to belong to a similar type of compound[3]. This compound was first synthesized by Wolffram[5], who obtained the red crystals of this compound by oxidizing an aqueous solution of tetrakis-(ethylamine)-platinum(II) chloride, $Pt(EA)_4Cl_2$, with hydrogen peroxide. Much later Reihlen and Flohr[6] considered the compound as containing divalent and quadrivalent platinum atoms, and ascribed the unusually deep colour of the compound to a special structure of the crystal lattice, which, however, was not explained at all. On the contrary, Drew and Tress[7] attempted to explain the deep colour of this compound on the assumption that the compound might involve a tervalent platinum atom. Establishing the diamagnetism of this compound, Jensen showed that the compound did not involve the platinum in the tervalent state. The deep colour of this compound, however, was still left unexplained[8].

The present work was undertaken in order to explain the color of Wolffram's salt and a related compound in relation to the structure and the probable aid in the comprehension of the charge transfer spectra.

1) Part XII of this series, S. Yamada and R. Tsuchida, This Bulletin, 29, 694 (1956).
2) Presented in part before the ninth annual meeting of the Japan Chemical Society, Kyoto, April 2nd, 1956.
3) R. Tsuchida and S. Yamada, *Nature*, 174, 1064 (1954); This Bulletin, 29, 421 (1956).
4) The notation, A, denotes a molecule of ethylamine.
5) H. Wolffram, Dissertation Königsberg, 1900.
6) H. Reihlen and E. Flohr, *Ber.*, 67, 2010 (1934).
7) H. D. K. Drew and H. J. Tress, *J. Chem. Soc.*, 1935, 1244.
8) K. A Jensen, *Z. anorg. allgem. Chem.*, 229, 252 (1936).

Experimental

Materials.—Tetratkis-(ethylamine)-platinum (II) chloride dihydrate was prepared according to the method of Reihlen and Flohr[5] as colourless crystals. The absorption spectrum was determined with the aqueous solution.

Dichloro-tetrakis-(ethylamine)-platinum(IV) chloride dihydrate was prepared by the method of Reihlen and Flohr[5] in pale-yellow crystals. The crystals of the compound are quite stable in the dark, but undergo decomposition on irradiation of ultra-violet light to form a red compound. The aqueous solution of the compound is rather stable in the light. The absorption spectrum was determined in an aqueous solution.

Wolffram's red salt, $Pt(ethylamine)_4Cl_3 \cdot 2H_2O$, was obtained by the method of Reihlen and Flohr[5] from $[Pt(EA)_4]Cl_2$ and $[Pt(EA)_4Cl_2]Cl_2$. Red crystals of the compound thus obtained show a striking dichroism; they are dark-red with polarized light having its electric vector along the needle axis and almost colourless with polarized light having its electric vector normal to the needle axis. The measurement of the dichroism was carried out along the above two directions.

Tribromo-tetrakis-(ethylamine)-platinum dihydrate, $Pt(EA)_4Br_3 \cdot 2H_2O$, was obtained by the method of Reihlen and Flohr from Wolffram's red salt. Green crystals thus obtained show a striking dichroism; they are dark-green with polarized light having its electric vector along the needle axis, and pale yellow with the electric vector normal to the needle axis. The measurement of the polarized absorption spectra was carried out in these two directions.

Dibromo-tetrakis-(ethylamine)-platinum (IV) bromide, $[Pt(EA)_4Br_2]Br_2$, was prepared in orange, crystalline powder by treating an aqueous solution of $[Pt(EA)_4]Cl_2$ with an excess of hydrogen peroxide and concentrated hydrobromic acid. The absorption spectrum was determined in an aqueous solution.

Measurement.—Quantitative measurements of absorption spectra of the crystals were made by Tsuchida—Kobayashi's microscopic method[9] with polarized light in the regions covering 2400 to 7500 Å. The notation, α, represents the absorption coefficient per mm. of a crystal. The c- and a-absorption denotes absorption with the electric vector parallel and normal to the needle axis, respectively.

Absorption spectra in solution were determined with a Beckman DU quartz-spectrophotometer. The symbol, ε represents a molar extinction coefficient.

Results and Discussion

Structure of Wolffram's Red Salt.—It seems to be obvious that Wolffram's salt, $Pt(EA)_4Cl_3 \cdot 2H_2O$, contains platinum atoms in bi- and quadri-valent states, but not the tervalent state, since the compound in its crystalline state proved to be diamagnetic[8]. The compound is obtained when evaporating a mixed solution of $[Pt(EA)_4]Cl_2$ and $[Pt(EA)_4Cl_2]Cl_2$. The red crystals of the compound dissolve in water to give a colourless solution from which the red crystals of the original compound separate out on cooling. All these facts indicate that Wolffram's salt may be formulated as $[Pt(EA)_4][Pt(EA)_4Cl_2]Cl_4 \cdot 4H_2O$.

Polarized absorption spectra of Wolffram's red salt in the crystalline state and absorption spectra of the component complexes in aqueous solution have been determined in the visible and ultra-violet region, and are shown in Fig. 1. It is seen from the curves that

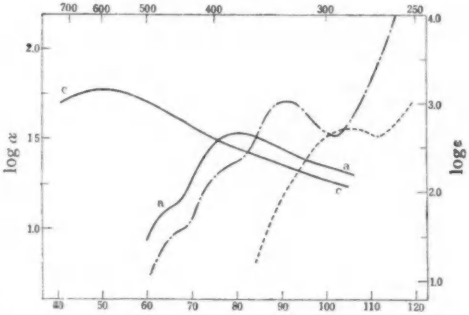

Fig. 1. Absorption spectra of $[Pt(EA)_4][Pt(EA)_4Cl_2]Cl_4 \cdot 4H_2O$ in the crystalline state (———), $[Pt(EA)_4]Cl_2$ in solution (– – – –) and $[Pt(EA)_4Cl_2]Cl_2$ in solution (·—·—).

$[Pt(EA)_4]Cl_2$ or $[Pt(EA)_4Cl_2]Cl_2$ does not show absorption in the visible region, only the tail of the latter absorption extending into the end of the visible region. Comparison of the absorption spectra of Wolffram's salt with those of the component complexes indicates that Wolffram's salt shows to the long wavelength side a new absorption band which is not observed with either of the component complexes alone. This fact implies that the component complexes in the crystal of Wolffram's salt undergo some great effect which does not exist in either of the component complexes alone. The nature of the effect may be judged from the polarization property of the new band at the long wavelength. The present measurement shows that the absorption occurs only with the electric vector along the needle axis, and does not with the electric vector normal to the needle axis. This relationship may be readily understood on the assumption that Wolffram's salt involves infinite chains consisting of the com-

9) R. Tsuchida and M. Kobayashi, "The Colours and the Structures of Metallic Compounds," Zōshindo, Osaka (1944), p. 180; This Bulletin, 13, 619 (1938).

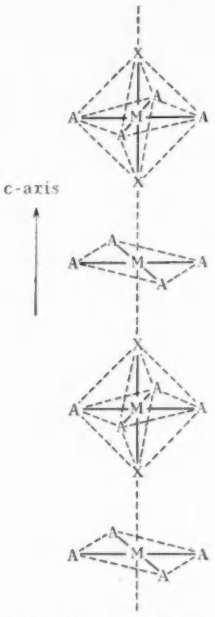

Fig. 2. Chain structure in the crystals of Wolffram's red salt and a related compound having the empirical formula, $Pt(EA)_4X_2 \cdot 2H_2O$.

ponent complexes arranged so that they are piled one just above another along the needle axis (Fig. 2).

In our former studies on the compounds of apparently tervalent platinum and palladium which display unusually deep colours, it was shown that some of those compounds involve infinite chains consisting of the metal atoms in two different oxidation states connected through halogen atoms, and that the chains give rise to a new kind of absorption polarized along the chains. This is quite similar to the relationships which are obtained with Wolffram's salt in the present work. Thus we are led to the conclusion that *the extraordinarily deep colour of Wolffram's salt in the crystalline state is due to the structure containing the infinite chains*, ---Cl—Pt^{IV}—Cl---Pt^{II}---Cl—Pt^{IV}—Cl---.

The new absorption observed with Wolffram's red salt at the longer wave-length, which has been assumed to be originated from the infinite chains, as shown above, may be considered as due to a charge transfer along the chains.

It was concluded in our former researches[2] that the crystal of [Pt en Cl_2][Pt en Cl_4][10], which has an unusually deep colour as compared with the colours of its component complexes, involves similar chains of ---Cl—Pt^{IV}—Cl---Pt^{II}---Cl—Pt^{IV}—Cl---, along which the crystals show a characteristic charge transfer band at about 59×10^{13}/sec. Wolffram's salt involving similar chains shows a charge transfer band at about 58×10^{13}/sec. Comparing the two compounds, the platinum atoms are co-ordinated through chloride ions and/or nitrogen atoms in both the compounds, and the difference between the two may be expected to be rather small, as far as the electronic state along the infinite chains is concerned. In fact, the charge transfer absorption characteristic of the infinite chains are observed at about the same wave-length. This also seems to support the above assumption of the chain structure.

It was formerly proposed that the compounds with apparently tervalent platinum and palladium which are dealt with in the present and former papers of this series might be dinuclear complexes of such a type as are represented by (1)[11]:

$$\left[A_4Pt^{II}\begin{matrix}X\\X\end{matrix}Pt^{IV}A_4\right]^{4+} \rightleftharpoons \left[A_4Pt^{IV}\begin{matrix}X\\X\end{matrix}Pt^{II}A_4\right]^{4+}. \qquad (1)$$

The evidence for this view, however, seems to be very insufficient. Since bivalent platinum usually assumes planar co-ordination, the supposed 6-co-ordination of the bivalent platinum is unusual. It may be impossible to suppose that the bivalent platinum should take octahedral 6-co-ordination which is equivalent to the octahedral co-ordination around the quadrivalent platinum so that the above resonance (1) might be allowed. The spectroscopic studies into polynuclear complexes, which will be reported elsewhere[12], indicate that the dibridged polynuclear complexes in general do not show their absorption in the wave-length regions much longer than the related monomeric compounds. Nor do they show any charge transfer band of the above sort. All these considerations, together with the X-ray structure analysis of a similar compound of tervalent platinum, $Pt(NH_3)_3Br_3$,

10) The notation, en, denotes a molecule of ethylenediamine.

11) See, for example, N. V. Sidgwick, "The Chemical Elements and Their Compounds. Vol. II". Oxford Univ. Press, London (1952), p. 1605, etc.

12) The work is concerned with halogen-bridged complexes: R. Tsuchida and S. Yamada, To be submitted soon.

seem to support our view that the appearance of a new absorption band at the long wave-length and the remarkable polarization of this new band along the *c*-axis in the crystal of Wolffram's red salt may be explained by the assumption of the infinite chains much better than by the model of the dinuclear complex.

In the coure of the present study, we have found that the crystal of $[Pt(EA)_4Cl_2]Cl_2 \cdot 2H_2O$ undergoes photo-decomposition with ultra-violet light. Thus on evaporating spontaneously an aqueous solution of $[Pt(EA)_4Cl_2]Cl_2$ in a sunny room, a small amount of Wolffram's salt is formed besides the crystals of the original compound. The compound, however, is quite stable to the visible light. On irradiating the crystal with a powerful tungsten lamp at a close distance, no decomposition has been observed. On the contrary, when the crystal was put into the light beam from the iron arc, photo-decomposition was found to take place in a few minutes, the crystal beginning to turn red. Observed under the microscope, red spots are formed here and there in the crystal, the spots getting larger and the number of the spots increasing. The red spots might possibly be due to the photo-reduction of the compound, followed by formation of the chain structure, which would be similar to Wolffram's salt. Thus we suppose the main change might be what follows:

$$[Pt(EA)_4Cl_2]^{2+} \xrightarrow{h\nu} [Pt(EA)_4]^{2+} + Cl_2. \quad (2)$$

This change seems to be rather incomplete in an aqueous solution. After the aqueous solution of the compound is exposed to the sun for scores of hours, the absorption spectrum is found to be slightly different from the absorption of the original compound before the irradiation. Thus the absorption at 76.8×10^{13}/sec. diminishes its intensity. This may be explained as due to the decomposition of $[Pt(EA)_4Cl_2]^{2+}$ and subsequent formation of the $[Pt(EA)_4]^{2+}$ ion, since the former has an absorption band at this wave-length whereas the latter shows no absorption at the same wave-length. A rough estimation indicates that about twenty percent of the original compound has undergone the photo-reduction after the exposure of the solution to the sun for about one hundred hours.

It was suggested in the former papers[3] that the formation of the infinite chains as assumed for Wolffram's salt would stabilize some complex radicals which would other-wise be rather unstable. In fact, the complex ion, $[Pt(EA)_4Cl_2]^{2+}$, in the crystal of Wolffram's salt is far more stable to the photo-decomposition than in the crystal of dichloro-tetrakis-(ethylamine)-platinum (IV) chloride. Thus Wolffram's salt does not undergo any change after irradiation with the iron arc for many hours. In the crystal of Wolffram's salt, the approach of the chloride ion in $[Pt(EA)_4Cl_2]^{2+}$ to the platinum(II) ion of an adjacent complex radical may partly diminish the negative charge on the chloride ion, suppressing the charge transfer from the chloride to the platinum(IV) ion, which is the reaction represented by (2). This also is an example of the stabilization of the otherwise unstable complex ions due to their incorporation into the chain structure[3].

There is known a similar type of compounds, such as $Pt(NH_3)pyCl_3$[13], $Pt(NH_3)(EA)Br_3$ and $Pt(NH_3)(EA)Cl_3$[14]. These compounds, which contain apparently tervalent platinum and show quite deep colours, may be believed to have a chain structure similar to that of Wolffram's salt. The unusually deep colour of those compounds may probably be due to the infinite chains in the crystalline state.

Structure of Reihlen's Green Salt.—On adding potassium bromide to a luke-warm, aqueous solution of Wolffram's salt, there are formed slender, green needles[3,15], which have an empirical formula, $Pt(EA)_4Br_3 \cdot 2H_2O$, analogous to that of Wolffram's red salt. Just as in the case of Wolffram's red salt, the crystals of the compound, Reihlen's green salt, dissolve in water to give an orangish-yellow solution, from which the green crystals of the original compound separate out on cooling. From these facts, it is supposed that this compound in the crystalline state may involve a structure similar to that of Wolffram's red salt, being formulated as $[Pt(EA)_4][Pt(EA)_4Br_2]Br_4 \cdot 4H_2O$.

Polarized absorption spectra of this compound have been determined, and shown in Fig. 3. It is seen from this measurement that this compound in the crystalline state shows to the long wave-length side a new absorption band, which may not be observed with the component complex ions alone. This shows that the complex ions in this crystal are subject to some effect. The present measurement also indicates that the new absorption band at the long wave length occurs only with the electric vector along the needle-axis, and not with the electric vector normal to the needle-axis. These re-

13) H. D. K. Drew, F. W. Pinkard, W. Wardlaw and E. G. Cox, *J. Chem. Soc.*, **1932**, 1004. The symbol, py, denotes a molecule of pyridine.

14) S. M. Jörgensen, *J. prakt. Chem.*, **33**, 489 (1886), etc.

15) The green compound is referred to tentatively as Reihlen's green salt in the present paper.

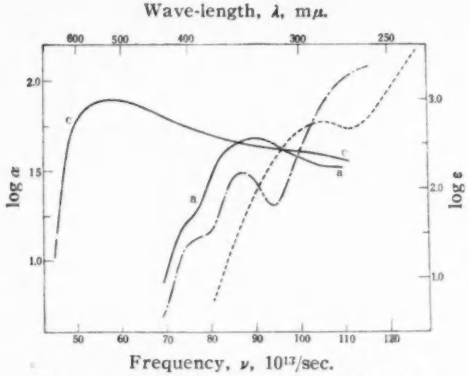

Fig. 3. Absorption spectra of $[Pt(EA)_4][Pt(EA)_4Br_2]Br_4 \cdot 4H_2O$ in the crystalline state (———), $[Pt(EA)_4]Cl_2$ in solution (– – – –) and $[Pt(EA)_4Br_2]Br_2$ in solution (·—·—·).

lationships, which are quite similar to those obtained with Wolffram's red salt, may be understood if we assume that the crystal of this compound involves a structure similar to Wolffram's red salt. Thus we are led to the presumption that the compound in the crystalline state contains infinite chains of ---Br—Pt^{IV}—Br---Pt^{II}---Br—Pt^{IV}—Br---. The absorption at about 51×10^{13}/sec. may possibly be due to the charge transfer along the infinite chains. It is concluded that *the deep colour of this compound is due to the formation of the infinite chains which are similar to those in the crystal of Wolffram's red salt.*

Charge Transfer Spectra.—It has been shown in the above discussion that the compounds with infinite chains of the above kind exhibit in the long wave-length regions charge transfer spectra which are polarized along the chains. Reviewing the data so far obtained, the following relationships on the charge transfer spectra may be derived. (1) *The charge transfer spectrum seems to be unrelated to the spectrum of both the components alone.* (2) *The spectrum is rather intense and broad.* (3) *The spectrum is strongly polarized along the infinite chains. That is, the spectrum is observed only with the electric vector along the infinite chains.*

These relationships are found to be consistent with the theory of the charge transfer spectra recently developed by Mulliken[16].

It is to be noted that the absorption normal to the infinite chains has in the long wave-length a shape similar to the superposition of the absorption spectra of the component complexes in solution. This fact seems to indicate that the absorption normal to the infinite chains may be more closely related to the linkages in the complex radicals.

Comparing the two compounds dealt with in the present work, it is seen that Reihlen's green salt shows its charge transfer band in the longer wave-length regions than the chlorine analogue, Wolffram's red salt. The difference in the wave-length of the charge transfer band between the two is found to be nearly equal to the difference in the ionization potential between the chlorine and bromine. This may also be explained on the basis of the assumption that the charge transfer takes place from the halide to platinum(II) ions.

Summary

Polarized absorption spectra of Wolffram's red salt, $Pt(EA)_4Cl_3 \cdot 2H_2O$, and a related compound, $Pt(EA)_4Br_3 \cdot 2H_2O$, EA being ethylamine, have been determined by Tsuchida-Kobayashi's microscopic method in the regions covering from 2400 to 7500 Å.

Both the compounds, which are supposed to be formulated by $[Pt(EA)_4][Pt(EA)_4X_2]X_4 \cdot 4H_2O$, have been found to show an absorption band that has not been observed with either of the components alone. Moreover, this band is strongly polarized along the needle axis. These relationships may be understood on the assumption that the crystals of these compounds involve infinite chains of ---X—Pt^{IV}—X---Pt^{II}---X—Pt^{IV}—X--- along the needle axis, X being chlorine or bromine.

The new absorption at the longer wave-length may be considered as a charge transfer band along the infinite chains as assumed above.

The present authors are indebted to Mr. H. Nakamura for assistance in the experimental work. The work reported here was supported by the grant in aid of the ministry of Education.

Department of Chemistry, Faculty of Science, Osaka University, Osaka

16) R. S. Mulliken, *J. Am. Chem. Soc.*, **72**, 600 (1950); **74**, 811 (1952). *J. Phys. Chem.*, **56**, 801 (1952).

Irreversible Photobleaching of the Solution of Fluorescent Dyes. II. Photobleaching of the Alcoholic Solution of Eosine in Vacuo

By Masashi IMAMURA and Masao KOIZUMI

(Received July 9, 1956)

Introduction

In the first paper of this series[1] kinetic studies on the photobleaching of eosine, erythrosine and uranine in aqueous solutions in the presence of oxygen were reported and some probable schemes were proposed for the primary processes of the reaction. In that paper the notable fact was found that the addition of ethyl alcohol to the aqueous solution of eosine caused a marked retardation on the rate of aerobic photobleaching. Thus in the mixture of water and ethyl alcohol 7: 3 in volume, the rate became practically negligible and in the pure alcoholic solution there was no photobleaching observed. But another remarkable fact then found was that if such solutions are deaerated, considerable rapid photobleaching takes place in contrast to the pure aqueous solution which shows no such photobleaching in vacuo at all.

Though it appears that the vacuum photobleaching (in alcohol) and the aerobic photobleaching (in aqueous solution) will proceed by different mechanisms, it is interesting to study about the primary processes of the former and about the retarding effect of oxygen. Moreover, it is not unexpected that the information obtained therefrom may be helpful for the further attack on the primary processes of the aerobic photobleaching in the pure aqueous solution.

The purpose of the present paper is to report some results obtained using methyl, ethyl, isopropyl and *n*-butyl alcohol as solvents and to make some discussions on the mechanism of the reaction.

Experimental

Procedure.—Eosine and the arrangements for irradiation were the same as those described previously[1,2]. Methanol, ethanol, isopropanol and *n*-butanol were purified by the method similar to that employed in the preceding paper for ethanol. Stock solutions of eosine in these alcohols were prepared at concentration of 10^{-3} mol./l. These solutions were diluted to the concentration of 10^{-5} mol./l. and were deaerated with much caution in view of the high solubility of oxygen in alcohols. The procedure was as follows. The solution was put into one of two ampoules attached to a reaction cell and was evacuated under cooling with use of a mercury diffusion pump. Then the alcohol was distilled into another ampoule and evacuated again. These processes were repeated four to six times.

Irradiated alcoholic solution of eosine in vacuo did not show any shift of the absorption maxima as compared with the initial solution, and the almost perfect absorption curve in visible region declined monotonously as the bleaching went on. Hence the change of the concentration of eosine could be followed by a photomultiplier and an interference filter in exactly the same way as described already[1,2].

Experiments were made on the oxygen effect on the rate, with use of the apparatus schematically shown in Fig. 1. At first, complete deaeration was accomplished by repeated vacuum distillation between E and F. Then a definite small amount of oxygen was taken between A and B manometrically and it was expanded to the right hand side of B, in which the solution F was being cooled with dry ice. (The volume of these two parts had been determined previously.) The oxygen pressure after expansion could easily be calculated. After C was fused off, oxygen was dissolved at room temperature into the solution, which was then poured into the cell, and D was fused off. Of course all the manipulations were made in the dark. The amount of oxygen in a reaction cell was calculated, employing the value

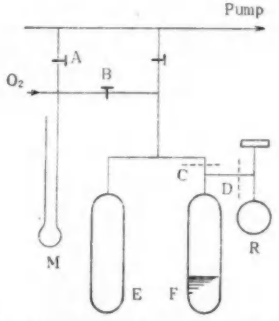

Fig. 1. Schematic diagram of the apparatus. M: manometer; R: reaction cell.

1) M. Imamura and M. Koizumi, This Bulletin, 28, 117 (1955).
2) M. Imamura, *J. Inst. Polytech. Osaka City Univ.*, 6, No. 1, Series C, 85 (1956).

of 0.14 as a Bunsen coefficient[3] for pure ethanol. and taking into account the volume of the solution and that of the gaseous phase.

Results

1. Photobleaching of the Alcoholic Solutions in Vacuo.—Investigations were carried out at 20°C with a filter Matsuda VGl. The intensity of light was varied with blackened metallic nets.

The rate of bleaching was relatively great compared with that of aerobic aqueous solution. Some examples of the bleaching curve are shown in Fig. 2, which includes a curve for the aerobic photobleaching of the aqueous solution for comparison. Absorption spectra of the irradiated solution are compared with the original one in Fig. 3.

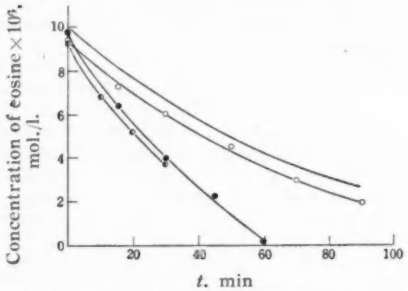

Fig. 2. Fading curves of eosine in vacuo at 20°C.

Full line: in aerobic aqueous solution, $I_0=1.74\times10^{15}$ $h\tilde{\nu}$/cm². sec.; ○: in methanol, $I_0=1.18\times10^{15}$ $h\mu$/cm². sec., ●: in ethanol, $I_0=1.41\times10^{16}$, ◐: in isopropanol, $I_0=1.18\times10^{15}$. In all cases $d=15$ mm.

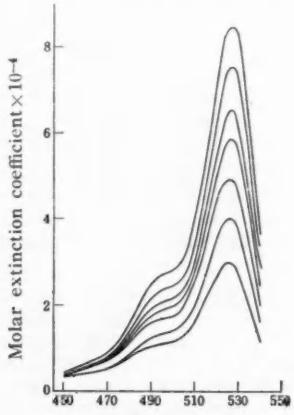

Fig. 3. Absorption spectra of irradiated eosine in EtOH in vacuo. At 34°C.

As anticipated from these figures, the experimental results obtained for every sort of alcohol except *n*-butanol could be represented satisfactorily by the same rate formula as that proposed in the previous paper[1].

$$-\frac{dc}{dt}=\frac{k}{d}I_0(1-e^{-\alpha cd})\times1000^* \tag{1}$$

$$S\equiv\ln(1-e^{-\alpha c_0 d})-\ln(1-e^{-\alpha cd})+\alpha d(c_0-c)=1000k\alpha I_0 t \tag{2}$$

where c and c_0 are the concentrations of dye in mol./l. at time $t=t$ and $t=0$, α the mean molar absorption coefficient, d the thickness of the solution in cm., I_0 the intensity of light in moles per cm² per sec., and k is the usual overall rate constant and is also considered as a quantum yield of bleaching. Mean molar absorption coefficients of eosine (α's) in methanol, ethanol, isopropanol were determined by a thermopile to be 4.8×10^4, 6.6×10^4, 6.1×10^4 and 5.2×10^4, respectively.

Some examples of the application of eq. (2) to the experimental results are shown in Fig. 4 and

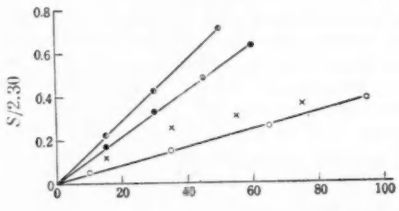

Fig. 4. Dependence of the left-hand side of eq. (2) divided with 2.30 (S/2.30) on irradiation time t. At 20°C.

○: in methanol, $I_0=0.69\times10^{15}$ $h\nu$/².cm sec.; ●: in ethanol, $I_0=0.83\times10^{15}$; ◐: in isopropanol, $I_0=0.69\times10^{15}$; ×: in *n*-butanol, $I_0=0.68\times10^{15}$.

TABLE I

QUANTUM YIELDS FOR PHOTOBLEACHING OF EOSINE IN MeOH, EtOH, AND i-PrOH AT 20°C

(k for aerobic photobleaching in aqueous solution is 1.8×10^4.)

Solvent	$I_0\times10^{15}$ $h\tilde{\nu}$/cm² sec.	$k\times10^4$	Solvent	$I_0\times10^{15}$ $h\tilde{\nu}$/cm² sec	$k\times10^4$
MeOH	0.69	5.3	EtOH	0.74	6.4
〃	〃	2.7	〃	0.83	4.4
〃	〃	4.0	〃	〃	4.6
〃	1.18	3.8	〃	1.25	5.4
〃	〃	3.7	〃	1.41	4.5
〃	〃	2.9	〃	〃	9.0
Average		(3.7)	Average		(5.6)
EtOH	0.35	4.2	*i*-PrOH	0.69	3.9
〃	0.39	4.3	〃	〃	7.4
〃	〃	4.5	〃	〃	7.8
〃	0.62	10.3	〃	1.18	4.6
〃	0.66	4.9	〃	〃	5.6
〃	〃	4.6	〃	〃	5.9
〃	0.74	6.4	Average		(5.9)
〃	0.83	4.4			

3) "International Critical Table", McGraw Hill, New York (1929), 3, p. 262.

the values of k's calculated are summarized in Table I. Though it is certain that eq. (1) can be applied to ethanol, methanol, and isopropanol, some fluctuations exist among the k-values of different runs. It may perhaps be due to the slight difference of the pretreatment of alcohols in view of the existence of the very sensitive effect of a trace of oxygen described below. In spite of these fluctuations, it is evident that the order of the rate of photobleaching in vacuo is MeOH< EtOH<i-PrOH. From the measurements made on the quantum yield of the ethanolic solution of eosine at various temperatures, it was found that the activation energy for the reaction in ethanol in vacuo was computed as 5 ± 1 kcal./mol., which is about the same as that obtained for aerobic aqueous solution of eosine[4].

As to the reaction products, qualitative tests of aldehyde and acid were applied to the vacuum distillate from the irradiated ethanolic solution of eosine.

Acidity was examined by a glass electrode pH meter and also by the spectroscopic measurements with some ordinary pH indicators. There was no change observed in pH.

Aldehyde, on the other hand, could be detected by every test employed, i.e., by Tollen's reagent (NH_3—$AgNO_3$ solution), by Schiff's reagent (reduced p-fuchsine solution) and by the method which utilized the catalytic action of aldehyde on the oxidation of p-phenylene diamin by hydrogen peroxide[4].

2. Effect of Small Amounts of Oxygen on the Photobleaching of Alcoholic Solution.—As mentioned above, aerobic pure alcoholic solution of eosine did not show any photobleaching. When a very small amount of oxygen was added to the completely evacuated solution, the photobleaching did not take place for a certain period which was almost proportional to the amounts of added oxygen, but after this induction period, the reaction began to proceed abruptly and with almost the same rate as that in the completely evacuated solutions.

Results are shown in Fig. 5, in which the number depicted along each curve is the oxygen pressure (mmHg) in the gaseous phase of a cell.

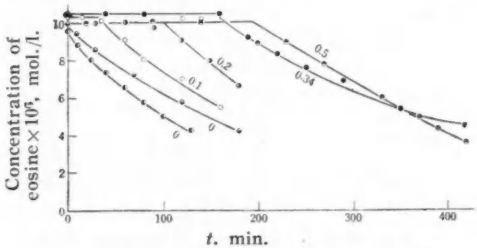

Fig. 5. Fading curves of eosine in EtOH in the presence of various amounts of oxygen. At 27°C.
The number depicted along each line is the oxygen pressure in mmHg. in the gaseous phase of a cell.

From the above results, there scarcely remains any doubt that a small amount of oxygen inhibits the photobleaching of eosine and this inhibiting action comes to its end when oxygen is used up by some unknown reaction. Thus it must be interpreted that during the induction period some photosensitized oxidation reaction is going on by virtue of eosine as a photosensitizer. As such a photosensitized oxidation, there will be no other possibility than that of the oxidation of alcohol to acid or aldehyde. Hence several tests for aldehyde and acid were tried for the irradiated aerobic alcoholic solution of eosine. The result was that the formation of aldehyde could not be detected by Tollens' and by Schiff's reagents, while the formation of acid was definitely established from the facts that reduction of pH could be observed by means of a glass electrode pH meter and by usual indicators spectroscopically.

Aldehyde would perhaps be oxidized to acid if it were produced, which was ascertained by an independent test that a small amount of aldehyde added to the aerobic alcohol solution was quickly converted to acid by irradiation. The acid formed would probably be acetic acid, but could not be identified because of its small quantity.

Another product confirmed in the irradiated aerobic alcoholic solution was hydrogen peroxide; it was detected by iodometry in nitrogen atmosphere and by titanium trichloride.

Assuming that the existing oxygen is exhausted during the induction period, the quantum yield for the photochemical disapperance of oxygen (γ) could be calculated from the data shown in Fig. 5. The ratio of γ to k (the quantum yield of photobleaching of eosine) is tabulated in Table II, which shows that the ratio is almost constant, independent of the quantity of oxygen; the value is about 3.

TABLE II
THE RATIO OF γ TO k

P_{O_2} (mmHg)	O_2 (10^{-7} mol.)	t_{ind} (min.)	γ/k
0.1	4.2	31	3.5
0.2	8.4	100	2.4
0.3	14.6	160	3.1
0.5	21.4	200	3.3
		Average	(3.1)

Discussion

Since the photobleaching of eosine in the evacuated alcoholic solution is accompanied by the production of aldehyde, it can be concluded that its primary process is the dehydrogenation of alcohol by the excited dye, most certainly in the triplet state;

$$D^t + RH \longrightarrow DH\cdot + R\cdot, \qquad \text{(i)}$$

where D^t is the excited dye in the triplet state, RH is alcohol, DH· a semiquinone-type intermediate and R· a radical from alcohol. The process (i) can also be considered as an

4) F. Feigl, "Spot Tests", Elsevier (1954), Vol. II, p. 146.

essential step of the photobleaching if one assumes, as is probable, that DH· is colorless or almost colorless. This is consistent with the experimental result that the rate of photobleaching depends only on the amounts of light absorbed; moreover, the fact that the rate increases in the order, MeOH<EtOH <i-PrOH, coincides nicely with the general trend of hydrogen releasing power of R· as observed, for example, in the oxidation of alcohol with Fenton's reagent[5]. Thus there scarcely remains any doubt about the primary process of the photobleaching in vacuo.

Turning to the inhibiting action of oxygen, although it is certain that oxygen oxidizes alcohol to acid by virtue of the excited dye, which acts as a sensitizer, there are two alternative mechanisms conceivable in respect to the step in which oxygen takes part. The one is

$$\begin{aligned} D^t+RH &\longrightarrow DH\cdot+R\cdot \quad (a)\\ DH\cdot+O_2 &\longrightarrow D+HO_2\cdot \quad (b) \end{aligned} \qquad (ii)$$

and the other is

$$\begin{aligned} D^t+O_2 &\longrightarrow D^t\cdots O_2 \quad (a)\\ D^t\cdots O_2+RH &\longrightarrow D+R\cdot+HO_2\cdot \quad (b) \end{aligned} \qquad (iii)$$

In general, two processes may occur simultaneously, but in the case of ethyl alcohol, the former is considered to be the principal process for the following reason.

As seen from Table II, the duration of the induction period during which photobleaching is completely suppressed, is roughly proportional to the amount of oxygen, and it reaches thirty minutes by the existence of as little oxygen as 4×10^{-8} mol., which corresponds to the oxygen concentration of 8×10^{-7} mol./l. in the solution. Thus it is almost certain that 10^{-8} mol./l. of oxygen or less is enough to completely prevent photobleaching.

This requires quite a long lifetime for the intermediate which is attacked by oxygen; it is estimated to be not less than 10^{-2}–10^{-3} sec. by the analogous argument performed in the previous paper[1]. Hence if the reactions (iii) are to occur, the lifetime of the triplet state must be of the same order. But in the case of the aerobic photobleaching in the aqueous solution, the lifetime of D^t is estimated to be 10^{-4} sec. or so if the reaction goes by (iii)**.

Thus the process (iii) can be denied unless one recognizes a very unprobable assumption that the lifetime of the triplet state differs markedly in water and in ethyl alcohol.

Next, let us consider the processes which follow the reaction (ii). There were some investigations published on the photoöxidation of alcohols sensitized by some substances such as azo-compounds[5], benzoquinone[7] and benzophenone[8]. In particular, a recent work of Bolland and Cooper[9], on the photoöxidation of ethanol by anthraquinone 2,6-disodiumsulfonate as a sensitizer afforded some detailed mechanism of the reaction. Applying it to our case it was really found, as shown below, that our experimental results concerning the reaction products and particularly the fact that the ratio τ/k is about 3 can all be explained satisfactorily.

For the photobleaching in vacuo, the mechanism in question can be written as follows:

$$D \xrightarrow{h\nu} D^* \qquad (iv)$$

$$D^* \longrightarrow D^t \qquad (v)$$

$$D^t+RH \longrightarrow DH\cdot+R\cdot \qquad (vi)\ (\text{same as (i)})$$

$$DH\cdot+DH\cdot \longrightarrow DH_2+D \qquad (vii)$$

$$DH_2 \longrightarrow \cdots \text{products} \qquad (viii)$$

$$R\cdot+R\cdot \longrightarrow RH+\text{aldehyde} \qquad (ix)$$

In this scheme, (vi) is the main step of photobleaching and DH· has the lifetime of 10^{-2}–10^{-3} sec. as stated above. On the other hand, D is regenerated according to (vii). Hence the k-value experimentally obtained is just one half of the rate constant for the formation of DH· by (vi).

When oxygen is present, the following reactions[10] would occur producing hydrogen peroxide and acetic acid and regenerating the original dye molecule. (Aldehyde produced by (xiv) will be further oxidized to acid).

$$R\cdot+O_2 \longrightarrow RO_2\cdot \qquad (x)$$

$$DH\cdot+O_2 \longrightarrow D+HO_2\cdot \qquad (xi)$$

$$RO_2\cdot+RO_2\cdot \longrightarrow 2\text{Acid}+H_2O_2 \qquad (xii)$$

$$HO_2\cdot+HO_2\cdot \longrightarrow H_2O_2+O_2 \qquad (xiii)$$

$$RO_2\cdot+HO_2\cdot \longrightarrow H_2O_2+\text{Aldehyde}+O_2 \qquad (xiv)$$

As regards the last three steps, the following three cases are possible:

5) J.H. Merz and W.A. Waters, *Faraday Soc. Discussion*, 2, 179 (1947); W.A. Waters, "The Chemistry of Free Radicals", Oxford (1946), p. 247.

* The rate formula $dc/dt=kI_0(1-e^{-\alpha cd})$ (3) written in the previous paper[1] must be corrected as above since all the evaluated values of k in that paper were the quantum yields and did not correspond to k in eq. (3). All the results and discussions given in it, however, are not affected by this modification.

** The proof that the primary process of the aerobic photobleaching of eosine in the aqueous solution is really $D^t+O_2 \rightarrow D^t\cdots O_2$ will be concluded in the next paper. Cf. G. Oster and A.H. Adelman, *J. Am. Chem. Soc.*, 78, 913 (1956).

6) B.E. Blaisdell, *J. Soc. Dyers & Colourists*, 65, 618 (1949).

7) A. Berthoud and D. Parret, *Helv. Chim. Acta*, 17, 694 (1934).

8) H.L.J. Bäckström, *The Suedberg (Mem. Vol.)*, 1944, 45; *C. A.*, 39, 1105 (1945); A. Berthoud, *Helv. Chim. Acta*, 16, 592 (1933).

9) J.L. Bolland and H.R. Cooper, *Proc. Roy. Soc. (London)*, 225, 405 (1954).

10) For the rapid reaction of radical R· with oxygen, see, for example, J. R. McNesby and C. A. Heller, Jr., *Chem. Rev.*, 54, 342 (1954).

(a) only (xii) and (xiii) take place;

(b) only (xiv) takes place;

(c) all the three processes take place simultaneously.

According to the above scheme the result, $\gamma/k=3$, can be accounted for as follows. For each DH· produced by (vi), two oxygen molecules are consumed in (x) and (xi), but in (xiii) and (xiv) one is regenerated. The total consumption of oxygen for one molecule of DH· thus becomes 3/2 for all the above three cases:

(a) $2-1/2=3/2$;

(b) $2-1+1/2=3/2$ (since 1/2 O_2 is necessary for the further oxidation of aldehyde);

(c) 3/2 (superposition of (a) and (b)).

In vacuo, on the other hand, for one DH· produced by (vi) 1/2 D should disappear since the process (vii) regenerates one D from two DH·.

Thus the ratio of the quantum yield for the oxygen consumption to that for the photobleaching should be $(3/2)/(1/2)=3$, which agrees very satisfactorily with the experimental values in Table II.

Here it is to be noted that from the above argument, the decomposition of dye through the interaction between DH· and R· can be practically neglected, for γ/k must otherwise be less than 3. Another fact to be added is that the reaction,

$$D^t+O_2 \longrightarrow D^t\cdots O_2,$$

is neglected in the above argument. But even if this reaction partially takes part, the products and the quantitative relation between γ and k are not affected, because, in this case, it is only necessary to replace (xi) by

$$D^t\cdots O_2+RH \longrightarrow D+R\cdot+HO_2\cdot \qquad (xv)$$

without any alterations for the succeeding steps.

Summary

Photobleaching of eosine in methanol, ethanol, isopropanol and *n*-butanol in vacuo was investigated and it was concluded that the primary process is the dehydrogenation of alcohols by the metastable excited eosine molecule. In the presence of oxygen, the photobleaching is suppressed completely, but the sensitized photoöxidation of alcohol takes place.

When a small amount of oxygen is added to the evacuated alcoholic solution of eosine, the induction period appears, after which the photobleaching proceeds with almost the same rate as that in the evacuated state. Both the quantum yield for the consumption of oxygen during the induction period (γ) and that of the photobleaching in vacuo (k) were determined and the ratio γ/k was found to be ca. 3. This result and the reaction products detected (aldehyde in vacuo, acid and hydrogen peroxide in the presence of oxygen) were satisfactorily explained by the mechanism proposed by Bolland and Cooper. Further results somewhat important from the general standpoint of photobleaching of dye are:

(1) The lifetime of the intermediate to be attacked by oxygen (which is most probably DH·) is not less than 10^{-2}–10^{-3} sec.

(2) The quantum yield for the primary process of the photobleaching $D \rightarrow D^* \rightarrow D^t(+RH) \rightarrow DH\cdot(+R\cdot)$ in pure ethanol is ca. 10×10^{-4} at 20°C.

(3) In pure ethanolic solution, the decomposition of dye by the interaction between DH· and R· practically does not occur.

The cost of the present research has been partly defrayed from the Scientific Research Grant from the Ministry of Education.

Institute of Polytechnics
Osaka City University
Osaka

*Reaction of Hydrogen Peroxide with Titanium(IV) at Different pH Values**

By Motoshichi MORI, Muraji SHIBATA, Eishin KYUNO and Syu ITO

(Received May 21, 1956)

Titanium(IV) gives the well-known orange coloration by the action of hydrogen peroxide on an acidified solution, and the production of color has been shown by Jahr and his co-workers[1] to be due to the $(TiO_2 \cdot aq)^{2+}$ ion. On the other hand a yellow compound is formed when ammoniacal hydrogen peroxide is added to a solution of a titanyl salt, and this compound has been regarded by Schwarz and Giese[2] as ortho-pertitanic acid, $Ti(OH)_3(OOH)$. Recently, Babko and Valkova[3] found that the orange color in an acidified solution faded away with the decreasing of the acidity and assumed the existence of different ion-species in solutions with different pH values.

pH below 3, $Ti^{4+}+H_2O_2 \rightleftarrows Ti(H_2O_2)^{4+}$ (orange)

pH 3–6, $Ti^{4+}+H_2O_2 \rightleftarrows Ti(HO_2)^{3+}+H^+$ or (colorless)

$Ti^{4+}\ \ H_2O_2 \rightleftarrows Ti(O_2)^{2+}+2H^+$

We have carried out a series of experiments with a view to finding out whether this assumption is correct.

Early in this work, our attention was attracted by a noteworthy fact that at least four different ion-species exist in solutions whose pH range 1 to 13. The first species, orange in color, appears in solutions of high acidity ($pH<2$), the second, the bright yellow kind, in solutions of lower acidity (pH 3–6), the third, the pale yellow kind, in slightly alkaline solutions ($pH<9$), and the fourth, which is colorless, exists in more strongly basic solutions ($pH>10$). Proceeding with our experiments we obtained various kinds of information about the behavior of these ions, and also devised a new method of volumetric analysis of titanium.

Experimental

Materials.—Stock solution of titanyl sulfate was prepared by carbonate-fusion and acid-digestion of titanium dioxide free from iron. Other reagents used were of analytical grade.

Measurement.—A Beckman Model DU Spectrophotometer and an Ito Spectrophotometer were used to obtain the absorptiometric data and all the measurements were made in matched 1.0 cm. cells. The Molar extinction coefficient was calculated from the titanium content of the solution.

Adjustment of pH was made with a buffer solution and the measurement of pH was made with a Mitamura pH meter. The content of structural water in the solid sample was estimated from the loss of weight of the sample by drying at 400°C by using a Shimazu Thermano Balance. The titanium content was determined by the usual gravimetric or colorimetric method depending upon the sample taken. Active oxygen was volumetrically estimated by using a standard permanganate solution. Molar ratio of hydrogen peroxide to titanium in colored solution was determined by the method of continuous variation. The analysis of the sulfate ion was made gravimetrically and that of potassium ion, alkalimetrically.

Results and Discussion

Appearances of Different Species of Ion with Changes of pH.—When an aliquot of the yellowish solution obtained by neutralizing titanyl sulfate solution with potassium carbonate and then adding a few drops of hydrogen peroxide was introduced into each of a number of buffer solutions, the resulting mixtures showed different colors ranging from orange to colorlessness according to the pH of each solution. The optical density of the colors was measured at 415 mμ, and the values were plotted against the pH (Fig. 1). The curve has its first point of inflexion in the range of pH 1 to 2, its second in that of pH 6 to 7 and the third, which is not so clear as the others, near pH 9. This information indicates the probability that there are at least four different ion-species, each of which exists in solutions having pH value within a certain range. Additional evidence for this was obtained through the measurement of absorption spectra of the solutions (Fig. 2). As shown in Fig. 2 the maximum on each absorption curve is shifted to the short wavelength side with increase of pH. Namely, the species arising from solutions with pH 1.5, 4.2 and 8.6 show the absorption maximum at 400, 330 and 313 mμ respectively. This may be attributed to co-ordination binding

* Presented at the Symposium on Co-ordination Compound, Osaka, October 29, 1955.

1) H. J. Emeleus and J. S. Anderson, "Modern Aspects of Inorganic Chemistry", D. Van Nostrand Co., Inc., N.Y., (1952), p. 375.

2) Schwarz und Giese, *Z. anorg. Chem.*, **176**, 209 (1928).

3) *C. A.*, **42**, 44836 (1948).

of the peroxide ion, O_2^{2-}, with the titanium ion since a certain μ-peroxo-cobalt (III) complex has a similar maximum at 330 mμ[4]. In a strongly alkalified solution (pH 13.0), the absorption band lies in far shorter region and has no maximum. This may be considered to be due to weaker co-ordination binding of the peroxide ion. Thus, it may be said that at least four different species exist separately in specified pH regions (i.e. pH<2, 3–6, 7–9 and 10<pH). Hereafter these species will be denoted by "A", "B", "C" and "D" respectively.

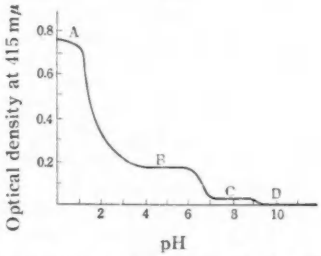

Fig. 1. Light absorption of the Ti(IV)-H_2O_2 system vs. pH. Concentration of Ti, approximately 1×10^{-3} mol./l.

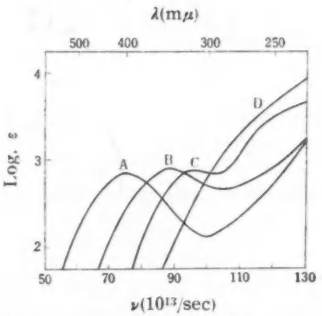

Fig. 2. Absorption spectra of various species.
A. at pH 1.5 B. at pH 4.2
C. at pH 8.6 D. at pH 13.0

Types of Behavior and Formulas.—In order to determine the chemical compositions of "B" and "C", continuous variation studies were carried out, and the results are shown in Fig. 3. In both species, titanium appears to combine with only one molecule of hydrogen peroxide. By the way, it has been well known that in highly acidified solutions they react in the one-to-one molar proportion[5].

4) S. Yamada, Y. Shimura and R. Tsuchida, This Bulletin, 26, 72 (1953).
5) Y. Shaeppi and W.D. Treadwell, *Helv. Chim. Acta*, 31, 577 (1948).

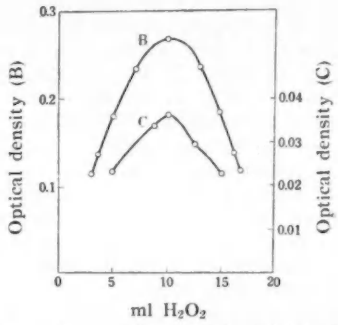

Fig. 3. Curves for graphical determination of ratio of H_2O_2 to Ti (λ=415 mμ). Concentrations of $TiOSO_4$ and H_2O_2, 7.2×10^{-3} M. Total volume, 20 ml.

Further experiments were conducted to isolate solids from the solutions containing each species of ions. Addition of a large amount of alcohol resulted in precipitation of solids. Namely, in the presence of potassium sulfate an orange-colored solid was isolated from the solution containing "A", and a yellow solid, from the solution containing "B". From solutions containing "C" and "D" a pale yellow and a white compound were isolated respectively in the absence of sulfate. After being washed with water, alcohol and finally ether, each precipitate was dried over sulfuric acid and kept for analyses. For convenience' sake they are denoted by A_1, B_1, C_1 and D_1. A_1 and D_1 were easily soluble, B_1 was slightly soluble in water, but C_1 was insoluble in water. All the solids were soluble in mineral acids. C_1 was stable at room temperature but B_1 underwent gradual decomposition. A_1 and D_1 were hygroscopic. Molar ratios of the various components to titanium were as follows.

For A_1: O, 1; H_2O, 3; SO_4, 2; K, 2; assumed composition, $K_2O\cdot TiO_3\cdot 2SO_3\cdot 3H_2O$. For B_1: O, 1; H_2O, 2.5; SO_4, 2.5; K, 4; $4K_2O\cdot Ti_2O_3\cdot 5SO_3\cdot 5H_2O$. For C_1: O, 1; H_2O, 2; $TiO_3\cdot 2H_2O$. For D_1: O, 2; H_2O, 1; K, 2; $K_2O\cdot TiO_4\cdot H_2O$.

On standing at room temperature the solution containing "A" acquired no turbidity, but pale yellow precipitates appeared in the solution containing "C" after standing for a little while, and on standing for several days the solutions containing "B" and "D" yielded a bright yellow and a pale yellow precipitate respectively. On heating them to about 70°C, however, the precipitation was quickly completed. After being washed with water, alcohol and ether, they were dried over sulfuric acid and kept in a vacuum desiccator for analysis. These are denoted

by B_2, C_2 and D_2. All the precipitates were insoluble in water and soluble in 3 N sulfuric acid. The analytical results were as follows.

For B_2: O, 0.9; H_2O, 1; assumed composition $TiO_3 \cdot H_2O$. For C_2 and D_2: O, 0.5; H_2O, 1; assumed composition, $Ti_2O_5 \cdot 2H_2O$.

Now, we are in a position to discuss the reactions taking place in solutions consisting of the titanium (IV)-hydrogen peroxide system. In addition to the absorptiometric and analytical results, the types of behavior of the species toward ion-exchangers are also useful for this discussion. Namely, "A" and "B" were held on a cation exchanger in Na-form (i.e. positively charged) and "D" was held on an anion exchanger in Cl-form (i.e. negatively charged), but "C" passed through both exchangers (i.e. uncharged). Thus, assuming that the co-ordination number of tetravalent titanium is four and that a hydrogen peroxide molecule can unite with the central ion through co-ordination linkage, the reactions involved may be represented as follows:

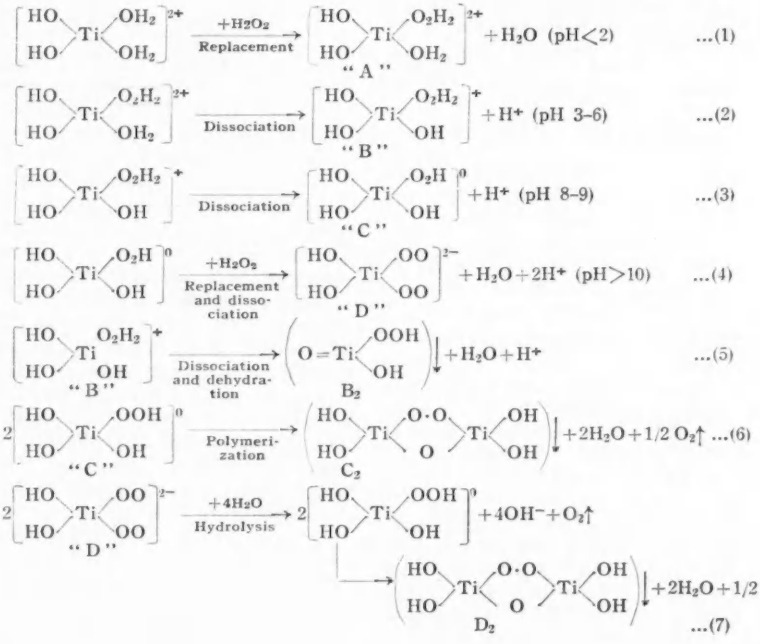

Among the hypothetical formulae, $[Ti(OH)_2(H_2O)(H_2O_2)]^{2+}$ is substantially identical with $(TiO_2 \cdot aq)^{2+}$, and its double salt $K_2SO_4 \cdot [Ti(OH)_2(H_2O)(H_2O_2)]SO_4$ is also identical with $K_2(TiO_2)(SO_4)_2 \cdot 3H_2O$[1]. The chemical formulae of B_1, C_1 and D_1 are presumed to be $4K_2SO_4 \cdot [Ti(OH)_3(H_2O_2)]_2SO_4$, $[Ti(OH)_3(O_2H)]$ and $K_2[Ti(OH)_2(O_2)_2]$ respectively.

Furthermore, the precipitation reactions taking place during the standing or heating of the solutions, may be represented by the following equations.

New Volumetric Analysis of Titanium

Procedure.—By means of a pipet, transfer a 10 ml. portion of the sample solution containing about 10 mg. of titanium (IV) to each of 300-ml. Erlenmeyer flasks, dilute them to about 150 ml. with distilled water and then add a saturated solution of potassium bicarbonate until each solution becomes alkaline and a white precipitate appears. Carefully add a few drops of 30% hydrogen peroxide; then the precipitate will be redissolved and the solution will become yellowish in color. Stand them on a water-bath in the neighborhood of 80°C until effervescence ceases (about two hours). During the time a pale yellow precipitate will separate out. Cool the contents to room temperature and dissolve the precipitate by adding about 50 ml. of 6 N sulfuric acid and standing the mixture about half an hour. Finally, titrate each of the orange-colored solutions with a 0.1 N permanganate solution by using a microburette. One ml of the 0.1 N solution corresponds to 0.00479 g. of titanium.

Discussion

Some of the results obtained by the procedure described above are given in Table I, which clearly shows that the procedure is

TABLE I
ANALYSIS OF TITANIUM

Expt. No.	0.1 N $KMnO_4$ (f=0.9763) ml.	Ti Found mg.	Ti Present mg.	Expt. No.	0.1 N $KMnO_4$ (f=0.9763) ml.	Ti Found mg.	Ti Present mg.
1	1.630	7.62	7.48	6	10.02	46.84	48.15
2	1.610	7.53	〃	7	10.54	49.27	〃
3	1.605	7.50	〃	8	10.19	47.64	〃
4	1.625	7.60	〃	9	10.40	48.62	〃
5	1.610	7.53	〃	10	11.30	52.83	〃

suited for the determination of titanium in quantities of the order of 10 mg. This method is based on the fact that when an alkaline solution containing a titanyl salt and hydrogen peroxide is heated, a pale yellow compound is formed in which the molar ratio of active oxygen to titanium is one to two. (Reaction (6)). By being dissolved with sulfuric acid, this compound decomposes into two components;

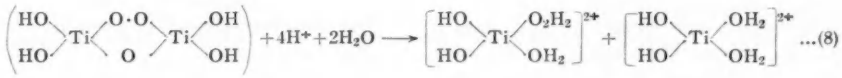

...(8)

Accordingly, it may be said that the reaction of hydrogen peroxide with a permanganate is applied to this method. Incomplete removal of the oxygen produced by reaction (6) and further decomposition of $[Ti(OH)_2(H_2O)(H_2O_2)]^{2+}$ into the hydrous oxide may interfere with the accuracy of the analysis and long and gentle heating on a water-bath and dissolution of the precipitates without heating should be resorted to in order to avoid these sources of error.

Summary

Reaction of hydrogen peroxide with titanium(IV) has been investigated over the range of pH 0 to 13. Below pH 2 this reaction gives orange-colored ion-species, $[Ti(OH)_2(H_2O)(H_2O_2)]^{2+}$ or $(TiO_2 \cdot aq)^{2+}$. In the range of pH 3 to 6 formation of a yellow species is observed and its chemical formula is presumed to be $[Ti(OH)_3(H_2O_2)]^{+}$. Existence of a species different from the above is indicated by the pale yellow color observed in the region of pH 7 to 9. This species is very unstable unless a large excess of hydrogen peroxide is present, and its chemical formula is presumed to be $[Ti(OH)_3(OOH)]^{0}$. At higher pH values (10<pH), the reaction mixture is colorless, and presumably contains $[Ti(OH)_2(O_2)_2]^{2-}$. All the tentative formulae of these species are based on the composition of isolated salts, the absorption spectra of the solutions etc. A solution containing $[Ti(OH)_2(H_2O)(H_2O_2)]^{2+}$ remains unchanged but a solution containing $[Ti(OH)_3(H_2O_2)]^{+}$ gives a yellow precipitate TiO(OH)(OOH), and one containing $[Ti(OH)_3(OOH)]^{0}$ or $[Ti(OH)_2(O_2)_2]^{2-}$ gives a pale yellow compound $(HO)_2Ti\langle^{O_2}_{O}\rangle Ti(OH)_2$, when left for a while at room temperature or more quickly when heated on a water-bath. The precipitation reaction of $(HO)_2Ti\langle^{O_2}_{O}\rangle Ti(OH)_2$ is taken advantage of in a new volumetric analysis suited for determination of titanium in quantities of the order of 10 mg.

Department of Chemistry, Faculty of Science, Kanazawa University
Kanazawa

A Kinetic Study of the Reaction of Substituted Benzyl Chlorides with Tertiary Amines

By Teruaki MUKAIYAMA and Hiromi TANAKA

(Received June 21, 1956)

Introduction

The kinetics of the bimolecular nucleophilic substitution of benzyl chlorides have been studied by many workers[1-9]. In a single stage process considered for the bimolecular substitution, bond formation between the central carbon atom and a nucleophilic reagent occurs simultaneously with bond fission between the central carbon atom and the halogen atom. The bond fission should be facilitated by electron releasing groups; however, the approach of the nucleophilic reagent, which is necessary for the bond formation is almost certain to be hindered by these substituents. The net result is a different effect and the polar effects of the substituents on the S_{N2} reaction can not be clear cut. In addition to the polar effect, the steric effect and the solvent effect to be considered in the reaction mechanism multiplies the difficulty for explaining the factors which determine the reactivity.

In the present experiment, the kinetics of the reaction of substituted benzyl chlorides with tertiary amines in benzyl alcohol solvent were studied in order to investigate the polar and the steric effects in the S_{N2} reaction by using the tertiary amines with bulky substituents as nucleophilic reagents.

Experimental

Materials.—Melting points, boiling points and literature references for benzyl chlorides, amines and benzyl alcohol are listed in Table I.

TABLE I

	M. p. or B. p. (°C)	Reference
Solvent		
Benzyl alcohol	112/20	
Amines		
Tri-*n*-butylamine	116/42	
Dimethylaminoethanol	135	
Diethylaminoethanol	42~44/8	
Diisopropylaminoethanol	104/39	(a)
Diisobutylaminoethanol	84/9	(a)
Di-*n*-butylaminoethanol	99/10.5	(b)
Benzyl chlorides		
H	69~70/17	
o-NO_2	[48]	(c)
p-NO_2	[71]	
o-Cl	94/10	
p-Cl	68/3	
o-CN	[60]	(d)
p-CN	[79]	(d)
o-CH_3	86~88/16	(e)
p-CH_3	63~65/5	(f)

a) Einhorn, Fiedler and Uhlfelder, *Ann.*, **371**, 145 (1909).
b) Kamm, Adams and Volwieler, U.S. Patent, 1,358, 750.
c) L. Vanino, "Handbuch der Präparativen Chemie", Bände II, 459.
d) C. Barkenbus and J.B. Holtzchaw, *J. Am. Chem. Soc.*, **47**, 2191 (1925).
e) I. Smith and L.J. Spillane, *J. Am. Chem. Soc.*, **62**, 2640 (1940).
f) M.G. Darzens and M.M. Delépine, *Compt. rend.*, **208**, 818 (1939).

Procedure.—In each run, 1 ml. of 0.1 N benzyl alcohol solutions of benzyl chlorides and amines were mixed into a 20 ml. reaction tube having a ground stopper. At appropriate intervals of time the reaction tubes placed in a thermostat were taken out and the reaction was stopped by rapid cooling with ice water. Then, the reaction mixture was washed out with 10 ml. of methanol and the chlorine ion formed was determined by titration with 0.01 N silver nitrate (Mohr's method). The temperature control was accurate to ±0.03° within the temperature ranges between 25°C–135°C.

The second order rate constant was calculated by equation 1

$$k_2 = \frac{1}{t} \cdot \frac{x}{a(a-x)} \qquad (1)$$

where k_2 is the second order rate constant; t, the time in seconds; x, the amount of chlorine ion

1) D.H. Peacock, *J. Chem. Soc.*, **1924**, 1975; **1925**, 2177.
2) P.P. Krichenko and V. Opotsky, *Ber.* **59B**, 2131 (1926).
3) H. Mc Combie, H.A. Scarborouch and F.P. Smith, *J. Chem. Soc.*, **1927**, 802.
4) B.V. Tronov and A.I. Gershevich, *C. A.*, **22**, 3397 (1928).
5) G.M. Bennett and B. Jones, *J. Chem. Soc.*, **1935**, 1815.
6) S.C.J. Olivier and A. Ph. Weber, *Rec. trav. chim. Pay-Bas*, **53**, 869, 899 (1934).
7) V.A. Hol'tsshmidt and N.K. Vorobev, *J. Phys. Chem.*, **13**, 473 (1939).
8) J.W. Baker and W.S. Nathan, *J. Chem. Soc.*, **1933**, 1128; **1934**, 987; **1935**, 519, 1840, 1844, 1847; **1936**, 236.
9) C.W.L. Bevan, E.D. Hughes and C.K. Ingold, *Nature*, **171**, 301 (1953).

formed at time t; a, the initial concentration of both benzyl chlorides and tertiary amines. As an example of a typical run, the reactions of benzyl chloride with diethylaminoethanol at the temperature between 55°C–95°C are shown in Fig. 1.

The rate constants of the reaction of benzyl chlorides with amines are shown in Table II.

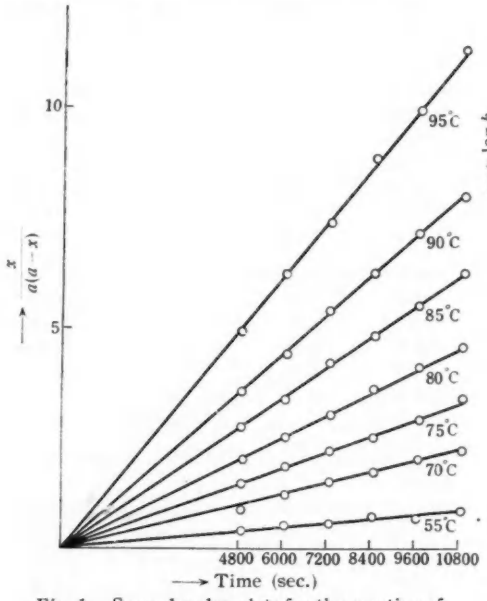

Fig. 1. Second order plots for the reaction of benzyl chloride with diethylaminoethanol.

The activation energies of the reactions were obtained from the linear relationship between log k and reciprocal absolute temperature. Typical runs are shown in Fig. 2. The rate constants, the activation energies and the entropies of activation obtained in this study are listed in Table III.

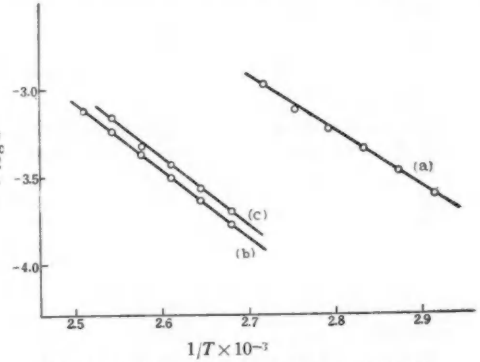

Fig. 2. The reaction of benzyl chloride with amines: the plot of log k against $1/T$. (a) diethylaminoethanol, (b) diisopropylaminoethanol, (c) diisobutylaminoethanol.

Results and Discussion

The experimental results listed in Table II are noted from the two different viewpoints, i. e. the effects of the substituents of amines (a) and those of benzyl chlorides (b), as follows.

TABLE II

THE RATE CONSTANTS OF THE REACTION OF BENZYL CHLORIDES WITH TERTIARY AMINES

$k_2 \times 10^4$ (mol.$\cdot$l.$^{-1}\cdot$sec.$^{-1}$), t(°C)

1) The reaction of benzyl chloride with amines.

t	k_2	t	k_2
(Dimethylaminoethanol)		(Diethylaminoethanol)	
25.0	2.21	55.0	0.824
30.0	3.26	70.0	2.09
35.0	4.74	75.0	3.40
40.0	6.84	80.0	4.57
		85.0	5.79
		90.0	7.43
		95.0	10.8
(Diisopropylaminoethanol)		(Diisobutylaminoethanol)	
100.0	1.66	95.0	1.39
105.0	2.31	100.0	2.01
110.0	3.10	105.0	2.70
115.0	4.21	110.0	3.44
120.0	5.67	115.0	4.66
125.0	7.55	120.0	7.02
(Di-*n*-butylaminoethanol)		(Tri-*n*-butylamine)	
80.0	2.44	80.0	0.622
85.0	3.24	85.0	0.834
90.0	4.23	90.0	1.11
95.0	5.52	95.0	1.46
100.0	7.48	100.0	1.93
120.0	21.22	105.0	2.36

2) The reaction of *o*-methylbenzyl chloride with amines.

(Dimethylaminoethanol)		(Diethylaminoethanol)	
25.0	2.68	60.0	1.29
30.0	4.10	65.0	1.83
35.0	5.99	70.0	2.59
40.0	9.00	75.0	3.56
		80.0	4.83
		85.0	6.50
(Diisopropylaminoethanol)		(Diisobutylaminoethanol)	
75.0	0.80	80.0	1.20
80.0	1.14	85.0	1.73
85.0	1.58	90.0	2.47
90.0	2.10	95.0	3.41
95.0	3.03	100.0	4.76
100.0	4.15	105.0	6.62

t	k_2	t	k_2
(Di-*n*-butylaminoethanol		(Tri-*n*-butylamine)	
75.0	2.21	54.5	0.740
80.0	3.02	60.0	1.16
85.0	4.05	65.0	1.67
90.0	5.81	70.0	2.67
95.0	7.85	75.0	3.40
100.0	10.55	80.0	5.04

3) The reaction of *p*-methylbenzyl chloride with amines.

(Dimethylaminoethanol)		(Diethylaminoethanol)	
20.0	2.85	60.0	2.40
25.0	4.27	65.0	3.44
30.0	6.46	70.0	4.96
35.0	9.77	75.0	6.66
		80.0	9.91
		85.0	13.5
(Diisopropylamino-ethanol)		(Diisobutylamino-ethanol)	
80.0	1.61	80.0	1.69
85.0	2.34	85.0	2.47
90.0	3.35	90.0	3.59
95.0	4.95	95.0	5.49
100.0	7.23	100.0	8.02
105.0	10.49	105.0	11.65
(Di-*n*-butylaminoethanol)		(Tri-*n*-butylamine)	
60.0	1.50	50.0	1.20
65.0	2.11	55.0	2.06
70.0	2.88	60.0	2.54
75.0	3.85	65.0	3.93
78.0	4.65	70.0	4.95
83.0	6.33	75.0	6.94

4) The reaction of *o*-chlorobenzyl chloride with amines.

(Dimethylaminoethanol)		(Diethylaminothanol)	
35.0	2.25	80.0	1.14
40.0	3.33	90.0	2.24
45.0	4.82	100.0	4.11
50.0	7.10	105.0	5.49
(Diisopropylamino-ethanol)		(Diisobutylamino-ethanol)	
110.0	0.870	110.0	1.36
115.0	1.18	115.0	1.72
120.0	1.52	120.0	2.27
125.0	2.07	125.0	2.98
130.0	2.76	130.0	3.99
135.0	3.67	135.0	5.05
(Di-*n*-butylaminoethanol)		(Tri-*n*-butylamine)	
95.0	1.76	85.5	3.45
100.0	2.33	90.0	4.17
105.0	2.80	95.0	4.89
115.0	4.65	100.0	7.06
120.0	5.99	105.0	8.66
125.0	8.21	110.0	11.3

5) The reaction of *p*-chlorobenzyl chloride with amines.

t	k_2	t	k_2
(Dimethylaminoethanol)		(Diethylaminoethanol)	
30.0	2.83	75.0	2.47
35.0	4.01	80.0	3.33
40.0	5.91	90.0	5.70
45.0	8.41	95.0	7.91
		100.0	11.25
(Diisopropylamino-ethanol)		(Diisobutylamino-ethanol)	
105.0	1.43	105.0	1.76
110.0	1.91	110.0	2.38
115.0	2.60	115.0	3.19
120.0	3.45	120.0	4.40
125.0	4.61	125.0	5.75
(Di-*n*-butylaminoethanol)		(Tri-*n*-butylamine)	
85.0	2.26	85.5	6.15
90.0	3.00	90.0	7.96
95.0	4.02	95.0	10.3
100.0	5.30	100.0	14.3
105.0	6.78	105.0	18.1
		110.0	22.2

6) The reaction of *o*-cyanobenzyl chloride with amines.

(Dimethylaminoethanol)		(Diethylaminoethanol)	
40.0	2.00	90.0	1.27
45.0	3.03	95.0	1.71
50.0	4.43	100.0	2.32
55.0	6.38	105.0	3.01
		110.0	3.82
(Diisopropylamino-ethanol)		(Diisobutylamino-ethanol)	
125.0	0.840	110.0	0.810
130.0	1.14	115.0	0.93
135.0	1.48	120.0	1.04
140.0	2.13	130.0	1.91
145.0	2.97	135.0	2.39
		140.0	3.01
		145.0	3.78
(Di-*n*-butylaminoethanol)		(Tri-*n*-butylamine)	
100.0	1.19	90.0	2.10
105.0	1.61	95.0	2.69
110.0	2.09	100.0	3.70
115.0	2.71	105.0	4.68
120.0	3.28	110.0	5.93
125.0	3.97	115.0	7.27

7) The reaction of *p*-cyanobenzyl chloride with amines.

(Dimethylaminoethanol)		(Diethylaminoethanol)	
40.0	2.58	90.0	2.26
45.0	3.94	95.0	3.02
50.0	5.75	100.0	3.99
55.0	8.21	105.0	5.32
		109.8	6.70

t	k_2	t	k_2
(Diisopropylamino ethanol)		(Diisobutylamino-ethanol)	
110.0	0.660	110.0	0.580
115.0	0.810	120.0	0.890
120.0	1.13	130.0	1.52
130.0	1.80	135.0	1.99
135.0	2.40	140.0	2.65
140.0	3.00	145.0	3.54
145.0	3.78		
(Di-*n*-butylaminoethanol)		(Tri-*n*-butylamine)	
100.0	1.80	90.0	2.86
105.0	2.35	95.0	3.63
110.0	3.10	100.0	4.81
115.0	4.11	105.0	6.42
120.0	5.00	110.0	7.93
		115.0	9.53

8) The reaction of *o*-nitrobenzyl chloride with amines.

t	k_2	t	k_2
(Tri-*n*-butylamine)			
105.0	3.66		
110.0	4.75		
115.0	6.34		
120.0	8.38		
125.1	11.3		

9) The reaction of *p*-nitrobenzyl chloride with amines.

(Dimethylaminoethanol)		(Diethylaminoethanol)	
40.0	2.56	95.0	3.28
45.0	3.67	100.0	4.32
50.0	5.33	105.0	5.49
55.0	7.37	110.0	6.79
		115.0	8.79
(Di-*n*-butylaminoethanol)		(Tri-*n*-butylamine)	
90.0	0.810	105.0	6.10
100.0	1.54	110.0	7.97
105.0	2.08	115.0	10.1
110.0	2.61	120.0	11.8
115.0	3.77	125.1	14.9
120.0	6.15	130.0	18.1

TABLE III

THE SUMMARY OF RATE CONSTANTS ($k_2 \times 10^4$ mol.$^{-1}$·l.·sec.$^{-1}$ at 105°C), THE ACTIVATION ENERGIES (E kcal.) AND THE ENTROPIES OF ACTIVATION ($\Delta S^{\neq}$ e. u.)

Amines	Dimethylaminoethanol			Diethylaminoethanol		
Benzyl chlorides	k_2	E	$\Delta S^{\neq}$	k_2	E	$\Delta S^{\neq}$
H	32.3	14.0	−28.8	19.2	15.5	−30.5
o-CH_3	596	15.2	−24.4	24.0	15.3	−30.9
p-CH_3	740	14.4	−25.7	46.0	16.7	−25.6
o-Cl	21.4	15.1	−26.7	5.52	15.9	−31.9
p-Cl	27.9	13.9	−29.4	13.6	14.9	−32.7
o-CN	7.38	16.0	−26.5	3.05	16.0	−32.8
p-CN	8.63	15.5	−27.5	5.32	15.6	−32.8
o-NO_2						
p-NO_2	6.56	14.4	−30.9	5.55	14.7	−35.1
	Diisopropylaminoethanol			Diisobutylaminoethanol		
H	2.30	17.8	−28.5	2.70	18.5	−26.4
o-CH_3	5.59	16.7	−29.7	6.58	18.1	−25.8
p-CH_3	9.57	18.9	−23.0	11.5	20.6	−18.0
o-Cl	0.650	17.4	−32.2	0.100	16.7	−33.2
p-Cl	1.43	17.4	−30.7	1.76	17.8	−29.1
o-CN	0.212	20.4	−26.5	0.526	15.5	−37.7
p-CN	0.459	16.9	−34.2	0.348	18.0	−31.9
o-NO_2						
p-NO_2						
	Di-*n*-butylaminoethanol			Tri-*n*-butylamine		
H	9.68	14.6	−34.2	2.36	14.1	−33.6
o-CH_3	14.3	16.5	−28.4	22.9	16.6	−27.2
p-CH_3	13.0	14.6	−33.6	41.3	16.2	−31.7
o-Cl	2.90	14.0	−38.3	0.866	15.2	−32.8
p-Cl	6.98	15.1	−33.6	1.81	15.1	−33.2
o-CN	1.59	15.9	−38.9	0.506	14.2	−41.2
p-CN	2.38	15.1	−35.7	0.642	14.1	−40.9
o-NO_2				0.370	16.1	−32.1
p-NO_2	2.07	17.2	−30.4	0.600	13.2	−38.8

I—a) The rate constants of the reaction of amines with benzyl chlorides at 105°C increase in the following order,

diisopropylaminoethanol, diisobutylaminoethanol≪di-*n*-butylaminoethanol, tri-*n*-butylamine, diethylaminoethanol≪dimethylaminoethanol.

As noted in the above sequence, dimethylaminoethanol reacts much faster than the other amines and amines with normal alkyl groups react faster than those with branched alkyl groups. I—b) The rate constants of benzyl chlorides with amines at 105°C increase in the following order,

$$p\text{-}CH_3 > o\text{-}CH_3 > H > p\text{-}Cl > o\text{-}Cl > p\text{-}CN > o\text{-}CN > p\text{-}NO_2 > o\text{-}NO_2 .$$

The rates of reaction decrease by introducing the electron attracting groups and the *para* derivatives react faster than the corresponding *ortho* derivatives.

II—a) The activation energies for amines increase in the following order,

dimethylaminoethanol, diethylaminoethanol, di-*n*-butylaminoethanol, tri-*n*-butylamine≪diisopropylaminoethanol, diisobutylaminoethanol.

Amines with the branched alkyl groups, such as isopropyl and isobutyl groups, require more energy than amines with normal alkyl groups, such as methyl, ethyl and *n*-butyl groups. The activation energies required for the latter four amines are nearly equal.

II—b) The activation energies for benzyl chlorides do not show the characteristic variation of the substituents as found in the rate constant, in which regular sequences are shown according to their polar effects.

The following relations are found for *ortho* and *para* derivatives of benzyl chlorides according to the nature of the attacking amines. *Ortho* derivatives require more energy of activation than *para* derivatives in the reaction with four amines with normal alkyl groups and the reversed order is found in the reaction with amines with branched alkyl groups.

III—a) The entropies of activation for amines increase in the following order,

tri-*n*-butylamine, di-*n*-butylaminoethanol, diethylaminoethanol<diisobutylaminoethanol, diisopropylaminoethanol<dimethylaminoethanol.

The entropy of activation for dimethylaminoethanol is less negative than the other amines. The slow rates of amines with normal alkyl groups, such as ethyl and *n*-butyl groups, which require the nearly equal energies of activation with dimethylaminoethanol are attributed to the more negative entropies of activation.

III—b) The linear relationship between the activation energy and the entropy of activation could not be found for benzyl chlorides; however, the results show a combined increase in the activation energy and decrease in the entropy of activation. Benzyl chlorides with electron attracting groups show more negative entropy of activation than those with the electron releasing groups.

Ortho derivatives show more negative entropy of activation than *para* derivatives in the reaction with amines with branched alkyl groups and the reversed relation is found in the reaction with the other four amines.

The single stage process is considered for the bimolecular nucleophilic substitution and, in the transition state, by the approach of the nucleophilic reagent, the bond formation occurs simultaneously with bond fission, in which chlorine atom ionizes by the interaction of the solvent molecule.

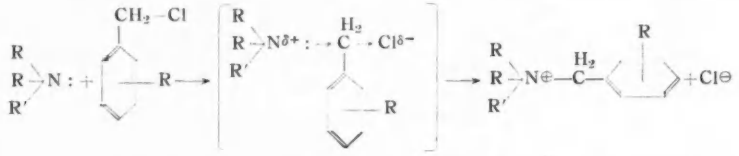

Assuming the above mechanism for the reaction, the effects of the substituents of amines are considered as follows. The electron density of the nitrogen atom in amines increases from methyl to *n*-butyl by an inductive effect, which is favorable for bond formation, but, the frontal strain considered in the transition state increases by the same sequence, which is unfavorable for the reaction. The simple explanation becomes difficult because of these two opposing effects, i.e.; polar effect and steric effect; however, the results that amines with bulky substituents always require 2-3 kcal. more activation energy than the other four amines may be due to the increased F-strain considered in the transition state.

As shown in II—b), the relative order of activation energies for *ortho* and *para* derivatives of benzyl chlorides are changed by the nature of the attacking amines. The lower activation energies for the reaction of

ortho derivatives with bulky amines may be explained by assuming the increased F-strain between *ortho* derivatives and the amines with bulky groups in the transition state, which causes the dissociation of chlorine atoms more readily.

The activation energies for the reaction of benzyl chlorides with electron attracting groups or electron releasing groups are nearly equal. These results may be due to the two opposing effects which are considered in the single stage process, namely the ionization of chlorine atom facilitated by the electron releasing groups and the approach of amine molecule to the central carbon atom retarded by the same substituents.

As shown in III—a), the entropy of activation for dimethylaminoethanol is less negative than the other four amines studied. This may be explained by assuming the solvation of amines, e.g. the interaction of protonic solvent with amines, in the ground state, which must be lost in the transition state. Dimethylaminoethanol solvates more than the other amines in which solvation is hindered by the increased B-strain due to their bulky substituents. Therefore, the entropies of activation for the latter amines are more negative than dimethylaminoethanol.

The results shown in III—b) are explained by a similar consideration in which the differences of the entropies of activation in the benzyl chloride series depend on the degree of solvation in their ground state. The solvation of benzyl chlorides to the chlorine atom by the protonic solvent, in the ground state, increases by introducing the electron releasing group, such as methyl group, but, in the transition state, the solvent interaction with the ionizing chlorine atom is nearly the same irrespective of the nature of their substituents. Therefore, the more negative entropies of activation of benzyl chlorides with electron attracting groups are expected.

In bimolecular nucleophilic substitution, the polar effects are not clearly shown as mentioned above, but, it can be concluded that the steric effect and the solvent effect play an important role for the reaction.

Summary

(1) The rate constants, the activation energies and the entropies of activation of the reaction of benzyl chlorides with tertiary amines in benzyl alcohol were determined.

(2) In the single stage process for the bimolecular nucleophilic substitution, the polar effects of the substituents are not clearly shown.

(3) Both steric and solvent effects play important roles on the reaction studied in this experiment.

The authors wish to express their hearty thanks to Prof. Toshio Hoshino for his encouragement and to Mr. Tsuyoshi Nakamura and Mr. Keiki Shibata for their help during the course of this experiment.

Department of Physics and Chemistry
Gakushuin University, Mejiro
Toshima-ku, Tokyo

Irreversible Photobleaching of the Solution of Fluorescent Dyes. III. Photoreaction of Eosine in the Aqueous Alcoholic Solutions under Evacuated State

By Masashi IMAMURA and Masao KOIZUMI

(Received July 9, 1956)

Introduction

In the preceding paper[1], the vacuum photobleaching of eosine in pure methanol, ethanol and isopropanol was investigated, and it was found that the absorption spectra decline steadily without any shift and that the rate depends only on the light absorbed.

Now as a natural extension of our research, the effect of water added on the vacuum photobleaching was examined, and a remarkable result was obtained; this was that the addition of water does cause a gradual displacement of the absorption spectra towards shorter wavelengths in the course of reaction and at the same time the solution becomes more and more fluorescent. The reaction is completely irreversible and the strongly fluo-

1) M. Imamura and M. Koizumi, This Bulletin, **29**, 000 (1956).

rescent product is very stable. Analyzing the absorption spectra carefully, this ultimate product was definitely confirmed to be uranine.

Kinetic studies were also undertaken, and from the results obtained, a conclusion was given as to the primary process of the aerobic photobleaching of eosine in the aqueous solution, which had remained undecided in the first paper[2] of this series.

Experimental Procedures and Results

1. Photobleaching in the Aqueous Alcoholic Solutions.—Materials were the same as before[1,2]. Concentrated aqueous solution of eosine was diluted with water and ethanol to a desired concentration of alcohol, the resulting concentration of eosine being kept constant as 10^{-5} mol./l.

Evacuation was done under repeated cooling with dry ice and melting for several times with the use of a mercury diffusion pump. Reaction was carried out in a cylindrical glass cell to which a cuvett (path length: 1 cm.) for Beckman spectrophotometer was attached. Evacuated samples were irradiated with a tungsten lamp and Matsuda color filter VG1 as before.

At some minutes' intervals the cell was taken out of a thermostat and the absorption spectra were measured by Beckman spectrophotometer model DU.

An example of a series of measurements is shown in Fig. 1. From Fig. 1, it is seen that the optical density gradually decreases and, at the same time, absorption maximum is displaced towards shorter wavelengths; the irradiated solution becomes more greenly fluorescent than the initial solution.

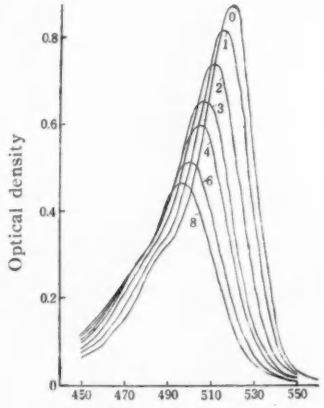

Fig. 1. Absorption spectra of the irradiated eosine in 10 vol. % EtOH solution in vacuo.
No.'s depicted indicate the order of measurement.

2. Analysis of the Absorption Spectra.—Although a gradual shift of the absorption maximum was observed during the reaction, its limiting position in every case was in the neighborhood of 490 mμ. Since the above results strongly suggest the formation of a coloring product from eosine, identification of the product was attempted from the analysis of absorption spectra. The method is essentially the same as reported by Blaisdell[3].

At various wavelengths, the ratio of the optical density of each irradiated solution to that of the initial solution was calculated, and the value of the minimum ratio was decided. For all the curves tried, the minimum points fell alike between 530 and 540 mμ. Minimum ratios thus obtained may be considered as relative measures of the concentration of eosine remaining.

Multiplying these values to the optical densities of the initial solution at each wavelength, the absorption curves could be drawn which may approximately be considered as the curves of eosine remaining in solution at each time.

Substracting these curves from the absorption curves of the original solutions, one can get the curves which may be attributed to intermediate products.

An example of such curves obtained is given in Fig. 2. It is seen from Fig. 2 that with decreasing concentration of eosine, optical density of the products increases moderately at the beginning, then more and more slowly, and at last begins to decrease very slowly. At the same time the position of the maximum is gradually displaced towards 490 mμ, where the displacement comes to a halt.

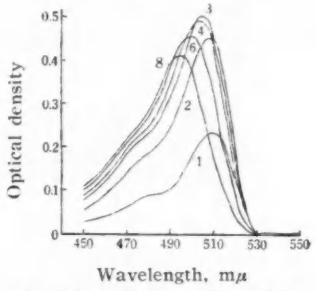

Fig. 2. Absorption spectra of the intermediates produced in 10 vol. % EtOH solution in vacuo.
No.'s depicted indicate the order of measurement. (cf. Fig. 1).

3. Identification of an Ultimate Intermediate Product.—The coloring product intermediately produced by the irradiation of the aqueous alcoholic solution of eosine has a strong green fluorescence and has its absorption maximum near 490 mμ as mentioned above.

From these facts, it seemed very plausible to suspect that this product would be fluoresceine-Na

2) M. Imamura and M. Koizumi, This Bulletin, 28, 117 (1955).

3) B. E. Blaisdell, *J. Soc. Dyers & Colourists*, 65, 619 (1949).

(uranine) (II) which is a debrominated product of eosine (I).

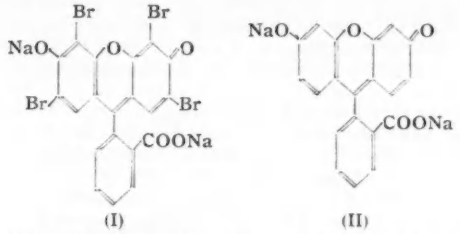

To confirm this conjecture, the following methods were adopted.

(*a*) *Comparison of Absorption Spectra.*—If the coloring material were uranine as supposed, then the separated absorption curves in the final stage of reaction should be the same as that of uranine, or of uranine which is partly photobleached in vacuo in the same aqueous alcoholic solution. Uranine in alcoholic or in aqueous alcoholic solution also decolorizes in vacuo, but no shift of spectrum such as for eosine is observed.

The comparison of the separated curves with that of uranine partly photobleached in vacuo is shown in Fig. 3. In Fig. 3 suitable normalization

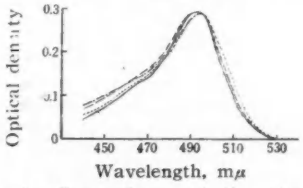

Fig. 3. Comparison of the absorption spectra.

———: Uranine partly photobleached in 10 vol. % EtOH solution;
– – – –: Separated curve for 5 vol. % EtOH solution;
·····: For 10 vol. % EtOH solution;
·—·—: For 20 vol. % EtOH solution;
(normalized at 495 mμ)

is done to make all the curves coincide at 495 mμ.

Absorption curves of an ultimate intermediate were measured in vacuo for the solutions in which the concentrations of alcohol were 5, 10 and 20 vol. per cent while the uranine partly photobleached was also measured in vacuo for 10 vol. per cent alcoholic solution. Agreement of all curves is satisfactory in view of the approximate nature of the analytical procedures.

(*b*) *Bromination.*—It is known that fluoresceine can easily be brominated by bromine into tetrabromofluoresceine[4,5]. In fact, uranine in aqueous alcoholic solution could be converted to eosine by adding few amounts of bromine and of sodium hydroxide. Hence similar bromination was applied to the 10 vol. per cent alcoholic solution in which eosine had almost completely disappeared in vacuo and the products were examined spectroscopically. The result is illustrated in Fig. 4.

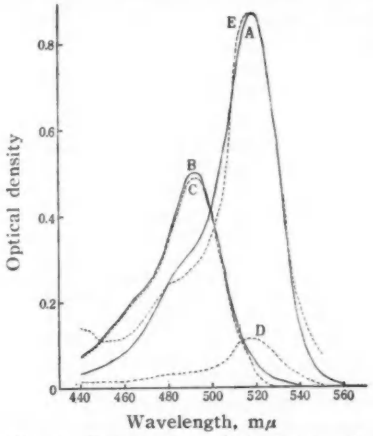

Fig. 4. Bromination of the intermediate. See sec. 3-b of procedures and results.

Curve A in Fig. 4 is an initial absorption curve of eosine in 10 vol. per cent alcoholic solution, B is the one after almost complete photobleaching of eosine in vacuo. Applying the analytical method mentioned in Sec. 2 to curve B, the resulting curve for intermediate is C. One drop of bromine and of concentrated sodium hydroxide solution were added to the irradiated solution of 10 ml.; then yellow color with strong green fluorescence instantly became reddish with weak fluorescence. Curve D indicates this color change. Levelling the curve D up to A at 520 mμ, the resultant is E.

If the intermediate, which is supposed to be uranine (curve C), be converted quantitatively to eosine by bromination, the maximum optical density of the curve D must be higher than the maximum optical density of the curve C*. The reason why the curve D is lower than the curve C in the present case, may plausibly be attributed to the simultaneous oxidative decomposition of uranine by bromine. When compared with the curve A, there scarcely remains any doubt that the curve E represents the absorption curve of eosine, although in the shorter wavelength region discrepancy is appreciable; this discrepancy may be due to the decomposition products.

(*c*) *Photobleaching of Uranine in Vacuo.*—When uranine in aqueous alcoholic solution was irradiated in vacuo under the same conditions as for eosine, it bleached in the same way but with a very slow rate and without any shift of its spectrum.

This behavior is qualitatively similar to that of the ultimate intermediate in eosine solution which was shown in Fig. 2.

From the facts mentioned above it can be concluded that the intermediate produced in the course of photobleaching reaction of eosine in aqueous alcoholic solution in vacuo is the debrominated eosine, that is, uranine.

* Maximum molar extinction coefficient of uranine is lower than that of eosine in aqueous or alcoholic solution.

4) K. Venkataraman, "The Chemistry of Synthetic Dyes", (1952) II, p. 747.

5) G. Schultz, "Farbstofftabellen", Leipzig (1931), I-2, p. 374.

4. Rate of the Conversion of Eosine.—The real rate of disappearance of eosine can be found by the method described in Sec. 2. It seems very natural to expect that the rate thus obtained be expressed, if I_{abs} is the light absorbed and is expressed in mol. per l. per sec., by the following equation:

$$-\frac{dc}{dt}=kI_{abs}, \tag{1}$$

since, as reported already[1], the photobleaching of eosine both in aerobic aqueous solution and in deaerated alcoholic solution obeys the following formula which is only a different form of Eq. (1).

$$-\frac{dc}{dt}=k\frac{I_0}{d}(1-e^{-\alpha cd})\times 1000. \tag{2}$$

It is to be noted, however, that in the present case there are more than two light absorbing species, eosine and intermediates, because the transmission of the filter covered the main absorption regions of them all. Hence, I_{abs} in Eq. (1) must be put as the portion of light actually absorbed by eosine, and this must be calculated as an integrated sum over the necessary wavelength regions, since the inner filter effect of the intermediates depends on the wavelength λ. Taking into account this fact, Eq. (1) is to be written as follows:

$$-\frac{dc_1}{dt}=1000k\int_{\lambda_1}^{\lambda_2}I_{0\lambda}\frac{\varepsilon_{1\lambda}c_1}{D_\lambda}(1-10^{-D_\lambda})d\lambda, \tag{3}$$

where $\varepsilon_{1\lambda}$, D_λ and $I_{0\lambda}$ are the molar extinction coefficient of eosine, the optical density of the solution and the incident light intensity all at λ, respectively. In making the computation of Eq. (3), values of $I_{0\lambda}$'s are necessary and these can be given as follows:

$$I_{0\lambda}=L_\lambda T_{f\lambda}=L_{\lambda max}T_{f\lambda}f_\lambda, \tag{4}$$

where,

L_λ: the light intensity per unit band of wavelength for a light source at λ,

$T_{f\lambda}$: transmission of the filter at λ.

f_λ: the intensity distribution fraction of the light source at λ.

Then I_0, the light intensity, is expressed as follows

$$I_0=\int_{\lambda_1}^{\lambda_2}I_{0\lambda}d\lambda=\int_{\lambda_1}^{\lambda_2}L_\lambda T_{f\lambda}d\lambda=L_{\lambda max}\int_{\lambda_1}^{\lambda_2}f_\lambda T_{f\lambda}d\lambda. \tag{5}$$

From Eqs. (3), (4) and (5),

$$-\frac{dc_1}{dt}=1000kI_0\frac{\int_{\lambda_1}^{\lambda_2}f_\lambda T_{f\lambda}\frac{\varepsilon_{1\lambda}c_1}{D_\lambda}(1-10^{-D_\lambda})d\lambda}{\int_{\lambda_1}^{\lambda_2}f_\lambda T f_\lambda d\lambda} \tag{6}$$

$$=1000kI_0f_{abs}.$$

f_λ's were calculated assuming that the temperature of the light source was 2500°K,[6] which gave just the same value of the mean molar absorption coefficient, α, of pure eosine as that determined experimentally by a thermopile.

The values of f_{abs} were calculated at several points of each run using the value of D_λ of the solution. The rate of the disappearance of eosine at the corresponding time-point was determined directly from the concentration-time curve, and dividing this by $1000I_0f_{abs}$, one could get the value of k. Values of k, which ought to be constant if Eq. (1) holds, are plotted against f_{abs}. Some examples are shown in Fig. 5. The constancy of k does not hold except for the solution in which alcohol concentration is high. In general, k decreases more and more as the reaction proceeds, in other words, as the quantity of coloring intermediate increases. But in the earlier stage of the reaction k does not change practically.

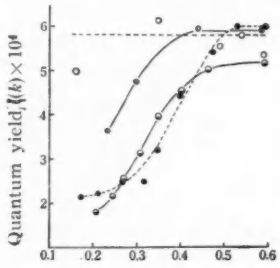

Fig. 5. Variation of the quantum yield with f_{abs}.
▬: 10 vol. %; ●: 20 vol. %;
◐: 50 vol. %; ○: 90 vol. %.

Although the above calculations are not altogether free from any ambiguity, there is no doubt about the general tendency that k-values decrease with the accumulation of the intermediate. Hence it was attempted to make clear some reasons for this behavior.

Supposedly Eq. (1) holds in the present case. One possible reason for this decrease might be the non-homogeneity of the irradiated solution; under the condition of non-stirring, intermediate coloring substances will become concentrated in the front part of the solution and this may cause a larger filter effect than that under the homogeneous condition which was assumed in the above calculation.

If this be the case, it should be possible to make this effect smaller with proper choice of experimental conditions. Some experiments were conducted for this purpose. Thus the initial concentration of eosine selected was half that of the ordinary one using another cell of 10 mm. path length (5 mm. shorter than ordinary cells) and the measurements of absorption spectra were made at shorter intervals. But the result is that there was no noticeable difference.

Another conceivable reason is some sort of retarding effect of the reaction products on the rate of photobleaching of eosine. The following experiments were conducted to examine this possibility. A definite amount of uranine was added previously to the pure ethanol solution of eosine and the rate of the photobleaching of the latter was measured by the usual method. It was definitely established by several experiments that

6) A. N. Lowan and G. Blanch, *J. Opt. Soc. Am.*, 30, 79 (1940).

the addition of uranine causes a marked retarding effect and that the effect increases greatly with the increase of added uranine. Some results are shown in Table I, where k values are calculated by the method analogous to that stated above, taking the filter effect of uranine into account.

TABLE I

QUANTUM YIELDS FOR THE VACUUM PHOTOBLEACHING OF EOSINE IN EtOH IN THE PRESENCE OF URANINE

$I_0 = 1.4 \times 10^{15} h\bar{\nu}$/cm^2. sec. 27°C

Conc. $\times 10^5$mol./l.		Quantum Yield, $k \times 10^4$
Eosine	Uranine	
10.0	—	6.0
10.0	2.5	3.4
10.0	5.0	1.0
10.0	10.0	0.5

From the above tests it is certain that the decrease of k is mainly due to the retarding effect of intermediates including uranine, although it is impossible, in the present stage of investigation, to interpret the matter quantitatively on the basis of the above data, in view of the facts that the experimental conditions of the above tests differ from those in the ethanol-water solutions which contain some other unknown intermediate products preceding final uranine production.

Thus the k-value extrapolated to t=0 can be accepted as a true one. Plotting the quantum yield thus obtained, against the concentration of ethanol, a curve is obtained which is shown in Fig. 6. As seen from Fig. 6, the quantum yield increases with increasing concentration of ethanol up to ca. 20 vol. per cent and then it becomes constant, the value being the same as that obtained in pure ethanol in vacuo.

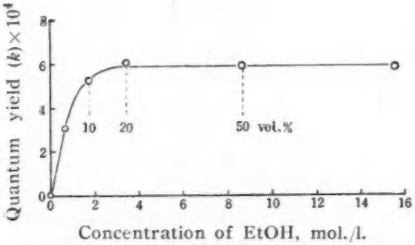

Fig. 6. Variation of the quantum yield with the concentration of EtOH.

Discussion

1. First the reliability of the evaluation of k-values and of the interpretation of the absorption spectra of intermediates will be discussed briefly. There is some suspicion that Blaisdell's method by which the minimum ratio of the optical density of the irradiated solution to that of the original one was taken for a measure of the concentration of the remaining eosine, might have given a smaller value than the real one, in view of the fact that the absorption curve of the intermediate is superposed on that of eosine in the whole range of wavelengths. But the superposition is negligible in the longer wavelength region above 530 mμ and the minimum ratio is exactly between 530 and 540 mμ without a single exception. Furthermore, the k-values in Fig. 6 are obtained from the initial rate which is scarcely affected by the reaction products. From these facts it is considered that the evaluation of k-values is very reliable.

As to the absorption spectra of the intermediates, there is no doubt that they are related only to the reaction products which are specific in the water-alcohol mixture. For, although there is another type of reaction which takes place in pure alcohol, the product of this reaction gives only a very small absorption band near ultraviolet and this band can not affect the present band even if the reaction of the latter type participates in wateralcohol mixture. Hence, the interpretation of the intermediates is considered to be fairly trustworthy.

2. From the fact that the quantum yield, k, is independent of the concentration of ethanol above 20 vol. per cent, it can be concluded that the primary processes in water-alcohol mixture are just the same as those in pure alcohol. They are

$$D \xrightarrow{h\nu} D^* \longrightarrow D^t \qquad \text{(i)}$$

$$D^t + RH \longrightarrow DH\cdot + R\cdot, \qquad \text{(ii)}$$

where D^t is eosine in the triplet state, RH is alcohol, and DH· is a colorless or almost colorless semiquinoid radical. This conclusion is further supported by the following preliminary experiments. Thus, similar experiments using methanol- and isopropanol-water mixtures were attempted and analogous spectral shifts due to the production of coloring intermediates were observed, the extent of which was less in methanol and was nearly equal or a little greater in isopropanol than in ethanol. This order is exactly the same as for the rate of photobleaching in pure alcohols as reported already[1], and the result is quite reasonable if the two types of reaction proceed via the common primary processes.

It is significant that water molecules act as retarders only below 20 vol. per cent of alcohol. This result shows evidently a strong reactivity of ethanol with D^t, while the reaction of water with D^t is negligible, if it exist, at least when the content of alcohol exceeds ca 20 vol. per cent.

The production of uranine can be interpreted as a result of further interaction of

DH· with water.

3. On the basis of the above results concerning the variation of k with the concentration of ethanol, a definite conclusion can be drawn about the primary processes of the aerobic photobleaching of eosine in aqueous solution which remained undecided in the first paper[2] of this series. The two schemes then proposed were

$$D^t + O_2 \longrightarrow D\cdots O_2 \xrightarrow{H_2O} \cdots\cdots \text{prod.} \qquad \text{(iii)}$$

$$D^t + H_2O \longrightarrow D\cdots HOH \xrightarrow{O_2} \cdots\cdots \text{prod.} \qquad \text{(iv)}$$

and it can now be said that the former is suitable. The reason for it is as follows. As reported previously[2], ethanol causes a marked retardation on the aerobic photobleaching, but, at the concentration of ethanol of 20 vol. per cent there is observed photobleaching to some extent with a quantum yield about 1/5 of that in the pure aqueous solution. Hence if aerobic photobleaching in the aqueous solution goes via (iv), water ought to show a retarding effect just as great or greater than this value on the photobleaching in vacuo. But the present investigation shows that it is not the case.

Thus it can be concluded that the primary process in the aerobic photobleaching in the pure aqueous solution is (iii), in which D^t primarily reacts with oxygen molecule to form a labile complex, $D\cdots O_2$. It is to be noted, however, that the data for k-values are rather few and it is desirable to accumulate them or to find some other facts in support of this mechanism. Further confirmations and somewhat quantitative discussions will be given in the next paper.

4. Though the detailed mechanism of the uranine-producing reaction is not yet clear, it is certain that uranine is not directly formed from eosine but is formed via some preceding intermediates, may be dibromo-compound, in view of the fact that the absorption for intermediates (Fig. 2) shows a gradual displacement of their maxima towards shorter wavelengths.

When the quantity of intermediates produced per unit quantity of decomposed eosine is evaluated from the absorption data and is plotted against time, then it is found from the value extrapolated to time zero that the reaction which produces coloring materials decreases with increasing concentration of alcohol. The molar extinction coefficient of the intermediates can be estimated to be roughly 10^5 from the data for the solution of low alcohol content. Hence, in the region of low concentration of alcohol (~20 vol. per cent), the principal reaction is an uranine-producing one, while, with rising concentration of ethanol, the reaction in pure ethanol becomes predominant.

It is to be added here that, according to our supplementary experiments, an uranine-producing reaction is sensitive to pH; the addition of a very small amount of acetic acid causes no shift of spectrum. Further, in the case of erythrosine, uranine is not so much produced as in the case of eosine under analogous conditions.

At any rate, the reaction of this type seems to be exceedingly curious from the standpoint of organic reactions and may be worthy of further research from this point of view, as well as from the view point of photochemistry.

Summary

The photoreaction of eosine has been studied in ethanol-water mixture in vacuo. Irradiated solution showed a gradual spectral shift towards shorter wavelengths. Analyzing the spectra and applying the chemical method, it was found that the spectral shift is due to the production of uranine.

The rate of disappearance of eosine increases with rising concentration of ethanol until 20 vol. per cent, at which it reaches its maximum and constant value, which is the same as that in pure ethanol.

The primary processes of the aerobic photobleaching of eosine in aqueous solution were discussed and it was concluded that the process must be

$$D^t + O_2 \longrightarrow D\cdots O_2 \xrightarrow{H_2O} \cdots \text{prod.} \qquad \text{(iii)}$$

The cost of the present research has been partly defrayed from the Scientific Research Grant from the Ministry of Education.

Institute of Polytechnics
Osaka City University
Osaka

*Partition Equilibrium of Cumene Hydroperoxide between Water and Cumene**

By Shigehiko YAMADA and Tokio KATŌ

(Received May 17, 1956)

In the "cumene process", the hydroperoxide (CHP) is sometimes obliged to come in contact with water chiefly because the latter is the general stabilizer to thermal decomposition of CHP in the oxidate. The contact is operated during and after the hydroperoxidation, where dissolution of CHP in the water phase cannot be neglected. In this relation, studies on the partition equilibrium of CHP between water and cumene seem to contribute to the solution of the problem, so the partition constant K and its dependence on the temperature and CHP concentration were investigated. We can find no description of such an investigation in the literature up to the present, though CHP is said to be insoluble in water[1].

Experimental

Apparatus and Sample.—Thermostat adjusted to ±1°C, and conical flasks of 200 cc. and 500 cc. with tight stoppers were used.

Cumene was prepared by alkylation of benzene with propylene in the presence of 90% sulfuric acid at 20~30°C. The fraction of the mixture after washing with concentrated sulfuric acid and 25% aqueous sodium hydroxide for more than 10 times, had b. p. 151~3°C.

CHP was prepared by the liquid phase oxidation of the cumene with oxygen gas at 128~132°C. The sodium salt was precipitated by shaking the steam-stripped oxidate with 25% aqueous sodium hydroxide, filtering off, washing with petroleum benzine, and dissolving in water. The solution was acidified with carbon dioxide, the oily layer extracted with petroleum ether, dried over anhydrous sodium sulfate, filtered and concentrated at 50~70°C under 1~3 mmHg pressure. The clear residue was found to contain 99% be weight of CHP by iodometry.

Method.—Several solutions, varying in concentration of CHP in the cumene were prepared in the flasks. Distilled water was added to the same volume as that of the oil and they were settled for a certain time after being subjected to vigorous shakings every 10~15 min. Volumes of samples employed for analysis were 1 or 5 cc. for the oily layer and 20 or 25 cc. for the aqueous layer according to the concentration of CHP in solution.

Each group of four samples was brought side by side in the thermostat for 2.5 hr. at 10, 20, 35, 50°C, and served for analysis.

Determination of Partition Constants.—We assume that v_1 is the volume (cc) of N/10 aqueous sodium thiosulfate consumed for 5 cc. of oily layer, v_2 that for 25 cc. of water, and c_1, c_2 moles of CHP per litre in the oily and aqueous layer respectively. Then the partition constant $K(t)$ at t°C is shown as follows.

$$K = c_2/c_1 = 0.2\, v_2/v_1$$

Results are given in Table I.

TABLE I

PARTITION CONSTANTS AT SEVERAL TEMPERATURES

t (± 1°C)	v_1 (cc.)	v_2 (cc.)	K (×10²)
10	9.46	1.75	3.7
	9.56	1.82	3.8
	19.70	3.12	3.2
	36.20	6.38	3.5
20	4.30	0.64	3.0
	9.10	1.48	3.3
	19.18	2.48	2.6
	32.45	4.00	2.5
35	5.40	0.62	2.3
	11.43	1.28	2.2
	23.03	2.32	2.0
	44.68	4.50	2.0
50	6.10	0.51	1.7
	11.40	1.10	1 9
	21.76	2.05	1.9
	39.73	3.37	1.7

The Time Required for the Equilibrium.—Some samples in Table I were further taken to determine K under the settling time of 1.5 hr., which however gave approximately the same value, as in the case of Table I. The following data show the variation of CHP concentration with the settling time. In these cases the temperature was subjected to the fluctuation ranging from 7 to 15°C and the shaking time of 10~15 min. was not exactly maintained.

A and B in Table II are the volume (cc.) of thiosulfate solution required for titrating 5 cc. of aqueous layer of the system, composed of 200 cc. of distilled water and 200 cc. of 15~20% CHP solution, prepared from pure CHP and the steam-stripped oxidate of cumene respectively.

* Presented at the 9th Annual Meeting of the Chemical Society of Japan held in Kyōto, April, 1956.

1) H. Hock and S. Lang, *Ber.*, 77, 259 (1944).

TABLE II

VARIATION OF CHP CONCENTRATION IN THE AQUEOUS LAYER WITH TIME AS EXPRESSED BY CC. OF THIOSULFATE SOLUTION

	10 min.	2 hr.	4 hr.	6 hr.	1 week
A	0.54	0.92	0.59	0.56	0.69
B	0.52	0.74	0.39	0.59	0.65

Data for the Practical Oxidate.—A similar method was applied for the practical oxidate of cumene prepared as mentioned above. Results are given in Table III.

TABLE III

PARTITION CONSTANT FOR THE PRACTICAL OXIDATE AT 10°C

v_1'	v_2'	K ($\times 10^2$)
6.18	1.25	1.0$_1$
12.70	2.41	0.9$_5$
24.40	4.75	0.9$_7$

v_1', v_2' are volumes for 1 cc. and 20 cc.

$$K=0.05\, v_2'/v_1'$$

Discussion

Concentration and Temperature Dependence of Equilibrium Constant K.—Constancy of K regardless of the change of CHP concentration at each temperature seems to be affirmed within the limits of experimental error, while its dependence on the temperature is shown in Table IV and Fig. 1.

TABLE IV

ARITHMETIC MEAN OF CONSTANT, $\bar{K}$ AT EACH TEMPERATURE

t (±1°C)	$\bar{K}$ ($\times 10^2$)
10	3.6
20	2.9
35	2.1
50	1.8

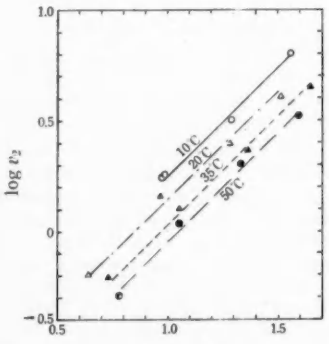

Fig. 1. Relation between log v_1 and log v_2.

Linear relation between log $\bar{K}$ and reciprocal of absolute temperature shown in Fig. 2. suggests that it will satisfy the following thermodynamic formula,

$$\ln K_2/K_1=-Q/R\cdot(1/T_1-1/T_2),$$

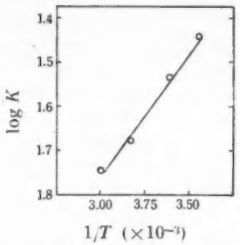

Fig. 2. Relation between log $\bar{K}$ and $1/T$.

where, R is the gas constant, and Q, the heat of transference of 1 mol. of CHP from cumene solution into water under the equilibrium condition. Thus, Q was determined as 3.16 kcal./mol. Accordingly, equilibrium constant K approximately satisfied the following formula,

$$K=1.3_4\times 10^{-4}e^{1580/T}$$

Other Problems.—From data in Table II the equilibrium is supposed to be established within two hours under these conditions. Further, values of K for the practical oxidate appear remarkably smaller than those for pure CHP series. A similar tendency was also observed in other practical cases which may presumably be explained as the influence due to the side products of the hydroperoxidation.

Summary

The partition equilibrium was investigated in relation to the steam-blowing and stripping, during and after the hydroperoxidation of cumene, and the following results were obtained.

1. Equilibrium constant K does not depend on the concentration of CHP within the limit of experimental error, but it depends on the temperature.

2. The partition constant, K approximately satisfies the following formula,

$$K=1.3_4\times 10^{-4}e^{1580/T}.$$

3. The heat of transference of 1 mol. of cumene hydroperoxide from cumene solution into water under the equilibrium condition, was determined as 3.16 k cal./mol.

This article is a part of the investigations of the cumene process which have been studied by many members of Tōkai Electrode Mfg. Co. The authors are grateful to them and wish to express their thanks to Dr. H. Sobue, professor of Tokyo University, for his valuable suggestions and discussions, to Mr. M. Nomaguchi, the chief of our laboratory for his instructive advice and encouragement, and to the authorities of Tōkai Electrode Mfg. Co. for the publication of this work.

Technical Research Laboratory
Tōkai Electrode Mfg. Co.
Fujisawa

*Antioxygenic Activity of α- and β-Glycerophosphoric Acids**

By Chieko URAKAMI, Yoshiko KAKUTANI and Hirotomo OKURA

(Received June 24, 1956)

Introduction

Since Bollmann[1] discovered antioxygenic activity of crude lecithin, a number of other investigators[2] have reported similar findings. However, Hilditch[3] found that purified lecithin did not show any antioxygenic activity in the autoxidized esters of the distilled fatty acids of olive oil. For the study of relations of molecular structures of phosphatides to antioxygenic activity, their hydrolysis products have been investigated by a number of workers. Olcott and Mattill[4] reported that cephalin among other phosphatides had the strongest activity and suggested that the phosphoryl group in the molecule has some relation to the activity. Strohecker, et al.[5] obtained the result that only choline among other hydrolytic products of cephaline was active against oils of plant origin, whereas Dutton, Olcott, and Mattill[6] observed that the phosphoryl residue in the cephalin or lecithin molecules possessed activity. Altman[7] reported that phosphatides, choline and amino acids were effective in rubber latex. Recently, Desneulle et al.[8] have found that the phosphatidyl choline which has been obtained from eggs did not possess antioxygenic activity in the methyl esters of sunflower seed oil fatty acids but the phosphatidic acids obtained on treating the phosphatidyl choline with phosphatase prepared from carrots exerted the activity. Calkin[9] proposed the theory that cephaline with one free hydroxyl gorup should show some activity but lecithin which has no free hydroxyl group in its molecule should have no activity.

It is conceivable that nothing definite has been established as to the relation of molecular structures of the phosphatides to antioxygeninc activity. It is, however, reasonable to assume that the phosphoryl group in these molecules would possess the activity since a number of organic esters of phosphoric acid[10] are known to be antioxygenic to fat-containing materials.

The confusing results[3,5,6] on the phosphatidic acids may be due to difference in composition of the hydrolysis products with respect to the α and β-structures of the glycerophosphoric acids, since the isomerization of the phosphoryl group has been found to occur in either acid or alkaline hydrolysis[11], to a greater extent with the former. Therefore, we have called our attention to the relation of the structural difference of the phosphatidic acid, to antioxygenic activity and, as a preliminary work, studied α and β-glycerophosphoric acids, relatively stable hydrolysis products of the phosphatides, in purified oleic acid.

Conditions for autoxidation were selected so that least kinds and amounts of by-products would be produced during autoxidation, as demonstrated by Swern, et al.[12] As the rate of oxidation of oleic acid is slow compared to that of methyl oleate, we chose 50°C for the temperature of autoxidation and compared activities of the glycerophosphoric acids with that of phosphoric acid in an early stage, up to peroxide value of about 10 mM per 100 g. of the acid. It was found that the α-compound was just as active as orthophosphoric acid but the β-isomer did not have any activity.

We have also investigated recovery of the water soluble glycerophosphoric acids during autoxidation to obtain some clue as to mechanism involved in the antioxygenic activity. Preliminary results showed that the recovery of the water soluble grycerophosphoric acids from the autoxidized oleic acid

* Presented in part at the 9th Annual Meeting of The Chem. Soc., Japan, April, 1956.

1) H. Bollmann. *U. S. Pat* 1, 575, 529 (1926).

2) G. I. Evans, *Ind. Eng. Chem...*, 27, 399 (1935); H. N. Holmes, R. E. Corbet and R. A. Ragatz, ibid., 28, 133 (1936); M. R. Sahasrabudhe, *J. Sci. Ind. Research*, 12B 63 (1953); H. J. Lips, *Food in Canada*, 12, No. 6, 9, 12 16 (1952).

3) T. P. Hilditch and S. Paul, *J. Soc. Chem. Ind*, 58, 21 (1939).

4) H. S. Olcott and H. A. Mattill, *Oil and Soap*, 13, 98 (1936).

5) R. Strohecker, W. Diemair and K. Reuland, *Z. Untersuch. Lebensm.*, 79, 23 (1940).

6) H. J. Dutton, H. S. Olcott, and H. A. Mattill, *J. Am. Oil Chemists' Soc.*, 26, 441 (1949).

7) R. F. A. Altman, *Trans. Inst. Rubber Ind.*, 23, 179 (1947).

8) P. Desneulle, R. Massoni and O. Benoit-Micaelli, *Bull. Soc. chim. France*, 1953, 595.

9) V. P. Calkins, *J. Am. Chem. Soc.*, 69, 384 (1947).

10) H. R. Kraybill and B. W. Beadle, *U. S. Pat.*, 2, 521, 856.

11) E. Baer and M. Kates, *J. Biol. Chem.*, 185, 615 (1950); E. Baer, H. C. Stancer and I. A. Korman, ibid., 200, 251 (1953).

12) H. B. Knight, J. E. Coleman and D. Swern *J. Am. Oil Chemists' Soc.*, 28, 498 (1951); ibid., 32, 135 (1955); D. H. Saunders, C. Ricciuti and D. Swern, ibid., 32, 79 (1955).

was very small, implying that a larger amount is associated with the fatty acid.

Experimental

Oleic Acid.—"Tokusei olein NTA 34" of the Nihon Yushi K. K.[13] was purified by recrystallization from acetone at low temperatures[14], first at −5° to remove stearic and other saturated acids present and then at −53° to removed linoleic and other highly unsaturated acids. The solvent was removed from the acetone solution containing chiefly oleic acid and the residue distilled three times. The sample thus prepared had the following constants: B.p., 220°/7 mm.and 221°/8 mm (220°/7 mm.).; Iodine number, 89.10 (89.9); Neutralization value, 199.7 (198.8); n_D^{20}, 1.4599, (1.4585, 1.4599). The figures given in the parentheses are those calculated or found in the literature.

Orthophosphoric Acid.—Analytical reagent (85%) of Mallinckrodt Chemical Works, U. S. A. was used. It was dehydrated in a vacuum desiccator over calcium chloride and then taken up in absolute alcohol. Its concentration was determined by Burmaster's method[15]. For the determination of absorption coefficients, Shimazu Model DF-11 with the filter no. 634 and 5 mm. cell were employed.

α-Glycerophosphoric Acid.—The barium ion of barium α-glycero-Phosphate[15] was removed in the form of sulfate by treating with 0.1 N sulfuric acid (adjusted to pH 1.5), followed by repeated washing with alcohol. The alcoholic solution was concentrated to 3 cc. in volume and the concentrate analyzed according to Burmaster's method. Analysis of 1 cc. of the alcoholic concentrate: inorganic P, 0.000 mg.; α-glycerophosphoric acid, 10.656 mg.; the β-isomer, 0.500 mg.

β-Glycerophosphoric Acid.—Sodium β-glycerophosphate suspended in alcohol was treated with 0.1N alcoholic HCl (adjusted to pH 1.5), the mixture concentrated under reduced pressure, and the residue washed several times with alcohol to remove the sodium chloride precipitated. The process was repeated several times to remove as much of the sodium chloride as possible, and the final alcoholic solution concentrated to give 3 cc. in volume. Analysis of 1 cc. of the solution: inorganic P, 0.000 mg.; α-glycerophosphoric acid, 0.600 mg.; the β-isomer, 20.960 mg.

Autoxidation of Oleic Acid.—After adding a sufficient amount of an alcoholic solution of the compound under consideration to 14 g. of oleic acid, the alcohol was removed at less than 40°C under reduced pressure and nitrogen atomosphere. The concentration of the compound in oleic acid was kept at 0.1%. The sample thus prepared was autoxidized at 50°C by passing purified air at a rate of 3l. per min. through a sintered glass funnel (a medium sized pore) without the sleeve. Aliquots were removed at intervals (into a weighing bottle containing 1–2 drops of a 0.05% solution of hydroquinone in isopropanol) and their peroxide values were determined according to Volz-Gortner's method[17], using 0.005N solution of sodium thiosulfate. The titration was carried out by using a 1 or 2 cc. pipette provided with a large injection needle at the tip end with the aid or rubber tubing and a long rubber tubing attached to a syringe at the other end. By manipulating the syringe, one cc. was cut into 70 drops. The method gave more accurate results than those obtained by using the microburette sold on the market. The error of average deviation involved was found to be 2% with peroxide values up to 1.5mM/100 g, 0.1% with 9 mM/100 g, and 0.5–1% for the intermediate values.

Recovery Test.—An aliquot of 0.1 cc. was removed at intervals during the autoxidation, weighed accurately, and dissolved in 2 cc. of ether. The ether solution was washed four times with 1 cc. portions of fresh water. The washing were combined, made up to a known volume and analyzed for the recovery of the glycerophosphoric acids. Blank tests were carried out in exactly the same manner with β-glycerophosphoric acid in non-autoxidized oleic acid.

Results

The effect of alcohol used as a solvent was observed, as shown in Tables I and II, higher peroxide values were obtained with the sample treated with alcohol. The results obtained with orthophosphoric acid, α and β-glycerophosphoric acids are shown in Tables III, IV and V, respectively. The maximum error

TABLE I

AUTOXIDATION OF OLEIC ACID AT 50°C

Time hr.	Peroxide Value m. mol./100 g.	Amount of Air Passed, Kl.
6.5	1.32±0.02	0.85
11.8	2.23±0.02	1.67
22.1	4.25±0.09	3.43
26.8	5.30±0.11	4.20
34.4	6.88±0.02	5.38
47.9	9.53±0.02*	7.68

* The determination was carried out 6 hr. after removing the sample from the autoxidation chamber.

TABLE II

AUTOXIDATION OF OLEIC ACID WITH TRACE OF ALCOHOL AT 50°C

Time hr.	Peroxide Value m. mol./100 g.	Amount of Air Passed, Kl.
5.9	1.56±0.02	0.95
18.4	4.00±0.06	3.15
23.0	5.01±0.02	3.86
28.1	6.20±0.04	4.66
43.8	9.70±0.04	7.28

13) We thank the Nihon Yushi K. K. Kenkyu-sho for the supply of the sample.

14) D. K. Kolb and J. B. Brown, *J. Am. Oil Chemists' Soc.*, **32**, 357 (1955).

15) C. F. Burmaster, *J. Biol. Chem.*, **164**, 233 (1946).

16) C. Urakami and Y. Kakutani, *Repts. Sci. Living, Osaka City Univ.*, Series D. No. 1, 3 (1953).

17) F. E Volz and W. A. Gortner, *J. Am. Oil Chemists' Soc.*, **24**, 417 (1947).

involved in the rates of aeration of the samples were found to be 5% but the rates were very close to each other in the samples containing α and β-glycerophosphoric acids.

TABLE III
AUTOXIDATION OF OLEIC ACID IN THE PRESENCE OF H_3PO_4 AT 50°C

Time hr.	Peroxide Value m. mol./100 g.	Amount of Air Passed, Kl.
5.8	0.73±0.02	0.75
20.6	1.84±0.04	3.02
30.2	2.72±0.02	4.05
44.7	4.44±0.07	6.48
53.2	5.60±0.04	7.90

TABLE IV
AUTOXIDATION OF OLEIC ACID IN THE PRESENCE OF α-GLYCEROPHOSPHORIC ACID AT 50°C

Time hr.	Peroxide Value m. mol./100 g.	Amount of Air Passed, Kl.
6.0	0.69±0.01	1.00
19.1	1.20±0.01	3.33
29.0	1.97±0.01	4.95
43.6	4.27±0.08	7.51
51.6	5.50±0.00	8.81

As shown in Tables IV and V, there is a distinct difference in antioxygenic activity between the two isomers, α-glycerophosphoric acid has the activity somewhat better than phosphoric acid while the β-isomer has no activity at all. The peroxide values for the latter are somewhat higher than those of

TABLE V
AUTOXIDATION OF OLEIC ACID IN THE PRESENCE OF β-GLYCEROPHOSPHORIC ACID AT 50°C

Time hr.	Peroxide Value m. mol./100 g.	Amount of Air Passed, Kl.
5.4	1.93±0.02	1.00
20.0	4.65±0.04	3.52
29.5	6.55±0.07	5.05
43.2	8.98±0.07	7.43
50.5	10.2 ±0.1	8.61

oleic acid alone but close to those of the blank run made with the addition of alcohol.

Recovery of water soluble β-glycerophosphoric acid from unautoxidized oleic acid was found to be 95%. However, there was a sharp drop in recovery of both α and β-glycerophosphoric acids from autoxidized oleic acid, 21–35% and 2–8%, respectively, as shown in Tables VI and VII. As the autoxidation progressed, a small amount of the α compound was detected in the β-sample.

Discussion

It has been demonstrated that α-glycerophosphoric acid has antioxygenic activity comparable to that of orthophosphoric acid in purified oleic acid but the β-isomer has no activity. According to Baer et al.[11] and Long and Maguire[18], alkaline or acid hydrolysis of the naturally occurring phosphatides results in migration of the phosphoryl radical. Consequently, the samples of glycero-

TABLE VI
RECOVERY OF α-GLYCEROPHOSPHORIC ACID FROM AUTOXIDIZED OLEIC ACID

Aliquot g.	Time of autoxidation, hr.	Absorbance* P			Microgram P				The Acids/0.2 g. Sample, μg.			Total recovery %
		H_3PO_4	α	Total	H_3PO_4	α	Total	β	α	β	H_3PO_4	
25 μl**		0.003	0.38	0.39	0.00	24.0	24.9	0.9	106.6 (96.4)	3.7 (3.4)		100
0.2408	29.0		0.113			6.9			63.6 (26.9)			
0.2421	〃			0.115			7.0			0.6 (0.25)		27.2
0.1907	43.4	0.008										
0.1899	〃		0.111			6.75			79.9 (33.8)			
0.1889	〃			0.115			7.0			2.3 (1.0)		34.8
0.2148	51.4	0.010			0.05						0.52 (0.2)	
0.1978	〃		0.062			3.5			39.3 (16.6)			
0.2164	〃			0.082			4.9			11.0 (4.7)		21.2

* The values were obtained by subtracting absorbance of blank from that of sample.
** Analysis of the alcoholic solution added to oleic acid. The figures in the parentheses are per cent recovery of the respective acid.

18) C. Long and M. F. Maguire, *Biochem. J.*, 54, 612 (1953).

TABLE VII

RECOVERY OF β-GLYCEROPHOSPHORIC ACID FROM AUTOXIDIZED OLEIC ACID

Aliquot g.	Time of Autoxidation, hr.	Absorbance* P			Microgram P			The Acid, 0.2 g. Sample, μg.		Total recovery %
		H_3PO_4	α	Total	H_3PO_4	α	Tatal	α	β	
10 μl**		0.004	0.017	0.295		0.50	18.88	5.8	218.5 (97.4)	100
0.2382	19.6		0.007							
0.2368	〃			0.037			1.83		17.07	7.6
0.2164	29.3		0.010			0.05		0.51 (0.2)		
0.2269	〃			0.037			1.83		17.40 (7.8)	8.0
0.1027	43.1	0.00								
0.2110	〃		0.010			0.05		0.52 (0.2)		
0.2125	〃			0.022			0.86		8.36 (3.7)	4.0
0.2070	50.3	0.00								
0.2146	〃		0.010			0.05		0.25 (0.2)		
0.2206	〃			0.018			0.55		4.82 (2.2)	2.4

* The values were obtained by subtracting absorbance of blank from that of sample.
** Analysis of the alcoholic solution added to oleic acid. The figures in the parentheses are per cent recovery of the respective acid.

phosphoric acids or the hydrolysates of phosphatides studied earlier for their antioxygenic activity might have been a mixture of the isomers in various proportions and this might have been responsible for the confusing results found in the literature.

Concerning mechanisms of antioxygenic activity of orthophosphoric acid, Quackenbush[19] reported that at a higher temperature phosphoric acid reacted with the peroxides of lard to give an oil soluble polymer-like substance. On the other hand, Calkin[9] suggested that the activated oleic acid adsorbs phosphoric acid molecules to form an ester-like intermediate, which on dissipating its energy disintergrates into the original substances, oleic acid and phosphoric acid. Our preliminary results in the recovery of the glycerophosphoric acids indicate that they are either adsorbed on the oleic acid molecules or transformed into some kind of oil soluble products. Further investigation on this point is of great interest and we are extending the study.

Faculty of Science of Living, Osaka City University, Osaka

19) F. W. Quackenbush and O. S. Privett, *J. Am. Oil Chemists' Soc.*, **31**, 225 (1954).

Metal Chelate Compounds with Higher Rings. I. The Preparations and Some Properties of Copper(II) Complexes of ω-Aminocarboxylic Acids

By Akitsugu NAKAHARA, Jinsai HIDAKA and Ryutaro TSUCHIDA

(Received July 21, 1956)

Introduction

It is well-known that chelation in metal chelate compounds is most favoured when the functional groups are in the 1, 4 or 1, 5 positions.

In fact, relatively few chelate rings containing more than six atoms have been prepared from bidentate compounds. But the formation of larger rings does not always seem to be difficult if the preparation is carried out in non-aqueous media such as alcohol, ether, or chloroform. Recently Pfeiffer[1,2], for instance, has succeeded in preparing 7-, 8-, and 9-membered rings by the reaction of tetra-, penta-, and hexa-methylenediamine, respectively, with some metal salts in organic solvents. In the case of dicarboxylic acid complexes, there have also been reported some other complexes containing 7- and 8-membered rings[3,4,5]. Those increasing examples of higher rings have led us to perform the further systematic researches of metal chelate compounds with higher rings. The chief purpose of this series of work is to establish experimental data concerning the relation between the stability and ring sizes.

First of all, we picked up copper(II) complexes of ω-aminocarboxylic acids which contain carbon atoms from C_2 to C_6, getting two new examples of higher rings and one new type of amino acid complex. They are copper(II) complexes of γ-aminobutyric*- and δ-aminovaleric-acid, and of ε-aminocaproic acid, respectively. This paper describes the preparations and some properties of those three new compounds with some discussion on their stabilities.

Experimental

General Method of Preparation.—Two methods were adopted for preparing copper(II) complexes of ω-aminocarboxylic acids. The one was a heterogeneous reaction, (**A**), of a ligand with copper(II) perchlorate in an organic solvent, while the other was a homogeneous reaction, (**B**), making use of the action of an overwhelming amount of a ligand in an aqueous solution. The product obtained by the method (**A**) necessitated to be recrystallized from a mixed solution of alcohol and water containing a large amount of the ligand. Therefore, the difference between the two methods was rather slight. When the preparation was performed on a small scale, however, the method (**A**) seemed to have much advantage over (**B**).

Preparation of Bis-(γ-aminobutyrato)-copper(II), $[Cu(NH_2(CH_2)_3COO)_2]\cdot 2H_2O$.—The method (**A**) was applied to prepare this compound. To a suspension of 4 g. of γ-aminobutyric acid in chloroform, was added 3.5 g. of copper(II) perchlorate hexahydrate. The heterogeneous mixture was shaken vigorously till the light blue of the copper(II) perchlorate changed to deep blue or violet. To complete the reaction the mixture was preserved overnight. The viscous product was freed from chloroform by blowing dry air on it after decantation. Then the crude product was dissolved in a small quantity of water, and the resulting solution was filtered quickly. A large amount of alcohol was added carefully to the clear deep blue filtrate. Within a few days fine crystals of $[Cu(NH_2(CH_2)_3COO)_2]\cdot 2H_2O$ were obtained. The yield of the reaction was almost quantitative, and the compound was pure enough at least for spectrochemical studies. The results of the analyses were as follows.

Anal. Found: C, 31.54; H, 6.49; N, 9.29; H_2O, 11.55. Calcd. for $[Cu(NH_2(CH_2)_3COO)_2]\cdot 2H_2O$: C. 31.57: H, 6.56: N, 9.21: H_2O, 11.84%.

Preparation of Bis-(δ-aminovalerato)-copper (II), $[Cu(NH_2(CH_2)_4COO)_2]$.—This compound was prepared by the method (**A**). In this case, however, there was provided twice the quantity of the ligand in mole ratio for the complex formation, since it was assumed that the complex might have less stability compared with bis-(γ-aminobutyrato)-copper(II). Other procedures for preparation were the same as those described above.

Anal. Found: C, 40.54; H, 7.09; N, 9.13. Calcd. for $[Cu(NH_2(CH_2)_4COO)_2]$: C, 40.60; H, 6.76; N, 9.47%.

Preparation of Tetrakis-(ε-carboxyamylamine)-copper(II) Perchlorate, $[Cu(NH_2(CH_2)_5COOH)_4](ClO_4)_2$.—To prepare this compound the method (**B**) was adopted as well as (**A**). Copper(II)

1) P. Pfeiffer, E. Schmitz and A. Böhm. *Z. anorg. allg. Chem.*, **270**, 287 (1952).
2) P. Pfeiffer, *Naturwiss.*, **35**, 190 (1948).
3) J. C. Duff, *J. Chem. Soc.*, **119**, 385, 1982 (1921); **123**, 560 (1923).
4) T.S. Price and S.A. Brazier, ibid., **107**, 1367 (1915).
5) T. S. Price and J. C. Duff, ibid., **117**, 1071 (1920).
* Although there are some descriptions of the complex formation of bis-(γ-aminobutyrato)-copper (II), the compound has never been isolated in the crystalline state up to date.

perchlorate hexahydrate was added to an aqueous solution which contained an over-whelming amount of ε-aminocarboxylic acid. After filtration of the deep blue solution, beautiful violet crystals were obtained. Within a couple of hours the deposition of the complex ended. The yield of the reaction was almost quantitative. The analyses of the compound were as follows.

Anal. Found: C, 36.52; H, 6.52; N, 7.02; Cu, 7.87; Cl, 9.39. Calcd. for $[Cu(NH_2(CH_2)_5COOH)_4](ClO_4)_2$: C, 36.62; H, 6.62; N, 7.12; Cu, 8.08; Cl, 9.01%.

The compound prepared by the method (**B**) was ascertained to be identical with that obtained by the method (**A**). However, (**B**) was much more convenient than (**A**), when the preparation was carried out on a large scale.

Preparation of Bis-(glycinato)-copper(II), $[Cu(NH_2CH_2COO)_2]\cdot H_2O$, and Bis-(β-alaninato)-copper(II), $[Cu(NH_2(CH_2)_2COO)_2]\cdot 6H_2O$.—Although there are some known methods, the above described method, (**A**), was also applied for preparing these two complexes. It was confirmed that there was no difference between the known and the present method.

Syntheses of the Ligands.—The synthesis of δ-aminovaleric acid was carried out by the method of Wallach[5] as shown in the following scheme:

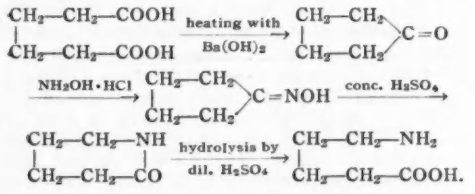

γ-Aminobutyric acid was obtained from pyrrolidone according to the direction of Tafel et al.[7] ε-aminocaproic acid was derived from caprolactam by heating with dilute hydrochloric acid[8].

Preparation of Bis-(hexamethylenediamine)-copper(II) Perchlorate, $[Cu(NH_2(CH_2)_6NH_2)_2](ClO_4)_2$.—The preparation of this compound was reinvestigated in order to clarify the ambiguity concerning the purity of the compound obtained by Pfeiffer[1]. Analytical values showed a good agreement with each other as follows: Pfeiffer's analyses (crude substance): Cu, 12.74; N, 11.34. Analysis in this work (pure crystal): N, 11.09. Calcd. for $[Cu(NH_2(CH_2)_6NH_2)_2](ClO_4)_2$: Cu, 12.85; N, 11.32%.

The recrystallization of Pfeiffer's crude substance was performed in the same way as that used in the preparation of bis-(γ-aminobutyrato)-copper(II).

Properties of the Three Amino Acid Complexes.—The crystal of bis-(γ-aminobutyrato)-copper(II) is very small and prismatic, and shows a remarkable dichroism on the prism face, that is, deep violet and almost colourless. Tetrakis-(ε-carboxyamylamine)-copper(II) perchlorate also shows a clear dichroism on the well-developed face of the acicular crystal, that is, violet and blue. In the case of bis-(δ-aminovalerato)-copper(II), no optical properties were observed cleary because the crystal was extremely small. All the three compounds are stable in the crystalline state but quite unstable in water, and decompose over 180°C.

It is impossible to get the 0.01 M-solution of bis-(γ-aminobutyrato)-copper(II) on account of its decomposition even in an aqueous solution containing 0.08 M of the ligand. In water containing over 1.5 M of the ligand, however, clear solutions of the complex are obtainable without any detectable decomposition. δ-Aminovalerato-complex resembles the γ-aminobutyrato-complex in many respects, but the former is still more unstable in water than the latter. Although the three complexes show different colours from one another in the crystalline state, it is impossible to discriminate one from the others when they are dissolved in water with a large amount of the respective ligand. With respect to their infrared spectra, only the ε-aminocaproic acid complex shows a widely different curve, suggesting a different type of structure[9].

Results and Discussion

In this work three new complexes were obtained as shown in the experimental part. They were bis-(γ-aminobutyrato)-copper(II), bis-(δ-aminovalerato)-copper(II) and tetrakis-(ε-carboxyamylamine)-copper(II) perchlorate. As is clear from the analytical values of those compounds the former two complexes must be metal chelate compounds of the bis-(glycinato)-copper(II) type in structure. (Fig. 1). On the other hand, the last complex must have a structure which corresponds to an amminederivative complex, containing four unidentate ligands, as is seen in Fig. 2.

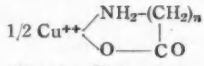

Fig. 1. Chelate-type.

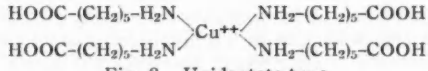

Fig. 2. Unidentate-type.

It is of interest to notice here that the stabilities of copper(II) complexes of ω-amino acids in aqueous solution decrease with an increasing length of the ligands. For example, bis-(glycinato)-copper(II) is so stable that it is quite easy to recrystallize the complex from a hot aqueous solution, while, in the case of bis-(β-alaninato)-copper(II), it is difficult to recrystallize the complex from a hot solution without any detectable decomposition. The comparison of the stabilities of β-alaninato- and γ-aminobutyrato-complex is

6) O. Wallach, *Ann.*, **312**, 179 (1900).
7) J. Tafel and M. Stern, *Ber.*, **33**, 2230 (1900).
8) J. C. Eck, Org. Syn., **17**, 7 (1937).
9) To be submitted later.

the same as that of glycinato- and β-alaninato-complex, that is, the former is less unstable than the latter. This tendency is well-observed in the comparison of γ-aminobutyrato- and δ-aminovalerato-complex, too.

Judging from this tendency, it may be supposed that ε-aminocaproato-complex would be extremely unstable, if it would coördinate to a copper atom as a chelate ligand. In fact, ε-aminocaproic acid does not behave as a chelate ligand but coördinates to a copper atom as an unidentate ligand, as was already shown in the preceding section.

Thus, we may conclude that 8-ring is the highest ring for the formation of metal chelate compounds, so far as the copper(II) complexes of ω-aminocarboxylic acids are concerned. On the other hand, Pfeiffer has succeeded in preparing a 9-membered ring by the reaction of hexamethylenediamine with copper(II) perchlorate according to the same method*. This indicates directly that hexamethylenediamine is more favoured than ε-aminocaproic acid in forming the chelate ring. In other words, those bidentate ligands which have two nitrogen atoms in the functional end groups can form more stable copper(II) chelate compounds than can those having one nitrogen and one oxygen atom. With respect to the ligand, ε-aminocaproic acid, there are two possible ways in coördinating to a copper atom as an unidentate ligand. The one corresponds to the case in which the nitrogen attaches directly to the copper atom, and the other the case in which the oxygen plays the part of the donor atom. In the present case, however, the former is more likely than the latter in many respects. For example, the color of the complex quite resembles that of the ammine-complex. Spectroscopic studies also support the above interpretation, and show the presence of free carboxyl groups[9]. Therefore, the structure of the copper(II) complex of ε-aminocaproic acid should coincide with that shown in Fig. 2, and the nomenclature of the complex should be "tetrakis-(ε-carboxyamylamine)-copper(II) perchlorate" taking the copper-nitrogen linkage into consideration. *In consequence, we reach a conclusion that nitrogen has a greater affinity than oxygen for copper.* In the case of chromium(III) complexes with amino acids[10], oxygen seems to be more favoured than nitrogen in uniting with chromium contrary to the case with copper.

* Pfeiffer's 9-membered ring seemed to be unreliable, since the reaction product obtained by heterogeneous reaction had not been recrystallized. According to our reinvestigation, however, the analytical value of the pure crystal which was obtained by the present authors showed a good agreement with that of Pfeiffer's product.

The Relation between Chelate Formation and Ring Sizes.—As is clear from the above described facts the greater the separation of the carboxyl and amino groups the less the tendency for chelate formation. In an aqueous solution, therefore, it is considered to be difficult to obtain a metal chelate compound which has a larger ring on account of the strong solvolytic aquation[11,12,13,14]. In this respect, the heterogeneous reaction method adopted in this work is quite suitable for the study of the metal chelate compounds with higher ring, since there are very few interrupting factors in the reaction system. But yet the 9-membered ring was too unstable to be included in this work. In connexion with this fact, it seems to be desirable to afford some elucidation concerning the reason why the stablities of metal chelate compounds decrease with an increasing number of ring members.

Firstly, we propose steric effects. With very few exceptions the recognized examples of steric influences on stability are based on qualitative observations which usually involve formation or non-formation of the metal complexes. In the present case, however, that is not the way to consider the subject, since it is clear through the examinations of models that there is hardly expected any remarkable difference between the steric condition of δ-aminovalerato-chelate and that of ε-aminocaproato-chelate. Judging from their lactam forms, the amino and carboxyl groups in the free molecules of δ-amino- and ε-aminocarboxylic acid are accessible to each other without any serious distortion. Therefore, it seems to be easy for both the ligands to arrange their functional groups about a central metal atom so that the respective metal chelate complex can be formed. Such being the case, the stability of higher rings is not fully explained from the standpoint of the steric effect, though it is considered to be a very important factor.

Secondly, electronic influences induced with the separation of the two functional groups probably play another important role for the chelate formation. According to the work of Ley[15], the acidity of ω-aminocarboxylic acid decreases with an increasing distance between carboxyl and amino groups, and there is the opposite inclination with respect-

10) R. W. Green and K. P. Ang, *J. Am. Chem. Soc.*, 77, 5482 (1955).
11) A. Werner, *Ber.*, 40, 15 (1907).
12) L. Tschugaeff, ibid., 39, 3190 (1906); *J. Prakt. Chem.*, [2] 75, 159 (1907).
13) P. Pfeiffer and M. Haimann, *Ber.*, 36, 1063 (1903).
14) P. Pfeiffer and E. Lübbe, *J. prakt. Chem.*, [2] 136, 321 (1933).
15) H. Ley, *Ber.*, 42, 354 (1909).

to the basicity. Thus, it is quite natural to expect a different affinity for a metal with the separation of the two functional groups.

It may be considered that the stability of higher chelate rings is mainly influenced by the above two factors. Probably accumulations of slight steric constraints and electronic influences may prevent the ε-aminocaproic acid from the chelate formation with copper. We are continuing the study of the stability of higher chelate rings from another point of view.

Summary

Three new compounds, bis-(γ-aminobutyrato)-copper(II), bis-(δ-aminovalerato)-copper (II), and tetrakis-(ε-carboxyamylamine)-coppe(II) perchlorate, have been prepared. The first and the second compound belong to the bis-(glycinato)-copper(II) type, having a 7- and 8-membered ring, respectively. The last compound has a structure of ammine-derivative complex. In all cases preparations were carried out in non-aqueous media such as ether and chloroform.

It has been concluded that the 8-membered ring is the highest ring for the formation of metal chelate compounds, so far as the copper(II) complexes of ω-aminocarboxylic acids are concerned.

Stability of higher chelate rings was considered as the functions of steric constraints and electronic influences which may be induced with the separation of the two functional groups.

The authors are grateful to Mr. Y. Kinoshita of the Toyo Rayon Co. and Mr. H. Sekiguchi of Osaka University for supplying part of the samples used in this work. This investigation was supported by a grant from the Ministry of Education.

Department of Chemistry, Faculty of Science, Osaka University, Osaka

Action of Emulsifier upon the Copolymerization of Acrylonitrile and Styrene

By Moriya UCHIDA and Hideo NAGAO

(Received June 21, 1956)

Introduction

The mechanism of emulsion polymerizations of water-insoluble monomers as styrene and isoprene has been shown by Harkins[1] and Smith[2]. However, the mechanism of emulsion polymerizations of water-soluble monomers as acrylonitrile seems to be different from that of styrene and isoprene. It has been known that the polymerization rate of acrylonitrile in water increases as the polymer forms[3]. It appears to be due to diffusion and adsorption of monomer to polymer precipitated in water[4]. It has been known that in heterogeneous polymerization the loci of polymer propagation reaction are the polymers adsorpted with monomers and the appearance of this polymerization looks like that of emulsion polymerization. It was already reported that the compositions of emulsion copolymers of water-soluble monomer as acrylonitrile and water-insoluble monomer as vinylidenechloride depended on the concentrations of emulsifier used in copolymerization[5]. The reactivity of acrylonitrile and styrene in emulsion copolymerization was studied by Fordyce and Chapin[6] and Smith[7]. Although they proved that the composition of formed copolymer depended on the composition of oil phase, the action of emulsifier has not been cleared up yet. In the present paper, in the first place, some observations in emulsifier-free copolymerization, and then the action of anionic emulsifier upon the rate of polymerization, the degree of polymerization and the composition of formed copolymer are given.

1) W. D. Harkins, *J. Am. Chem. Soc.*, **69**, 1428 (1947).
2) W. V. Smith and R. H. Ewart, *J. Chem. Phys.*, **16**, 592 (1948).
3) P. J. Flory, "Principles of Polymer Chemistry", Cornell University Press (1953), p. 208.
4) H. Nagao, M. Uchida and T. Yamaguchi, *J. Chem. Soc. Japan* (in Japanese) **59**, 695 (1956).
5) H. Nagao, M. Uchida and T. Yamaguchi, *J. Chem. Soc. Japan*, in press.
6) R. G. Fordyce and E. C. Chapin, *J. Am. Chem. Soc.*, **69**, 581 (1947).
7) W. V. Smith, *J. Am. Chem.Soc.*, **70**, 2177 (1948).

Experimental

Acrylonitrile (AN).—Redistilled American Cyanamid Co. material was used for all experiments.

Styrene Monomer (St).—Redistilled commercial material was employed.

Emulsifier (Sodium Dodecyl Sulfate).—Recrystallized Kao Soap Co. material was used.

Polymerization Procedure.—A stirred 1-liter, four-necked-fiask placed in a water bath maintained at 45±0.1°C was charged by the additions of the required emulsifier aqueous solution and monomers. The air in the flask was purged by the introduction of nitrogen. Then the catalyst (potassium persulfate) 0.8 weight % and the reductant (sodium bisulfite) 0.8 weight % were added after the flask had attained thermal equilibrium. These weight % concentrations were based on total monomers. The mixer of the flask was rotated at 300 revolution per minute. The latex was coagulated in water or in a calcium chloride solution which contained hydroquinone as an inhibitor. Conversion data were based on total solid determinations. η_{sp}/c was measured in 2 g./l. dimethylformamide solution at 25°C. The combined acrylonitrile in copolymer was determined by Kjeldahl analysis.

Results and Discussion

(1) Rate of Polymerization in Emulsifier-free Copolymerization

The mixture of water-soluble monomer as acrylonitrile and water-insoluble monomer as styrene in the presence of suitable water-soluble redox initiating reagents is capable of undergoing copolymerization in water without the assistance of emulsifying agents. The relation between conversion and polymerization times is shown in Fig. 1.

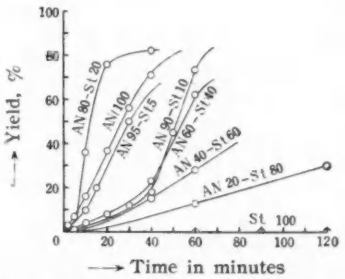

Fig. 1. Rate of polymerization of acrylonitrile and styrene in aqueous solution.

The rate of polymerization was very slow in only styrene and became faster as the mixture of monomer contained much acrylonitrile. The polymerization of water-insoluble monomer as styrene without soap or with a very small amount of soap was very slow, and the degree of polymerization of the formed polymer was low[8]. The water-soluble monomer as acrylonitrile was absorbed remarkably in the initial polymer in water[4], so that the rate of polymerization would be fast and the degree of polymerization of the formed polymer would be high even if the emulsifier was not used. The difference of the property as above existed between the two monomers used. The copolymerization rate of these monomers was dependent upon the average water-solubility of their mixture. It has been known that the rate of polymerization is roughly proportional to the solubility of the monomer in water in case of polymerization of water-soluble momomer such as methyl-methacrylate, vinylacetate or acrylonitrile[8]. Consequently, the solubilized amount of monomer in water must depend on the rate of polymerization. Whitby, Gross, Miller and Costanza[9] found that the addition of a small amount of acrylonitrile in copolymerization of styrene and butadiene accelerated the rate of reaction and the polymerization rate of styrene containing 5–10% methacrylonitrile was faster than that of only styrene.

It has been known that the initiation of polymerization occurs in water phase in these polymerization systems. When a layer of styrene is placed on a column of a dilute potassium persulfate solution in water and the system is allowed to stand for several days, the aqueous phase slowly becomes cloudy. If substances with greater solubility in water, e. g., methacrylic ester, vinyl acetate or acrylonitrile, are used, the cloudiness appears much more rapidly although the area of the interface is the same as before. Moreover, if a small amount of an inhibitor is added to monomer phase, the course of the polymerization in the aqueous phase is not noticeably affected; if, however, the same amount is added to the aqueous phase, the appearance of the cloudiness is considerably delayed.

This is an indication that at least the formation of active nuclei takes place in the aqueous phase.

Fryling and Harrington[10] observed that, in the case of the layer polymerization of acrylonitrile on top of an aqueous potassium persulfate solution, the aqueous phase remains clear and transparent for a distance of about five millimeters below the interface, indicating that no polymer is actually being formed at

8) W. P. Hohenstein and H. Mark, *J. Polymer Sci.*, **1**, 549 (1946).
9) G. S. Whitby, M. D. Gross, J. R. Miller and A. J. Costanza, *J. Polymer Sci.*, **16**, 549 (1955).
10) C. F. Fryling and E. W. Harrington, *Ind. Eng. Chem.*, **36**, 114 (1944).

the interface itself but that the dissolved monomer is the principal center for the formation of polymer. Moreover, the active center produced by interaction of monomer and potassium persulfate in water, can grow in the aqueous phase without being in any direct contact with liquid monomer and the adsorption rate of monomer to active center is greater than the consumption rate of monomer as we reported[4], so the propagation reaction seems to occur in the polymer adsorpted monomer.

It has been found that the polymer of water-insoluble monomer as styrene was slowly formed in the aqueous phase outside of the droplet by the observation of the behavior of small droplets of styrene in aqueous solutions of peroxides under the microscope[8]. The interface between monomer and aqueous solution of catalyst seems not to be appropriate locus for the initiation and propagation of polymer. Consequently, it is thought that the initiation of polymer occurs also in aqueous phase in copolymerization of acrylonitrile and styrene, and is remarkable because of the increase of active centers in water as the amount of acrylonitrile is great in the mixture of monomer so that the rate of polymerization increases.

At the same time the reactivity of monomers must also be taken into account. The monomer reactivity ratios in the copolymerization of acrylonitrile and styrene were the following[11].

r_1 (Styrene)	r_2 (Acrylonitrile)	
0.41 ± 0.08	0.04 ± 0.04	60°C

Consequently, the rate of addition of acrylonitrile to styrene radical is faster than that to acrylonitrile radical, and the rate of addition of styrene to acrylonitrile radical is faster than that to styrene radical. The rate of propagation reaction must be maximum in the mixture of equal molecules of monomers according to the above-mentioned concept.

This concept will be applied to the copolymerization of acrylonitrile (r_1, 0.91 ± 0.10) and vinylidenechloride (r_2, 0.34 ± 0.10). It has been reported that the maximum rate of polymerization related to the compositions of monomer mixtures appears in the mixture of almost equal molecules of acrylonitrile and vinylidene chloride[5]. Accordingly the maximum of the rate in the emulsifier-free copolymerization of acrylonitrile and styrene seems to be due to the effect of monomer reactivity which overlapped the effect of average water-solubility of the mixture of monomer and appears in the acrylonitrile richer composition.

11) F. M. Lewis, F. R. Mayo and W. F. Hulse, *J. Am. Chem. Soc.*, **67**, 1701 (1945).

(2) Rate of Polymerization in Emulsion Copolymerization

The results of emulsion copolymerization rate which used emulsifier 0, 0.1, 0.2, 0.4, 0.6, 1.0, 1.5 weight % to total monomer are given in Figs. 2, 3, 4, 5, 6, 7, 8 and 9.

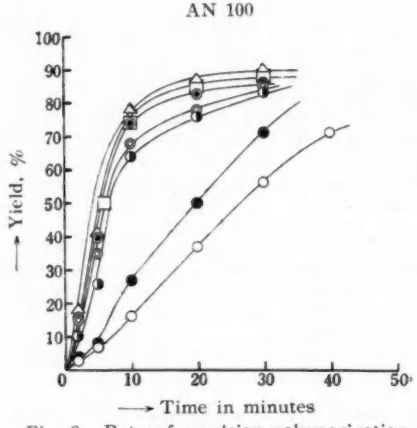

Fig. 2. Rate of emulsion polymerization, No. 1.

Emulsifier (to Total Monomers)
□ 1.5% △ 1.0% ⊙ 0.6%
◎ 0.4% ◑ 0.2% ● 0.1%
○ 0%

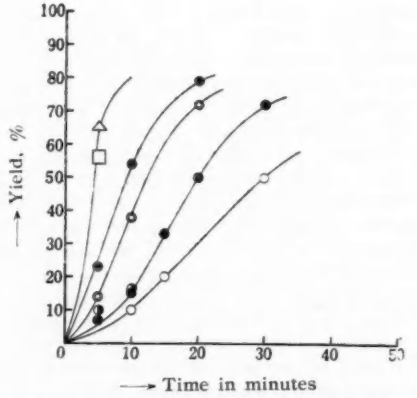

Fig. 3. Rate of emulsion polymerization, No. 2.

Emulsifier (to Total Monomers)
□ 1.5% △ 1.0% ⊙ 0.6%
◎ 0.4% ◑ 0.2% ● 0.1%
○ 0%

AN 90–St 10

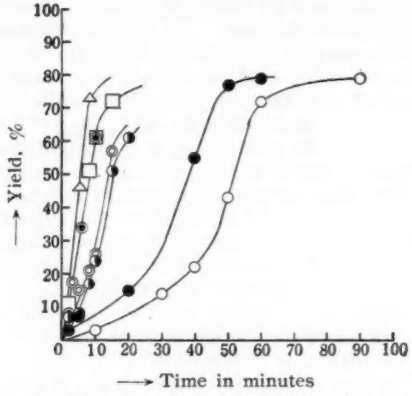

Fig. 4. Rate of emulsion polymerization, No. 3.
Emulsifier (to Total Monomers)
□ 1.5% △ 1.0% ⊙ 0.6%
◎ 0.4% ◑ 0.2% ● 0.1%
○ 0%

AN 80–St 20

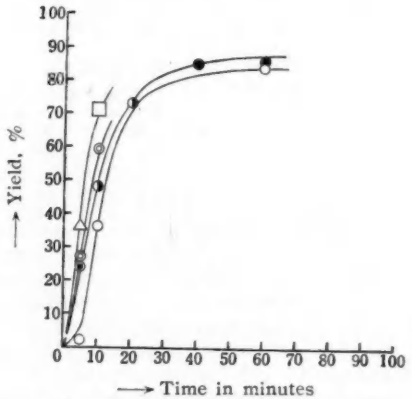

Fig. 5. Rate of emulsion polymerization, No. 4.
Emulsifier (to Total Monomers)
□ 1.5% △ 1.0% ⊙ 0.6%
◎ 0.4% ◑ 0.2% ● 0.1%
○ 0%

AN 60–St 40

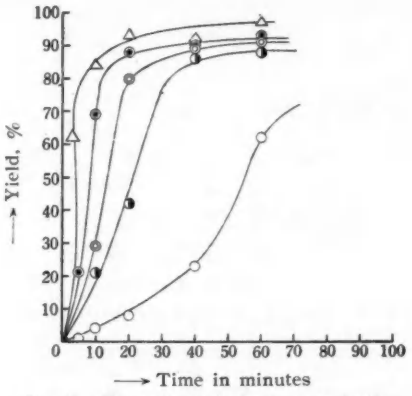

Fig. 6. Rate of emulsion polymerization, No. 5.
Emulsifier (to Total Monomers)
△ 1.0% ⊙ 0.6% ◎ 0.4%
◑ 0.2% ● 0.1% ○ 0.0%

AN 40–St 60

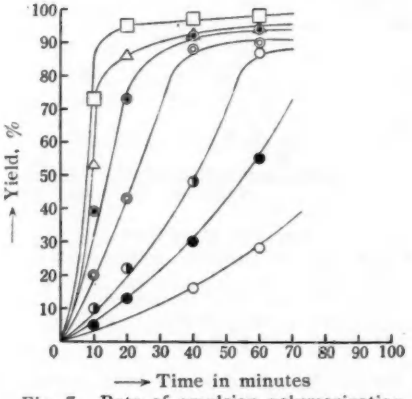

Fig. 7. Rate of emulsion polymerization, No. 6.
Emulsifier (to Total Monomers)
□ 1.5% △ 1.0% ⊙ 0.6%
◎ 0.4% ◑ 0.2% ● 0.1%
○ 0%

The situation changes significantly if soap solutions are used instead of pure water. Hess and his co-workers[12,13,14] found the presence of lamellar soap micelles from the observation of the diffraction of X rays by soap solutions. The increase of average distance of adjacent lamellae due to solubilization of hydrocarbon was observed by McBain and Harkins[15–20]. The water-soluble initiator is allowed free-diffusion and the formation of active center seems to occur mainly in micelles for these micelles contained monomer

12) K. Hess and J. Gundermenn, *Ber.*, **70**, 1800 (1937).
13) K. Hess and W. Philippoff, *Ber.*, **70**, 1808 (1937).
14) K. Hess, W. Philippoff and H. Kiessig, *Naturwissenschaften*, **26**, 184 (1938).
15) J. W. McBain, *Trans. Faraday Soc.*, **9**, 99 (1913).
16) W. D. Harkins, R. W. Mattoon and M. L. Corrin, *J. Am. Chem. Soc.*, **68**, 220 (1946); *J. Colloid Sci.*, **1**, 105 (1946).
17) J. W. McBain, "Advance in Colloid Science" Interscience Publishers, Inc., New York, N. Y. (1942), Vol. 1, p. 124.
18) W. D. Harkins, *J. Chem. Phys.*, **13**, 381 (1945).
19) W. D. Harkins, *J. Chem. Phys.*, **14**, 47 (1946).
20) W. D. Harkins and R. S. Stearns, *J. Chem. Phys.*, **14**, 215 (1946).

AN 20–St 80

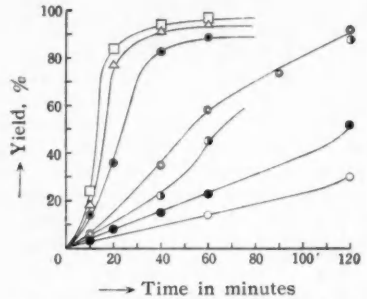

Fig. 8. Rate of emulsion polymerization, No. 7.
Emulsifier (to Total Monomers)
□ 1.5% △ 1.0% ⊙ 0.6%
◎ 0.4% ◑ 0.2% ● 0.1%
○ 0%

St 100

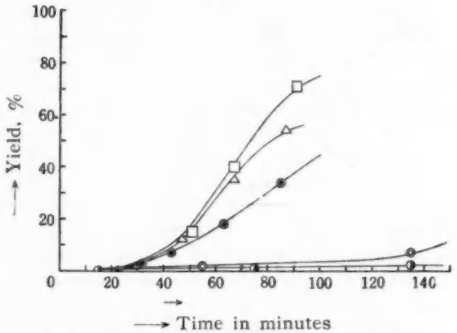

Fig. 9. Rate of emulsion polymerization, No. 8.
Emulsifier (to Total Monomers)
□ 1.5% △ 1.0% ⊙ 0.6%
◎ 0.4% ◑ 0.2%

and swelled by water in the soap concentrations of our polymerization systems as Fikentscher[21] and Hohenstein[22] have shown. The rate of polymerization increased as the emulsifier was used much, for the formation of an active center in a micelle increased as above mentioned. Moreover, it seemed to depend upon the average water-solubility of mixture of monomers, for it increased as the mixture contained much acrylonitrile. If the initiation occurs by the interaction between the radical of catalyst and monomers solubilized in micelles, according to Harkins' theory, the reaction rate will vigorously increase in the critical micelle concentration of emulsifier. The critical micelle concentration of Sodium Dodecyl Sulfate used as emulsifier has been known to be 0.05–0.2% aqueous solution[23,24]. It has been known that the critical micelle concentration becomes low by the addition of polar organic materials[25], so that 0.1–1.0 weight % (to total monomer) solution of emulsifier corresponds to about 0.01–0.15 weight % aqueous solution, that is to say, critical micelle concentration. In fact, the increase of reaction rate was found in this concentration range. The rate of polymerization seems also to depend upon the average water-solubility of monomer mixture, for it depends upon the solubilized volume of monomer in emulsion polymerization. Accordingly, it increases as the mixture of monomers contains much acrylonitrile having good ability of solubilization[26].

The rates of polymerization shown in about 40% conversion in various system are given in Table I.

TABLE I
RATE OF POLYMERIZATION (%/min.)

Amount of Emulsifier % to Total Monomer	Acrylonitrile mol. % in Monomer Mixture							
	100	95	90	80	60	40	20	0
1.5	16	16	9.0	7.1	—	7.0	5.0	1.7
1.0	19	16	9.0	7.1	9.0	5.0	4.2	1.2
0.6	14	6.0	7.0	—	8.1	3.5	3.2	0.7
0.4	12	4.8	6.0	6.8	4.8	2.2	1.1	0.3
0.2	8.6	—	5.0	6.6	2.9	1.4	0.6	0.02
0.1	2.4	3.5	3.0	6.1	—	1.2	0.4	0.01
0	2.0	2.1	2.8	6.1	2.0	0.7	0.3	0.0

Its maximum appeared in the composition of acrylonitrile 80 mol. % and styrene 20 mol. %. This seems to depend upon the effect of the monomer reactivity which overlapped that of the average water-solubility of monomer mixture as above described. The rate of acrylonitrile rich polymerization shows maximum in the concentration nearly 1% (to total monomer) of emulsifier. The emulsifier acts less upon the polymerization of water-soluble monomer than that of water-insoluble monomer, for the initiation of water-soluble monomer is easy even in emulsifier-free polymerization. It appears to be the cause of rate maximum related to emulsifier aqueous concentration that the monomer solubilized in water makes critical micelle concentration lower and in more high concentration of emulsifier the radical diffusion into micelle

21) H. Fikentscher, *Angew. Chem.*, **51**, 433 (1934).
22) W. Hohenstein, S. Siggia and H. Mark, *India Rubber World*, **111**, 173 (1944).
23) R. Goto, "Outlook of High Polymer", Association of High Polymer Chemistry, Kyoto, Japan (1951), Vol. 5, p. 47.
24) K. A. Wright, A. D. Abbott, V, Sivertz and H. V. Tartar, *J. Am. Chem. Soc.*, **61**, 549 (1939).
25) K. Schinoda, *J. Phys. Chem.*, **58**, 1136 (1954).
26) S. Okamura and T. Motoyama, *J. Chem. Soc. Japan*, **57**, 930 (1954).

becomes difficult due to the fact that the wall of micelle is thick or the solubilized amount of monomers decrease because of the excess of emulsifier[27]. Consequently, the maximum will easily appear in the polymerization of acrylonitrile rich monomer mixtures.

(3) Degree of Polymerization

The relations between $\eta sp/c$ and conversion are given in Figs. 10, 11, 12, 13 and 14.

AN 95-St 5

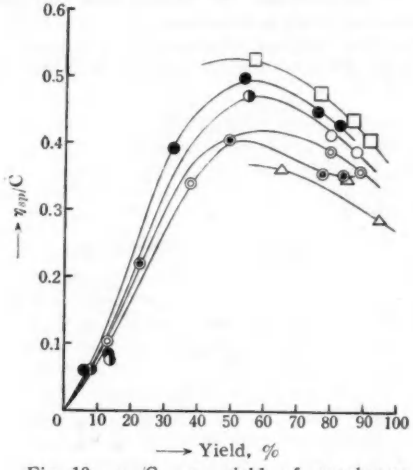

Fig. 10. η_{sp}/C vs. yield of copolymer, No. 1.
Emulsifier (to Total Monomers)
□ 1.5% △ 1.0% ⊙ 0.6%
◎ 0.4% ◑ 0.2% ● 0.1%

AN 80-St 20

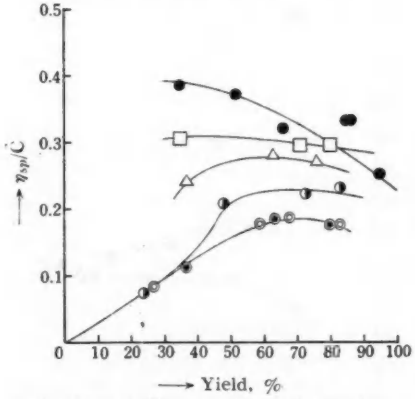

Fig. 11. η_{sp}/C vs. yield of copolymer, No. 2.
Emulsifier (to Total Monomers)
□ 1.5% △ 1.0% ⊙ 0.6%
◎ 0.4% ◑ 0.2% ● 0.1%

27) K. Kanamaru et al., *J. Chem. Soc. Japan*, **58**, 221 (1955).

AN 60-St 40

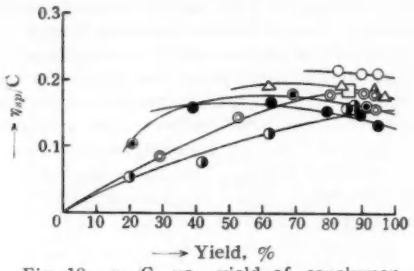

Fig. 12. η_{sp}/C vs. yield of copolymer, No. 3.
Emulsifier (to Total Monomers)
□ 1.5% △ 1.0% ⊙ 0.6% ◎ 0.4%
◑ 0.2% ● 0.1% ○ 0%

AN 40-St 60

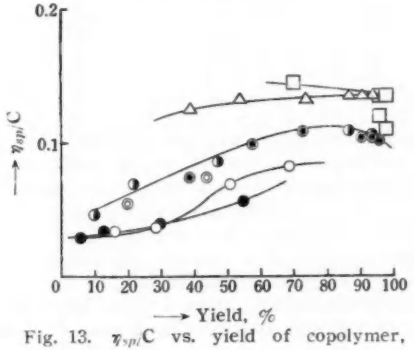

Fig. 13. η_{sp}/C vs. yield of copolymer, No. 4.
Emulsifier (to Total Monomers)
□ 1.5% △ 1.0% ⊙ 0.6% ◎ 0.4%
◑ 0.2% ● 0.1% ○ 0%

AN 20-St 80

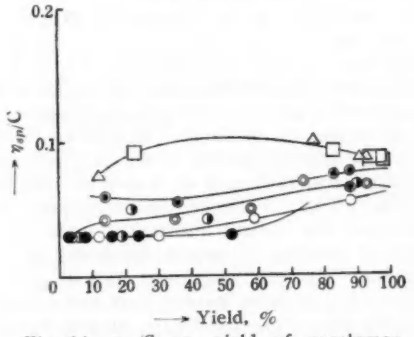

Fig. 14. η_{sp}/C vs. yield of copolymer, No. 5.
Emulsifier (to Total Monomers)
□ 1.5% △ 1.0% ⊙ 0.6% ◎ 0.4%
◑ 0.2% ● 0.1% ○ 0%

In the polymerization of styrene rich monomer $\eta sp/c$ increases with much using of

emulsifier and is proportional to the tendency of polymerization rate and it seems that the increase of the active center also brings the increase of the degree of polymerization according to its rate. However, $\eta sp/c$ in the polymerization of the monomer containing acrylonitrile decreases, shows the minimum and increases as the concentration of emulsifier becomes thick. The used amounts of emulsifier when $\eta sp/c$ becomes minimum are given in the following Table.

TABLE II

The Composition of Monomer Mixture		The Amount of Emulsifier Minimunized $\eta sp/c$
Acrylonitrile (mol. %)	Styrene (mol. %)	(weight %)
0	100	0
20	80	0.1
40	60	0.1
60	40	0.2
80	20	0.4–0.6
95	5	1.0
100	0	1.0

It has been known that the initiation of styrene occurs in micelle, so the increase of emulsifier brings the increase of polymerization rate due to the increase of active center and the increase of the degree of polymerization due to the decrease of termination. But the diffusion of water-soluble monomer as acrylonitrile in water is very faster than that of styrene, so that the degree of polymerization of monomers containing acrylonitrile becomes high even in emulsifier-free polymerization. The second radical can be more easy to diffuse into polymer swelled by water and to combines with polymer radical as the concentration of emulsifier becomes thick, so that the polymerization degree of formed polymer becomes low. In thicker concentration, the diffusion of the second radical may be hindered by the thick wall of emulsifier, so that the degree of polymerization seems to be large. In any case, the degree of polymerization of formed polymer depends upon the state of water in micelles and the affinity between monomer, polymer, emulsifier and radical due to the water-solubility of monomer. $\eta sp/c$ decreased as the monomer mixture contained much acrylonitrile. It has been known that the relation between $\eta sp/c$ and the degree of polymerization varies with the composition of the copolymer, but $\eta sp/c$ of copolymer becomes great even in the same molecular weight as the used solvent becomes poor solvent to copolymer as Maeda, Kawai and Yamaguchi[28] mentioned in regard to the copolymer of vinylchloride and vinylacetate. Dimethylformamide which is used for the measurement of $\eta sp/c$ in this paper is a good solvent for the copolymers containing much acrylonitrile unit in their structure. Consequently, the degree of polymerization becomes greater because of the increase of the solubilized amount of monomer due to its containing richer acrylonitrile.

28) K. Maeda et al., *J. Chem. Soc. Japan*, 58, 502 (1955).

(4) Composition of Copolymer on the Process of Polymerization

The compositions of copolymers formed in various conversions are given in Figs. 15, 16 and 17.

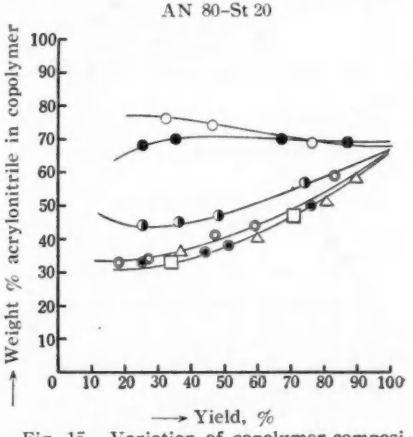

Fig. 15. Variation of copolymer composition with yield, No. 1.
Emulsifier (to Total Monomers)
□ 1.5% △ 1.0% ⊙ 0.6% ◎ 0.4%
◑ 0.2% ● 0.1% ○ 0%

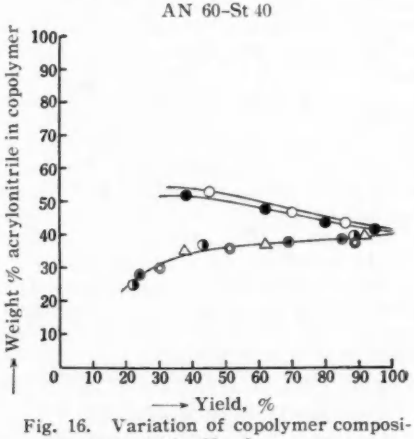

Fig. 16. Variation of copolymer composition with yield, No. 2.
Emulsifier (to Total Monomers)
△ 1.0% ⊙ 0.6% ◎ 0.4%
◑ 0.2% ● 0.1% ○ 0%

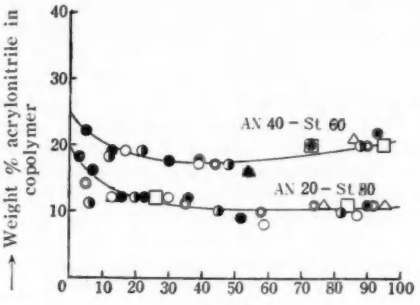

Fig. 17. Variation of copolymer composition with yield, No. 3.
Emulsifier (to Total Monomers)
□ 1.5% △ 1.0% ◉ 0.6%
◎ 0.4% ◑ 0.2% ● 0.1%
○ 0%

It has been reported that in emulsion copolymerization of acrylonitrile and vinylidene chloride, the compositions of formed copolymers depended upon the concentration of emulsifier used and the copolymer produced in low concentration of emulsifier contained much acrylonitrile[5,29].

The same phenomena were observed in the copolymerization of acrylonitrile and styrene. It is supposed that the water-solubility of monomer depends upon the compositions of copolymer, for these copolymerizations are those of water-soluble monomer and water insoluble monomer. The variation of the composition is especially great in the copolymerization of almost equal weight water-soluble and water-insoluble monomer.

29) H. Nagao, M. Uchida and T. Yamaguchi, *J. Chem. Soc. Japan*, in press.

Conclusion

From the copolymerization of acrylonitrile and styrene done in emulsion and suspension, the following facts were found.

1. The polymerization rate becomes fast as the mixture of monomer contains much acrylonitrile and reaches the maximum in the mixture of acrylonitrile 80 mol.% and styrene 20 mol.%.

2. The polymerization rate becomes generally fast as the concentration of emulsifier becomes thick; however, it is maximum at about 1.0 weight % emulsifier (to total monomer) in the copolymerization of monomers containing above 80 mol.% acrylonitrile.

3. η sp/c becomes great as the mixture of monomers contains much acrylonitrile.

4. η sp/c becomes small, reaches the minimum and then becomes great as the concentration of emulsifier becomes thick.

The concentration of emulsifier giving η sp/c minimum becoms thick as the mixture of monomers contains much acrylonitrile.

5. The composition of copolymer depends upon the concentration of emulsifier and it contains less acrylonitrile as the concentration becomes thick.

Research Institute of Teikoku Rayon Co. Ltd., Iwakuni

---

*Some Optical Properties of Zinc Sulfide Phosphors Doubly Activated with Copper and Manganese**

By Shigeo SHIONOYA

(Received July 14, 1956)

Introduction

The sensitized luminescence in doubly activated phosphors has been one of the most interesting problems in the field of solid-state luminescence in recent years. In these phosphors two kinds of activating impurity, called "sensitizer" and "activator", are incorporated. The activator is sensitized to emit luminescence as a result of the absorption of excitation energy by the sensitizer and of the subsequent radiationless transfer of this energy from the sensitizer, in such a spectral region that the activator has no appreciable absorption band unless the sensitizer is incorporated. In most cases the sensitizer causes also the luminescence of its own, so that these phosphors show two

* A part of this work was read at the Symposium on Photochemistry held by the Chemical Society of Japan on Sept. 25, 1954, and at the 8th Annual Meeting of this Society on Apr. 1, 1955, and was briefly reported in *J. Chem. Phys.* **23**, 1173, 1976 (1955).

kinds of emission band.

Generally, the sensitizer is an atom or ion of heavy metals such as lead, thallium, copper, antimony and other metals, while the activator is an ion of transition metals such as manganese and samarium. Manganese incorporated as a divalent ion is most popular as the activator, and known to be apt to show a strong luminescence by sensitization because the optical transition involved which leads to the luminescence is a forbidden one[1].

The sensitized phosphors recently developed and investigated are confined almost entirely to non-photoconductive phosphors such as $CaSiO_3$:(Pb+Mn)[2,3,4], $Ca_3(PO_4)_2$:(Ce+Mn)[4,5], $3Ca_3(PO_4)_2$-$Ca(Cl, F)_2$:(Sb+Mn)[5], and CaF_2:(Ce+Mn)[7]. On the other hand, the investigation for photoconductive ones such as the sulfide type are rather few except those by Makishima[8] for calcium sulfide type, CaS:(Bi+Sm), CaS:(Pb+Sm), CaS:(Bi+Mn) and others, and those by the author[9] for self and manganese-activated zinc sulfide.

The theory of sensitization mechanism has been developed by Botden[5] and more fundamentally by Dexter[10], and it was concluded that the resonance transfer of excitation energy from sensitizer to activator is responsible for the sensitization process in non-photoconductive phosphors. However, in photoconductive phosphors the possibility of sensitization due to the mechanism which will be described below may be also taken into consideration, namely the mechanism by the transfer of photoelectrons through the conduction band simultaneously accompanied by the migration of holes through the filled band[11,12,13].

The present work was undertaken in order to investigate the sensitization process in photoconductive phosphors and to discuss the mechanism by which the process is governed. Zinc sulfide doubly activated with copper and manganese was taken up as an example to be investigated, and its optical properties, the emission, absorption and excitation spectra, thermoluminescences and photoconductivities, were measured. This phosphor seems to be suitable for the present purpose, since zinc sulfide singly activated with copper and that with manganese are both very familiar and their properties are well-known. The results presented below will show that in this phosphor, manganese emission is really sensitized by copper incorporated as a sensitizer, and that some interesting phenomena characteristic of sensitized luminescence take place.

Experimental

1 Preparation of the Samples.—The preparation of the samples was carried out according to the method currently used. Several series of the samples were prepared, in which the copper concentration was fixed to be constant, 3×10^{-5}g./g.ZnS*, and the manganese concentration was varied from zero to 3×10^{-3}g./g.ZnS. These were fired at 1200°C for one hour in air with the flux of sodium or potassium chloride (0.02–0.05g./g.ZnS). Each series was fired at one time so as to keep the firing condition completely constant.

2 Emission.—As is well konwn, copper-activated zinc sulfide phosphor and that which is manganese- activated show the yellow green and orange luminescence, respectively. A series of the doubly activated ones with a constant copper concentration and varying manganese concentrations shows the luminescence with colors varying from yellow green to orange with the increase of manganese concentrations under 3650Å excitation.

The exmission spectra were measured under 3650Å excitation at room temperature with a glass monochromator of constant deviation type and a photomultiplier, RCA 931A or 1P21. The excitation source was a high pressure mercury discharge lamp, Matsuda SHL-100, with a Matsuda UV-D1 filter. The output of the photomultiplier was further amplified with either of two kinds of high sensitive amplifier, a *dc* or *ac* amplifier. The *dc* amplifier was constructed by using a vacuum tube 954 operating as an electrometer tube[14]. The current amplification was about 80–100db. In the case of the *ac* amplifier, the light emitted by the phosphor was interrupted and modulated to 200cps by means of a rotating sector set just before the entrance slit of the monochromator, and the *ac* output of the photomultiplier was amplified with the *ac* amplifier tuned to this frequency, the design of which follows closely to the one devised by Yamada et al[15]. The gain of the *ac* amplifier was almost the same as that of the *dc* amplifier. The spectral sensitivity of the photomultiplier set just behind the exit slit was determined by

1) C. C. Klick, *Brit. J. Appl. Phys.*, Sup. No. 4 ("Luminescence"), 74 (1955).
2) J.B. Merril and J.H. Schulman, *J. Opt. Soc. Am.*, 38, 471 (1948).
3) J. H. Schulman, R. J. Ginther and C. C. Klick, *J. Electrochem. Soc.*, 97, 123 (1950).
4) Th. P.J. Botden and F.A. Kröger, *Physica*, 18, 553 (1948).
5) Th. P.J. Botden, *Philips Res. Rep.*, 7, 197 (1952).
6) H.G. Jenkins, A.H. McKeag and P.W. Ranby, *J. Electrochem. Soc.*, 96, 1 (1949).
7) R. J. Ginther, *J. Electrochem. Soc.*, 101, 248 (1954).
8) S. Makishima, Doctral Thesis (1945).
9) S. Shionoya, *Bull. Fac. Eng.*, Yokohama Natl. Univ. 3, 97 (1954).
10) D.L. Dexter, *J. Chem. Phys.*, 21, 836 (1953).
11) N.F. Mott and R.W. Gurney, "Electronic Processes in Ionic Crystals", (1940), p. 207.
12) M. Schön, *Z. Phys.*, 119, 463 (1942).
13) H.A. Klasens, W. Ramsden and C. Quantie, *J. Opt. Soc. Am.*, 38, 60 (1948).

* Concentrations of activating impurities are given in weight ratios, g./g.ZnS, throughout this paper.
14) H. Matsuda and K. Ogata, *J. Appl. Phys. Japan*, 20, 229 (1951).
15) M. Yamada, K. Mitsuhashi and K. Akagi, *Tech. J. Japan Broadcasting Corp.*, 13, 29 (1953).

measuring the emission spectrum of a tungsten-incandescent lamp having the approved true temperature, including not only the spectral sensitivity of the photomultiplier itself but also the variation of the dispersion of the monochromator with wavelength and the absorption by glass.

Some typical results are shown in Fig. 1. The

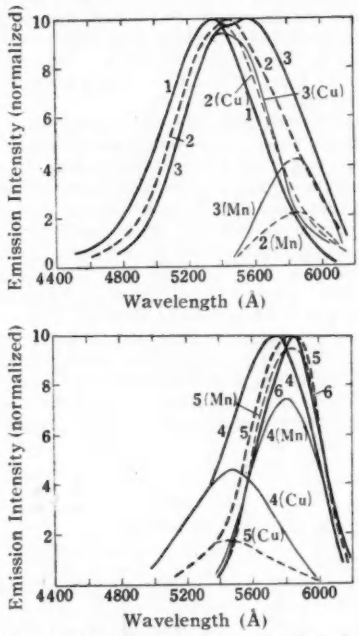

Fig. 1. Emission spectra of (1) ZnS:Cu and (2)–(6) ZnS:(Cu+Mn) under 3650 Å excitation. The Mn concentrations are (2) 2×10^{-4}, (3) 4×10^{-4}, (4) 8×10^{-4}, (5) 1.5×10^{-3} and (6) 3×10^{-3}. The Cu concentration is always 3×10^{-5} for all of the samples in this paper.

emission of manganese increases with the increase of its concentration, the emission of the copper decreasing simultaneously. Because of the overlap of the copper band with the manganese band, the samples showing both the copper and manganese emissions have broad bands, which are divided graphically into the copper and manganese bands as shown in the figure. The samples containing less than 1×10^{-4} manganese show the manganese emissions scarcely observable, those containing $2\text{–}8\times10^{-4}$ show distinctly both the copper and manganese emissions and those containing more than 1.5×10^{-3} show the predominant manganese emissions, while the copper emissions almost disappear. These concentrations of manganese are varied slightly by the firing conditions.

The emission peaks of copper and manganese are located at 5350–5450Å and about 5850Å, respectively, both being almost unchanged from those of the case where each of them is singly incorporated[16]. The copper peak has a tendency to shift slightly towards longer wavelength with the increase of manganese concentration. The reason for this effect is considered to be that since manganese is incorporated substitutionally into zinc sulfide, forming a solid solution[17] and causing the expansion of the lattice, the forbidden gap of the host lattice is made smaller, and then the energy of the copper emission becomes smaller.

3 Absorption.—The measurements of absorption were made by measuring the diffuse reflectivity from a layer of phosphor with an effectively infinite thickness. A Hitachi's quartz monochromator of Littrow type and an integrating sphere, which was set behind the exit slit, were used. The excitation source was a tungsten incandescent lamp. The intensity of the reflected light was measured with a photomultiplier, 1P28, attached to the *dc* amplifier mentioned above, and the reflectivity was determined as the ratio to that of magnesium oxide powder. An ultraviolet transmitting filter, Corning No. 9863 or Matsuda V-V1, was inserted between the integrating sphere and the photomultiplier so as to separate the reflected light from the luminescence, in the spectral region 3200–4800Å where the incident light excites the phosphor.

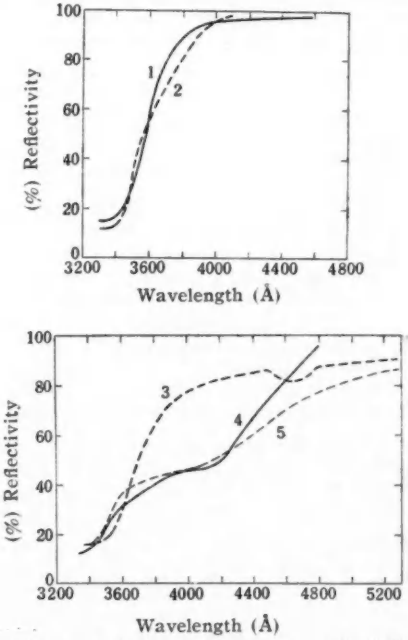

Fig. 2. Reflection spectra of (1) ZnS unfired, (2) ZnS fired without any activating impurities, (3) ZnS:Mn (Mn: 1×10^{-2}), (4) ZnS:Cu and (5) ZnS:(Cu+Mn) (Mn: 8×10^{-4}).

16) R.H. Bube, *Phys. Rev.*, **90**, 70 (1953).
17) F.A. Kröger, *Z. Krist.*, **100**, 543 (1939).

Results of reflection spectra at room temperature are shown in Fig. 2, including those for ZnS unfired, ZnS fired without activating impurities and ZnS: Mn (Cu not in corporated). The long wavelength threshold of the fundamental absorption of zinc sulfide host crystal is located at about 3400Å which is nearly in agreement with the value reported by Piper[18] for single crystals of zinc sulfide. In the long wavelength region beyond the fundamental absorption, the absorption bands due to copper and manganese appear. The copper band seems to be located from 3600 to 4200Å. The manganese band has a small peak at 4600–4700Å.

4 Excitation. — The excitation spectra were measured with the same quartz monochromator and the excitation source as used in the case of absorption. The phosphor sample was coated uniformly on a glass plate in a thin layer of the thickness, 2.5mg./cm², by means of the sedimentation method, and was set just behind the exit slit. The intensity of the emission was measured through suitable filters with the photomultiplier, 1P21, set behind the plate of the phosphor, the output photocurrent being amplified by the *dc* amplifier. The copper and manganese emissions were isolated from each other with filters, namely Matsuda V-Y1 plus V-B2 for copper and V-O2 or V-R3 for manganese.

Results at room temperature are shown in Fig. 3, including those for ZnS: Mn (Cu not incorporated). All of the samples have a strong excitation peak near 3400Å. This corresponds to the

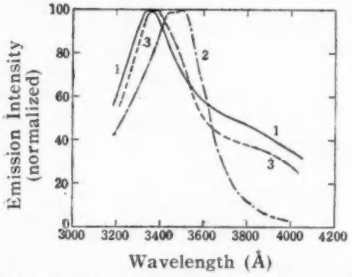

Fig. 3. Excitation spectra for (1) Cu emission of ZnS: Cu, (2) Mn emission of ZnS: Mn (Mn: 1×10^{-2}) and (3) Mn emission of ZnS: (Cu+Mn) (Mn: 8×10^{-4}).

fundamental absorption edge of the host crystal as seen at a glance by comparing it with the reflection spectra, so that this peak is regarded as the one due to the absorption of the host crystal. ZnS: Cu has, in addition, the broad excitation band the peak of which seems to be located at about 3800Å. This band is regarded as the one due to the absorption of copper impurity by comparing it with reflection spectra. These results are nearly in agreement with those of Bube[16]. While manganese in ZnS: Mn has only the excitation band due to the host crystal, manganese in ZnS: (Cu+Mn) has, in addition, the excitation band regarded as the one due to copper. It is no doubt obvious that this additional band is attributed to the absorption of copper, since its shape is very similar to that for copper in ZnS: Cu. This result shows that manganese emission is really sensitized by copper behaving as a sensitizer.

According to Bube[16], the excitation spectrum of manganese in ZnS: Mn shows, in addition to the host excitation band, four excitation peaks due to the forbidden transition within Mn^{+2} ion itself in the wavelength region 3900–5100Å, namely 3980, 4320, 4770 and 5060Å peaks. However, they were not found in the present phosphors, and this fact seems to be probably due to the effect of impurity, especially oxygen.

As thus found, ZnS: (Cu+Mn) has two kinds of excitation band, one due to the host crystal and the other due to the copper sensitizer. Then a new problem arises whether the emission spectra are different under the host or copper excitation. As the excitation source to be used for these excitations, an ordinary 100 W. tungsten incandescent lamp was used, selecting only the necessary wavelength region for each of these excitations with suitable filters; namely Matsuda UV-D1 plus nickel sulfate solution filter (the concentration: $NiSO_4\cdot7H_2O$, 100g./*l.*; the optical path: 5 cm) for the host xcitation, and Matsuda UV-D1 plus V-B2 for the copper excitation. The transmission spectra of these filters are shown in Fig. 4. Since this

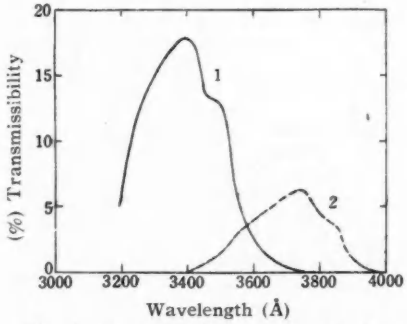

Fig. 4. Transmission spectra of filters for (1) the host and (2) Cu excitations.

excitation source was too weak to measure the emission spectra, only the ratios of the emission peak intensities of manganese to those of copper, *R*, were determined by separating these two kinds of emissions with filters.

It was found that the values of the ratios under the host excitation, R_{host}'s, are about 1.2 times R_{3650}'s for all the phosphors, while R_{Cu}'s are about 0.8 times R_{3650}'s. It may be suggested that the excitation energy absorbed by the host crystal is shared between copper and manganese in proportion to their capture cross sections under the host excitation, whereas under the copper excitation a part of the excitation energy absorbed by copper is transferred to manganese. This results shows that the transfer probability from copper to manganese is rather small as compared with the probability that manganese captures the

18) W.W. Piper, *Phys. Rev.*, **92**, 23 (1953).

host absorbed energy. R_{3650}'s shows the intermediate values between R_{host}'s and R_{Cu}'s, since 3650Å line lies just at a middle position between the two excitation peaks, and consequently causes the both kinds of excitation.

5 Thermoluminescence.—The thermoluminescence for both the copper and manganese emissions after both the host and copper excitations were measured with a specially designed Dewar vessel shown in Fig. 5, using liquid air as

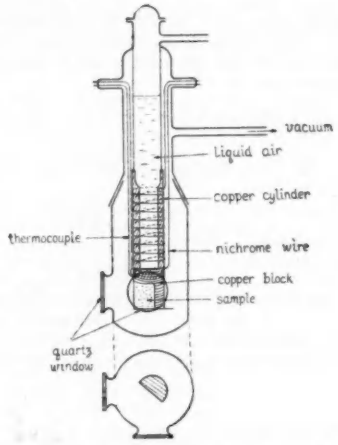

Fig. 5. An apparatus for the thermoluminescence measurement.

a coolant. The phosphors were coated with distilled water on an aluminum plate, which was attached to the copper block. The excitation source was the same as mentioned just above, the tungsten incandescent lamp with filters. The phosphors were excited up to the saturated emission intensities at a liquid air temperature, and then heated by means of nichrome wire with a constant rate, 0.22°K/sec., after allowing the emission to decay for six minutes, detecting the glow intensities with the photomultiplier attached to the *ac* amplifier mentioned in Sec. 2. The copper and manganese emissions were isolated from each other with filters.

Examples of the results are shown in Fig. 6. Every phosphor shows the main glow peak in the temperature range 230-300°K. Low temperature peaks associated with shallow traps were not found, because the emissions were allowed to decay for six minutes after the ceasing of the excitation. In ZnS: Cu, the glow curves for the copper emission after the host and copper excitations are similar to each other, showing main glow peaks at about 240°K. On the other hand, in ZnS: (Cu +Mn) (Mn: 8×10^{-4}) with the copper and manganese emissions which are both distinct, the glow curves for the copper and manganese emissions after the copper excitation are very similar to each other having the main glow peaks at 265°K, whereas those after the host excitation are remarkably different from each other, the main glow peaks

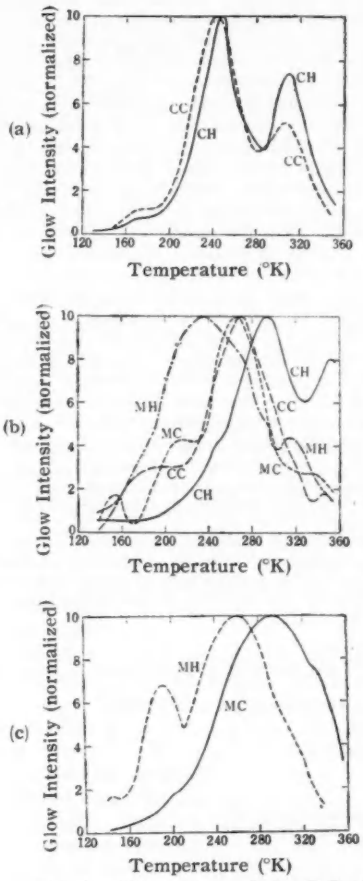

Fig. 6. Glow curve of (a) ZuS: Cu, (b) ZnS: (Cu+Mn) (Mn: 8×10^{-4}) and (c) ZnS: (Cu+Mn) (Mn: 3×10^{-3}).
CH: Cu glow after the host excitation
CC: Cu glow after the Cu excitation
MH: Mn glow after the host excitation
MC: Mn glow after the Cu excitation

being at 295°K for the copper emission and at 235°K for the manganese emission. This result should be strongly noticed in connection with the sensitization mechanism. Also in ZnS: (Cu+Mn) (Mn: 3×10^{-3}) with the predominant manganese emission, the two manganese glow curves are different depending on either the host or copper excitation.

Analyses for the main glow peaks were carried out in the usual manner. The thermoluminescence is produced when the trapped electrons are released by the thermal energy and recombine with the holes in the ground states of the luminescence centers. In the photoconductive phosphors such as zinc sulfide, it is suggested that this process is governed by the bimolecular

mechanism. However, Randall and Wilkins[19,20] found that the phosphorescence and thermoluminescence in the sulfide type phosphors can be explained by the monomolecular mechanism rather than by the bimolecular one. Also, Williams and Eyring[21] established fairly conclusively that the rate-determining process for the glow emission of ZnS: Cu is predominantly monomolecular, based on the analysis of the shape of the glow curve. The reason for these results appears to be that the number of electrons escaping from traps is much smaller than the number of holes in luminescence centers, and so the thermoluminescence process is determined by the rate at which electrons escape from traps, or in other words that the time necessary for the release of electrons from traps is much larger than that during which electrons stay in the conduction band. Furthermore, the effect of the retrapping of thermally released electrons should be also taken into consideration in the photoconductive phosphors. However, Randall and Wilkins[19,20] showed that the retrapping is a negligible process during luminescence, although an empty luminescence center and an empty electron trap have similar cross-sections for electron capture.

Therefore, the analyses were done assuming the monomolecular kinetics and the negligible retrapping. The distribution of trap depth was also ignored. In the case of the monomolecular kinetics, the intensity of the glow emission, I, is given by

$$I=-\alpha \mathrm{d}n/\mathrm{d}t=akn, \tag{1}$$

where n is the number of electrons in the trap at any instant and k is the specific rate constant for the thermal release of trapped electrons. The rate constant is expressed by

$$k=s\exp(-E/kT), \tag{2}$$

where s is the frequency factor and E is the activation energy, i.e. the trap depth. Integrating Eq. (1),

$$n=n_0\exp\left(-\int_{t_0}^{t}k\mathrm{d}t\right) \tag{3}$$

where n_0 is the number of electrons in the trap at time t_0. Introducing the heating rate, $\beta=\mathrm{d}T/\mathrm{d}t$,

$$n=n_0\exp\left(-\frac{1}{\beta}\int_{T_0}^{T}k\mathrm{d}T\right). \tag{4}$$

The emmission intensity is given by inserting Eq. (4) into Eq. (1),

$$I=\alpha n_0 k\exp\left(-\frac{1}{\beta}\int_{T_0}^{T}k\mathrm{d}T\right). \tag{5}$$

From Eq. (4),

$$k=\frac{\mathrm{d}}{\mathrm{d}T}\left[-\beta\ln\frac{n}{n_0}\right]=\beta\frac{\mathrm{d}}{\mathrm{d}T}\left[-\ln\left(1-\frac{n_0-n}{n_0}\right)\right]. \tag{6}$$

Assuming that the number of trapped electrons which undergo radiationless transition is negligible, n_0 and (n_0-n) can be expressed in terms of the light sums, i.e.

$$n_0=\frac{1}{\alpha\beta}\int_{T_0}^{\infty}I\,\mathrm{d}T \quad \text{and} \quad n_0-n=\frac{1}{\alpha\beta}\int_{T_0}^{T}I\,\mathrm{d}T. \tag{7}$$

Hence, the rate constant is given as a function of observables,

$$k=\beta\frac{\mathrm{d}}{\mathrm{d}T}\left[-\ln\left(1-\frac{\int_{T_0}^{T}I\,\mathrm{d}T}{\int_{T_0}^{\infty}I\,\mathrm{d}T}\right)\right]. \tag{8}$$

With this equation both the frequency factor and activation energy can be calculated, although absolute intensities are not observed.

In Table I, The calculated values for the main peaks of the glow curves shown in Fig. 6 are given. The trap depth for the copper main peaks are 0.21–0.23 e.V., irrespective of either the host or copper excitation. The frequency factors for these are made a bit smaller by the incorporation of manganese. The trap depth for the manganese main peak of ZnS: (Cu+Mn)(Mn: 8×10^{-4}) after the copper excitation shows a similar value to that for copper, whereas that after the host excitation shows a considerably different value from that for copper, namely, a smaller one 0.15 e.V., as expected from the results of Fig. 6. Similarly for ZnS: (Cu+Mn) (Mn: 3×10^{-3}), the manganese trap depth after the host excitation is smaller than that after the copper excitation, although both show smaller values than those for ZnS: (Cu+Mn)(Mn: 8×10^{-4}). This effect of trap shallowing by the increased concentration of manganese appears to be caused by the same reason as suggested for the effect that the copper emission peak shifts towards a longer wavelength with the increase of manganese concentration.

TABLE I

TRAP DEPTHS AND FREQUENCY FACTORS FOR THE MAIN PEAKS OF THE GLOW CURVES

Phosphor	Emission	Excitation	Trap Depth e.V.	Frequency Factor (sec^{-1})
ZnS: Cu	Cu	host	0.23	4×10^{2}
		Cu	0.23	6×10^{2}
ZnS: (Cu+Mn) (Mn: 8×10^{-4})	Cu	host	0.21	2×10
		Cu	0.21	6×10
	Mn	host	0.15	1×10
		Cu	0.23	2×10^{2}
ZnS: (Cu+Mn) (Mn: 3×10^{-3})	Mn	host	0.14	2
		Cu	0.18	7

19) J.T. Randall and M.H.F. Wilkins, *Proc. Roy. Soc.* (London), **A184**, 347, 365, 390 (1945).

20) G.F.J. Garlick, "Luminescent Materials", Oxford Press (1949), Chap. II.

21) F.E. Willams and H. Eyring, *J. Chem. Phys.*, **15**, 289 (1947).

The values of Table I are characterized by the unusually low values of frequency factors, resulting from the fact that the width of the main glow peaks are rather broad. The neglect of trap depth distribution seems predominantly responsible for this result. If the trap depth were not a single one, but had a distribution, or two or more traps which could not be resolved by the heating rate used were involved, the broad glow peak would result, which would give the apparent low value of the frequency factor by the analysis on the assumption of the single trap depth. The ignoring of the effect of the retrapping can be also considered as the cause of the low frequency factor. It was shown by Randall and Wilkins[19,20] that when retrapping is present the half-width of the peak for the same values of trap depth and frequency factor becomes much larger. Therefore, if retrapping were involved, it would give the apparent low value of the frequency factor similarly to the trap depth distribution.

The aforementioned results may be reasonably explained by the following inference, if an assumption is made that two kinks of main traps are involved in these phosphors, the deep one associated with copper and the shallow one associated with manganese, as indicated in Fig. 8 in Discussion 2. Under the copper excitation, the freed electron from the copper center enters only into the copper associated trap, and the thermal release from it is the rate-determining step for both of the copper and manganese main glow peaks. On the other hand, under the host excitation, the freed electron from the host lattice enters, probably through the conduction band, into either of the copper and manganese associated traps, and the thermal release from either of them is the rate-determining step for each of the copper and manganese main glow peaks. On the nature of these traps nothing can be discussed here from only this experiment.

6 Photoconductivity.—Only a preliminary experiment was done on the photoconductivity. Cells were made by packing the phosphor powder between a conductive glass and an aluminum plate in the thickness of 1mm. Photocurrents induced by applying *dc* electric field of 280V./cm. under 3650Å excitation were detected by means of a sensitive amplifier constructed with a Matsuda UX-54 vacuum tube and a galvanometer.

In Fig. 7 the relative photoconductive response of a series of ZnS: (Cu+Mn) with a constant copper concentration and varying manganese concentrations are given as the function of manganese concentrations. The response of the samples with higher manganese concentrations are by far smaller than those with lower concentrations. Comparing this with the results of emission spectra, it is shown that the photoconductive response changes abruptly to the smaller value at the manganese concentration at which the manganese emission becomes distinct.

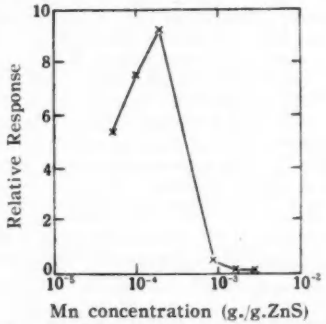

Fig. 7. The relative photoconductive response of a series of ZnS: (Cu+Mn) as the function of the manganese concentration.

Discussion

1 The Range of Energy Transfer from Copper to Manganese.—As mentioned in Experimental 4, the manganese emission in zinc sulfide phosphor is really sensitized by copper behaving as a sensitizer. In other words, a part of the excitation energy absorbed by copper is transferred to manganese to give rise to its emission. The extent of the range surrounding the sensitizer where this energy transfer takes place can be estimated from the relation between the concentrations and luminescent intensities of the sensitizer and activator, based on the assumption that they are distributed at random over the whole lattice sites[9].

Defining z as the number of lattice sites (substitutional or interstitial, or both) surrounding a given sensitizer, it is assumed that if any one of these z sites is occupied by an activator the sensitization can take place with the probability of unity, but that if none of them is occupied by an activator the emission of the sensitizer itself is caused. Then, the mole fraction of the sensitizer incapable of the sensitization and responsible for its own emission is given by

$$C_s(1-C_a)^z, \tag{9}$$

where C_s and C_a are the mole fraction of the sensitizer and activator, respectively. Therefore, the mole fraction of the sensitizer capable of the sensitization, which corresponds to the mole fraction of the activator to be sensitized, is given by

$$C_s[1-(1-C_a)^z]. \tag{10}$$

Under the excitation by the sensitizer absorption, the emission of both the sensitizer and activator are caused only by the light absorption of the sensitizer. Accordingly, the ratio of the number of the quanta emitted by the activator, N_a, to that emitted by the sensitizer, N_s, is expressed by the ratio of Eq. (10) to (9), i.e.

$$B=\frac{N_a}{N_s}=\frac{1-(1-C_a)^z}{(1-C_a)^z}=\frac{1}{(1-C_a)^z}-1 \tag{11}$$

This equation holds if only the following

three conditions are satisfied; the first is that no transfer of the excitation energy between the sensitizers takes place, the second is that the concentrations of both the sensitizer and activator are so low that we may permit the concentration quenching of luminescences among themselves to be neglected, and the third is that the radiationless transition of excitation energy does not occur. It is known[22,23] that for both copper and manganese in zinc sulfide the temperatures at which the radiationless transition begins to occur are higher than room temperature. Then, the value of z is calculated by

$$z=-\frac{\log(B+1)}{\log(1-C_a)}. \qquad (12)$$

The values of B can be estimated by the shapes of the emission bands and the peak intensities for the sensitizer and activator.

In Table II, the values of z calculated for a series of ZnS:(Cu+Mn) with a fixed copper concentration and varied manganese concentrations under the copper excitation are given. The sensitization is shown to take place over the range of 400–500 lattice sites.

TABLE II

THE CALCULATION OF THE VALUES OF z FOR ZnS:(Cu+Mn) UNDER THE COPPER EXCITATION

R: The ratio of the peak intensity of manganese to that of copper.

B: The ratio of the number of quanta emitted by manganese to that emitted by copper.

Mn conc. (g./g.ZnS)	R	B	z	
1×10^{-4}	0.13	0.095	500	Mean 440
2×10^{-4}	0.18	0.13	360	
4×10^{-4}	0.37	0.28	350	
8×10^{-4}	1.3	0.96	470	
1.5×10^{-3}	4.3	3.2	530	

The values of z were already estimated for several non-photoconductive phosphors, such as $CaSiO_3$:(Pb+Mn)[3,9], $Ca_3(PO_4)_2$:(Ce+Mn)[5], and CaF_2:(Ce+Mn)[7]. All of them lie between 10 and 70. The one calculated here for ZnS:(Cu+Mn) is characterized by a value one order of magnitude larger than these.

2 Sensitization Mechanism.—In the photoconductive phosphors two kinds of sensitization mechanism, the resonance transfer and the photoelectron transfer, are suggested as the possible mechanisms, as already mentioned in Discussion 1.

Dexter[10] has developed a quantum-mechanical theory of the sensitized luminescence due to the resonance transfer in non-photoconductive phosphors. He has calculated the probability of the energy transfer by the following mechanisms, i.e. the overlapping of the electric dipole fields of sensitizer and activator, the overlapping of the dipole field of sensitizer with the quadrupole field of activator, and the exchange effect, and has concluded that these mechanisms will give rise to the sensitization of about 10^3–10^4, 10^2 and 30 lattice sites surrounding each sensitizer in typical systems.

The energy levels of doubly ionized manganese in the gaseous state are ^6S, ^4G, ^4P, ^4D and ^4F starting with the lowest term[24]. Based on the experimental results of magnetic susceptibility change accompanying the optical excitation for ZnF_2:Mn[25] and ZnS:Mn[26] and on the comparision of the excitation spectra of phosphors containing manganese with the energy levels in the gaseous state[27], it is indicated[1] that the excited state leading to the luminescence of divalent manganese has four of the 3d electrons with parallel spins and one anti-parallel, while the ground state has all electrons with parallel spins. The luminescence may be suggested to correspond to $^4G\rightarrow{}^6S$ transition.

Although it seems difficult to determine whether the dipole-quadrupole or the exchange transfer is responsible for the sensitized luminescence of divalent manganese in non-photoconductive phosphors, the experimentally derived values of z for these phosphors agree with the theoretical one for the exchange transfer, giving a suggestion that this transfer might be the case. The value of z for ZnS:(Cu+Mn) here calculated is too large to assume the exchange transfer, and still large even for the dipole-quadrupole transfer. This result seems to preclude these mechanisms. However, this value is the one calculated from the assumption that sensitizers and activators are distributed at random, so that the true value might be much smaller if they had a tendency to approach to each other in the host crystal.

Manganese will be distributed at random, since it is incorporated substitutionally forming a solid solution, but copper would not be so. The author has shown[28] in the

22) G.F.J. Garlick and A.F. Gibson, *J. Opt, Soc. Am.*, **39**, 935 (1949).

23) S. Makishima, J. Yamauchi, T. Mukaibo and S. Shionoya. *Ann. Rept. Eng. Res. Inst.*, Fac. Eng., Univ. Tokyo, No. 9, 33 (1951).

24) M.A. Catalan and O. Garcia-Riquelme, "Atomic Energy Levels", National Bureau of Standards, Washington (1952), Vol. 2, Circular 647.

25) P.D. Johnson and F.E. Williams, *J. Chem. Phys.*, **17**, 435 (1949).

26) K. Oshima and H. Nagano, *J. Chem Phys.*, **23** 1473 (1955).

27) C.C. Klick and J.H. Schulman, *J. Opt. Soc. Am.*, **42**, 910 (1952).

28) S. Shionoya and K. Kikuchi, *J. Chem. Soc. Japan, (Pure, Chem. Sect.)*, **77**, 291 (1956).

study of the diffusion of copper into zinc sulfide crystal that copper seems to diffuse, not through the perfect lattice, but along the internal surface, grain boundary or dislocation line. Diemer[29] has studied light patterns in electroluminescent zinc sulfide single crystals activated by the diffusion of copper, and shown that at temperatures a little above room temperature copper diffuses into the bulk of the crystal along certain imperfections which are supposed to be screw dislocations. Therefore, it is likely that copper incorporated as an activating impurity is situated at the vicinity of crystal imperfections. Substitutionally incorporated manganese will give rise to a small disturbance of lattice. Hence, the above assumption that copper and manganese have a tendency to approach to each other might be rather reasonable.

According to Bube[16] zinc sulfide activated with copper shows a photoconductivity by the absorption of copper as well as by the host absorption. Therefore, there is a possibility that the sensitization by photoelectron transfer may occur. This mechanism is shown schematically in Fig. 8. As a result of the

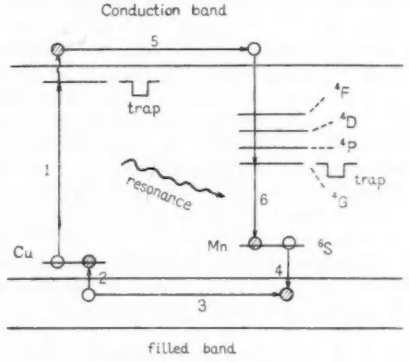

Fig. 8. An energy level diagram for ZnS: (Cu+Mn).

excitation of the copper sensitizer, the electron is raised directly or thermally into the conduction band (process 1). The hole left in the ground state of the sensitizer is released thermally (2), migrates through the lattice (3), and is trapped at the ground state of the manganese activator (4). The electron in the conduction band is transferred to the excited state of the activator (5), and then recombines with the hole producing the luminescence of the activator (6).

For the occurrence of this mechanism, it is needed that the thermal energy for the process 2 is supplied, and that the hole in the filled band has an appreciable mobility. This thermal energy will be so little, the order of 10^{-1} e. V. or less, as to be easily supplied, because the energy for the process 1 is 3.3 e. V. (3800 Å) and that for the host absorption which corresponds to the band gap is 3.6 e. V. (3400 Å). Nothing is yet known for the mobility of holes in zinc sulfide. It was shown in the measurement of thermoelectric effect[22] and in the study of the modulation of luminescence by an *ac* electric field[30] that the dominant charge carriers in zinc sulfide are electrons, and not holes. If the hole mobility were very small, the sensitization by photoelectron transfer mechanism would not occur with an appreciable probability.

In the continuation of this study, it was examined whether heavy metals other than copper which are capable of having luminescence of their own caused by allowed transitions when incorporated in zinc sulfide can act as effective sensitizers for divalent manganese[31]. The results of the study were that lead can sensitize manganese whereas silver or bismuth cannot. This gives a suggestion for the sensitization mechanism. Silver in zinc sulfide is known[16] to show a photoconductivity by the absorption of its own likewise to copper. Also in the case of lead or bismuth the sameness may be expected. If the photoelectron transfer mechanism is the case, any sensitizer which has a photoconductivity in its own absorption band should alway be able to sensitize manganese although the sensitization probability may vary with the kinds of sensitizer used. The above fact that silver and bismuth cannot sensitize manganese at all seems to argue against this mechanism. Thus it appears reasonable to conclude tentatively in the present situation that the resonance transfer rather than the photoelectron transfer is the predominant mechanism. The different behavior of silver and bismuth from that of copper and lead might be attributed to the difference of the electronic state between these two groups.

The results of thermoluminescence are considered to be favorable to the resonance transfer mechanism. If it is assumed that the manganese thermoluminescence after the copper excitation is caused by the photoelectron transfer, it would show the same glow curve as after the host excitation, since

29) G. Diemer, *Philips Res. Rept.*, **10**, 194 (1955).

30) R. E. Halsted, *Phys. Rev.*, **99**, 1897 (1955).

31) S. Shionoya and K. Amano, *J. Chem. Phys.*, **25**, 380 (1056).

electrons raised into the conduction band seem to behave irrespectively of their history, whether they have originated from the host crystal or the coppzer sensitizer. Therefore this assumption appears inconsistent with the experimental results. On the assumption of the resonance transfer, however, the experimental results that the thermoluminescence of copper and manganese after the copper excitation are very similar to each other may be reasonably understood.

The results of photoconductivity measurement might also present a support for the occurrence of sensitized luminescence by the resonance transfer. As mentioned in Experimental 6 the photoconductive response for ZnS: (Cu+Mn) decreases with the increase of the manganese concentration. The similar experiment was done for ZnS:(Ag+Mn), but such an effect was not observed. This difference between copper and manganese seems to be correlated with the different behavior as a sensitizer between them. This effect in the case of copper is explained as follows if the resonance transfer is assumed. The life-time of the excited electron of copper sensitizer, which, it is considered, gives rise to photoconductivity owing to the thermal excitation, will be made shorter by the sensitization of manganese, so that the photoconductive response should becomes smaller with the increase of manganese concentrations.

A tentatively determined energy level diagram for ZnS:(Cu+Mn) is given in Fig. 8. As already mentioned in Experimental 4 manganese in ZnS:Mn has four excitation peaks due to the forbidden transitions within Mn^{+2} ion, i.e. 5060, 4770, 4320 and 3980 Å peaks, which were found by Bube[16]. They are considered to correspond to the excitation from ^6S ground state to ^4G, ^4P, ^4D and ^4F excited states, respectively. Since the energy of the manganese ground level is not yet determined, its position is written arbitrarily. If the resonance transfer is responsible for the sensitized luminescence, the overlap of the emission band of sensitizer with the excitation band of activator is required essentially, and the sensitization probability is proportional to this overlap[10]. Since the emission peak of copper is located at 5350–5450 Å, the excitation energy will be transferred directly to ^4G state of manganese, the lowest excited state from which the luminescence is emitted.

Summary

Optical properties of ZnS:(Cu+Mn) phosphors have been extensively studied with the purpose to investigate the phenomena of sensitized luminescence in photoconductive phosphors. Spectra of emission, absorption and excitation, thermoluminescence and photoconductivity were measured. It was confirmed from the measurement of excitation spectra that the manganese emission is really sensitized by copper behaving as a sensitizer. Some interesting phenomena ascribed to this sensitization were found in the measurements of thermoluminescence and photoconductivity. The mechanism of the sensitization was discussed exhaustively. It appears reasonable to conclude tentatively in the present situation that the resonance transfer rather than the photoelectron transfer is the predominant mechanism.

The author would like to express his thanks to Prof. S. Makishima, University of Tokyo, Dr. Y. Kotera, Government Chemical Industrial Research Institute, Tokyo, and Assist. Prof. K. Oshima, University of Tokyo, for their encouragement and discussions, and to Mr. S. Kamiya*, Mr. W. Ichise** and Mr. K. Amano of this laboratory for their assistance in the experimental works.

A Part of the expense of this study was defrayed by the Grant in Aid of the Ministry of Education for Scientific Research.

Department of Electrochemistry, Faculty of Engineering, Yokohama National University, Minami-ku, Yokohama

* At present: Matsushita Electronics Ind. Co.
** At present: Tokyo Shibaura Electric Co.

SHORT COMMUNICATIONS

New Photometric Method for Determining Thallium with Rhodamine B

By Hiroshi ONISHI

(Received July 17, 1956)

A satisfactory color or fluorescence reagent for thallium is lacking. The photometric methods available at the present time are either indirect or insensitive. A procedure for detecting traces of thallium with rhodamine B has recently been described by Feigl and his coworkers[1]. It does not appear, however, that a quantitative method based on this reaction has been reported. The difficulty in developing the method was ascribed by MacNulty and Woollard[2] to the instability of the higher valency compounds of thallium. According to them, no oxidizing agent has been found that will consistently retain thallium in a higher valency state until the complex with rhodamine B is formed and extracted.

The present author has found that the oxidation of univalent thallium to trivalent with bromine is a satisfactory method preparatory to rhodamine B-benzene extraction. The absorbance-concentration curve shown in Fig. 1 was obtained by the following procedure: Take 0, 2, 4, 6 and 8 μg. of thallium (as Tl_2SO_4) into beakers respectively, add 5.0 ml. of 2.0 N hydrochloric acid and 0.5 ml. of saturated bromine water. Heat near the boiling point and keep heating until immediately after the color due to bromine has disappeared. Cool to room temperature, transfer the solution to a 10-ml. volumetric flask and dilute to the mark with 2.0 N hydrochloric acid. Transfer the solution to a separatory funnel, add 1.0 ml. of 0.20% (w/v) aqueous rhodamine B solution and mix. Add 10.0 ml. of pure benzene and shake for one minute. When the two phases have separated, drain off the aqueous phase, transfer and centrifuge the benzene phase until a clear solution has been obtained. Measure the absorbance of the benzene extract at 560 mμ.

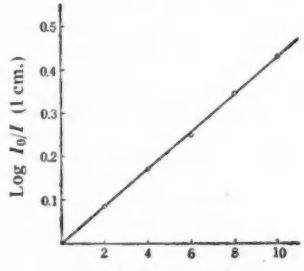

Fig. 1. Absorbance-concentration curve of thallium. Hitachi spectrophotometer, EPB-U, 560 mμ, temperature 18–26°C.

Absorbance is proportional to thallium concentration in the range 0.1 to at least 1 p. p. m. (based on the amount of thallium present originally in the aqueous phase). At 560 mμ the molar extinction coefficient is about 87,000, or 0.0023 μg. Tl/cm^2 corresponding to log $I_0/I=0.001$. Thus the method appears to offer a good basis for the photometric determination of traces of thallium. Details of the study will be published later.

Government Industrial Research Institute, Nagoya

1) F. Feigl, V. Gentil and D. Goldstein, *Anal. Chim. Acta*, **9**, 393 (1953).
2) B. J. MacNulty and L. D. Wollard, ibid., **13**, 154 (1955).

Spatial Configurations and Ultraviolet Absorption Spectra of Some 2,2'-Bridged Biphenyl Derivatives

By Hiroshi SUZUKI

(Received July 19, 1956)

Previously, the present author calculated with certain simple assumptions the quantitative relations between the degree of deviation from coplanarity of molecular configuration and the ultraviolet absorption spectrum as well as the extent of conjugation for stilbene derivatives[1] and also for biphenyl-type compounds[2] by the molecular orbital method, and clarified the theory that the absorption maximum is shifted toward shorter wavelengths with increasing angle between the two benzene rings in the case of biphenyls, and between the benzene rings and the plane

TABLE

Compound	Conjugation band* $\lambda_{max.}$ (Å)	$\varepsilon_{max.}$	$\Delta E(\beta)$	α	R.E. (β)	θ	θ (from model)*
3, 4, 5, 6-Dibenzocyclohepta-3, 5-diene-1-carboxylic Acid	2490	15300	1.653	0.550	0.120	48.4°	ca. 50°
Methyl 3, 4, 5, 6-dibenzocyclohepta-3, 5-diene-1-carboxylate	2485	15500	1.657	0.543	0.117	49.0°	〃
1-Hydroxymethyl-3, 4, 5, 6-dibenzocyclohepta-3, 5-diene	2485	15400	1.657	0.543	0.117	49.0°	〃
Ethyl 4, 5, 6, 7-dibenzocycloocta-4, 6-diene-1, 1, 2, 2-tetracarboxylate	2395	13100	1.723	0.432	0.075	58.0°	60–65° (or 75–80°)
Methyl 4, 5, 6, 7-dibenzocycloocta-4, 6-diene-1, 2-dicarboxylate	2365	12700	1.747	0.392	0.062	61.1°	〃

* According to G.H. Beaven and others, loc. cit.

of the central ethylenic linkage in the case of stilbenes, and further, demonstrated the fact that the values of the angle of twist computed by this method from the observed positions of the absorption maxima agree satisfactorily well with those deduced from scale models or by other methods such as the electron diffraction analysis in almost all the examples cited in both the cases.

Applying the same method to some 2, 2′-bridged biphenyl derivatives with seven- and eight-membered homocyclic rings, whose absorption spectra in 96% ethanol solutions have recently been reported by G.H. Beaven and others[3], the results summarized in the Table are obtained. The notation used here is the same as in the previous paper[2]: ΔE is the energy difference between the lowest vacant orbital and the highest occupied orbital, α is a parameter by which allowances are made for the situation that the value of the exchange integral for the 1–1′ bond varies with the angle of twist θ and the length of the bond, and R.E. is the extra-resonance energy, representing the extent of conjugation. Agreements between the values of the angle of twist computed from the absorption maxima and those deduced from scale models are fairly good also here.

The College of General Education
The University of Tokyo
Tokyo

1) H. Suzuki, This Bulletin, 25, 145 (1952).
2) H. Suzuki, This Bulletin, 27, 597 (1954).
3) G. H. Beaven, Gwendoline R. Bird, D. Muriel Hall, E. A. Johnson, Joan E. Ladbury, Mary S. Lesslie and E. E. Turner, *J. Chem. Soc.*, 1955, 2708.